An Investigation into the Mechanism of Intercomponent Motion in Mechanically Interlocked Molecules

By

Phillip Nash

Degree of Doctor of Philosophy

Department of Chemistry

University of Edinburgh

October 2003

EDINBURGH UNIV. LIBR.

Dedicated to Hélène Turpin,
whose love and support made it
possible to for me to work hard
and achieve this.

And to my parents, Peter and Maureen
whose belief in me and constant
encouragement helped me to continue
and complete this thesis.

And last, but not least,
to my brother Edward, who
always said I could do it.

Table of Contents

Abstract		iv
Declaration		vi
Acknowledgements		vii
List of Abbreviations		viii
General Remarks on the Experimental Data		ix
Chapter 1:	Introduction	1
Chapter 2:	Macrocycle Racing 1: Measuring the Rate of Macrocycle Movement along a Polymer Backbone in [2]Polyrotaxanes Grown by Atom Transfer Radical Polymerisation (ATRP)	41
Chapter 3:	A Tight Fit: Rotaxane Formation with a Highly Preorganised Template Assisted by Aromatic Stacking Interactions	85
Chapter 4:	Macrocycle Racing 2: Using Telechelics to Form [2]Polyrotaxanes	110
Chapter 5:	Using Symmetrical Molecular Shuttles to Study the Mechanism of Intercomponent Motion in Rotaxanes	136
Chapter 6:	Entropy-Driven Translational Isomerism: a Tristable Molecular Shuttle	182

Abstract

Research into interlocked architectures has now progressed to a point where the design and synthesis of 'molecular machines' is now becoming a reality. Despite this, some of the fundamental properties of simple interlocked molecules are not fully understood. The mechanism of intercomponent motion is one such phenomenon that has not been investigated, *e.g.* how does a macrocycle move within an interlocked system? This motion is difficult to observe because the components spend the majority of their time over a binding station, and the methods of study are usually time-averaged techniques, *e.g.* Nuclear Magnetic Resonance. An understanding is not essential to the design of molecular machines, but would allow us to better predict the behaviour of these systems, and enable us to determine whether interlocked components experience microscopic equivalents of macroscopic phenomena such as inertia, momentum and friction.

The aim of this research was to investigate intercomponent motion by employing systems where the motion, although difficult to observe directly, has an observable effect on a measurable property in the systems of study. The initial target of this research was to synthesise a [2]polyrotaxane. On cleaving a removable stopper the macrocycle would be free to translate along the backbone of the polymer chain before being irreversibly lost to the system in solution. The initial research presents the attempts to functionalise a rotaxane auxiliary with a polymer chain, firstly by Atom Transfer Radical Polymerisation (ATRP) of a rotaxane initiator, and then by attaching a poly(ethylene glycol) monomethyl ether chain to a rotaxane auxiliary. The design and application of a new rotaxane template motif is also presented. An alternative approach to the study of intercomponent motion is then presented. A series of symmetrical molecular shuttles, defined as a [2]rotaxane comprised of two identical stations that are separated by an alkyl chain, was synthesised. The macrocycle in such systems is known to 'shuttle' between the two stations, spending roughly half the time on each station, and this rate can be observed and measured. By reducing the length of the alkyl chain between the two stations, a faster rate of shuttling between the stations was observed. The series incorporated shuttles with

different length alkyl (C2, C4, C6, C8, C10, C12) spacers, different stations and different macrocycles. Shuttling or site exchange rates were measured by ^{1}H Nuclear Magnetic Resonance using Spin Polarisation Transfer by Selective Inversion Recovery (SPT-SIR) technique. We attempt to use the experimental results to validate a theoretical model for the intercomponent motion. Finally a study of a unique tristable molecular shuttle is presented. This unique system displays some of the unanticipated behaviour that highlights our incomplete understanding of interlocked systems.

Declaration

The scientific work described in this thesis was carried out in the Department of Chemistry at University of Warwick between November 1999 and September 2001 and in the Department of Chemistry at University of Edinburgh between September 2001 and October 2003. Unless otherwise stated, it is the work of the author and has not been submitted in whole or in support of an application for another degree or qualification of this or any other University or institute of learning.

Acknowledgements

I would like to thank my supervisor Prof. David Leigh for giving me the opportunity to work in his group, for giving me challenging projects and for allowing me the freedom to pursue my own ideas. Towards the end of my PhD, I am grateful to him for the useful discussions, and for helping make this part of my four years an enjoyable and intellectually stimulating period.

To those who I spent the whole PhD experience with, a big thanks to: Gianni, a sincerely joyous character who made me laugh a lot; Jeff whose synthetic and general knowledge was invaluable, and who most closely understood what this experience has been like for me; Andrea for the laughs.

From Edinburgh, I would like to thank: Elena for being an amazing friend who would listen and chat, and make me laugh, and counsel, and support and give me a proverbial 'kick' when I needed it; Emilio, who helped make my days enjoyable with good laughs and interesting discussions, and of course for his work with the NMR; my good friend Trent for putting me up, and putting up with me, for my last month, and for making the intensive write-up period more enjoyable than it should have been; Steph also for interesting chats, Ale (not only) for the use of her mug, Paul, Clare, Andrea, Popi, Euan, Drew, Isabel, Jose, Smilja, Barney (esp. for footy), Louise, all the new people and anyone I've forgotten (sorry).

From Warwick, I'd like to thank: Jason and Matt for many hours fun at the table-football table; Ged for being a very good friend; Ale F. for some good times and some bad; Also Guy, Frankie, Miguel, Ben, Sandra, Andy, Tony, and anyone else, especially those who played in the footy tournament.

From outside the group in Edinburgh: Fraser for making me feel welcome in Scotland, and being a good mate; the KB staff, esp. Alan and Chris, for the extra food; and anyone else who knows me.

List of Abbreviations

δ	chemical shift
ΔG°	Gibbs energy
Calcd.	calculated
COSY	COrrelation SpectroscopY
CPK	Corey-Pauling-Koltun
4-DMAP	4-dimethylaminopyridine
DMF	*N,N'*-dimethylformamide
DMSO	dimethylsulphoxide
E	*trans* isomer
EDCI·HCl	1-(3-dimethylaminopropyl)-3-ethyl-carbodiimide hydrochloride
Et	Ethyl
FAB	Fast Atom Bombardment
g	grams
HMBC	Heteronuclear Multiple-Bond Correlation
HMQC	Heteronuclear Multiple-Quantum Correlation
HRMS	High Resolution Mass Spectrometry
Me	Methyl
mins	minutes
mL	millilitres
m.p.	melting point
NMR	Nuclear Magnetic Resonance
NOESY	Nuclear Overhauser Enhancement SpectroscopY
ppm	part per million
rt	room temperature
SPT-SIR	Spin Polarisation Transfert by Selective Inversion Recovery
THF	tetrahydrofuran
TFA	trifluoroacetic acid
TLC	Thin Layer Chromatography
VT	Variable Temperature
Z	*cis* isomer

General Remarks of Experimental Data

All the melting points (m.p.) were determined using a Electrotermal 9100 melting point apparatus and are uncorrected. ^{1}H (400 MHz) and ^{13}C (100 MHz) NMR spectra were recorded on a Bruker DPX 400 MHz spectrometer using dilute solution in $CDCl_3$, CD_2Cl_2, d_6-DMSO, $C_2D_2Cl_4$ without any internal reference and referenced to the residual solvent signal as internal standard ($CHCl_3$ at δ_H = 7.27, s; δ_C = 77.0, t; CD_2Cl_2 at δ_H = 5.32, t; δ_C = 53.5, m; d_6-DMSO at δ_H = 2.54, m; δ_C = 40.5, m; $C_2D_2Cl_4$ at δ_H = 5.96, s; δ_C = 78.0, t) and the chemical shifts are reported in part per million (ppm) from low to high field. All the ^{1}H and ^{13}C NMR spectra were recorded at 298K unless otherwise stated. The FIDs were processed by the software WinNMR or Mestre-C and where it was necessary the FIDs were treated with different kind of apodization functions. ^{1}H NMR are reported as follows: br = broad, s = singlet, d = doublet, dd = doublet of doublets, t = triplet, dt doublet of triplets, q = quartet, m = multiplet, ^{2}J(H,H) = geminal coupling constant, ^{3}J(H,H) = vicinal coupling constant, ^{4}J(H,H) = dihedral coupling constant. ^{13}C NMR are reported as follows: Ar*C* (ipso) = quaternary aromatic, Ar*C*H = non quaternary aromatic. H-H COSY, HMQC, HMBC, NOESY 2D were also recorded for some compounds to enable more detailed assignment of ^{1}H and ^{13}C signals. Rotaxanes and their respective threads have been named using IUPAC/ACD software. Column chromatography was carried out using Kiesegel C60 (Merck) as stationary phase. TLC detection was performed on silica gel plates (0.25 mm thick, 60 F254, Merck, Germany). The TLC plates were observed under UV light or stained with iodine vapours, or spotted using different developing solutions as 8% sulfuric acid, 0.1N $KMnO_4$ or 0.2% ninhydrin in EtOH and successively heated using a heatgun. Mass spectrometry and HRMS analyses were performed by the University of Warwick and University of Edinburgh mass spectrometry service using fast atom bombardment (FAB) from *m*-nitrobenzyl alcohol matrix unless otherwise stated. Elemental analyses were performed by the University of Warwick and University of Edinburgh elemental analysis service. The CD measurements were recorded in the range 235-320 nm on a JASCO J-810 spectropolarimeter at 0.1 mM substrate concentration with a path length of 0.1 cm. The path length allowed the reproducible measurements of the CD spectra even in

$CHCl_3$ in the range 235-320 nm, despite the strong absorbance of the solvent at these wavelengths. Photo-isomerizations were carried out in quartz vessels using a multilamp photoreactor model MLU18 manufactured by Photochemical Reactors Ltd, Reading UK. Reagents and anhydrous solvents used for the reactions were purchased from Aldrich and were in general used without further purification. Isophthaloyl dichloride was routinely recrystallized from hexane and *para*-xylylenediamine was distilled under reduced pressure. Anhydrous chloroform used for the rotaxane formation reactions was stabilized with amylenes.

Chapter 1

Introduction

1.1 Historical Summary

The unique properties of interlocked architectures, such as rotaxanes and catenanes are only recently being exploited. Indeed, they have only been synthesised in useful quantities in the last twenty years, and in that time, have opened up new areas of research into functional molecules.

In the early 1900s, Willstatter first discussed the possibility of synthesis of linked macrocyclic rings.[1] Interlocked architectures of this type were not isolated for many decades after this initial suggestion. In 1960, Wasserman reported the synthesis of the first interlocked species.[2] Since that time rotaxanes and catenanes have been the subject of growing interest, but it was not until 1984[3] that a new era of the chemistry of interlocked molecules dawned with the use of self-assembly and template directed synthesis, utilising non-covalent interactions.

Nature has long since mastered the use of non-covalent interactions for all manner of functions essential to life. For example, proteins maintain their well-defined structures in solution through the use of many weak inter- and intra-molecular interactions, and they are able to recognise and bind specific molecules, without the need of covalent bonds.[4] Chemists have been inspired to utilise the lessons learnt from nature for as long as biologists have been able to study and elucidate its detailed workings. The study of non-covalent interactions and self-assembly in nature has been key to improving our understanding of how these processes work, and of how we can utilise them. They have been used successfully in the synthesis of interlocked architectures, which have allowed further study and helped us to improve our understanding of them further.

This short review, which is by no means exhaustive, serves to provide a general introduction to the chemistry of interlocked architectures. Their origins will be discussed in more detail, then advances such as the use of template directed synthesis, and thermodynamic control in self-assembly will be introduced. Finally, an insight into their properties and future potential will be discussed.

1.2 Catenanes, Rotaxanes, and Knots

Non-covalent interactions have been utilised for a wide variety of self-assembly processes including molecular zippers[5] and all manner of host-guest complexes (supramolecular chemistry).[6] Interlocked architectures have received a growing amount of interest because of their inherent properties: - the individual components can move independently of each other, but cannot be separated without the cleavage of a covalent bond. The three types of interlocked architectures are catenanes (from the Latin *catena* meaning chain), rotaxanes (from the Latin *rota* and *axis* meaning wheel and axle respectively) and knots (figure 1.1).

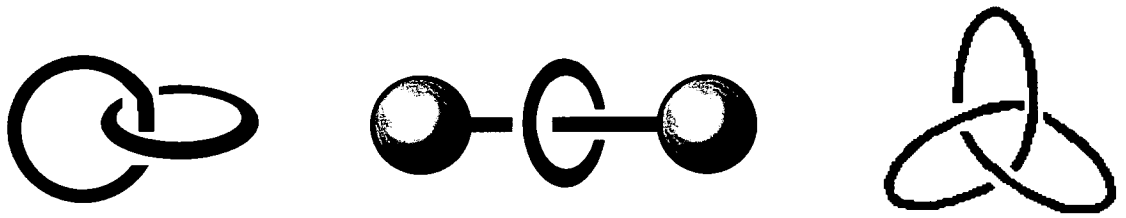
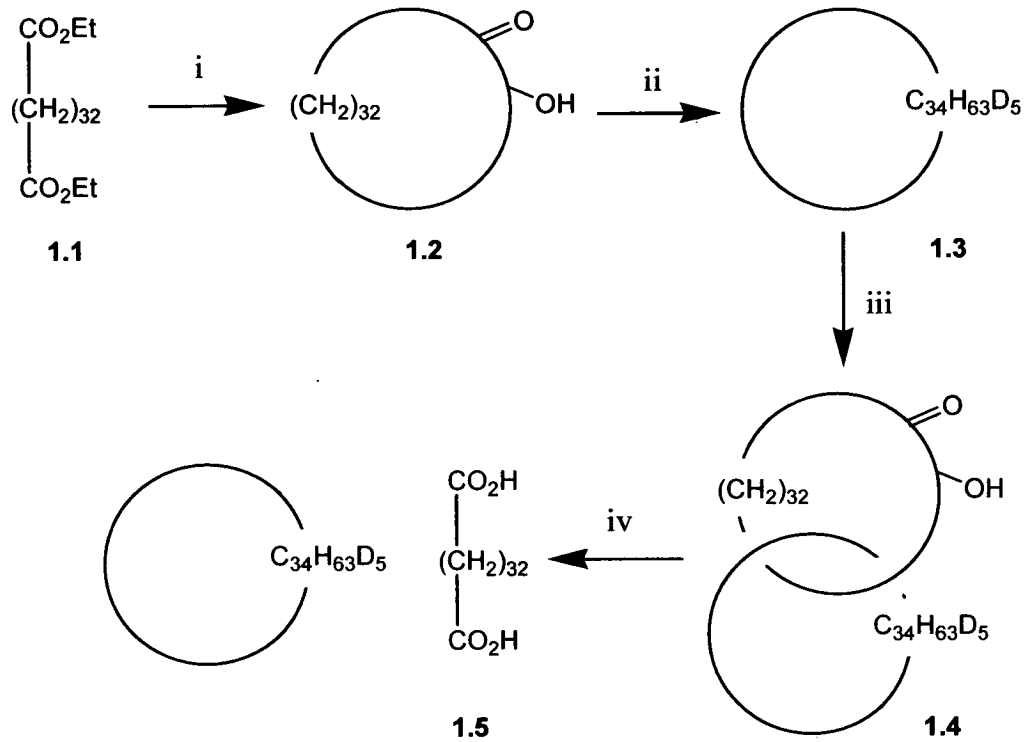


Figure 1. 1 Examples of Interlocked Architectures

Catenanes are two or more mechanically interlocked macrocycles. Rotaxanes are species that have one or more macrocycles, interpenetrated by another molecule (referred to as a 'thread'). The thread is terminated with bulky groups ('stoppers') to prevent unthreading. Without the stoppers, the association complex of macrocycle and thread is known as a pseudorotaxane. Knots are made of a single linear component, looped and threaded through itself, and are topological isomers[7] of a macrocycle.

1.3 Statistical Methods

Early attempts at the synthesis of interlocked molecules were performed by statistical threading methods. The first catenane synthesis by Wasserman[2] was designed to prove the existence of linked products in macrocyclisation reactions (scheme 1.1).



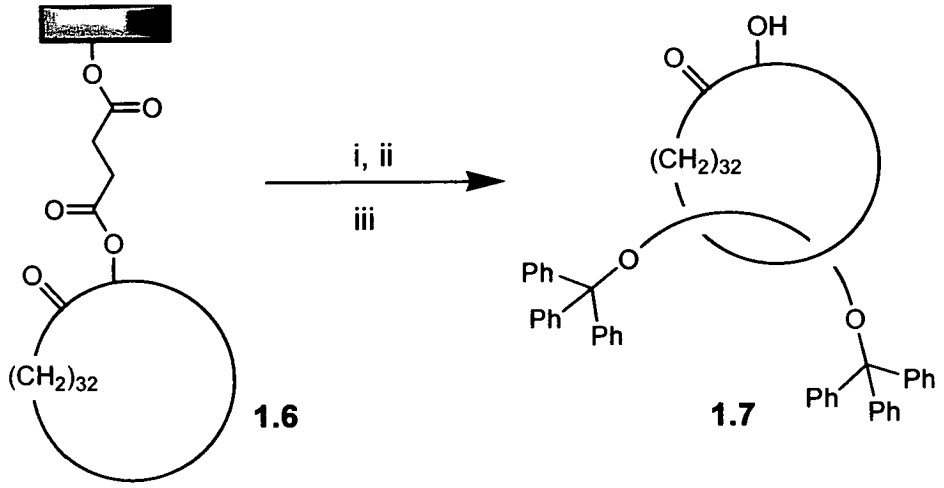
Scheme 1. 1 First Synthesis of a [2]Catenane.

Conditions: (i) Na, xylene; (ii) Zn, DCl; (iii) bis-ester 1.1, Na, xylene; (iv) H_2O_2 / OH^-

Acyloin condensation of the linear diester **1.1** gives over 70% acyloin macrocycle **1.2**, which was reduced and deuterated to give macrocycle **1.3**. Acyloin condensation of the linear diester **1.1** was repeated in the presence of this deuterated hydrocarbon macrocycle **1.3**. The mixture of macrocycles was easily separated by chromatography, but the purified acyloin macrocycle was still found to contain deuterium by IR spectroscopy. Oxidative cleavage of the product gave the di-acid **1.5** and approximately 1% of the deuterated macrocycle **1.3**. The most likely explanation

quoted was that some linear precursors threaded through deuterated macrocycles before being macrocyclised to form some catenane. Indeed, the catenane was isolated and reported in 1962.[8]

In 1967, Harrison and Harrison reported the synthesis of the first rotaxane by using a macrocycle attached to a solid support (scheme 1.2).[9]



Scheme 1. 2 First Synthesis of a Rotaxane.

Conditions: (i) decane-1,10-diol, trityl chloride, pyridine, dimethylformamide; (ii) wash resin; repeat i) and ii) 70 x; (iii) Na_2CO_3, MeOH.

The macrocycle was tethered to a Merrifield resin, and rotaxane synthesis relied on the statistical threading of decane-1,10-diol through the macrocycle before being stoppered with trityl groups. The resin was washed and the reaction was repeated seventy times. When the link to the resin was cleaved, the [2]-rotaxane **1.7** was obtained in 6% yield.

The low yield highlights the problem of using statistical methods, as there is no thermodynamic driving force to facilitate the formation of interlocked species. Correspondingly, Schill and Lütteringhaus described these stategies as "synthetically useless".[10]

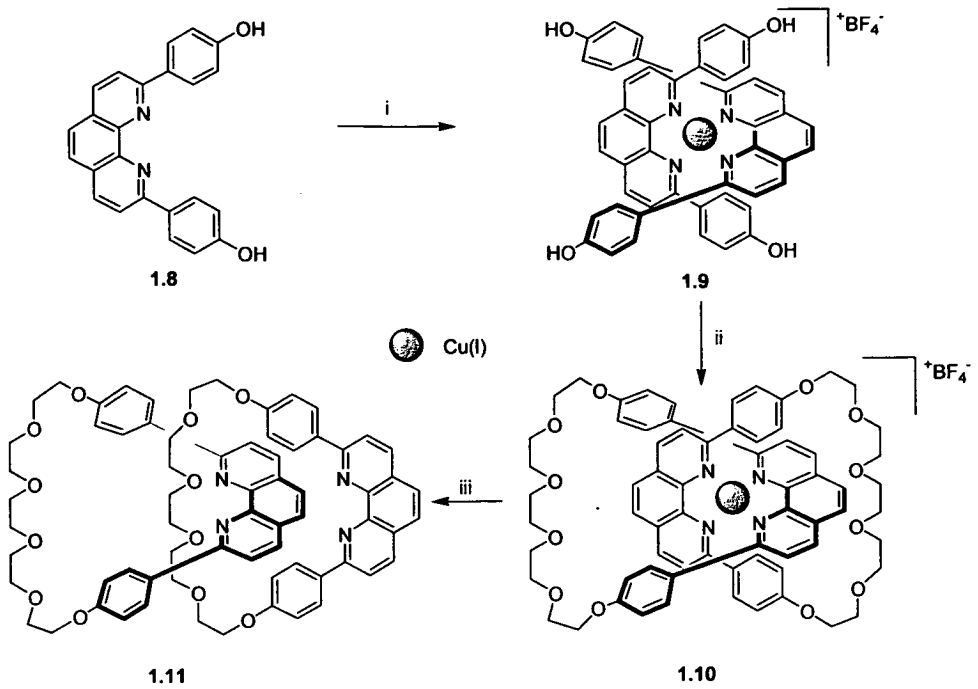
Although researchers aimed to improve the yield using covalent templates, such as möbius strip[7] and directed synthesis methods,[11] little improvement was seen.

1.4 The Dawn of Template Directed Synthesis of Interlocked Architectures

Thus far, interlocked architectures had been seen only as chemical curiosities and synthetic challenges, and received little by way of interest. The advent of non-covalent templates heralded a new era for interlocked architectures, utilising non-covalent interactions to form stable interlocked complexes (or complexes preorganised for interlocking). Final covalent modification of these complexes has resulted in the synthesis of interlocked molecules in high yields.

1.4.1 Metal Templates

In 1984, Sauvage reported the first catenane synthesis using a non-covalent template.[3] Rather than relying on statistical threading, a catenane formation was directed by a copper (I) ion templating two 1,10-phenanthroline derivatives **1.8** in a locked, mutually-orthogonal orientation (scheme 1.3)



Scheme 1. 3 The First Template Directed Synthesis of a [2]Catenane

Conditions: (i) $Cu(CN)_4BF_4$, MeCN; (ii) 1,14-diiodo-3,6,9,12-tetraoxotetradecane, $CsCO_3$; (iii) KCN, H_2O / MeCN

The preorganised, interlocked core of the catenate* **1.9** was formed in quantitative yield. The subsequent ring closure step (ironically, a statistical reaction) proceeded poorly and catenate **1.10** was only isolated in 27% yield. Subsequent demetallation to remove the metal template gave the catenand* **1.11** in quantitative yield.

This represented a vast improvement in the yield compared to statistical methods. The remarkable feature of this system is that the metal ion was used to template the core of the catenate, which was preorganised towards catenane formation and provided the necessary thermodynamic driving force to form the interlocked species.

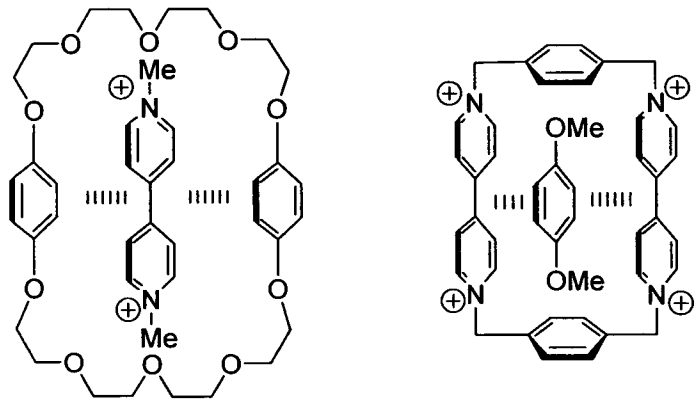
Sauvage has since improved the yield of [2]catenate[12] to over 90% using ring-closing metathesis to close the macrocycles.

* Catenate and catenand are variations of catenane derived from the nomenclature of coordination chemistry (*cf* ligate and ligand)

The transition metal template has since been used to form a wide variety of interlocked species, including rotaxanes,[13] the first knot[14] and multi-ring catenates.[15]

1.4.2 π - π Stacking Interactions

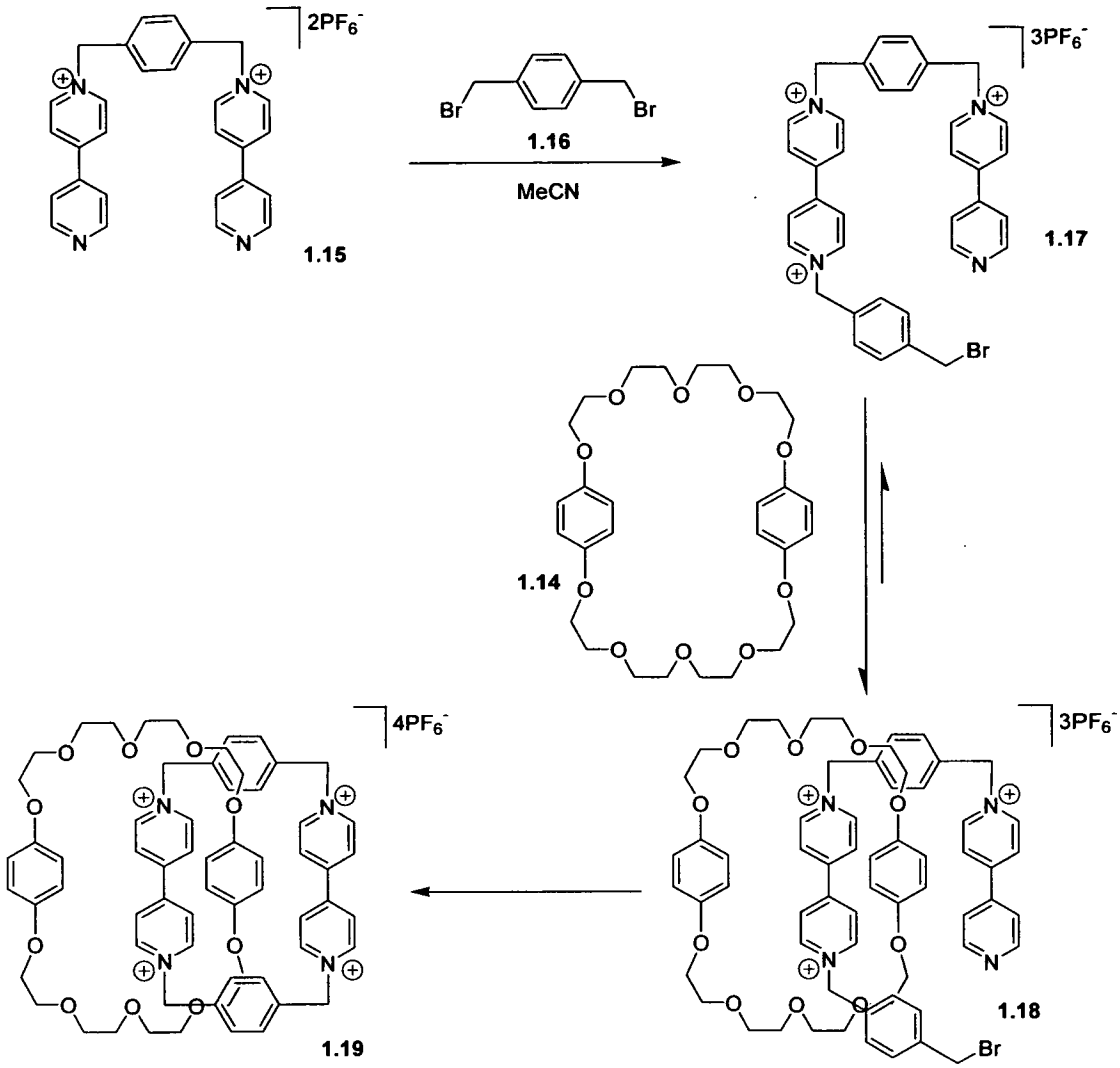
In 1989, Stoddart reported the synthesis of a [2]catenane utilising aromatic π-π stacking interactions.[16] Previous research[17] in his group had studied the inclusion complexes of electron-deficient paraquat with electron-rich crown ethers **1.12**, and the analogous π-deficient tetracationic receptor with π-rich guests such as 1,4-dimethoxybenzene **1.13** (figure 1.2).



1.12 **1.13**

Figure 1. 2 Inclusion Complexes Utilising Aromatic π - π Stacking Interactions

Stoddart utilised these π - π stacking interactions as a template to synthesise a catenane incorporating two different macrocycles (scheme 1.4). By reacting the 'u-shape' precursor **1.15** with *p*-xylylenedibromide **1.16** in the presence of the 24-crown-8 macrocycle **1.14** the [2]catenane **1.19** was obtained in 70% yield. The high yield is remarkable, considering the fact that there is no initial association between **1.14** and **1.15**. After a single reaction of **1.15** with **1.16** has occurred, the bipyridinium unit is sufficiently electron-deficient for a favourable interaction to occur with the electron-rich crown ether **1.14**, and the inclusion complex **1.18** is formed. This precursor then undergoes intramolecular ring closure ('clipping') to give the highly coloured [2]catenane **1.19**.



Scheme 1. 4 [2]Catenane Synthesis using Aromatic Interactions

Conditions: Anion Exchange of Br^- with PF_6^- is carried out using NH_4PF_6

Stoddart developed the field of interlocked architectures by using π-donor - π-acceptor templates to synthesise a range of [2]rotaxanes by different methods (figure 1.3). The majority of rotaxane syntheses can be attributed to one of these three methods.

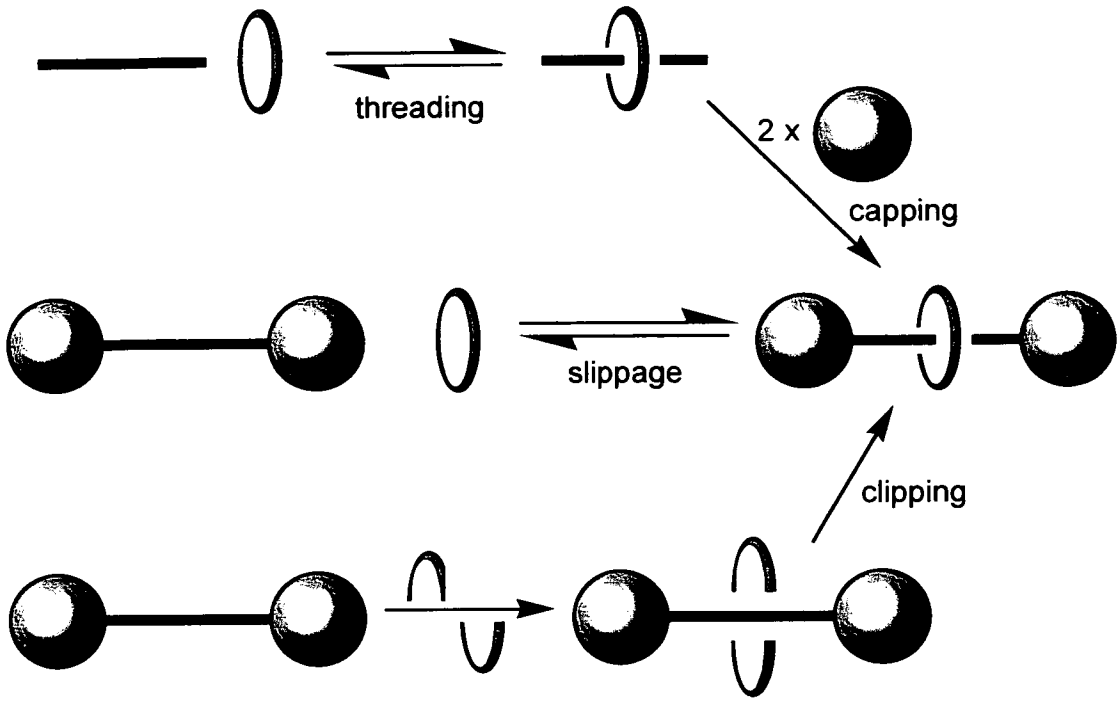


Figure 1. 3 Methodologies Used in Rotaxane Synthesis

'Threading'[18] involves the binding of the unstoppered thread to the macrocycle to form an inclusion complex, or pseudo-rotaxane. The threading process is in equilibrium with the unthreading process. The rotaxane is formed when the included thread is 'capped' with bulky stopper groups.

'Clipping'[19] involves the use of a preformed thread, with bulky stopper groups, which templates the formation of a macrocycle around it to give the rotaxane.

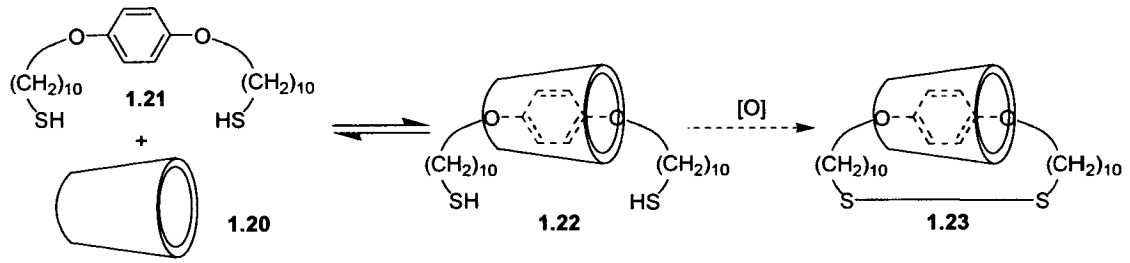
'Slippage'[20] involves the use of a carefully designed, pre-stoppered thread and preformed macrocycle. At elevated temperatures, the macrocycle has sufficient energy to slip over the bulky stopper group and an equilibrium between the free components and the inclusion complex is established. On lowering the temperature the macrocycle in the inclusion complex is trapped on the thread giving the rotaxane.

Many interlocked architectures have since been synthesised using π - π stacking interactions including multi-ring catenanes,[21] [3]rotaxanes,[22] and many other interesting architectures.[23]

1.4.3 Solvophobic Effects

Although the solvophobic effect does not involve the favourable enthalpic interaction between two species, but is driven by entropically favourable desolvation, it is a very useful tool for the synthesis of interlocked architectures.

The first example of an attempted [2]catenane synthesis using the hydrophobic effect was by Lüttringhaus[24] in 1958. On mixing dithiol **1.21** and cyclodextrin **1.20** in water the inclusion complex, or pseudo-rotaxane, **1.22** was formed. Intramolecular oxidative coupling of the two thiols theoretically should have produced the [2]catenane **1.23**, but only starting materials were isolated.



Scheme 1. 5 Attempted Synthesis of a [2]Catenane using the Hydrophobic Effect

Anderson has used the hydrophobic effect to template the synthesis of a water-soluble [3]rotaxane[25] **1.24** in reasonable yield by threading dicationic macrocycles onto a singly-stoppered hydrophobic thread before capping (figure1.4).

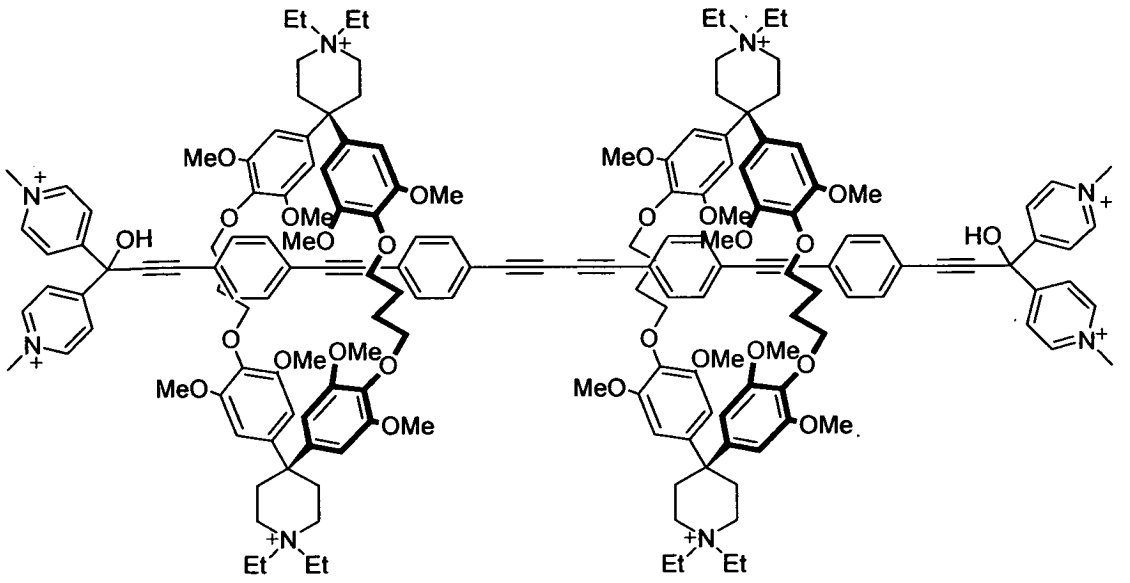


Figure 1. 4 [3]Rotaxane[25] Assembled using the Hydrophobic Effect

1.4.4 Hydrogen Bonds

Hunter reported the first example of a catenane formed using hydrogen bonds[26] in 1992. Vögtle published a similar synthesis shortly afterwards.[27] Hunter's serendipitous discovery was made when he tried to make a receptor for quinone[28] (figure 1.5). The receptor utilises hydrogen bonding and CH - π interactions to bind its guest.

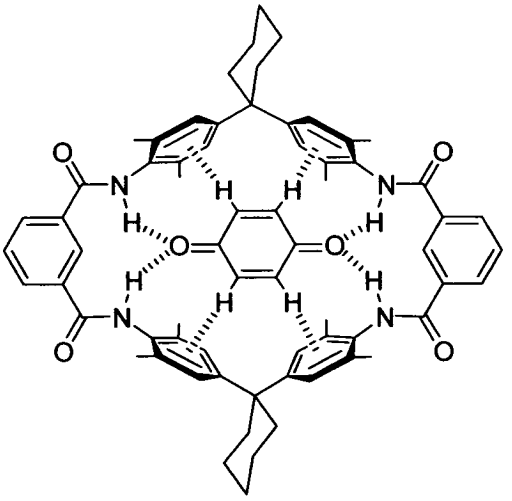
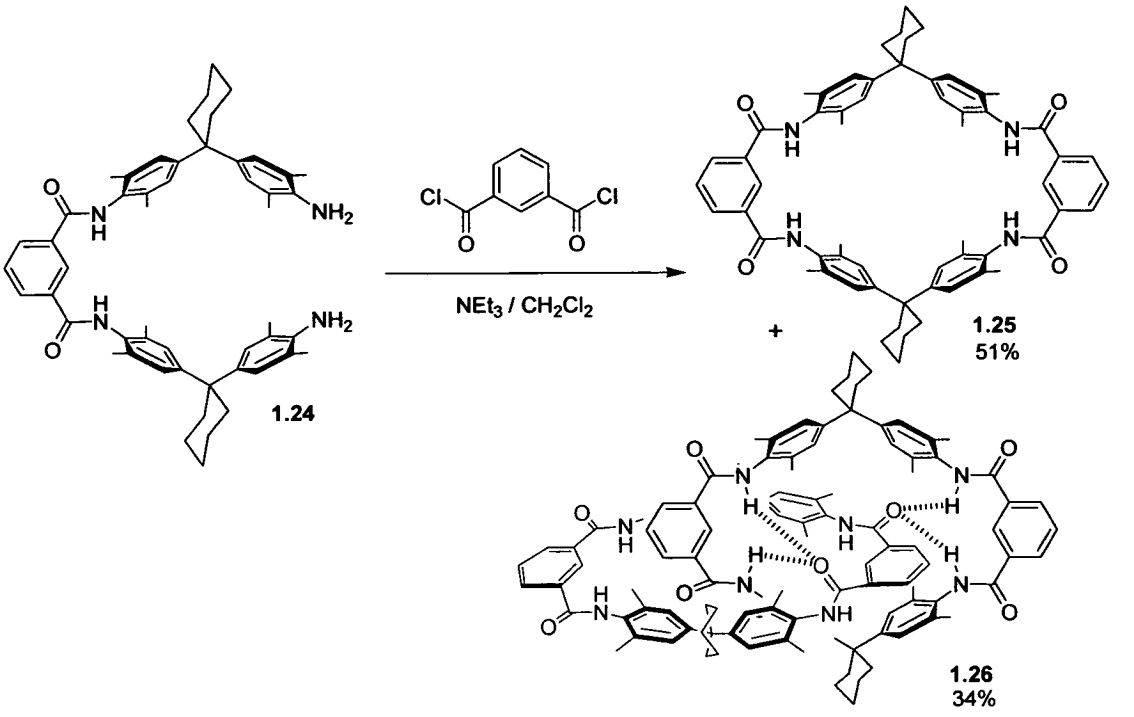


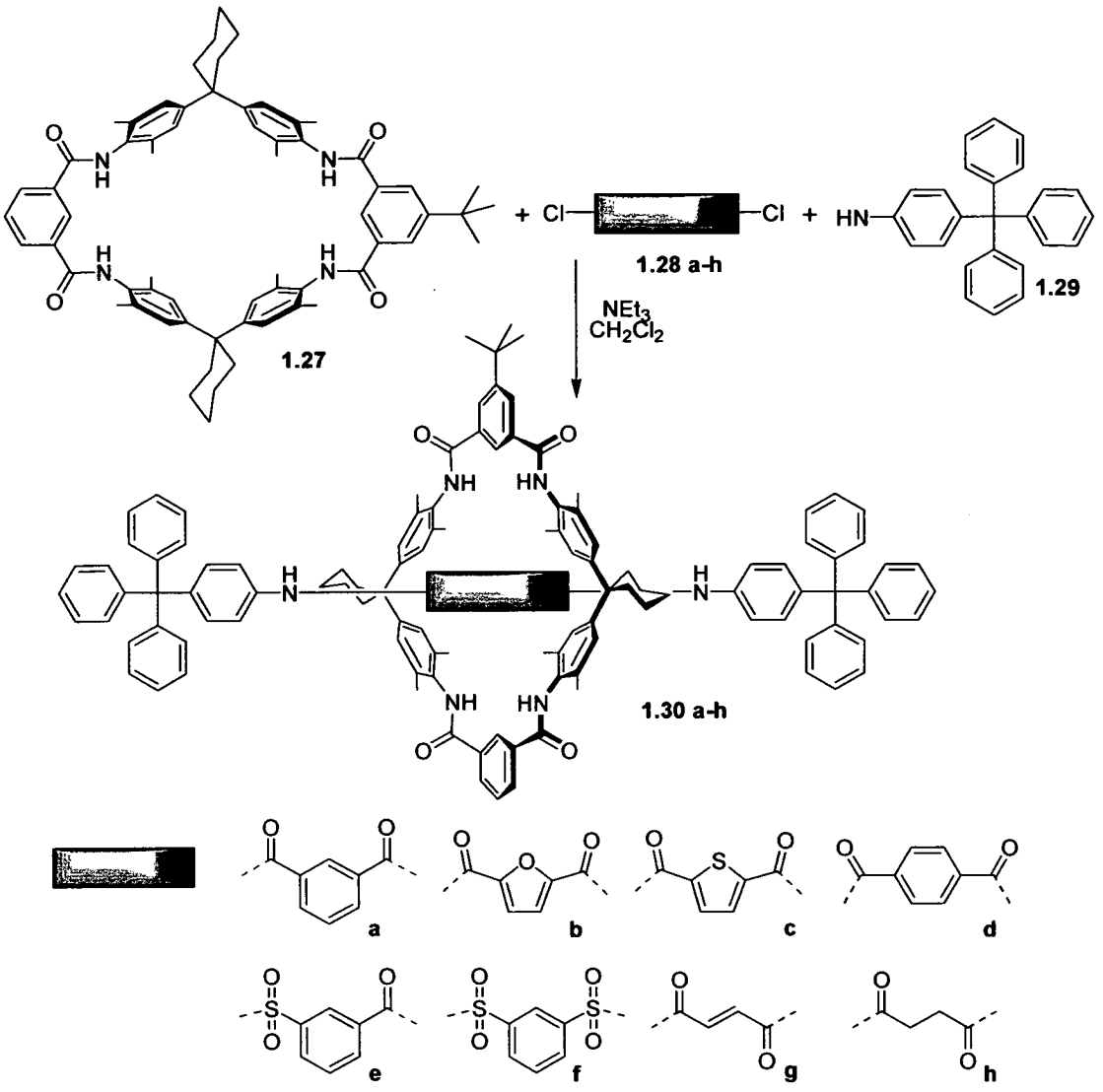
Figure 1. 5 Hunter's Quinone Receptor

In an attempt to synthesise the receptor, a 'U-shaped' precursor **1.24** was reacted with isophthaloyl dichloride under high dilution conditions (scheme 1.6). The macrocyclic receptor **1.25** was synthesised in 51% yield, along with an unexpected [2]catenane **1.26** in 34% yield.



Scheme 1. 6 First [2]Catenane Synthesis using Hydrogen Bonds

Vögtle has since developed a range of catenanes.[29] He initially proposed (incorrectly) that catenane synthesis occurred through initial binding of an acid chloride by a preformed macrocycle.[30] Since then he has synthesised a number of rotaxanes **130 a-h**,[31] by using the macrocycle **1.27**, diacid chlorides **1.28 a-h** (scheme 1.7), and the stopper **1.29**.



Scheme 1. 7 Vögtle [2]Rotaxanes using Different Hydrogen Bonding Templates

He used these rotaxanes to probe the mechanism of interlocking. He proposed a more plausible theory that after an initial amide formation reaction, the thread forms an inclusion complex with the macrocycle,[32] prior to the second amide reaction to stopper the thread and form the [2]rotaxane (threading followed by capping). The synthesis of rotaxanes **130 a-h** demonstrated the wide structural diversity and versatility possible using a hydrogen-bonding template.

In another serendipitous discovery, Leigh reported the synthesis of the smallest [2]catenane in 20% yield by means of an eight molecule condensation.[33] The aim

was to synthesise a receptor (**1.31**) for carbon dioxide (figure 1.6) using a [2+2] high dilution condensation of isophthaloyl dichloride with *p*-xylylenediamine.

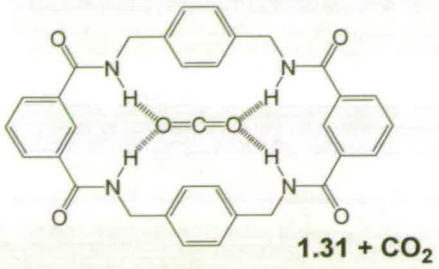
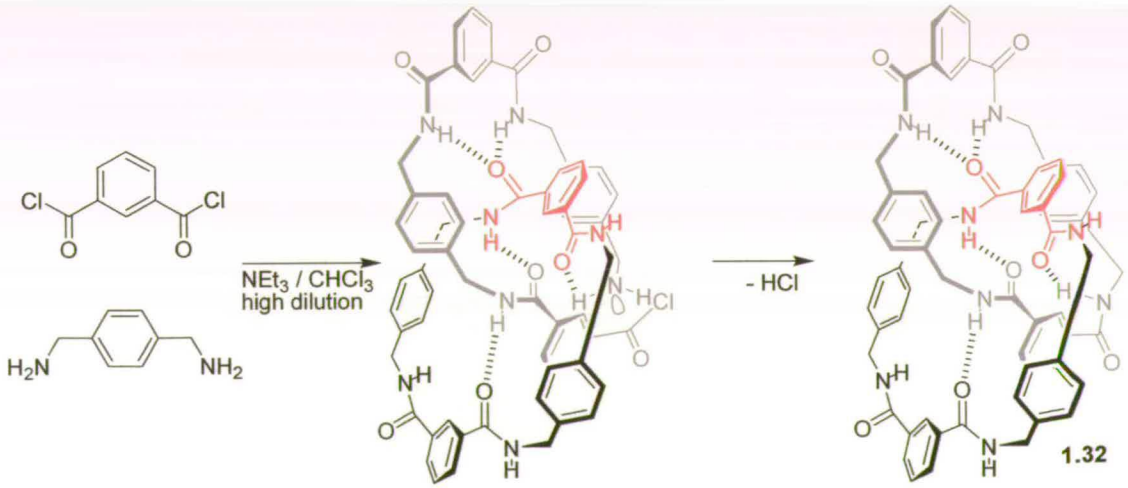


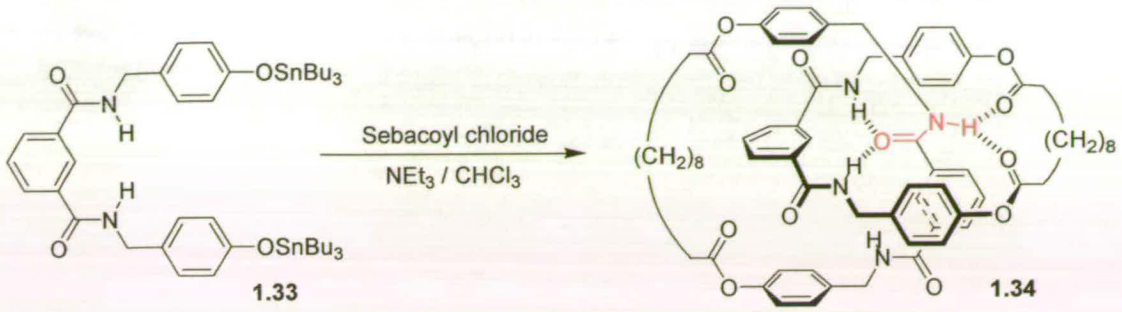
Figure 1. 6 Leigh's Receptor for Carbon Dioxide

No macrocycle **1.31** could be isolated, intractable from a mixture of higher cyclic oligomers and polymers precipitated out of solution. Indeed, [2]catenane **1.32** was the only product left in solution. The reason for its solubility, over the other reaction products, is that the [2]catenane has satisfied its internal hydrogen bonding requirements intramolecularly (scheme 1.8). The other products have no such facility available, and therefore must aggregate to hydrogen bond intermolecularly. The synthesis proved tolerant to a variety of different acid chlorides and diamines to produce a range of hydrogen bond-assembled [2]catenanes.[34]



Scheme 1. 8 [2]Catenane Formation by an Eight Molecule Condensation

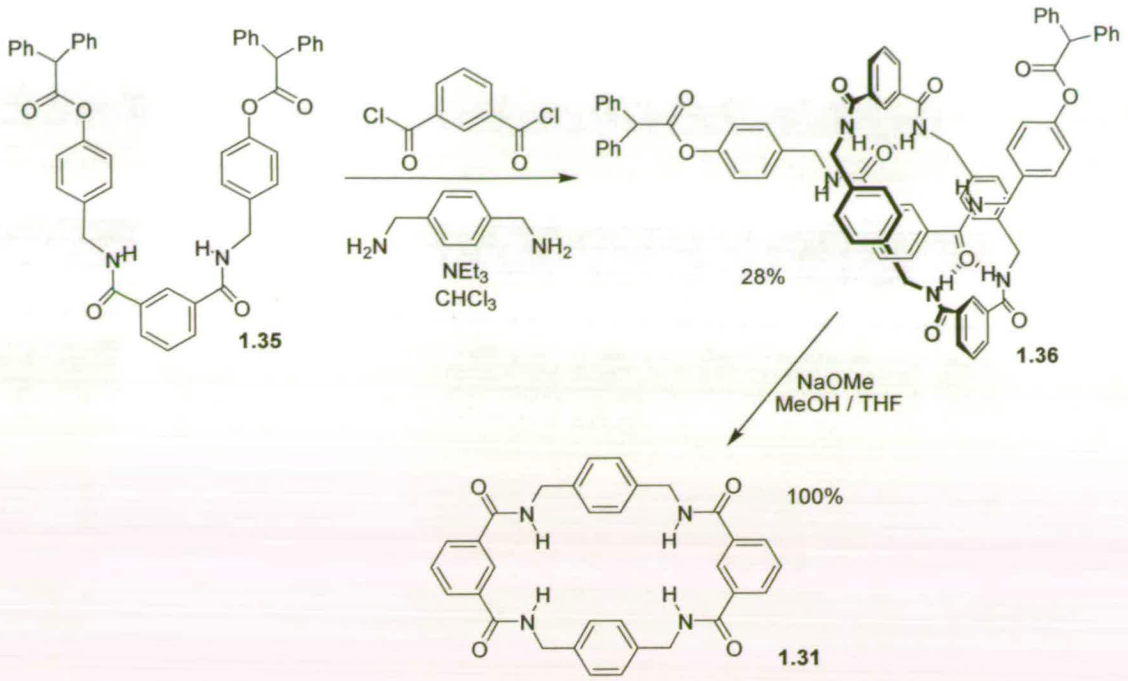
Subsequent studies into the requirements for catenane formation revealed only one isophthalamide unit in each macrocycle was necessary. Reaction of precursor **1.33** with sebacoyl dichloride and triethylamine in chloroform at high dilution resulted in the formation of a mixed benzylic amide/ester catenane **1.34** in 18% yield. This amphiphilic [2]catenane exhibited solvent dependent translational isomerism.[35]



1.33 **1.34**

Scheme 1. 9 Synthesis of an Amphiphilic [2]Catenane

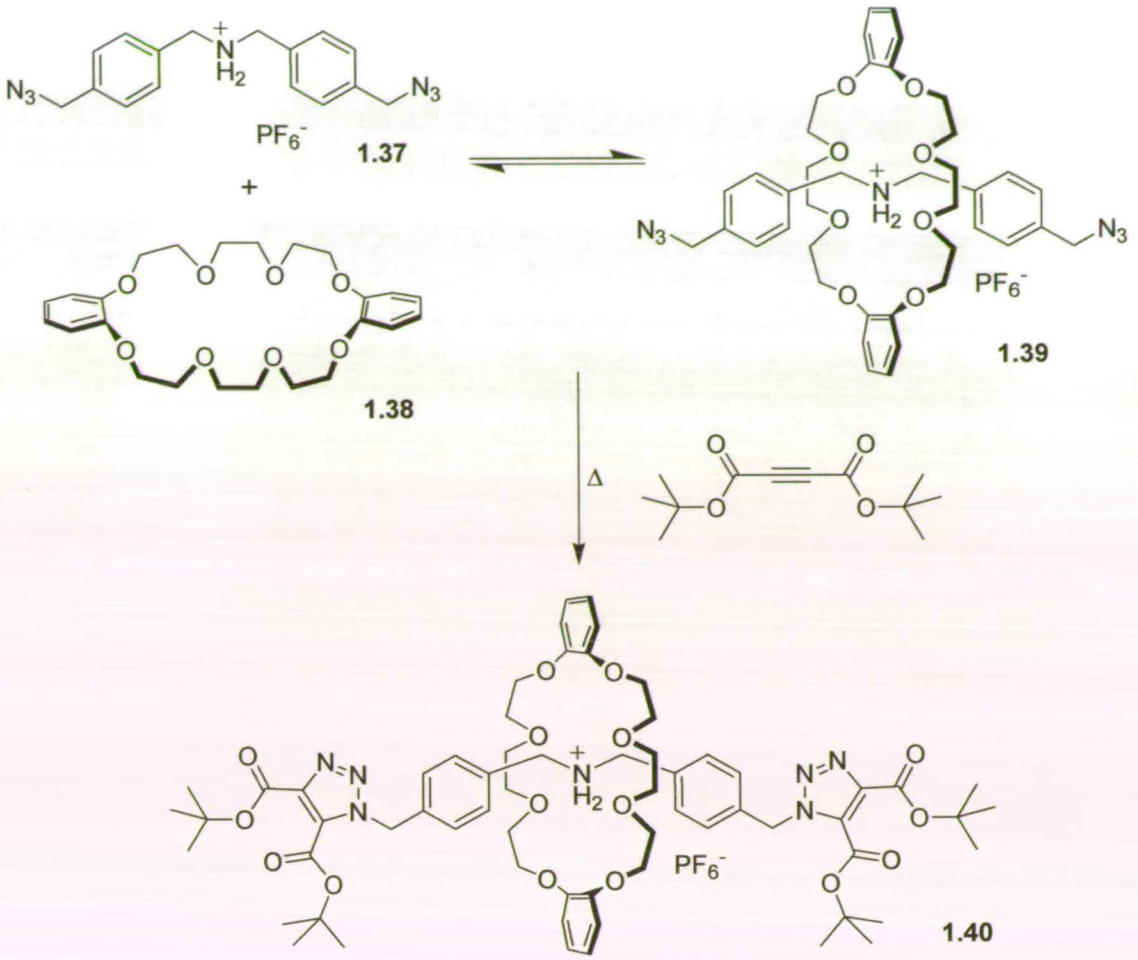
After having failed to recover any of the desired receptor **1.31** by the [2+2] condensation, Leigh *et al.* adopted a different strategy and synthesised it by means of a rotaxane intermediate, which could be isolated and purified (scheme 1.10).[36] A stoppered thread **1.35**, designed to mimic the catenane template, was subjected to the same conditions used to form the [2]catenane.[33] The [2]rotaxane intermediate **1.36** was synthesised in 28% yield along with the [2]catenane. Removal of the stopper groups by saponification caused the macrocyclic receptor **1.31** to precipitate out of solution, and it was isolated pure by filtration.



Scheme 1. 10 Synthesis of Receptor **1.31** by means of a [2]Rotaxane Intermediate

Leigh developed a wide variety of templates to probe the structural requirements and tolerances of benzylic amide [2]rotaxane formation.[37] These included synthetic peptide rotaxanes,[38] and the remarkably efficient fumaramide template,[39] which gives almost quantitative yield of rotaxane.

Stoddart has used crown ethers and dialkylammonium salts to form rotaxanes, templated by hydrogen bonding.[40] Using crown ethers with 24 ring atoms or more, it was possible to form pseudo-rotaxane complexes,[41] which could be capped to form rotaxanes (scheme 1.11). The first example[22] used dibenzo-24-crown-8 **1.38** in methylene chloride in the presence of dialkylammonium salt **1.37** to form the complex **1.39**. Addition of excess di-*tert*-butyl acetylenedicarboxylate and refluxing for several days gave the [2]rotaxane **1.40** in 31% yield.



Scheme 1. 11 Crown Ethers Binding of Secondary Ammonium Salts Followed by Covalent Modification to form [2]Rotaxanes[22]

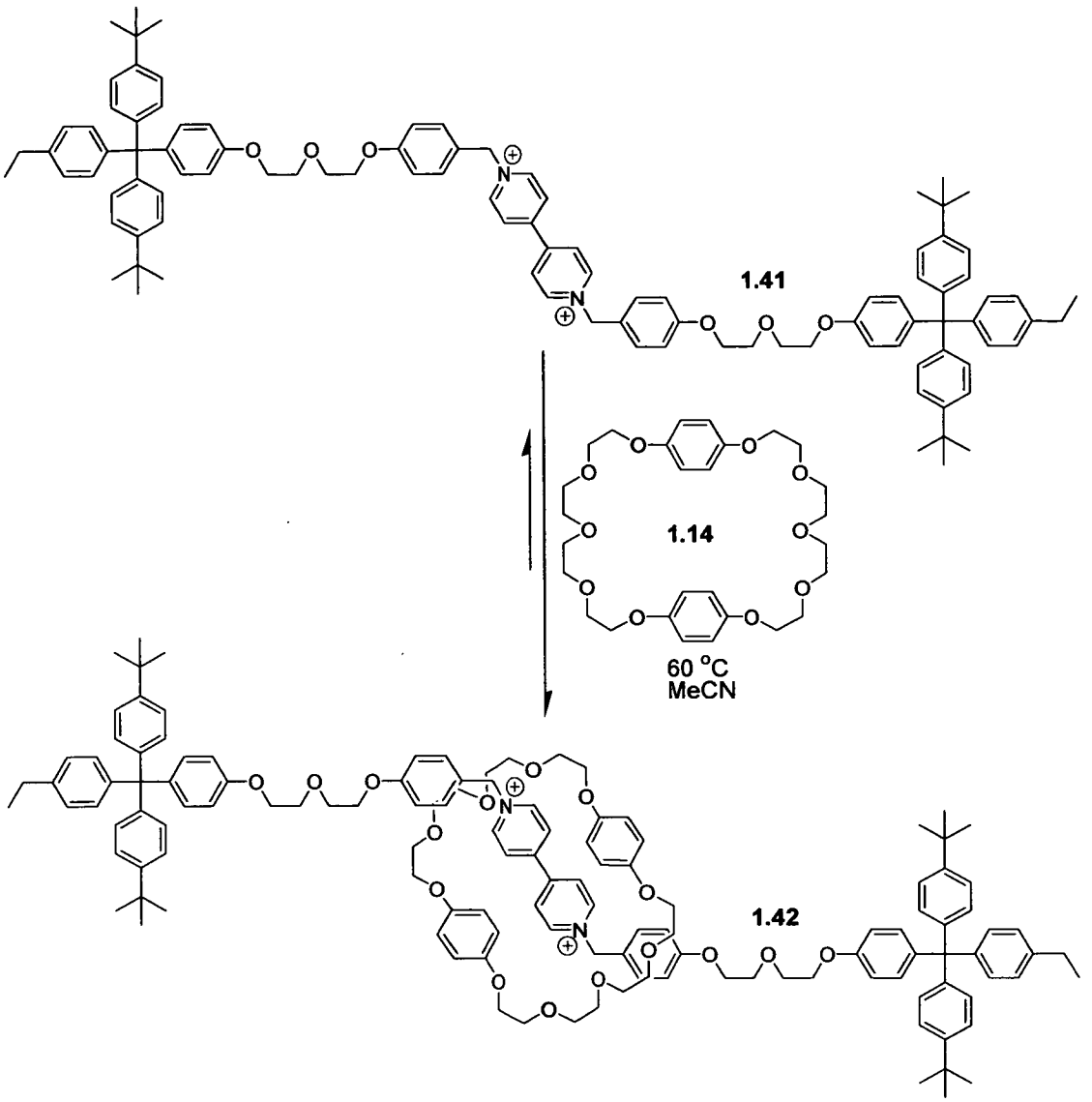
1.5 Synthesis of Interlocked Architectures under Thermodynamic Control

Self-assembly processes that occur in nature work under thermodynamic control; they are reversible processes. This allows for 'error checking' whereby incorrectly assembled structures can be disassembled then reassembled to give the most energetically stable, correct product. Most of the syntheses of interlocked architectures discussed so far have ultimately been done under kinetic control. During the synthesis of catenanes, and rotaxanes by the threading and clipping

methodologies, an equilibrium is set up between the free and complexed species. The complex (interlocked precursor) is the lower energy species, but because the final reaction (clipping or capping) is an irreversible, kinetically controlled reaction, both complexed and uncomplexed precursors are targeted indiscriminately, giving the system no chance to re-equilibrate. Thermodynamic control over this final reaction would allow the reverse reaction to occur, allowing the system to re-equilibrate and allowing the most thermodynamically stable product to form in greatest yield. Therefore the synthesis of interlocked architectures under thermodynamic control is desirable, as it would allow the 'correcting of mistakes' during synthesis.

1.5.1 Slippage Route to Rotaxanes

The first examples of rotaxane synthesis under thermodynamic control come via the slippage methodology.[20] This strategy relies on the macrocycle being able to squeeze over a judiciously chosen bulky stopper group at elevated temperatures. An equilibrium is established between the threaded and free species in which the non-covalent interactions stabilise the complex. On lowering the temperature, the interlocked components no longer have sufficient energy to separate. Stoddart first utilised this methodology successfully (scheme 1.12).[42] Heating the stoppered thread **1.41** in the presence of bis-parphenylene-34-crown-10 **1.14** at 60°C in acetonitrile gave the [2]rotaxane **1.42** in 52% yield. On using ten equivalents of macrocycle **1.14** the yield could be increased to 82%.[20]

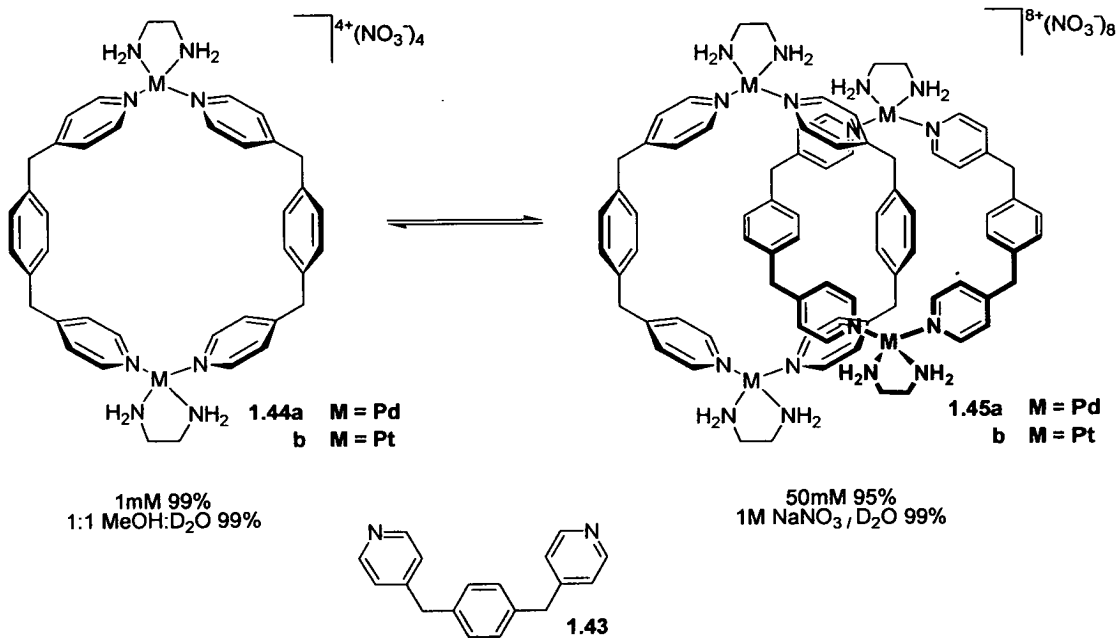


Scheme 1. 12 [2]Rotaxane synthesis by the Slippage Route

Although this synthesis represents a remarkable achievement, in that no chemical reaction takes place during the synthesis, there is an inherent problem with the slippage route to rotaxanes. At the elevated temperatures required for synthesis, the binding energy is lessened, and the complex is no longer as strongly favoured in the equilibrium, therefore lower yields of interlocked products are observed.

1.5.2 Control through the use of Reversible Bond Formation

A more viable approach to thermodynamic control lies in the use of reversible bond-forming reactions to form the interlocked architectures. Coordination chemists utilise the reversible nature of ligand coordination by certain metal centres. In a celebrated example,[43] Fujita designed a dynamic system in which ligands assemble to form macrocycle or [2]catenane, and can equilibrate between the two forms (scheme 1.13).



Scheme 1. 13 Fujita's 'Molecular Lock':[43,44] Catenane Synthesis under Thermodynamic Control

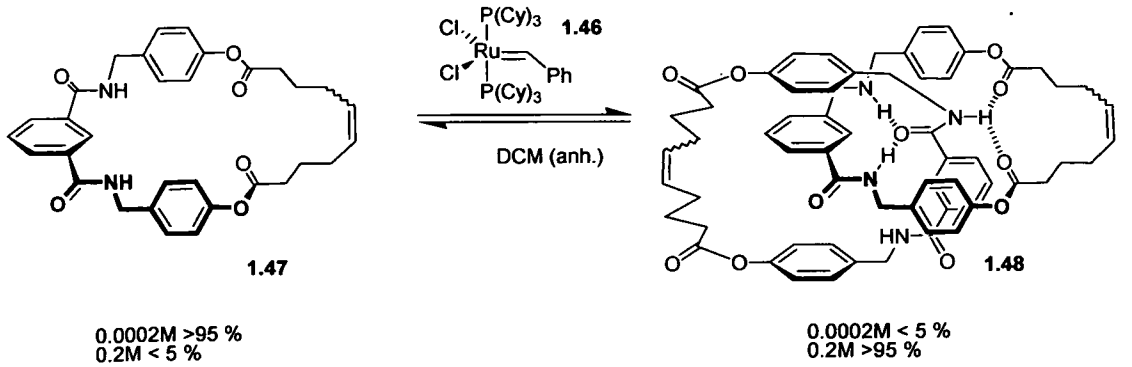
A mixture of $Pd(en)(NO_3)_2$ and pyridine ligand **1.43** in solution resulted in formation of macrocycle **1.44a** and [2]catenane **1.45a**.[43] As the coordinate bonds are kinetically labile, ligand exchange is facile and an equilibrium between the [2]catenane and free macrocycle is established. Subsequent altering of the conditions changes the position of the equilibrium. In one molar aqueous sodium nitrate, the hydrophobic ligands want to shield themselves from the polar environment, and interlocking is favoured, giving 99% catenane **1.45a**. In a methanol and water mix, the pyridine ligands associate with the solvent to give macrocycle **1.44a**. Altering the concentration also affects the distribution of products. At 1mM, macrocycle **1.44a** is almost exclusively observed, whereas at 50mM the equilibrium lies in favour of the catenane **1.45a**. It

was also possible to obtain a kinetically stable product, if the less labile platinum metal was used.[44] In these systems, heat was required to establish the equilibrium. Macrocycle **1.44b** heated in highly polar medium, resulted in the formation of the interlocked catenane **1.45b**, which upon cooling proved to be kinetically stable. Fujita described this system as a 'molecular lock'.

The application of thermodynamic control has been extended to organic systems. The breaking of covalent bonds in a reversible reaction is a much slower process than the breaking of non-covalent bonds, because of the inherent difference in strength between each bond. Reactions of this type often require a catalyst to increase the rate of bond-making / bond-breaking processes, and the interlocked products can often be trapped by removal of the catalyst to form a kinetically stable product.

Sauvage first identified the potential of applying this to the synthesis of interlocked architectures. Sauvage used olefin metathesis to form catenanes in high yield.[12] In his systems, the metal template irreversibly binds the two ligands and preorganises them for interlocking. The application of metathesis simply ensured that the subsequent macrocyclisations occurred with the desired selectivity in good yield (see scheme 1.3).

Sanders[45] attempted to use the metathesis reaction to introduce true thermodynamic control into his systems, but suffered from poor yields as a result of the slow reaction kinetics. Leigh actually achieved this goal with organic ring systems using hydrogen bond-mediated assembly to reversibly form catenanes in greater than 95% yield (scheme 1.14). [46]



Scheme 1. 14 Leigh's 'Magic Rings': Catenane Synthesis under Thermodynamic Control

When the macrocycle **1.47** is exposed to Grubbs' catalyst **1.46**, it is reversibly ring-opened. The linear species is then able to thread through another macrocycle, and subsequent ring-closure gives the [2]catenane **1.48**. This ring-opening / ring-closing process continues until equilibrium is established. Again, changing the concentration can alter the equilibrium. At high concentration (0.2M), 95% catenane **1.48** is formed, and at low concentration (0.0002M) catenane **1.48** can be converted to the macrocycle **1.47** in 95% yield. It is also possible to 'switch off' catenane formation by masking the recognition features of the molecules. Trifluoroacetylation of the amide groups within the catenane **1.48**, followed by metathesis at high concentration and then deprotection results in just macrocycle **1.47** formation. This high yield system incorporates reversibility, allowing equilibrium of the components to be established, and switchable recognition, by 'disabling' the hydrogen bonding motif.

These examples highlight the advantages of applying thermodynamic control[47] to the synthesis of interlocked architectures. The ability to self-assemble and isolate the most energetically favourable products is a great step forward in the synthesis of useful quantities of these interlocked species. Much interest is being shown in this area, or 'dynamic covalent chemistry' as it is has been referred to in the literature.[48]

1.6 Properties of Interlocked Architectures

Although the synthesis of interlocked architectures has proved a suitable challenge for chemists, utilising non-covalent interactions and more recently thermodynamic control, the synthesis alone is not enough to sustain interest in these species. Much effort is being applied to the application of such molecules. Their interlocked nature means they have properties that rigid, fully covalent structures do not, and research is being directed towards creating functional molecules.

1.6.1 Molecular Machines

> *What would be the utility of such machines? Who knows? I cannot see exactly what would happen, but I can hardly doubt that when we have some control of the arrangement of things on a molecular scale we will get an enormously greater range of possible properties that substances can have, and of the different things we can do.*
>
> Richard P Feynman (1959)[49]

This famous, and insightful quote was seen by many as a challenge to utilise the power and properties of molecules to create artificial machines. The advances made in supramolecular chemistry have provided new tools with which to explore these possibilities. Since the elucidation of structures and mechanism of some key biological devices, for example the unidirectional rotary motor of ATP synthase,[50] much interest has been stimulated in developing artificial molecular machines,[51] and with the realisation that the top-down approach to miniaturisation is reaching its limit, confidence is growing that a bottom-up (chemical) approach can one one-day replace it.

It would be impossible to review all the recent advances made in this field. The reader is encouraged to refer to the many excellent reviews that have been published on this subject for more detailed information.[51] Instead, a few examples will be provided to highlight the origins and the potential of interlocked architectures as molecular machines.

Rotaxanes and catenanes have the unique features compared with rigid, covalent structures, and indeed with their unlinked, individual components, in that the two (or more) interlocked components can move independently of one another without separation (translational isomerism).[52] For example, the macrocycles of a [2]catenane may be free to rotate with respect to one another, and a macrocycle in a [2]rotaxane may rotate and translate along the thread. Such large amplitude intramolecular motions appear well suited to the development of molecular machinery.

In the metal templated [2]catenate **1.10** of Sauvage, it was found that the two ring components were locked in position by the metal (see scheme 1.3).[53] In the catenand **1.11**, obtained by demetallation of **1.10**, the macrocycles, no longer held in position, were observed to rotate about one another ('pirouetting').[54] Since the metal can also be reintroduced, this represents one of the first examples of a molecular switch: where an internal process can be regulated by application of an external stimulus.

Another early example of a molecular machine was the molecular shuttle, in which a macrocycle shuttles between two identical stations in a [2]rotaxane. Stoddart created the first molecular shuttle using π - π stacking interactions,[55] but Leigh developed a shuttle using hydrogen bonds which better displays the versatility of such a system, due to its ability to be tuned on altering the conditions (figure 1.7).[56]

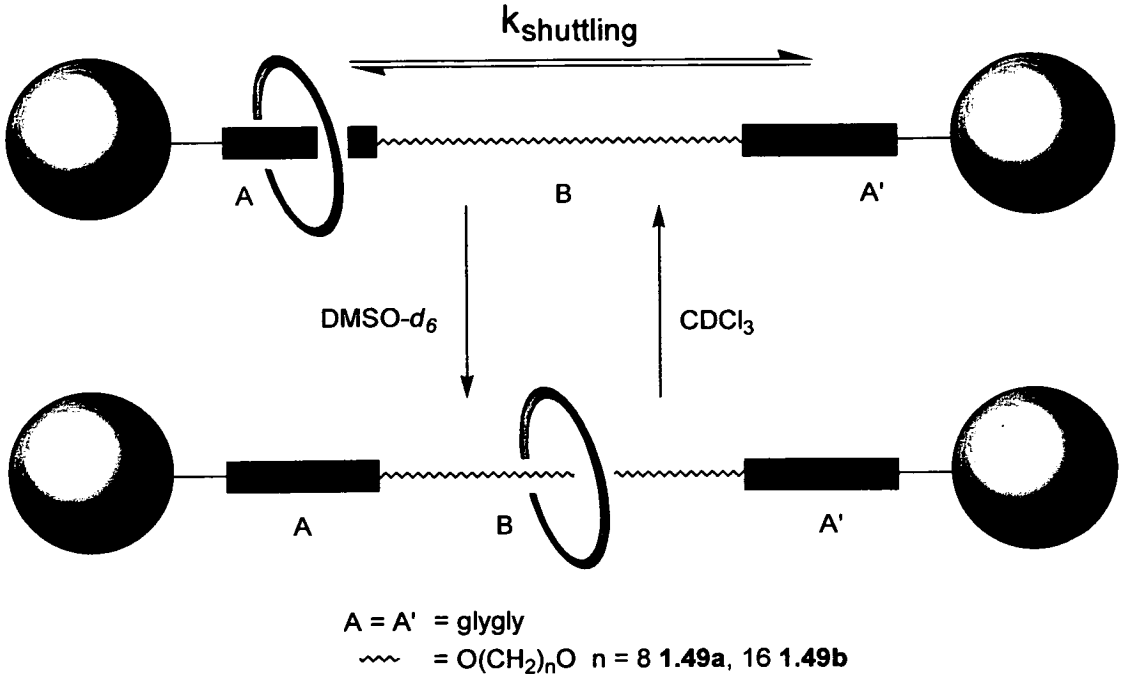
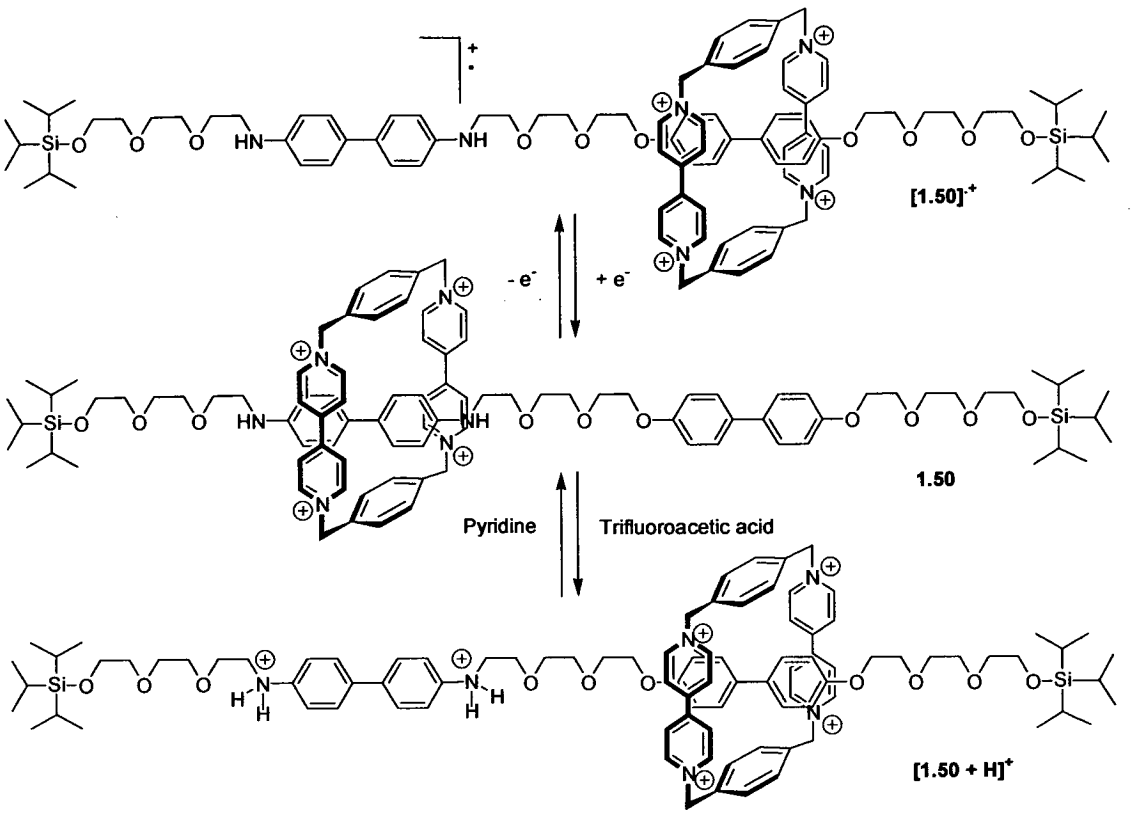


Figure 1. 7 Cartoon Representation of Leigh's Molecular Shuttle

Several two-station [2]rotaxanes **1.49a,b** comprised of a thread with two identical glycylglycine stations separated by an alkyl chain, and one tetrabenzylicamide macrocycle were studied. The two stations are degenerate, and therefore in non-polar solvents, the macrocycle shuttles between the two stations, spending roughly half of its time on each one. The rate of shuttling depends on the distance between the two stations, with the macrocycle shuttling more rapidly by an order of magnitude over the short alkyl chain in rotaxane **1.49a** than the longer one in **1.49b**. Lowering the temperature also slowed the rate of shuttling, whereas the introduction of methanol, which disrupts the strength of the hydrogen bonding at each station, increased the speed of shuttling. In strongly polar solvents, the shuttling process was 'switched-off', with the macrocycle spending the majority of its time on the alkyl chain.

In synthesising an unsymmetrical two-station rotaxane, Stoddart was the first to show that it is possible to influence the preferred position of the macrocycle by altering the strength of each station's interaction with macrocycle (scheme 1.15).[57]



Scheme 1. 15 An electrochemically and chemically addressable rotaxane

In the [2]rotaxane **1.50**, the macrocycle spends the majority of its time on the benzidine station due to its better π-donor ability relative to the bisphenol ether. Protonation **[150 + H]**$^{+}$ (chemical stimulus) or oxidation **[150]**$^{\cdot+}$ (electrochemical stimulus) generates positive charge on the benzidine station, and the electrostatic repulsion causes the macrocycle to sit preferentially over the bisphenol ether station. The reverse operation (deprotonation or reduction) can be applied to the system to restore the initial state.

Since the synthesis of these interlocked molecules, many more recent and sophisticated examples have appeared in the literature[51] including addressable [2]catenanes,[58] molecular muscles,[59] and a light-powered molecular piston.[60]

1.6.2 Applications in Materials Science

Interlocked architectures have resulted in some surprising changes in physical properties of molecules. Encapsulation, for example, has already been shown to provide a safe environment for unstable or very reactive molecules.[61] Several groups have observed changes in the properties of small molecules on forming their interlocked counterparts. Anderson has shown that encapsulation of 'molecular wires' within the cavity of cyclodextrins ('sheathed molecular wires') in a [3]rotaxane has increased the stability of polyethynes.[25] The same shielding from the environment effect has been observed with dyes also.[62] Sauvage has observed that his [2]catenanes form unusually stable complexes with low oxidation state transition metals.[53] Leigh has also increased the solubility of a tetraamide macrocycle 10^6 fold in chloroform by the inclusion of a thread in rotaxane formation.[36]

These changes in physical properties of interlocked molecules over their uninterlocked counterparts have attracted the interest of chemists who wish to exploit these properties in macromolecules.[63] The incorporation of rotaxanes and catenanes into the covalent polymer structure would allow the investigation of any new properties resulting from mechanical and non-covalent bonds within the structure.

There are several different architectures available from the synthesis of interlocked polymeric structures. These include main-chain, and side-chain polyrotaxanes (figure 1.8) and polycatenanes (figure 1.9).

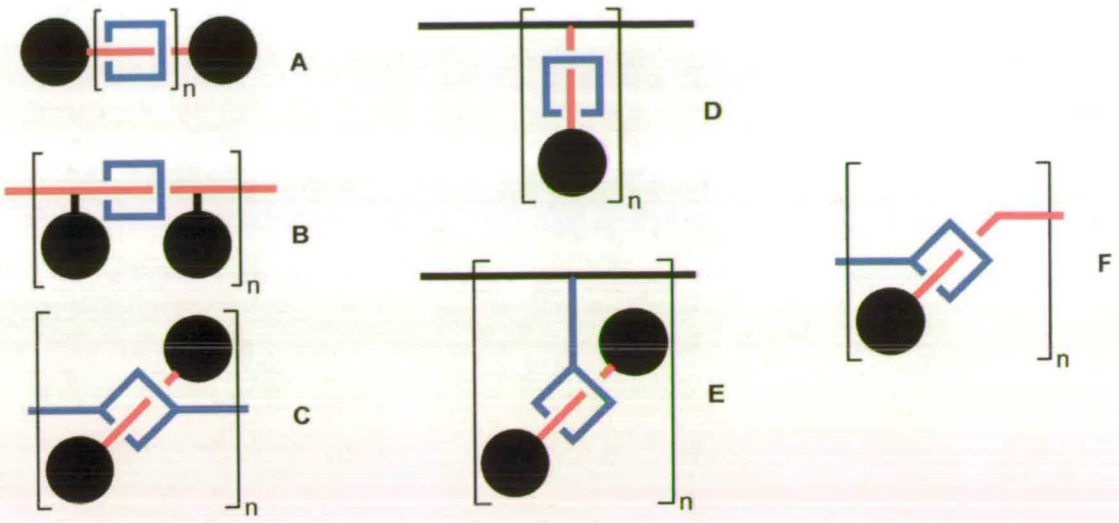


Figure 1. 8 Examples of Main-Chain (**A**,**B**,**C**), Side-Chain (**D**,**E**) and Daisy-Chain (**F**) Polyrotaxanes

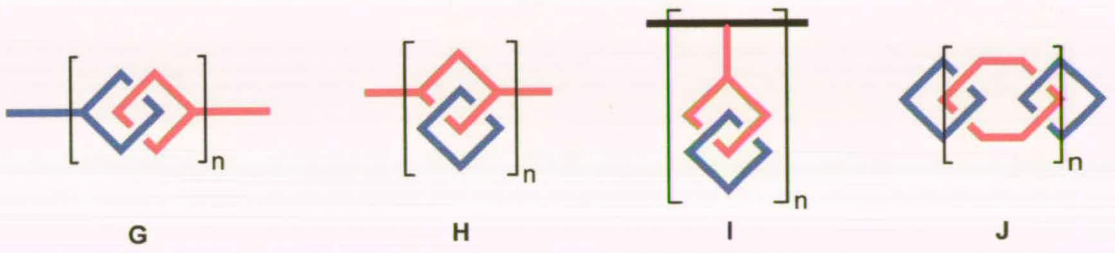


Figure 1. 9 Examples of Main-Chain (**G**,**H**) and Side-Chain (**I**) Poly[2]Catenanes and Polycatenanes (**J**)

Main-chain polyrotaxanes (**A, B, C**) and polycatenanes (**G**, **H**, **J**) have interlocked components incorporated into the main polymer backbone. Side-chain polyrotaxanes and polycatenanes (**D**, **E**, **I**) have the interlocked components pendant to the main polymer backbone. Daisy-chain polyrotaxanes (**F**), poly[2]catenanes (**G**) and polycatenanes (**J**) are polymers which incorporate mechanical bonds into the main polymer backbone. Whereas poly[2]catenanes (*e.g.* **G**) have catenane units linked by linear chains, polycatenanes (**J**) are polymers extended solely by means of mechanical bonds.

Many poly[2]catenanes have been synthesised to date using hydrogen bonds,[64] metal templating[65] and aromatic interactions,[66] but polycatenanes still represent an intriguing challenge and have yet to be synthesised. Polyrotaxanes and

pseudopolyrotaxanes (their unstoppered counterparts) have been synthesised using cyclodextrins,[67] crown ethers,[68-70] and cyclophanes.[71] Pseudopolyrotaxanes exhibit remarkable stability[69,70,72] with respect to their interlocked components compared to pseudorotaxanes. Pseudorotaxanes dissociate readily in solution under equilibrium conditions, whereas random coiling of the polymeric backbone, and the fact that many macrocycles are threaded over a single end-group means dethreading is a much more difficult process in pseudopolyrotaxanes.

The inclusion of mechanical links and/or non-covalent bonds in interlocked macromolecules has resulted in some remarkable changes in their physical properties over conventional polymers.

Interlocking polymers with macrocycles can change the solubilities compared to the individual components. Harada has synthesised pseudopolyrotaxanes by threading α-cyclodextrins over poly(ethylene glycol) chains.[73] Both components individually are water soluble, yet the pseudopolyrotaxanes are not. The opposite behaviour has been observed for a pseudopolyrotaxane of poly(acrylonitrile) with crown ether macrocycles synthesised by Gibson.[68] The interlocked macromolecule is soluble in methanol, whereas the parent molecule is insoluble.

Other phenomena have been observed. Aggregation[74,75] to form gels and micelles after threading of crown ethers has been noted. Glass transition temperatures can be significantly changed.[75,76] Melting points of polymers are also affected by interlocking. In pseudopolyrotaxanes where macrocycles have freedom of movement along the polymer backbone, aggregation, nucleation and crystallisation have all been observed,[75] and two distinct melting points, both slightly lower than those of the separate components, can often be observed. Hydrodynamic volumes also increase compared to the separate components, and therefore the intrinsic viscosities.[77] This has been used as a technique to monitor the threading process.[78] Threaded macrocycles can also inhibit entanglement of polymers backbones in melts of polyesters.[70] As a result, melt viscosities are much lower for these polyrotaxanes, which will improve their processabilities.

As well as simply observing changes in physical properties, some detailed structural investigations have been conducted. The detailed structures of some interlocked macromolecules have been studied by a variety of techniques, including NMR,[73,79,80] X-ray crystallography[81] and scanning tunnelling microscopy.[82] They have revealed some interesting structural features of certain polyrotaxanes.[83]

Harada has formed polyrotaxanes from poly(ethylene oxides) and α-cyclodextrin.[73,80] Using ^{1}H NMR, it was found that these polyrotaxanes or 'molecular necklaces' have a 2:1 stoichiometric composition that is usually independent of the molecular weight of polymer used. As two ethylene oxide units fit within the cavity of α-cyclodextrin, this suggests the α-cyclodextrin rings within the polyrotaxane are packed tightly next to one another, utilising intercomponent hydrogen bonds to stabilise such close packing. X-ray studies suggest that the cyclodextrin molecules arrange along a common symmetry axis, and scanning tunnelling microscope visualisation[82] has shown cyclodextrin-based polyrotaxanes to appear as rod-like structures with length equal to that of the stretched polymer and width equal to that of the macrocycle. It was found that on polyrotaxane formation, the observed rod-like conformations were spontaneously formed from the random coils of polymer chains in solution (figure 1.10).[84]

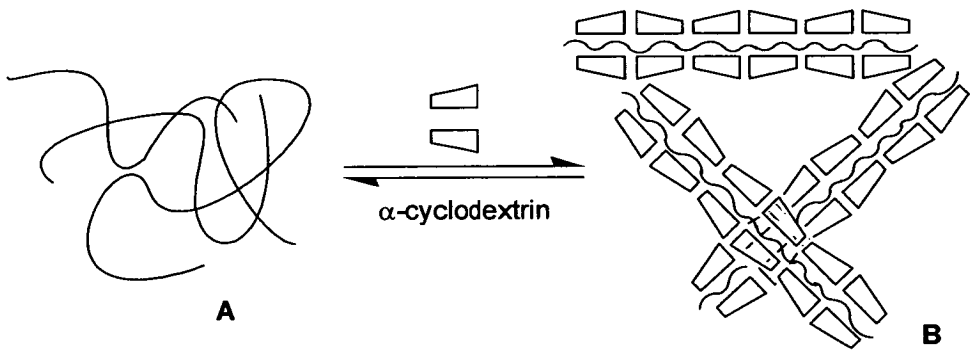
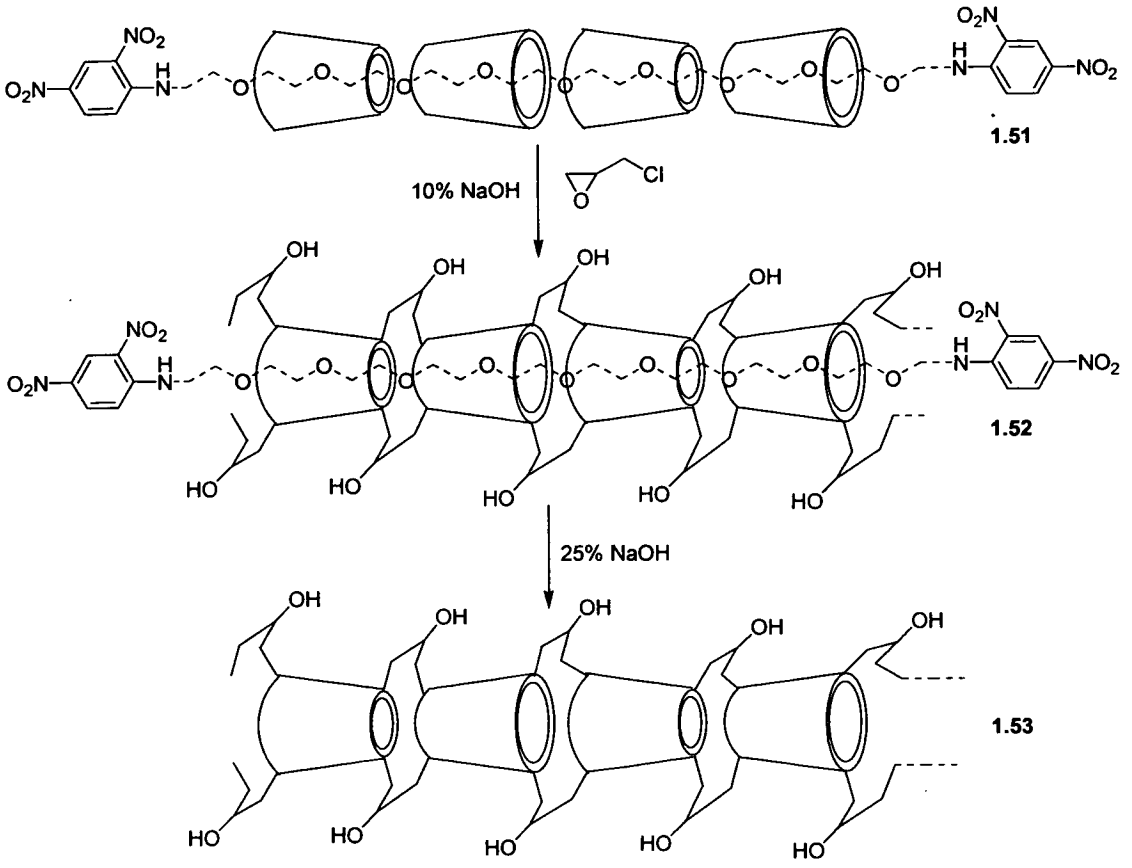


Figure 1. 10 Random Coils (**A**) to Rod-Like Structures (**B**) on (Pseudo)Polyrotaxane Formation with α-Cyclodextrin

Harada demonstrated and utilised this tight packing of cyclodextrins in polyrotaxanes in the synthesis of a 'molecular tube'.[85] The polyrotaxane acts as an intermediate in

the tube synthesis, as the cyclodextrin units are preorganised on the polymer chain for covalent linking to form a tubular polymer. (scheme 1.16).



Scheme 1. 16 Synthesis of Molecular Tubes using a Polymer as a Template

A polyrotaxane **1.51** consisting of poly(ethylene glycol) and α-cyclodextrins was formed. Analysis showed that the α-cyclodextrins were very closely packed together. On dissolving in 10% sodium hydroxide solution with epichlorohydrin, the α-cyclodextrins were cross-linked. On heating with 25% sodium hydroxide solution, the bulky stopper groups were cleaved and the cross-linked molecular tube was be separated from the poly(ethylene glycol) by chromatography. The molecular tube was estimated to have a molecular weight of 17000 and was isolated in 92% yield.

Attempts to synthesise a molecular tube from α-cyclodextrins in solution only gave randomly crosslinked α-cyclodextrins with no order or central cavity. The polymer

backbone was used to preorganise the α-cyclodextrins to facilitate the formation of the molecular tube.

The synthesis of interlocked macromolecules is still in the early stages of development. The properties of these novel polymers are still being investigated, as are new methods of synthesising them. These preliminary studies have revealed the difference in physical properties between these new macromolecules and conventional polymers. Further study and research will no doubt yield new macromolecules with remarkable properties, and functional uses.

1.7 Conclusions and Outlook

The study of interlocked architectures has come a long way since their humble origins in the 1960s as chemical curiosities. Our understanding of self-assembly and the use of templates has developed since the initial use of non-covalent interactions in templating interlocked molecules nearly twenty years ago. Now such molecules can be synthesised with relative ease.

New and more complicated designs have been encouraged with our ability to perform detailed studies on such molecules with the advent of powerful techniques, such as NMR and probe microscopy. The creation of functional molecules is now a distinct possibility.

Besides finding applications for new interlocked molecules, they still represent an opportunity for us to study more common structures and improve our understanding of non-covalent interactions. Much attention is focussed on their potential as molecular machines, but there is still a place for the investigation of their inherent properties, in order to improve our understanding of how such architectures behave. It is very easy to compare, for example, a molecular shuttle with its macroscopic analogue, but understanding intercomponent movement and interaction on the

molecular level will further increase our knowledge of such systems, aid in the development of functional molecules, and is an attractive research goal.

1.8 References

(1) Schill, G. *Catenanes, Rotaxanes, and Knots*; Academic Press: New York, 1971; Frisch, H. L.; Wasserman, E., *J. Am. Chem. Soc.*, **1961**, *83*, 3789-3795.

(2) Wasserman, E., *J. Am. Chem. Soc.*, **1960**, *82*, 4433-4434.

(3) Dietrich-Buchecker, C. O.; Sauvage, J. P.; Kern, J. M., *J. Am. Chem. Soc.*, **1984**, *106*, 3043-3045.

(4) Branden, C.-I.; Tooze, J. *Introduction to Protein Structure*; 2nd ed.; Garland Publishing: New York, London, 1999.

(5) Bisson, A. P.; Carver, F. J.; Hunter, C. A.; Waltho, J. P., *J. Am. Chem. Soc.*, **1994**, *116*, 10292-10293; Bisson, A. P.; Carver, F. J.; Eggleston, D. S.; Haltiwanger, R. C.; Hunter, C. A.; Livingstone, D. L.; McCabe, J. F.; Rotger, C.; Rowan, A. E., *J. Am. Chem. Soc.*, **2000**, *122*, 8856-8868; Hunter, C. A.; Jones, P. S.; Tiger, P. M. N.; Tomas, S., *Chem. Commun.*, **2003**, 1642-1643.

(6) Lehn, J.-M. *Supramolecular Chemistry: Concepts and Perspectives.*; VCH: Weinheim, Germany, 1995.

(7) Walba, D. M., *Tetrahedron*, **1985**, *41*, 3161-3212.

(8) Wasserman, E., *Scientific American*, **1962**, *207*, 94.

(9) Harrison, I. T.; Harrison, S., *J. Am. Chem. Soc.*, **1967**, *89*, 5723-5724.

(10) Schill, G.; Lüttringhaus, A., *Angew. Chem.*, **1964**, *73*, 567-568.

(11) Schill, G.; Lüttringhaus, A., *Angew. Chem., Int. Ed.*, **1964**, *73*, 546.

(12) Mohr, B.; Weck, M.; Sauvage, J.-P.; Grubbs, R. H., *Angew. Chem., Int. Ed.*, **1997**, *36*, 1308-1310.

(13) Wu, C.; Lecavalier, P. R.; Shen, Y. X.; Gibson, H. W., *Chem. Mat.*, **1991**, *3*, 569-572.

(14) Dietrich-Buchecker, C. O.; Sauvage, J. P., *Angew. Chem., Int. Ed.*, **1989**, *28*, 189-192.

(15) Bitsch, F.; Dietrich-Buchecker, C. O.; Khemiss, A. K.; Sauvage, J. P.; Van Dorsselaer, A., *J. Am. Chem. Soc.*, **1991**, *113*, 4023-4025.

(16) Ashton, P. R.; Goodnow, T. T.; Kaifer, A. E.; Reddington, M. V.; Slawin, A. M. Z.; Spencer, N.; Stoddart, J. F.; Vicent, C.; Williams, D. J., *Angew. Chem.*, **1989**, *101*, 1404-1408.

(17) Ashton, P. R. O., B.; Reddington, M.V.; Slawin, A.M.Z.; Stoddart, J. F.; Williams, D. J., *Angew. Chem., Int. Ed.*, **1988**, *27*, 1550-1554.

(18) Anelli, P. L.; Spencer, N.; Stoddart, J. F., *J. Am. Chem. Soc.*, **1991**, *113*, 5131-5133; Ashton, P. R.; Philp, D.; Spencer, N.; Stoddart, J. F., *J. Chem. Soc., Chem. Commun.*, **1992**, 1124-1128.

(19) Ashton, P. R.; Grognuz, M.; Slawin, A. M. Z.; Stoddart, J. F.; Williams, D. J., *Tetrahedron Lett.*, **1991**, *32*, 6235-6238.

(20) Raymo, F. M.; Stoddart, J. F., *Pure Appl. Chem.*, **1997**, *69*, 1987-1997.

(21) Amabilino, D. B.; Ashton, P. R.; Boyd, S. E.; Lee, J. Y.; Menzer, S.; Stoddart, J. F.; Williams, D. J., *Angew. Chem., Int. Ed.*, **1997**, *36*, 2070-2072.

(22) Ashton, P. R.; Glink, P. T.; Stoddart, J. F.; Tasker, P. A.; White, A. J. P.; Williams, D. J., *Chem. Eur. J.*, **1996**, *2*, 729-736.

(23) Amabilino, D. B.; Stoddart, J. F., *Chem. Rev.*, **1995**, *95*, 2725-2829.

(24) Lüttringhaus, A.; Cramer, F.; Prinzbach, H.; Henglein, F. M., *Liebigs Ann. Chem.*, **1958**, *185*, 613.

(25) Anderson, S.; Anderson, H. L., *Angew. Chem., Int. Ed.*, **1996**, *35*, 1956-1958.

(26) Hunter, C. A., *J. Am. Chem. Soc.*, **1992**, *114*, 5303-5311.

(27) Vögtle, F.; Meier, S.; Hoss, R., *Angew. Chem., Int. Ed.*, **1992**, *31*, 1619-1622.

(28) Hunter, C. A., *J. Chem. Soc., Chem. Commun.*, **1991**, 749-751.

(29) Ottens-Hildebrandt, S.; Nieger, M.; Rissanen, K.; Rouvinen, J.; Meier, S.; Harder, G.; Vogtle, F., *J. Chem. Soc., Chem. Commun.*, **1995**, 777-778.

(30) Vögtle, F.; Dünnwald, T.; Schmidt, T., *Acc. Chem. Res.*, **1996**, *29*, 451-460.

(31) Händel, M.; Ottens-Hildebrandt, S.; Schmidt, W.; Vögtle, F., *Synthesis*, **1996**, 353-356; Händel, M.; Meier, S.; Ott, T.; Ottens-Hildebrandt, S.; Schmidt, T.; Vögtle, F., *Liebigs Annalen/Recueil*, **1995**, 739-743; Jäger, R.; Baumann, S.; Fischer, M.; Safarowsky, O.; Nieger, M.; Vögtle, F., *Liebigs Annalen/Recueil*, **1997**, 2269-2273.

(32) Hübner, G. M.; Safarowsky, O.; Seel, C.; Vögtle, F., *J. Org. Chem.*, **1999**, *64*, 7236-7242.

(33) Johnston, A. G.; Leigh, D. A.; Pritchard, R. J.; Deegan, M. D., *Angew. Chem., Int. Ed.*, **1995**, *34*, 1209-1212.

(34) Johnston, A. G.; Leigh, D. A.; Nezhat, L.; Smart, J. P.; Deegan, M. D., *Angew. Chem., Int. Ed.*, **1995**, *34*, 1212-1216.

(35) Leigh, D. A.; Moody, K.; Smart, J. P.; Watson, K. J.; Slawin, A. M. Z., *Angew. Chem., Int. Ed.*, **1996**, *35*, 306-310.

(36) Johnston, A. G.; Leigh, D. A.; Murphy, A.; Smart, J. P.; Deegan, M. D., *J. Am. Chem. Soc.*, **1996**, *118*, 10662-10663.

(37) Clegg, W.; Gimenez-Saiz, C.; Leigh, D. A.; Murphy, A.; Slawin, A. M. Z.; Teat, S. J., *J. Am. Chem. Soc.*, **1999**, *121*, 4124-4129.

(38) Leigh, D. A.; Murphy, A.; Smart, J. P.; Slawin, A. M. Z., *Angew. Chem., Int. Ed.*, **1997**, *36*, 728-732.

(39) Gatti, F. G.; Leigh, D. A.; Nepogodiev, S. A.; Slawin, A. M. Z.; Teat, S. J.; Wong, J. K. Y., *J. Am. Chem. Soc.*, **2001**, *123*, 5983-5989.

(40) Ashton, P. R.; Campbell, P. J.; Chrystal, E. J. T.; Glinke, P. T.; Menzer, S.; Philp, D.; Spencer, N.; Stoddart, J. F.; Tasker, P. A.; Williams, D. J., *Angew. Chem., Int. Ed.*, **1995**, *34*, 1865-1869.

(41) Ashton, P. R.; Chrystal, E. J. T.; Glink, P. T.; Menzer, S.; Schiavo, C.; Spencer, N.; Stoddart, J. F.; Tasker, P. A.; White, A. J. P.; Williams, D. J., *Chem. Eur. J.*, **1996**, *2*, 709-728.

(42) Ashton, P. R.; Belohradsky, M.; Philp, D.; Stoddart, J. F., *J. Chem. Soc., Chem. Commun.*, **1993**, 1269-1274.

(43) Fujita, M.; Ibukuro, F.; Hagihara, H.; Ogura, K., *Nature*, **1994**, *367*, 720-723.

(44) Fujita, M.; Ibukuro, F.; Yamaguchi, K.; Ogura, K., *J. Am. Chem. Soc.*, **1995**, *117*, 4175-4176.

(45) Hamilton, D. G.; Feeder, N.; Teat, S. J.; Sanders, J. K. M., *New J. Chem.*, **1998**, *22*, 1019-1021.

(46) Kidd, T. J.; Leigh, D. A.; Wilson, A. J., *J. Am. Chem. Soc.*, **1999**, *121*, 1599-1600.

(47) Philp, D.; Stoddart, J. F., *Angew. Chem., Int. Ed.*, **1996**, *35*, 1155-1196.

(48) Rowan, S. J.; Cantrill, S. J.; Cousins, G. R.; Sanders, J. K. M.; Stoddart, J. F., *Angew. Chem. Int. Ed.*, **2002**, *41*, 898-952.

(49) Feynman, R. P., *Eng. Sci.,* **1960**, *23*, 22-36; Feynman, R. P., *Saturday Rev.,* **1960**, *43*, 45-47.

(50) Stock, D.; Leslie, A. G. W.; Walker, J. E., *Science,* **1999**, *286*, 1700-1705.

(51) Balzani, V.; Credi, A.; Raymo, F. M.; Stoddart, J. F., *Angew. Chem. Int. Ed.,* **2000**, *39*, 3348-3391.

(52) Ashton, P. R.; Blower, M.; Philp, D.; Spencer, N.; Stoddart, J. F.; Tolley, M. S.; Ballardini, R.; Ciano, M.; Balzani, V.; et al., *New J. Chem.,* **1993**, *17*, 689-695.

(53) Dietrich-Buchecker, C. O.; Sauvage, J. P.; Kern, J.-M., *J. Am. Chem. Soc.,* **1989**, *111*, 7791-7800.

(54) Cesario, M.; Dietrich-Buchecker, C. O.; Guilhem, J.; Pascard, C.; Sauvage, J. P., *J. Chem. Soc., Chem. Commun.,* **1985**, 244-247.

(55) Anelli, P.-L.; Asakawa, M.; Ashton, P. R.; Bissell, R. A.; Clavier, G.; Gorski, R.; Kaifer, A. E.; Langford, S. J.; Mattersteig, G.; Menzer, S.; Philp, D.; Slawin, A. M. Z.; Spencer, N.; Stoddart, J. F.; Tolley, M. S.; Williams, D. J., *Chem. Eur. J.,* **1997**, *3*, 1113-1135.

(56) Lane, A. S.; Leigh, D. A.; Murphy, A., *J. Am. Chem. Soc.,* **1997**, *119*, 11092-11093.

(57) Bissell, R. A.; Cordova, E.; Kaifer, A. E.; Stoddart, J. F., *Nature,* **1994**, *369*, 133-137.

(58) Balzani, V.; Credi, A.; Mattersteig, G.; Matthews, O. A.; Raymo, F. M.; Stoddart, J. F.; Venturi, M.; White, A. J. P.; Williams, D. J., *J. Org. Chem.,* **2000**, *65*, 1924-1936; Asakawa, M.; Ashton, P. R.; Balzani, V.; Credi, A.; Hamers, C.; Mattersteig, G.; Montalti, M.; Shipway, A. N.; Spencer, N.;

Stoddart, J. F.; Tolley, M. S.; Venturi, M.; White, A. J. P.; Williams, D. J., *Angew. Chem. Int. Ed.,* **1998**, *37*, 333-337; Gunter, M. J.; Johnston, M. R., *J. Chem. Soc., Chem. Commun.,* **1994**, 829-830.

(59) Consuelo Jimenez, M.; Dietrich-Buchecker, C. O.; Sauvage, J. P., *Angew. Chem. Int. Ed.,* **2000**, *39*, 3284-3287.

(60) Brouwer, A. M.; Frochot, C.; Gatti, F. G.; Leigh, D. A.; Mottier, L.; Paolucci, F.; Roffia, S.; Wurpel, G. W. H., *Science,* **2001**, *291*, 2105-2106.

(61) Cram, D. J.; Tanner, M. E.; Thomas, R., *Angew. Chem., Int. Ed.,* **1991**, *30*, 1024-1027.

(62) Anderson, S.; Claridge, T. D. W.; Anderson, H. L., *Angew. Chem., Int. Ed.,* **1997**, *36*, 1310-1313.

(63) Amabilino, D. B.; Parsons, I. W.; Stoddart, J. F., *Trends Polym. Sci.,* **1994**, *2*, 146-152.

(64) Geerts, Y.; Muscat, D.; Muellen, K., *Macromol. Chem. Phys.,* **1995**, *196*, 3425-3435; Muscat, D.; Witte, A.; Kohler, W.; Mullen, K.; Geerts, Y., *Macromol. Rapid Commun.,* **1997**, *18*, 233-241; Muscat, D.; Koehler, W.; Raeder, H. J.; Martin, K.; Mullins, S.; Mueller, B.; Muellen, K.; Geerts, Y., *Macromolecules,* **1999**, *32*, 1737-1745.

(65) Shimada, S.; Ishikawa, K.; Tamaoki, N., *Act. Chem. Scand.,* **1998**, *52*, 374-376; Weidmann, J.-L.; Kern, J.-M.; Sauvage, J.-P.; Geerts, Y.; Muscat, D.; Muellen, K., *Chem. Commun.,* **1996**, 1243-1244.

(66) Hamers, C.; Raymo, F. M.; Stoddart, J. F., *Eur. J. Org. Chem.,* **1998**, 2109-2117; Menzer, S.; White, A. J. P.; Williams, D. J.; Belohradsky, M.; Hamers,

C.; Raymo, F. M.; Shipway, A. N.; Stoddart, J. F., *Macromolecules,* **1998**, *31*, 295-307.

(67) Harada, A., *Acta Polymerica,* **1998**, *49*, 3-17; Weickenmeier, M.; Wenz, G., *Macromol. Rapid Commun.,* **1997**, *18*, 1109-1115; Herrmann, W.; Keller, B.; Wenz, G., *Macromolecules,* **1997**, *30*, 4966-4972.

(68) Gibson, H. W.; Engen, P. T., *New J. Chem.,* **1993**, *17*, 723-727.

(69) Gibson, H. W.; Liu, S.; Lecavalier, P.; Wu, C.; Shen, Y. X., *J. Am. Chem. Soc.,* **1995**, *117*, 852-874.

(70) Gibson, H. W.; Liu, S.; Gong, C.; Ji, Q.; Joseph, E., *Macromolecules,* **1997**, *30*, 3711-3727.

(71) Mason, P. E.; Parsons, I. W.; Tolley, M. S., *Angew. Chem., Int. Ed.,* **1996**, *35*, 2238-2241; Mason, P. E.; Parsons, I. W.; Tolley, M. S., *Polymer,* **1998**, *39*, 3981-3991.

(72) Wu, C.; Bheda, M. C.; Lim, C.; Shen, Y. X.; Sze, J.; Gibson, H. W., *Polym. Commun.,* **1991**, *32*, 204-207; Gong, C.; Gibson, H. W., *Macromolecules,* **1996**, *29*, 7029-7033; Gong, C.; Ji, Q.; Glass, T. E.; Gibson, H. W., *Macromolecules,* **1997**, *30*, 4807-4813; Gong, C.; Gibson, H. W., *Macromolecules,* **1997**, *30*, 8524-8525.

(73) Harada, A.; Li, J.; Kamachi, M., *Macromolecules,* **1993**, *26*, 5698-5703.

(74) Li, J.; Harada, A.; Kamachi, M., *Polym. J.,* **1994**, *26*, 1019-1026.

(75) Shen, Y. X.; Xie, D.; Gibson, H. W., *J. Am. Chem. Soc.,* **1994**, *116*, 537-548.

(76) Born, M.; Ritter, H., *Angew. Chem., Int. Ed.,* **1995**, *34*, 309-311.

(77) Gibson, H. W.; Liu, S.; Shen, Y. X.; Bheda, M.; Lee, S. H.; Wang, F. In *Molecular Engineering for Advanced Materials*; Becher, J., Schaumburg, K., Eds.; Kluwer Academic Publishers: Dordrecht, 1995, pp 41-58.

(78) Wenz, G.; Keller, B., *Angew. Chem., Int. Ed.,* **1992**, *31*, 197-199.

(79) Harada, A.; Kamachi, M., *Macromolecules,* **1990**, *23*, 2821; Harada, A.; Li, J.; Kamachi, M., *Nature,* **1992**, *356*, 325; Harada, A.; Kamachi, M., *J. Chem. Soc., Chem. Commun.,* **1990**, 1322-1323.

(80) Harada, A.; Li, J.; Suzuki, S.; Kamachi, M., *Macromolecules,* **1993**, *26*, 5267-5268.

(81) Harada, A.; Okada, M.; Kamachi, M., *Acta Polymerica,* **1995**, *46*, 453-457; Kamitori, S.; Matsuzaka, O.; Kondo, S.; Muraoka, S.; Okuyama, K.; Noguchi, K.; Okada, M.; Harada, A., *Macromolecules,* **2000**, *33*, 1500-1502; Harada, A.; Okada, M.; Li, J.; Kamachi, M., *Macromolecules,* **1995**, *28*, 8406-8411.

(82) Yoshida, M.; Shimomura, T.; Ito, K.; Hayakawa, R., *Langmuir,* **1999**, *15*, 910.

(83) Panova, I. G.; Topchieva, I. N., *Rus. Chem. Rev.,* **2001**, *70*, 23-44.

(84) Panova, I. G.; Gerasimov, V. I.; Kalashnikov, F. A.; Topchieva, I. N., *Dokl. Chem. Technol., Dokl. Chem.,* **1997**, *355*, 641; Panova, I. G.; Gerasimov, V. I.; Kalashnikov, F. A.; Topchieva, I. N., *Polym. Sci., Ser. B,* **1998**, *40*, 2077.

(85) Harada, A.; Li, J.; Kamachi, M., *Nature,* **1993**, *364*, 516.

Chapter 2

Macrocycle Racing 1: Measuring the Rate of Macrocycle Movement along a Polymer Backbone in [2]-Polyrotaxanes grown by Atom Transfer Radical Polymerisation (ATRP)

Declaration: Dr. Adrian Carmichael, working under Professor David Haddleton at the University of Warwick, conducted all the polymerisation work.

2.1 Introduction

The utilisation of the large amplitude motion of rotaxane components with respect to one another is seen as a possible route to the development of molecular machinery.[1] Despite comparisons to macroscopic devices such as an abacus or a switch where components have defined loci, or on / off positions, controlling the translational motion in rotaxanes is not straightforward. The components of molecular shuttles spend the majority of their time in the most energetically favourable position, but they are not fixed there and are free to move away from the station.

Symmetrical molecular shuttles provide an interesting example of the time-averaged location of components.[2-4] The macrocycle in a two identical-station [2]rotaxane will appear to spend half of its time on each binding site by shuttling between the two degenerate stations. As the chain length increases or as the temperature is reduced, the rate of shuttling will decrease until the symmetry of the station occupancy is destroyed and the macrocycle occupies only one station in the time-period of observation. Therefore, the symmetry of the stations depends on the time-scale of observation. At any particular instant the macrocycle will have an indeterminate, but

definite position somewhere along the linear thread, either on one station, or the other or in-between. Because the measurements are made on many molecules at once, and because the macrocycle spends a relatively long time on the stations, the macrocycle is not observed directly when in the process of shuttling between the stations. Due to this lack of observational evidence, the actual mechanism of macrocyclic motion is somewhat of a mystery.

The mechanism of macrocycle movement,[2] once it has left the station, is probably a result of Brownian motion (or one-dimensional diffusion), a random walk between stations, but it is unknown whether the macrocycle experiences any of the properties associated with macroscopic motion, such as inertia, momentum and friction. For example, a molecular shuttle studied by Leigh displays an unexpected shuttling behaviour (figure 2.1).[3] The rate of shuttling between degenerate stations separated by a short, sulfur-containing alkyl chain was determined by ^{1}H NMR experiments. Derivatisation of the sulphur atom by oxidation with MCPBA to the sulfoxide (0 °C, 1 hr), or the sulfone (25 °C, 6 hr) had no effect on the rate of shuttling, despite the apparent change in size and hydrogen bonding ability of the sulfur group. Only on the introduction of a large, steric barrier by tosyl imination was the shuttling disrupted.

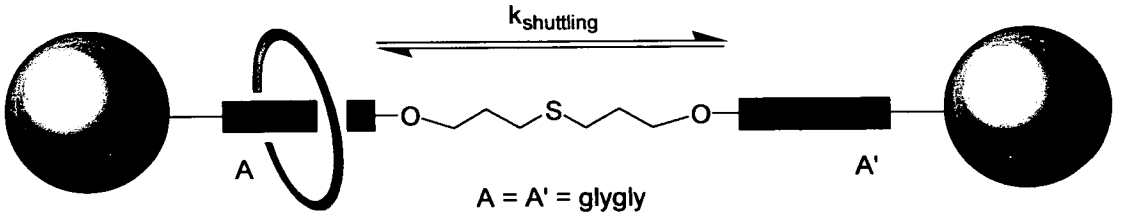


Figure 2. 1 Leigh's molecular shuttle

The study of pseudopolyrotaxanes, formed by threading of macrocycles onto a preformed polymer chain, offers an unprecedented opportunity to study macrocycle movement. The property that makes pseudopolyrotaxanes unique over the analogous pseudorotaxanes is that they incorporate many binding sites, but only have two chain ends over which the macrocycle can thread.

Wenz *et. al.* have used this property of multiple threading over chain ends to study and model the threading of multiple α-cyclodextrins onto a polymer, which incorporates multiple binding sites separated by bulky groups.[5] Using experimental kinetic and thermodynamic data, they quantitatively described the inclusion process using a Monte Carlo simulation. They reasoned that each macrocycle threads at a chain end, then must move away before the next may thread. The macrocycles move between sites via a consecutive hopping process (figure 2.2), where the macrocycles move over energy barriers between binding sites, but have equal probability of moving to an adjacent binding site in either direction along the polymer chain, as long as it is free.

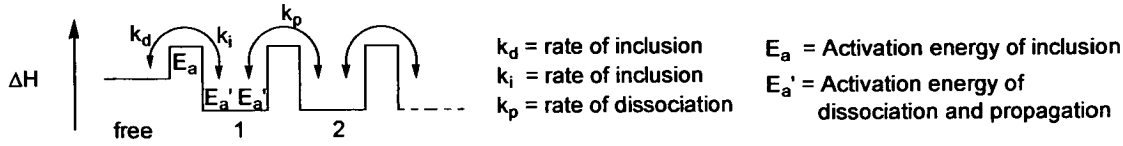


Figure 2. 2 Schematic representation of the energy profile of the inclusion process in pseudopolyrotaxanes

Studies by Gibson and co-workers highlight the problems of studying macrocycle movement in pseudopolyrotaxanes.[6] They observed that macrocycles towards the interior of the polymer chain experience restricted freedom of motion due to collision with other macrocycles. Only macrocycles near the chain ends could exchange with free macrocycles in solution, with macrocycles at the interior being effectively trapped there.

These results suggest that in pseudopolyrotaxane systems, free movement of the macrocycle is restricted by the presence of many other macrocycles, and in general, the overall direction of macrocycle movement is governed by macrocycle-macrocycle interactions.

It would be desirable to study the free motion of a macrocycle along a polymer chain where macrocycle-macrocycle interactions or collisions (*i.e.* one macrocycle blocking the path of another) do not feature (figure 2.3). This could be achieved by

looking at a polymer with a single macrocycle at its interior, or at one stoppered end. These [2]pseudopolyrotaxanes have not been studied due to their difficulty in synthesis and isolation, but in these systems, one could study the free motion of a macrocycle along the polymer backbone, which may provide evidence on whether a macrocycle possesses momentum, carrying it predominantly in one direction, or experiences friction on overcoming steric obstacles.

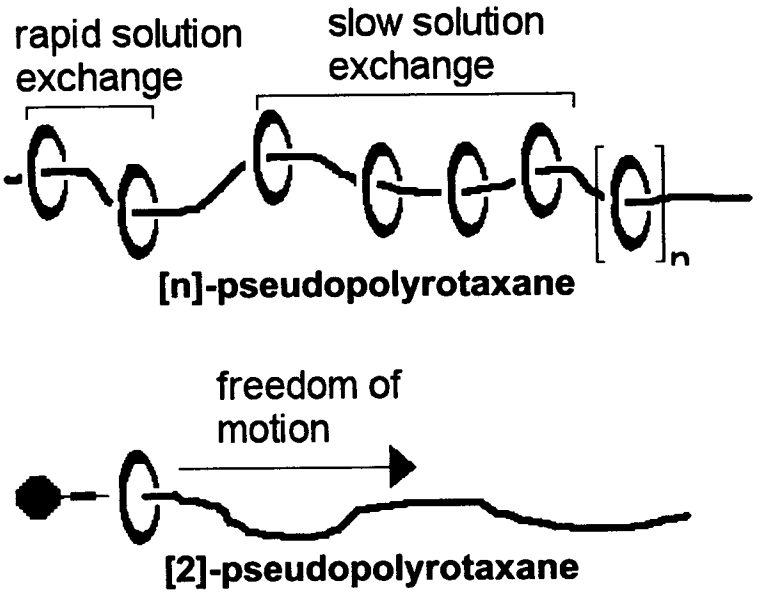


Figure 2. 3 Indicating Restricted Macrocycle Motion in [n]Pseudopolyrotaxanes and Freedom of Motion in [2]Pseudopolyrotaxanes.

One method to synthesise a [2]pseudopolyrotaxane would be to utilise a rotaxane template, or 'mechanically interlocked auxiliary', functionalised with a removable stopper and an atom transfer radical polymerisation (ATRP)[7] initiator (figure 2.4). Once the rotaxane is formed, the polymer is grown using ATRP methodology. The ATRP procedure is an attractive form of polymerisation as it is easy-controlled and produces non-terminated, low polydispersity polymers of predictable size. On cleaving the removable stopper group of the [2]polyrotaxane, the macrocycle is free to move along the polymer backbone. Disrupting the hydrogen bonding interaction at the template, either by using a competing hydrogen-bonding solvent[3,8], such as DMSO, or by switching-off the template[9] (e.g. by cis-trans isomerism of the fumaramide template), would encourage the macrocycle to move along the polymer

backbone until it dethreads from the chain end, at which point the free macrocycle can be detected.

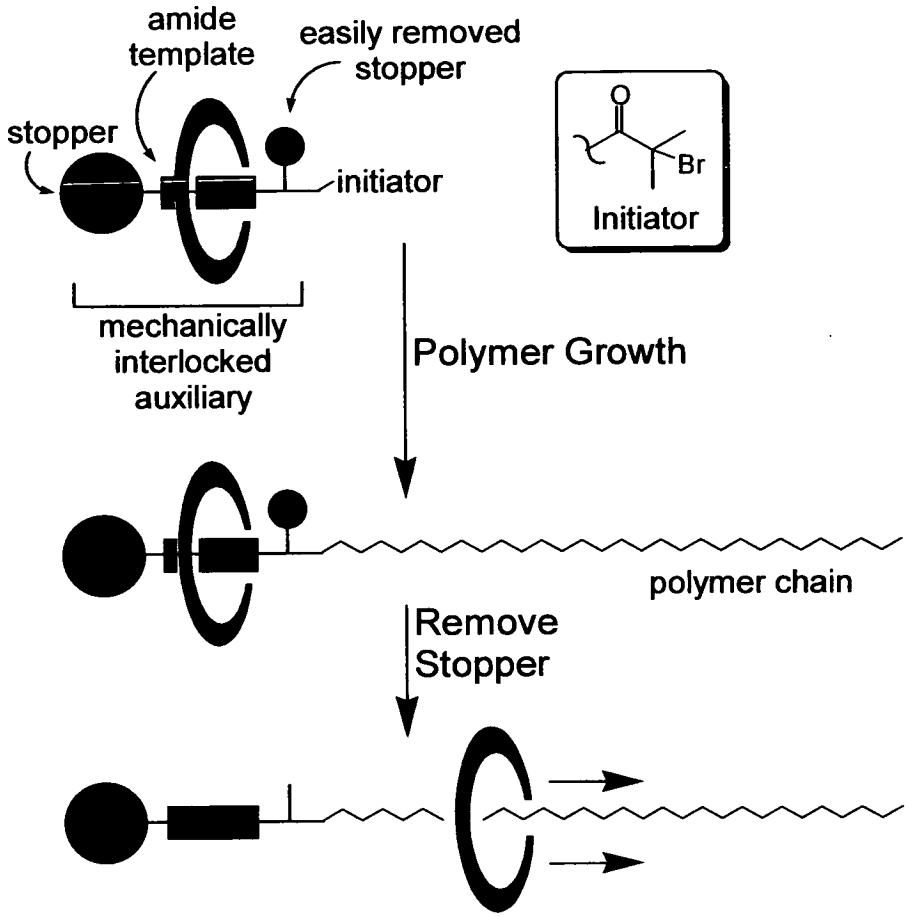


Figure 2. 4 Synthesis of a [2]Polyrotaxane and the Study of Free Macrocycle Movement

By changing the length or composition of the polymer backbone, for example by introducing bulkier groups, the effects on macrocycle motion along the polymer chain can be studied. By comparing the dethreading times and dethreading distribution of a series of different length, and different composition [2]pseudopolyrotaxanes, a model can be constructed to describe the macrocyclic motion over the polymer backbone.

2.2 Results and Discussion

2.2.1 Attempts to synthesise a rotaxane initiator for atom transfer radical polymerisation (ATRP).

Based on the previous work discussed in the introduction, a new thread was designed (figure 2.5).

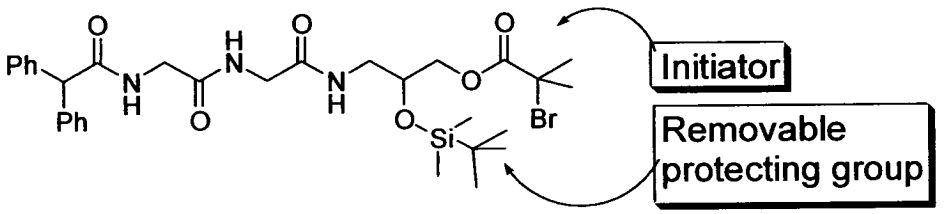
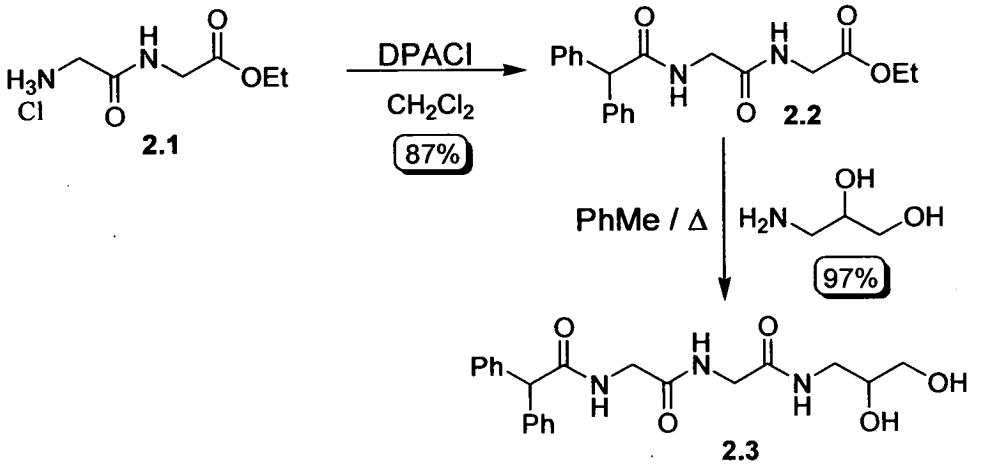


Figure 2. 5 Design of the ATRP Initiator Thread

The thread incorporates the necessary features discussed during the introduction. The glycylglycine unit has previously been used to template the formation of the benzylic amide rotaxane in 62% yield.[10] An aminopropan-1,2-diol unit was chosen as a linker unit for attaching the removable stopper and ATRP initiator groups. The amine can be attached to the template to provide another amide unit and perhaps improve the yield of rotaxane formation. The primary and secondary hydroxyl groups can be functionalised selectively to allow the efficient addition of the different stopper groups. A *tert*-butyldimethylsilyl protecting group was chosen as the removable stopper group as it stable to the reaction conditions necessary for polymerisation, but is readily cleaved under the appropriate conditions. Finally, the α-bromoester group is a widely used initiator for ATRP. During the course of this discussion the α-bromoester will be referred to as the initiator, and diphenylacetylglycylglycine-2,3-dihydroxy-1-propanamide (**2.3**) will be referred to throughout as the diol **2.3**.

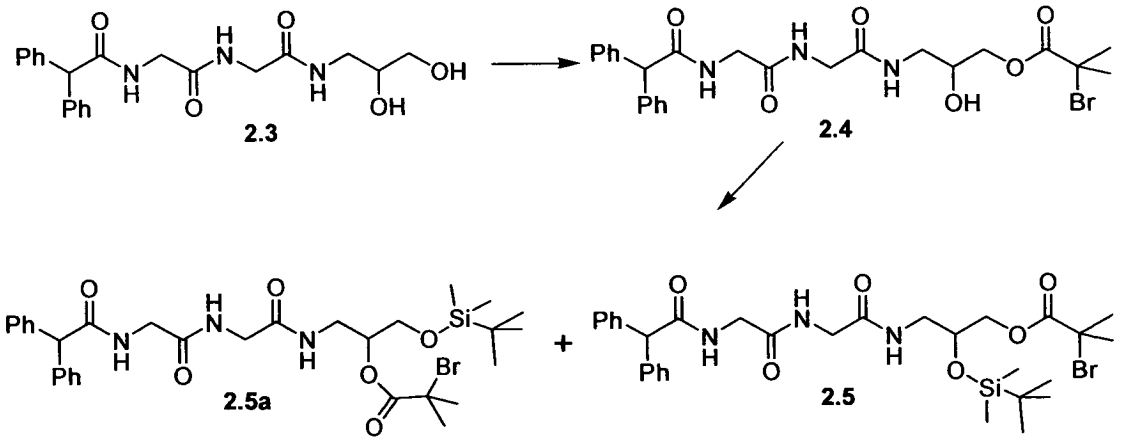
The diol **2.3** was synthesised in two steps (scheme 2.1). Glycylglycine ethyl ester hydrochloride salt (**2.1**) was reacted with diphenylacetyl chloride and triethylamine (CH_2Cl_2, 2 hr, 87%) to give product **2.2** as a colourless solid. Product **2.2** was then

treated with racemic 1-aminopropan-1,2-diol (PhMe, 110 °C, 4 hr, 97%) to give product **2.3** as a colourless solid. As the diol is racemic, stereochemistry is not indicated in any subsequent diagrams.



Scheme 2. 1 Diol **2.3** Synthesis

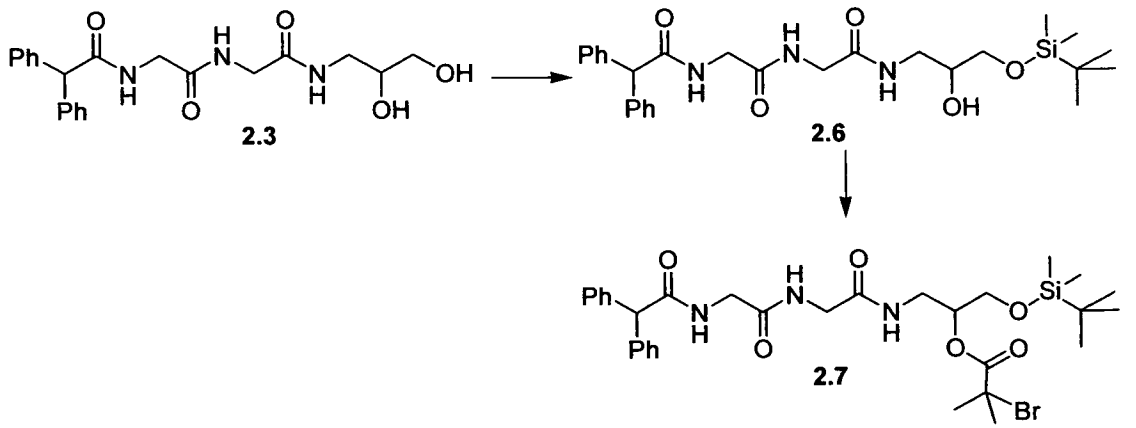
The initial approach to the target synthesis was to selectively acylate the primary position of the diol **2.3** with the initiator using 2-bromo-2-methylpropionic acid and EDCI (scheme 2.2). Subsequently, the secondary hydroxyl group would be protected with a silyl group.



Scheme 2. 2 Proposed Route to the Initiator Thread **2.5**

The diol **2.3** (1eq.) was coupled to 2-bromo-2-methylpropionic acid (1.2eq) using EDCI (1.05eq) and DMAP (dimethylformamide, 0 °C, 24 hr, 41%) to give product **2.4** in good selectivity. The next step was to add the *tert*-butyldimethylsilyl (TBDMS) group to the remaining hydroxyl group at the secondary position. The ester product **2.4** was reacted with TBDMS chloride (1.1eq), imidazole (1.5eq) and DMAP (CH_2Cl_2, 48 hr) to give a mixture of products **2.5** and **2.5a**. The two compounds could not be separated. Analysis of the ^1H NMR showed the characteristic peaks expected for the product, these being a six proton signal at 1.9ppm, a nine proton signal at 0.9ppm (*t*-butyl Si) and a six proton signal at 0.04ppm (Me_2Si). TLC analysis of the product showed only one spot, but the complex nature of the propandiol unit signals in the ^1H NMR spectrum indicated that the product was not pure, but a mixture of compounds. As the reaction had not occurred cleanly and the product could not be readily purified, it was decided to try a different approach.

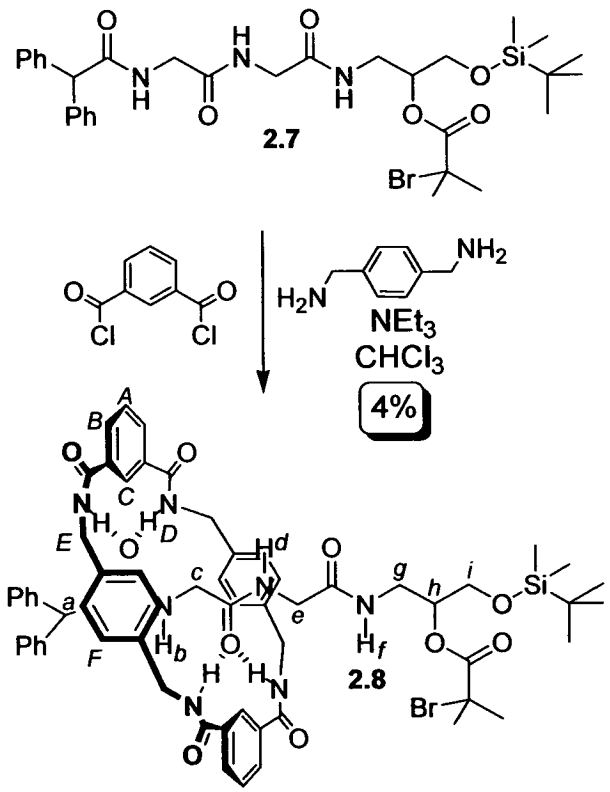
The diol **2.3** would be selectively silylated at the primary hydroxyl position followed by subsequent acylation at the secondary position to produce the thread **2.7** (scheme 2.3).



Scheme 2. 3 An Alternative Route to the Initiator

The diol **2.3** was reacted with TBDMS chloride, imidazole and DMAP (CH_2Cl_2, 48 hr, 90%) to yield the desired product **2.6**. In the subsequent synthesis of the thread **2.7**, product **2.6** was treated with 2-bromo-2-methylpropionyl bromide and imidazole (CH_2Cl_2, 30 min, 55%).

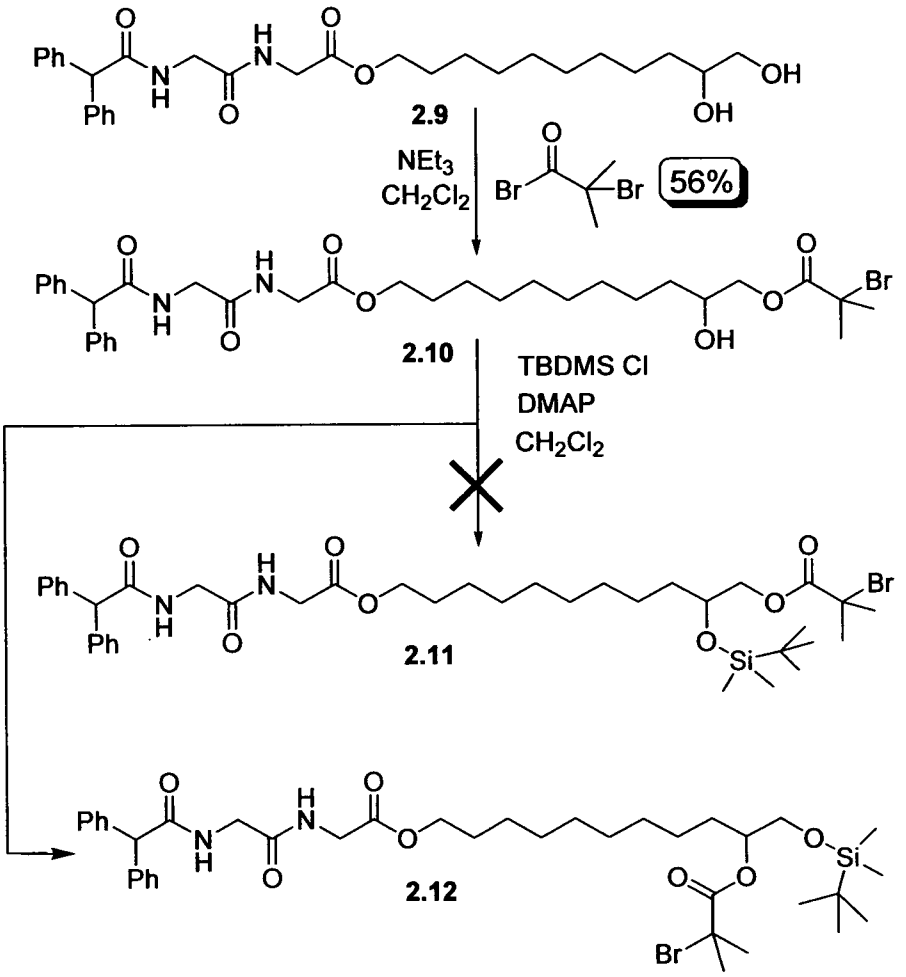
A rotaxane formation was attempted on the thread **2.7** (scheme 2.4). The thread **2.7** and triethylamine (30eq) were treated with *p*-xylylenediamine (12eq) and isophthaloyl dichloride (12eq) ($CHCl_3$, 3 hours) to give rotaxane **2.8** in a disappointing 4% yield. The ^1H NMR of the rotaxane **2.8** in $CDCl_3$ showed only a small impurity, but on removing the sample from the spectrometer a white precipitate was visible in the previously clear solution in the NMR tube. ^1H NMR analysis of the filtrate in d_6-DMSO showed the precipitate to be macrocycle, indicating that the rotaxane had decomposed in solution. Cleavage of the silyl group would have allowed the macrocycle to dethread and precipitate. The poor yield of rotaxane could also be attributed to similar decomposition during purification on silica.



Scheme 2. 4 Rotaxane Formation around Thread **2.7**

An alternative approach using a different starting material (**2.9**) was chosen (scheme 2.5). This starting material is a similar diol to **2.3**, but contains a long aliphatic chain. The purpose of this was to assist in the synthesis of the target, as the long chain diol

was more soluble in methylene chloride, and to decrease the steric crowding from around the diol. The approach adopted (see scheme 2.5) was to take the diol **2.9** and attach the initiator using the acid bromide and triethylamine in methylene chloride. Once the desired product was recovered, the remaining hydroxyl group would be protected with a silyl group.

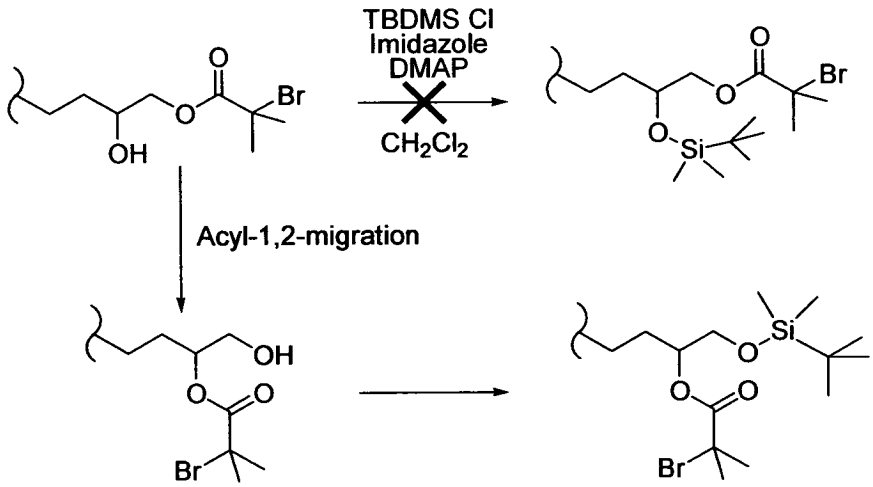


Scheme 2. 5 An Alternative Thread

The diol **2.9** was treated with 2-bromo-2-methylpropionyl bromide and triethylamine (CH_2Cl_2, 1 hr, 56%) to give the desired product **2.10**, after separation from a mixture of di-substituted, and the other mono-substituted product (15%). The clean product **2.10** was dissolved in methylene chloride with imidazole (3 eq), *tert*-butyldimethylsilyl chloride (1.2eq) and DMAP (cat). The TLC of the crude product showed starting material still present and another spot, assumed to be the desired product **2.11**. The first compound recovered was what was initially assumed to be the

desired product **2.11** (20%), but on closer analysis turned out to be the regioisomer **2.12**. The other material taken off the column turned out to be a mixture of starting material **2.10** and another compound (60%). The two compounds ran together on TLC and on looking at the ^{1}H NMR spectrum, the other compound was identified as the mono-ester, but with the ester group on the secondary position, *i.e.* the acyl group had migrated onto the secondary position during the course of the reaction.

With these being the only products recovered from the reaction, it seems that the silyl chloride does not react at the secondary hydroxyl group to yield the desired product **2.11**. Instead the reaction proceeds firstly by migration of the acyl group from the primary to the secondary position, followed by silylation at the primary position to give product **2.12** (scheme 2.6), either because the silyl group is too bulky to react at the secondary position or intramolecular acyl-migration is a much faster process under the reaction conditions.



Scheme 2. 6 Acyl Migration

In order to avoid the problems with acyl migration and silyl cleavage, a new thread was designed (figure 2.6).

EDINBURGH UNIV. LIBR.

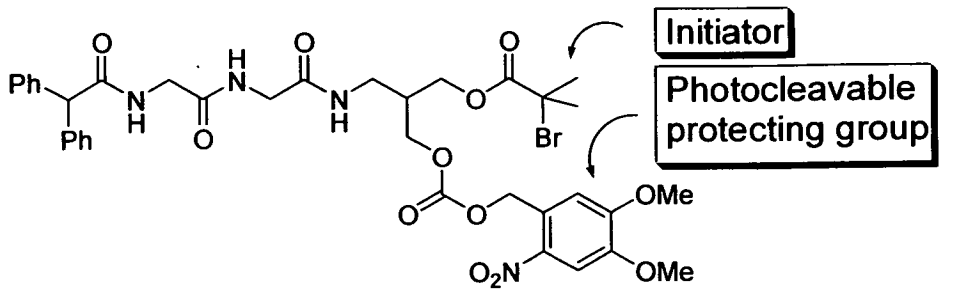
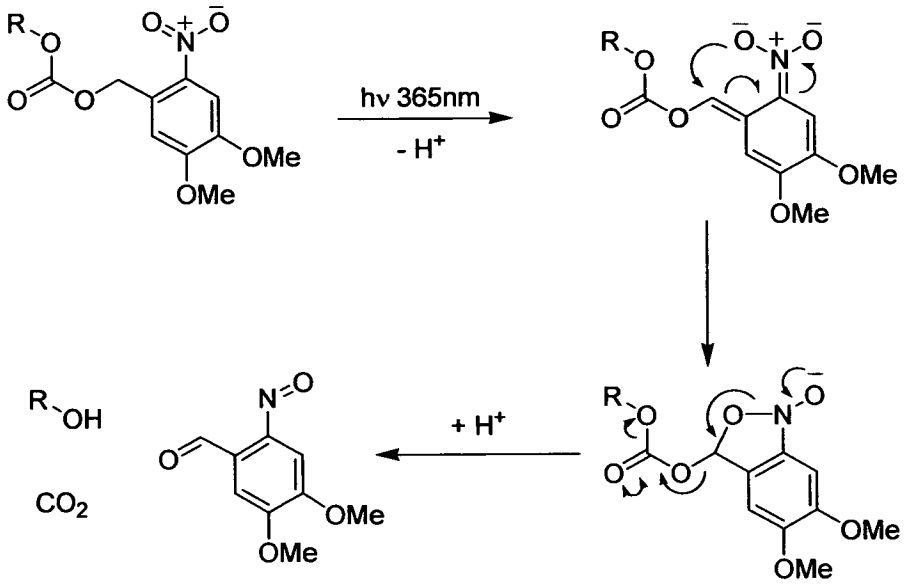


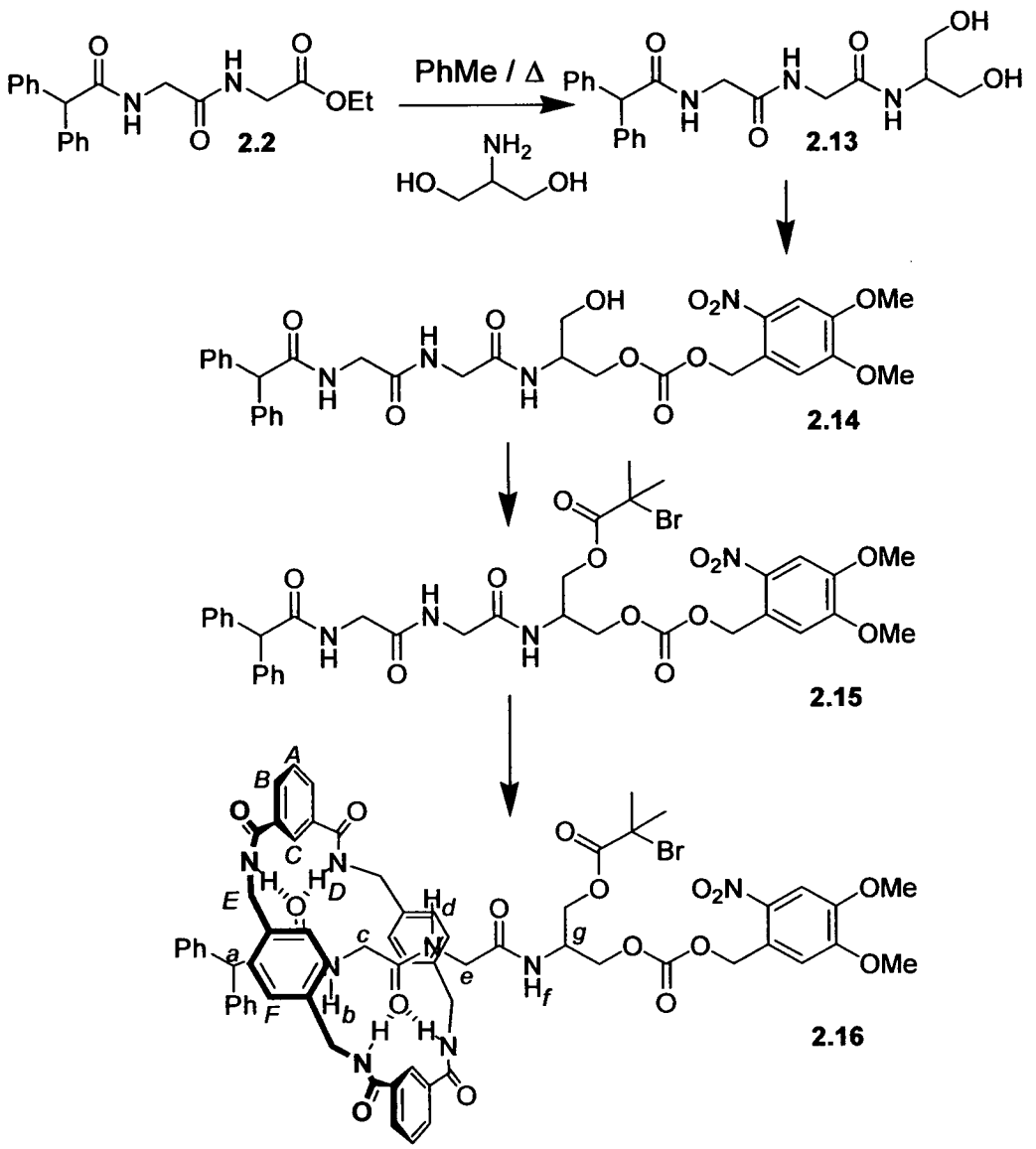
Figure 2. 6 A New Design of Thread

Instead of using the 1-aminopropanol-1,2-diol, serinol (2-aminopropan-1,3-diol) was used instead. This immediately eliminates the problems of migration because both hydroxyl groups are equivalent. A photocleavable protecting group has been incorporated into the design to avoid problems with silyl cleavage. The 5-nitroveratryl formylcarbonate group is cleaved using UV light at 365 nm (scheme 2.7).[11]



Scheme 2. 7 Mechanism of Photocleavage

The new thread was synthesised in three steps and the subsequent rotaxane was formed without problem (scheme 2.8).



Scheme 2. 8 Synthesis of Rotaxane Initiator **2.16**

The ester **2.2** was reacted with serinol (PhMe, 110 °C, 95%) to give the diol **2.13**. The yellow product **2.14** was formed by treating an excess of diol **2.13** with 5-nitroveratryl chloroformate (pyridine / $CHCl_3$, 56%). The unconsumed diol **2.13** was precipitated out of solution by the addition of an excess of chloroform. The initiator was coupled onto the remaining hydroxyl position of **2.14** using 2-bromo-2-methylpropionic acid with EDCI and DMAP (CH_2Cl_2, 0 °C, 94%) to give thread **2.15**. This was then treated *p*-xylylenediamine and isophthaloyl chloride (chloroform, 3 hr) to form the rotaxane **2.16** in 4% yield.

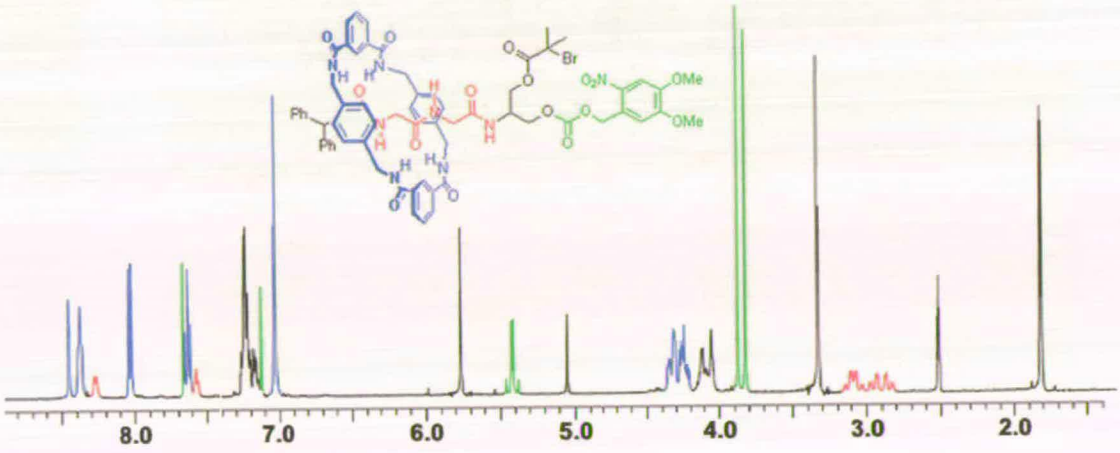
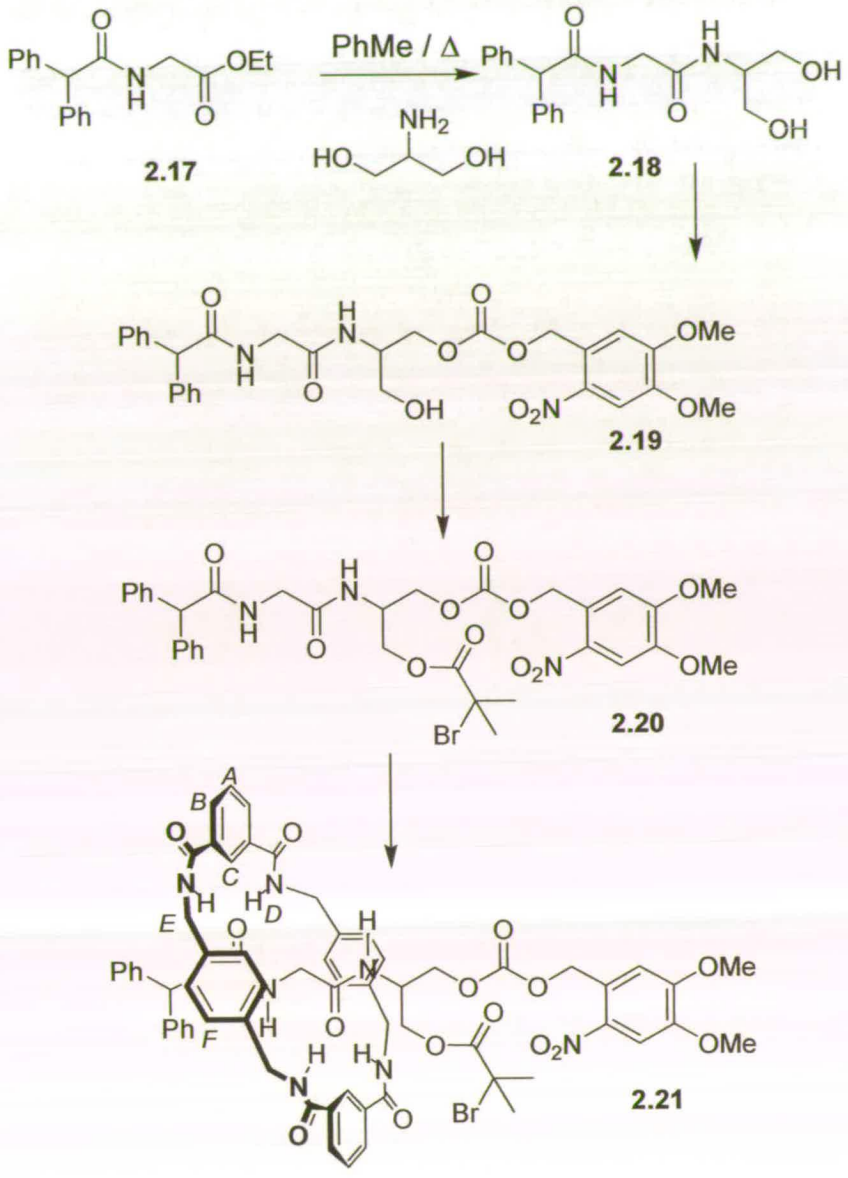


Figure 2. 7 ^{1}H NMR (400 MHz, d6-DMSO) of Rotaxane **2.16**

The disappointing rotaxane yield of 4% is not sufficient to efficiently produce large quantities of rotaxane initiator. Rotaxanes formed using the glycylglycine template, C-terminated with an ester, have been reported with yields of up to 62%. The addition of an extra amide unit to the glycylglycine template has decreased the yield dramatically. The lower than expected yield may be a result of the tri-peptide thread folding in the non-polar solution; also a problem observed in peptide synthesis. In the folded state the thread forms intra-molecular hydrogen bonds and therefore become a much poorer template for the macrocyclic precursor in solution, resulting in the observed low rotaxane yield.

It was decided to repeat the syntheisis using a single glycine template within the thread. The thread was synthesised in three steps, similar to the previous thread (scheme 2.9).



Scheme 2. 9 Thread **2.21** Synthesis Using a Single Glycine Template

Glycine ethyl ester and triethylamine in methylene chloride were reacted with diphenylacetyl chloride over one hour. The reaction was washed, and after removal of the solvent the resulting yellow-solid was recrystallised from toluene to give the pure white product **2.17** in 92% yield.

The ester **2.17** and serinol were refluxed in toluene overnight to produce an off-white precipitate. This was filtered and recrystallised from ethanol / hexane to yield the product **2.18** as a white solid in 91% yield.

An excess of the diol **2.18** was dissolved in a mixture of pyridine, methylene chloride and dimethylformamide, and nitroveratrylchloroformate was added. On completion of the subsequent reaction, the solution was diluted with diethyl ether to precipitate out the excess starting diol **2.18**, which was recovered by filtration and washed. The remaining solution was washed with acid, base and water and the crude product was purified by column chromatography on silica with methanol / methylene chloride to give the pure product **2.19** as a yellow solid in 32% yield.

The mono-hydroxy product **2.19** was coupled to 2-bromo-2methylpropionic acid with EDCI and DMAP in methylene chloride at 0°C. The reaction was washed with acid, base and water, and the crude product was purified by column chromatography on silica with methylene chloride to give the pure thread **2.20** as a yellow powder in 83% yield.

The subsequent rotaxane formation was carried out by reaction of dropwise additions of *p*-xylylenediamine and isophthaloyl dichloride in chloroform in the presence of the thread **2.20** and triethylamine. The completed reaction was filtered and washed through a silica plug with 10% methanol / methylene chloride. The crude mixture was then purified by column chromatography on silica to recover the unconsumed thread (60% recovery) and the rotaxane **2.21** as a bright yellow powder in 22% yield.

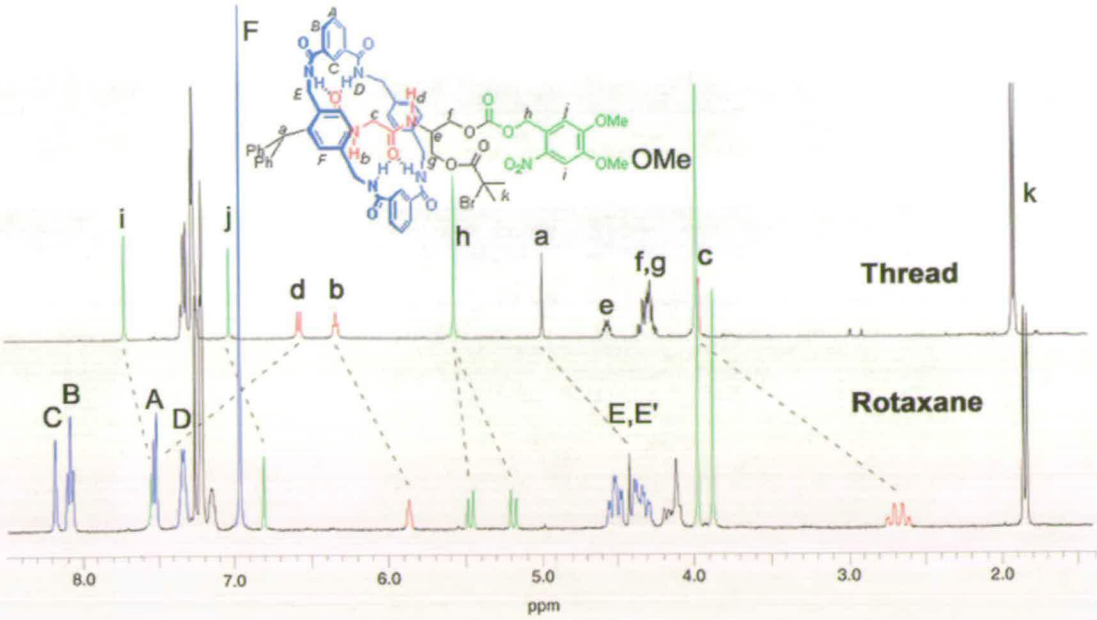


Figure 2. 8 ^{1}H NMR spectra (400 MHz, $CDCl_3$) of the Thread **2.20** and Rotaxane **2.21**

Comparison of the ^{1}H NMR spectrum of the thread and rotaxane shows the usual features associated with rotaxane synthesis. Characteristic macrocycle peaks are present in the spectrum (figure 2.8). Many of the thread signals appear at higher field in the rotaxane, due to shielding from the macrocycle. The most significant shifts due to shielding are seen for the methylene protons *c*, the diphenylacetyl proton *a*, and the amide proton *b* (δ 3.86, 4.89, 6.57 in thread to δ 2.64, 4.40, 5.86 in the rotaxane respectively). The amide proton *d* is heavily hydrogen bonded, and despite shielding from the macrocycle, appears further downfield (δ 6.88 in the thread and δ 7.16 in the rotaxane). The methoxy groups, an equivalent six-proton signal in the thread, are now two three-proton singlets separated by 0.10 ppm due to their differing proximities to the macrocycle. The nitroveratryl benzylic protons have become strongly desymmetrised. The protons *h*, a symmetrical singlet in the thread, now appear as two doublets separated by 0.28 ppm.

Synthesis of the thread and rotaxane were repeated until a quantity of rotaxane **2.21** sufficient for polymerisation (two grams in total) had been generated.

2.2.2 Attempts to grow a polymer chain from the rotaxane initiator by atom transfer radical polymerisation (ATRP).

The next step after the synthesis of sufficient quantities of rotaxane **2.21** was polymerisation (ATRP) using methyl methacrylate (MMA) from the rotaxane initiator **2.21**. The polymerisation was conducted in a NMR tube, and the kinetics followed by ^{1}H NMR. After an initial slow increase in rate, the polymerisation was found to be first order in terms of monomer conversion with time (figure 2.9).

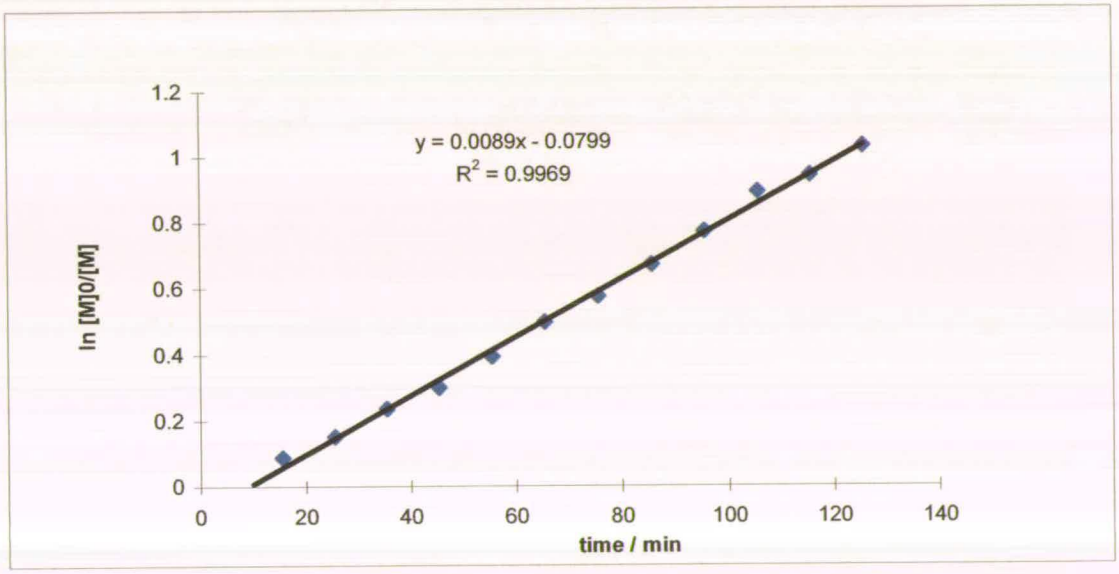


Figure 2. 9 First order kinetics plot for the ATRP of MMA initiated by rotaxane **2.21**

A hundred and fifty fold excess (with respect to the initiator) of methyl methacrylate was polymerised by ATRP at 90°C in toluene solution, initiated using the rotaxane **2.21** in conjunction with a (*N*-*n*-pentyl-2-pyridylmethanimine)copper(I) bromide complex formed in situ. The polymerisation was quenched at 60% conversion by cooling the sample. The catalyst removed by filtration through a silica plug, before isolating the polymer by precipitation into hexanes.

The polydispersity (PDI) was narrow at 1.19 as analysed by GPC (figure 2.10). The ATRP reaction appears to have been operating effectively, *i.e.* living / controlled

polymerisation, as established by: (i) a linear first order kinetics plot, (ii) narrow polydispersity (PDI < 1.5), and (iii) an increase in the number average molecular weight (M_n) of polymer as the conversion proceeds. Thus far the polymerisation from initiator **2.21** has satisfied points (i) and (ii). It was impossible to determine (iii) the increase in M_n throughout the course of the reaction, as samples could not be taken from the small scale, NMR tube reaction for GPC analysis.

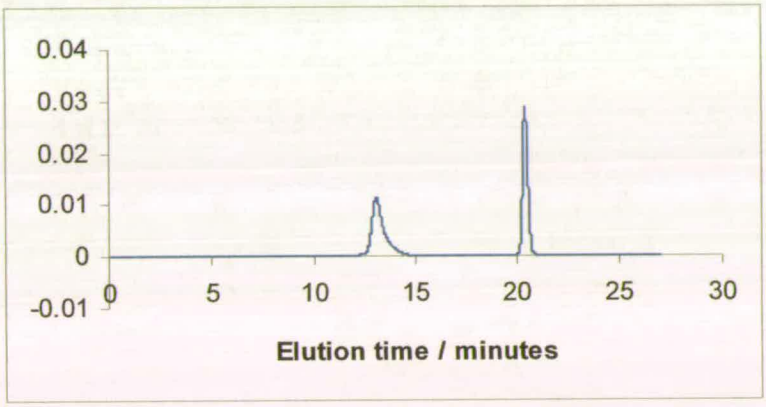


Figure 2. 10 GPC trace used to determine polydispersity (PDI)

Analysis of the isolated polymer indicated that the number averaged molecular weight (M_n) at 17.8 kD was in fact much higher than the theoretical value at 10.5 kD for 64% conversion (figure 2.11).

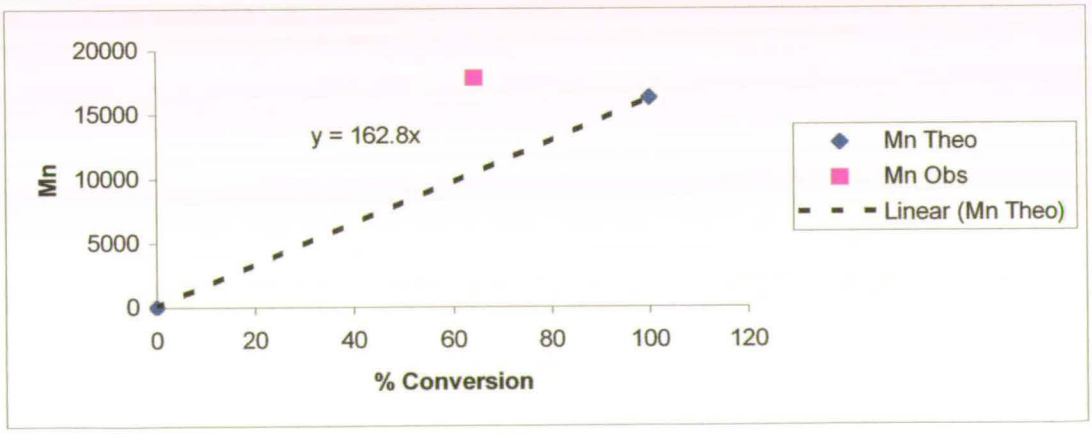


Figure 2. 11 Theoretical Number Average Molecular Weight (M_n) and Actual M_n against % conversion

The reason for this discrepancy is probably a result of the poor solubility of the initiator in toluene. In this case, initiation is the rate-determining step in polymerisation, as the rate of initiation is determined by the solubilisation of initiator. This means that the polymerisation is uncontrolled, and proceeds by polymerisation of solubilised initiator, before more initiator is dissolved. Polymerisation appears to terminate at the observed 17.8 kD. This hypothesis is supported by the presence of insoluble solid within the NMR tube.

Despite these observations, the obtained [2]polyrotaxane was cleaved using 365 nm ultraviolet light. Experiments were conducted in the solid-state, and in solutions of $CDCl_3$ and d_6-DMSO. The solid-state photocleavage was conducted using a film of material within an NMR tube. The film was created by dissolving a sample of material in 0.5 mL methylene chloride, injecting into the bottom of a NMR tube, bubbling nitrogen through to reduce the solvent to a small volume, and finally rotating the tube whilst under vacuum to leave a thin film. The NMR tube was irradiated for 20 min. The ^{1}H NMR in d_6-DMSO showed that the peaks corresponding to the photocleavable group disappeared and indicated that the group was removed. On observing the photocleaved polymer by ^{1}H NMR, no change could be detected at room temperature over a period of one week, and for a further week at 60°C with the macrocycle appearing to still be positioned over the template. Even after column chromatography on silica of the photocleaved polymer, the macrocycle could still be observed on the glycine unit of the recovered polymer.

A model was built using CPK. The macrocycle appears to easily fit over the monomer unit of methyl methacrylate. In poly(methyl methacrylate) (pMMA), the macrocycle can fit over the isotactic arrangement of monomer units within the chain (with groups arranged on the same side), but cannot fit over the syndiotactic arrangement (with groups on alternating sides) (figure 2.12). Since the stereochemistry of pMMA is most probably atactic (random arrangements), the polymer acts as a stopper for the rotaxane, and forces the macrocycle to remain on the template.

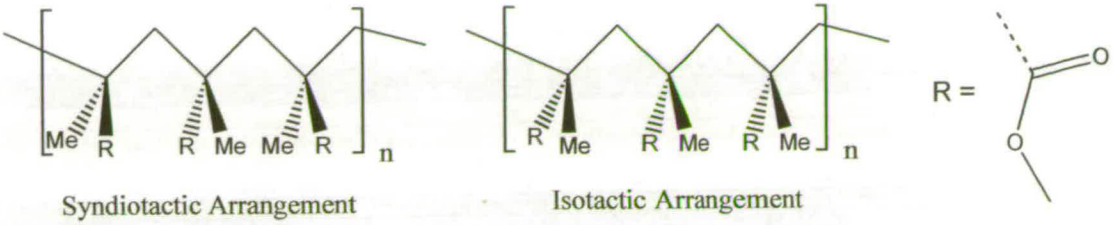


Figure 2. 12 Isotactic and Syndiotactic Arrangements in pMMA

CPK modelling showed that poly(methyl acrylate) (pMA) was small enough to allow the macrocycle to fit over and polymerisation was attempted with methyl acrylate as the monomer.

Polymerisation was conducted in the same manner as reported for pMMA. Again a linear first order kinetic plot was observed (figure 2.13).

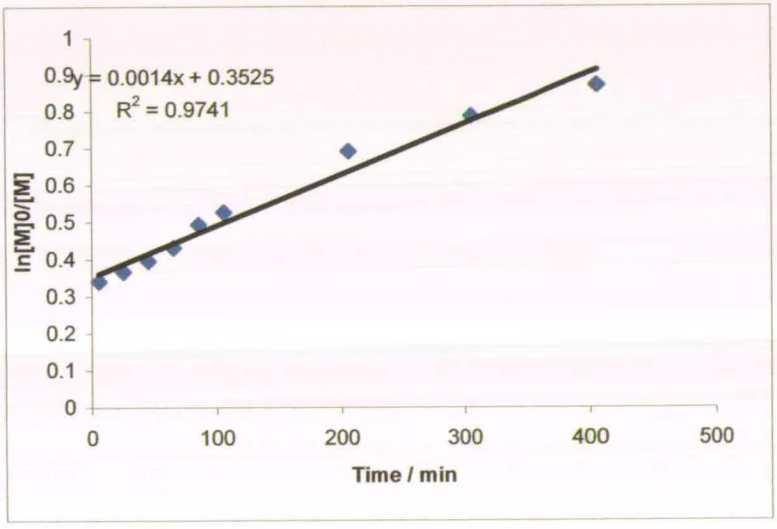


Figure 2. 13 First Order Kinetic Plot for Methyl Acrylate ATRP Initiated by Rotaxane **2.21**

Although a linear plot is observed, polymerisation appears to occur very rapidly initially with very rapid monomer consumption before the initial reading was taken. This could be as a result of polymerisation occurring on addition, or before reaching 90°C when the first reading was taken. The rate of polymerisation tails off, before ceasing completely.

The GPC trace of the polymer showed that the polydispersity was much broader than observed previously for pMMA (figure 2.14). Analysis showed that the polydispersity was greater than 1.5. This suggests that the polymerisation was uncontrolled. Unpolymerised initiator can also be observed in the GPC trace. The number average molecular weight (M_n) was recorded as 9.8 kD.

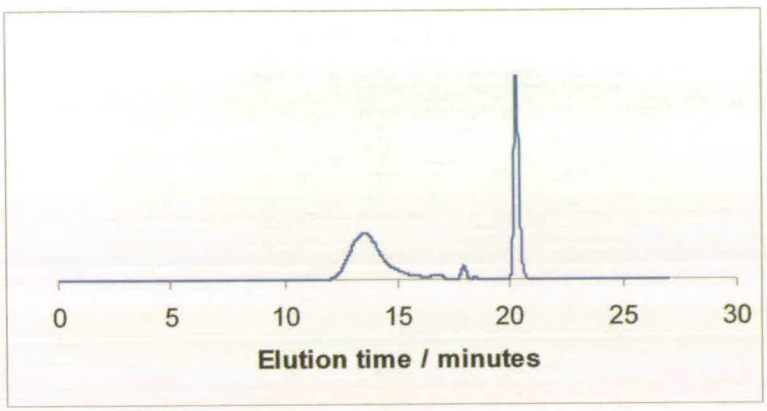


Figure 2. 14 GPC Trace used to determine polydispersity (PDI)

The polymerisation was repeated on a larger scale, and samples were extracted every ten minutes in order to obtain a range of polymers with different molecular weights (M_n). GPC analysis showed all samples to have molecular weights of around 10 kD.

This surprising result suggests that the polymerisation proceeds by the mechanism discussed before. Uncontrolled polymerisation occurs on the fraction of initiator in solution, before terminating somehow at or before molecular weight 10 kD. As the polymerisation occurs and the growing chains become more soluble, more initiator is dissolved and the cycle repeats, until the polymerisation is quenched. The initiator remaining could either not be dissolved before the reaction is quenched, or have been washed onto the walls of the NMR tube, and therefore removed from the reaction.

The mode of termination is uncertain, but could most likely influence the results of any further study. The methyl acrylate radical at the end of a growing chain is much less stable than the methyl methacrylate radical, as it is located on a secondary carbon instead of a tertiary carbon. This, in turn, means that the methyl acrylate

radical is more reactive, and could cause the polymerisation to proceed in an uncontrolled manner with side-reactions or branching occurring.

Photocleavage of the recovered polymer did not appear to proceed smoothly in either solid-state, or in solution of d_6-DMSO or $CDCl_3$. The ^1H NMR spectra appeared very messy, and could not be assigned. Further exposure to ultraviolet light at 365 nm intensified this effect. It appeared that the polymer was decomposing under the photocleavage conditions, despite trying photocleavage in the solid-state, or in d_6-DMSO or $CDCl_3$ solution.

It was decided that the methyl acrylate was too unstable and too difficult to polymerise in a controlled reaction. With methyl methacrylate being too large to accommodate the macrocycle, and no smaller monomers available, this meant that further progress using ATRP could not be achieved.

2.2.3 Cleavage study on thread and short chain (C18 and C30) rotaxanes.

In order to prove that the designed rotaxane initiator could be photocleaved without decomposition, photocleavage experiments were conducted on the thread **2.20** and rotaxane initiator **2.21**. These studies would prove photocleavage in the solid-state, and in solution, could be achieved and that the poly(methyl acrylate) was causing the observed problems during photocleavage.

Initial studies were conducted with a sample of thread **2.20** in d_6-DMSO. Cleavage occurred cleanly over a period of 4 hours in solution. ^1H NMR was used to follow the cleavage. The disappearance of the peaks corresponding to the photocleavable group and the doublet amide can clearly be observed, along with the emergence of a new doublet amide peak and a shift in the adjacent methylene peak. The experiment was repeated by photocleaving in the solid-state, followed by dissolution in $CDCl_3$ to observe the changes in ^1H NMR spectrum. The same results could be observed, and again for cleavage in $CDCl_3$.

Photocleavage studies were then conducted on the rotaxane initiator **2.21**. Initial studies were conducted in d_6-DMSO solution and ^{1}H NMR was used to follow the degree of cleavage over time. It is apparent that the photocleavage occurs cleanly without side reactions to yield one product, *i.e.* the two separate rotaxane components (figure 2.15).

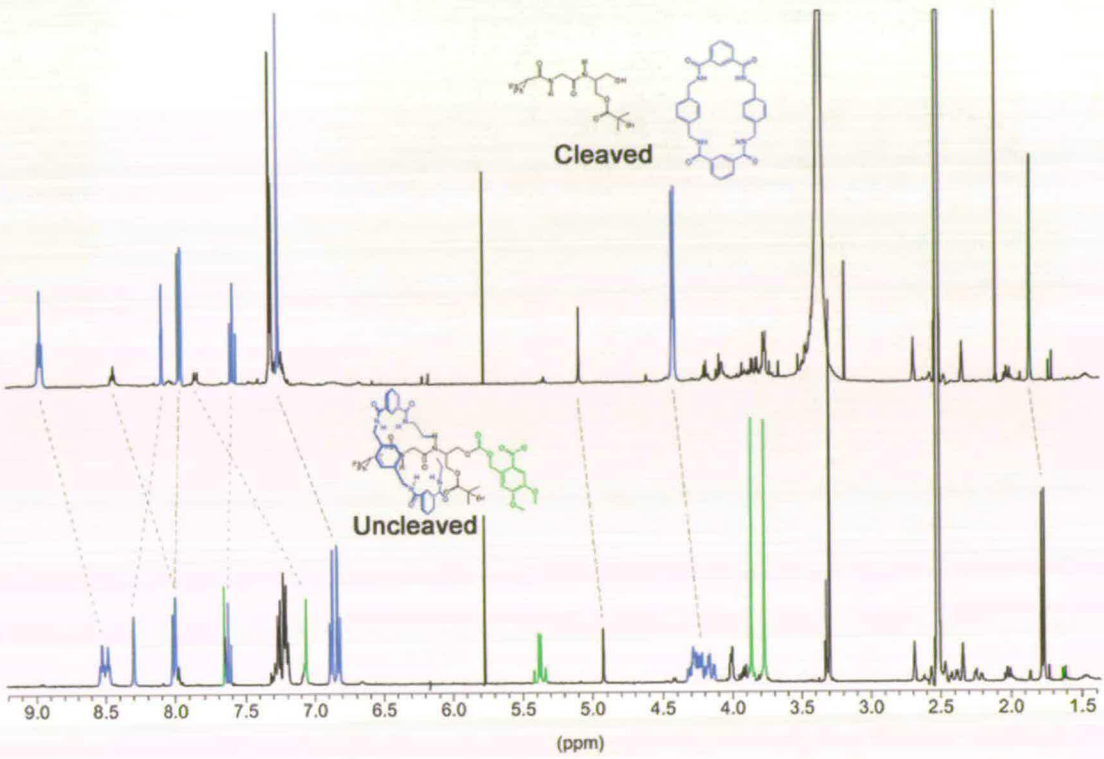


Figure 2. 15 ^{1}H NMR spectra (400 MHz, d_6-DMSO) of the Rotaxane Initiator **2.21** and the photocleaved products.

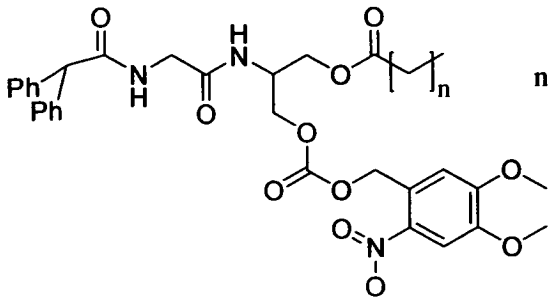
From the ^{1}H NMR of the uncleaved and cleaved rotaxane it is clear that the photocleavage reaction occurs cleanly without any side reactions. It is also clear that there is a dramatic change in the rotaxane spectrum on cleavage. The photocleaved group crystallises out of solution and disappears from the spectrum. The macrocycle is now free in solution as indicated in the cleaved product. The desymmetrised peaks of the benzylic and xylylene protons in the rotaxane become symmetrical peaks on cleaving, as they are no longer made enantiotopic by the thread. Also the amide

protons of the macrocycle are shifted 0.5 ppm downfield as a result of the increased hydrogen bonding to the solvent when free in solution.

The photocleavage experiment was repeated in $CDCl_3$. During the photocleavage a white precipitate appeared in the solution, which inhibited further reaction. This was found to be the macrocycle, known to be insoluble in chloroform. Cleavage in the solid-state occurred just as cleanly. After one hour in the photoreactor, dissolution and ^1H NMR analysis showed complete cleavage with an identical spectrum to that of the reaction in d_6-DMSO.

Clean photocleavage had been shown to occur with thread and rotaxane in the solid-state, and in solutions of chloroform and dimethyl sulfoxide. Although this result does not help determine the cause of problems with the poly(methyl acrylate) polymer, it does prove that the cleavage is clean and effective on the rotaxane **2.21**, which incorporates an ATRP radical initiator. Further study could determine specific problems, but it was decided that an alternative method of attaching polymers would be more desirable, considering the problems encountered during polymerisation and in identifying any inherent problems.

As a final study on photocleavable rotaxanes, [2]polyrotaxane models were synthesised. Instead of attaching a radical initiator, a long alkyl chain would be attached to show that designed [2]polyrotaxanes could have worked according to plan, i.e. that the macrocycle would move from the station, over the polymer chain (in this case an alkyl chain), and fall off the end, if not for unanticipated problems with the [2]polyrotaxanes studied, and the polymerisation procedure in general. To that end two new threads were synthesised incorporating a C18 acid **2.22** (stearic acid) and a C30 acid **2.23** (triacontanoic acid) (figure 2.16).



	thread	rotaxane
n = 16	**2.22**	**2.24**
28	**2.23**	**2.25**

Figure 2. 16 Threads **2.22**, **2.23** and Corresponding Rotaxanes **2.24**, **2.25** Incorporating C18 and C30 Acids Respectively

Synthesis of the C18 thread **2.22** was achieved by firstly forming the stearic acid chloride using oxalyl chloride and dimethylformamide in methylene chloride. This was used without further purification, and was added to a solution of thread precursor **2.19** and triethylamine in methylene chloride. The reaction was washed and the product **2.22** was isolated without the need for further purification. The rotaxane **2.24** was formed by the usual method and was purified by chromatography on silica. The ^{1}H NMR spectrum of rotaxane **2.24** looked very similar to the rotaxane initiator **2.21** spectrum, showing the usual characteristic rotaxane features.

Synthesis of the C30 thread **2.23** was achieved using EDCI to couple triacontanoic acid directly to the hydroxyl of precursor **2.19**. The rotaxane **2.25** was formed and isolated by the same method as before, and ^{1}H NMR showed the usual characteristic rotaxane features.

Cleavage of the two rotaxanes **2.24** and **2.25** in d_6-DMSO again occurred cleanly. In the ^{1}H NMR spectra of the both samples, the free macrocycle and thread could exclusively be seen in solution. During cleavage in $CDCl_3$, traces of the telltale white precipitation of macrocycle could be observed within ten minutes, long before complete photocleavage. This indicates that macrocycle movement is occurring much faster than the cleavage reaction. Cleavage in the solid-state was then conducted in a NMR tube. The samples were cleaved for one hour and NMR solutions made up immediately before ^{1}H NMR analysis. Again, only free

macrocycle could be observed in d_6-DMSO, and white precipitate could be observed on addition of $CDCl_3$.

Although these model systems proved unsuitable for a kinetic study, these observations prove that the system design does work. The rotaxane is stable and can be isolated and purified without the macrocycle being able to move or unthread. The rotaxane can be cleaved cleanly. Once cleaved, the macrocycle can translate along the alkyl chain and unthread. Observing the changes in the ^1H NMR spectrum or monitoring the precipitation of macrocycle in chloroform can be used detect the unthreaded macrocycle.

2.3 Conclusions

In order to synthesise a variety of [2]polyrotaxanes, a number of attempts were made to synthesise a template that would yield useful quantities of [2]rotaxane initiators for polymersation. Throughout the course of this research, the thread design has changed, incorporating different functionalities, to improve upon and avoid any problems associated with the previous attempt. The final thread was produced by an easier synthetic route, was more stable, and produced rotaxane in higher yield (from 4% to 22%) than the initially synthesised thread.

The attempts to synthesise [2]polyrotaxanes by ATRP polymerisation of the [2]rotaxane initiators proved unsuccessful. The polymerisation could not be controlled to produce a mono-disperse selection of polymers of different molecular weights. The polymers that were produced using methyl methacrylate and methyl acrylate, despite undergoing stopper photocleavage, displayed no evidence of the macrocycle leaving the thread onto the polymer backbone.

Although no kinetic study could now be carried out using [2]polyrotaxanes, [2]rotaxanes with alkyl chains instead of polymers were synthesised. These behaved exactly as expected, undergoing stopper photocleavage, followed by motion of the

macrocycle along the alkyl chain and unthreading into solution. Although unthreading occurred much too quickly for the kinetics to be measured, these model systems proved the design principle worked.

2.4 Experimental

Throughout the experimental section common abbreviations have been used.

(2-Diphenylacetylamino-acetylamino)-acetic acid ethyl ester (2.2)

To a stirred solution of glycylglycine ethyl ester hydrochloride **2.1** (10 g, 50.9 mmol) and triethylamine (21.3 mL, 152 mmol) in CH_2Cl_2 (200 mL) under a nitrogen atmosphere was added diphenylacetyl chloride (12.9 g, 56.0 mmol) in methylene chloride (50 mL) dropwise over 1 h and left to stir for 24 h. The reaction was then washed with saturated sodium bicarbonate solution (3 x 100 mL) and water (3 x 100 mL), dried over Na_2SO_4, filtered and concentrated under reduced pressure. Recrystallisation of the resulting yellow solid from toluene yielded the product as a white solid (**2.2**, 15.8 g, 87.4 %); ^{1}H NMR (400 MHz, CDCl3) δ 7.32 (10H, m, Ph), 6.73 (1H, t, J = 5.0 Hz, NH), 6.54 (1H, t, J = 5.0 Hz, NH), 5.01 (1H, s, $Ph_2C\underline{H}$), 4.23 (2H, q, J = 7.0 Hz, $OC\underline{H}_2CH_3$), 4.03 (2H, d, J = 5.0 Hz, $NHC\underline{H}_2$), 3.98 (2H, d, J = 5.0 Hz, $NHC\underline{H}_2$), 1.14 (3H, t, J = 7.0 Hz, $OCH_2C\underline{H}_3$); ^{13}C NMR (100 MHz, $CDCl_3$) δ 173.1, 169.8, 169.3, 139.4, 129.3, 129.2, 127.8, 62.0, 59.2, 43.8, 41.7, 14.5; HRFAB-MS (3-NOBA matrix): m/z = 355.16552 (calcd. for $C_{20}H_{23}N_2O_4$, $[M]H^+$, 355.16578).

***N*-({[(2,3-Dihydroxy-propylcarbamoyl)-methyl]-carbamoyl}-methyl)-2,2-diphenyl-acetamide (2.3)**

A stirred mixture of diphenylacetylglycylglycine ethyl ester **2.2** (10.3 g, 28.9 mmol) and 1-amino-2,3-propandiol (2.8 g, 30.4 mmol) in toluene (200 mL) was heated under reflux for 12 h. An off-white precipitate had appeared during the course of the reaction. The solid product was filtered and recrystallised from ethanol / hexane to

yield a white solid (**2.3**, 11.4 g, 98 %); ^{1}H NMR (400 MHz, d_6-DMSO) δ 8.50 (1H, t, J = 6.0 Hz, NH), 8.16 (1H, t, J = 6.0 Hz, NH), 7.81 (1H, t, J = 6.0 Hz, NH), 7.34-7.21 (10H, m, Ph), 5.09 (1H, s, $Ph_2C\underline{H}$), 4.73 (1H, d, J = 5.0 Hz, CHO$\underline{H}$), 4.52 (1H, t, J = 5.0 Hz, $CH_2O\underline{H}$), 3.79 (2H, d, J = 6.0 Hz, NHC$\underline{H_2}$), 3.72 (2H, d, J = 6.0 Hz, NHC$\underline{H_2}$), 3.49 (1H, m, C$\underline{H}$OH), 3.29 (2H, dt, J = 2.0 Hz and 5.0 Hz, $CH_2O\underline{H}$), 3.22 (1H, dt, J = 14.0 Hz, 6.0 Hz and 2.0 Hz, NHC$\underline{H}$H'CHOH), 2.99 (1H, dt, J = 14.0 Hz, 6.0 Hz and 2.0 Hz, NHCH$\underline{H}$'CHOH); ^{13}C NMR (100 MHz, d_6-DMSO) δ 172.0, 169.4, 140.6, 128.9, 128.6, 127.0, 70.6, 64.0, 56.6, 42.6, 42.5; HRFAB-MS (3-NOBA matrix): m/z = 400.18689 (calcd. for $C_{21}H_{26}N_3O_5$, $[M]H^+$, 400.18725).

2-Bromo-2-methyl-propionic acid 3-[2-(2-diphenylacetylamino-acetylamino)-acetylamino]-2-hydroxy-propyl ester (2.4)

A solution of diol **2.3** (500 mg, 1.25 mmol), 2-bromo-2-methylpropanoic acid (260 mg, 1.5 mmol), EDCI (242 mg, 1.26 mmol) and a catalytic ammount of 4-(dimethylamino)pyridine in anhydrous tetrahydrofuran (25 mL) and Dimethylformamide (7 mL) under a nitrogen almosphere was allowed to stir for 5 days. The mixture was then concentrated under reduced pressure, partitioned between ethyl acetate (50 mL) and water (150 mL). The aqueous layer was washed with ethyl acetate (3 x 25 mL). The combined organic washings were further washed with dilute HCl (3 x 25 mL), saturated sodium bicarbonate solution (3 x 25 mL), brine (3 x 25 mL), dried over Na_2SO_4, filtered and concentrated under reduced pressure to yield a pale yellow oil (**2.4**, 281 mg, 41 %); ^{1}H NMR (400 MHz, d_6-DMSO) δ 8.51 (1H, t, J = 6.0 Hz, NH), 8.17 (1H, t, J = 6.0 Hz, NH), 7.91 (1H, t, J = 6.0 Hz, NH), 7.35- 7.19 (10H, m, Ph), 5.19 (1H, d, J = 6.0 Hz, OH), 5.08 (1H, s, Ph_2CH), 4.08-3.98 (2H, m, $C\underline{H_2}OCO$), 3.79 (2H, d, J = 6.0 Hz, NHC$\underline{H_2}$), 3.76 (1H, m, CHOH), 3.72 (2H, d, J = 6.0 Hz, NHC$\underline{H_2}$), 3.25-3.16 (1H, m, NHC$\underline{H}$H'CHOH), 3.14-3.06 (1H, m, NHCH$\underline{H}$'CHOH), 1.92 (1H, s, $(C\underline{H_3})_2CBr$); HRFAB-MS (3-NOBA matrix): m/z = 548.13915 (calcd. for $C_{25}H_{31}BrN_3O_6$, $[M]H^+$, 549.13962).

2-Bromo-2-methyl-propionic acid 2-(*tert*-butyl-dimethyl-silanyloxy)-3-[2-(2-diphenylacetylamino-acetylamino)-acetylamino]-propyl ester (2.5)

A solution of **2.4** (1.39 g, 2.53 mmol) and *tert*-butyldimethylsilyl chloride (420 mg, 2.78 mmol), imidazole (260 mg, 3.79 mmol) and 4-(dimethylamino)pyridine in CH_2Cl_2 (50 mL) was stirred under nitrogen for 24 h. The solution was then washed with dilute acid (3 x 50 mL) and brine (3 x 50 mL), dried over Na_2SO_4, filtered and dried under reduced pressure. The crude was product obtained was shown by ^1H NMR to be a complex mixture of primary and secondary ester products, as a result of unwanted acyl-migration reactions. The compound was not further purified; FAB-MS: m/z = 662, $[M]H^+$;

_N_-[({[3-(*tert*-Butyl-dimethyl-silanyloxy)-2-hydroxy-propylcarbamoyl]-methyl}-carbamoyl)-methyl]-2,2-diphenyl-acetamide (2.6)

A mixture of **2.3** (2g, 5.0 mmol), *tert*-butyldimethylsilyl chloride (830 mg, 5.5 mmol), imidazole (510 mg, 7.5 mmol) and a catalytic amount of 4-(dimethylamino)pyridine in CH_2Cl_2 (100 mL) was stirred under a nitrogen atmosphere for 14 h. The reaction was then washed with acid (3 x 50 mL), base (3 x 50 mL) and water (3 x 50 mL), dried over Na_2SO_4 and filtered. Petroleum ether was added to the CH_2Cl_2 and the solvent was decanted off to leave a yellow oil. On drying under vacuum the product was obtained as an off-white foam (**2.6**, 2.35 g, 90 %); ^1H NMR (400 MHz, $CDCl_3$) δ 7.34-7.27 (11H, m, Ph and NH), 6.98 (1H, t, J = 6.0 Hz, NH), 6.93 (1H, t, J = 6.0 Hz, NH), 5.00 (1H, s, $Ph_2C\underline{H}$), 3.88-3.83 (4H, m, 2x $NHC\underline{H}_2$), 3.64 (1H, m, $C\underline{H}OH$), 3.55-3.51 (2H, m, $C\underline{H}_2OSi$), 3.48-3.42 (1H, m, $NHC\underline{H}H'CHOH$), 3.16-3.09 (1H, m, $NHCH\underline{H}'CHOH$), 0.91 (9H, s, $(C\underline{H}_3)_3CSi$), 0.07 (6H, s, $(C\underline{H}_3)_2Si$). ^{13}C NMR (100 MHz, $CDCl_3$) δ 173.9, 169.9, 169.8, 139.4, 129.3, 129.2, 127.8, 81.7, 77.6, 71.1, 65.4, 58.8, 43.9, 43.2, 43.1, 26.3, 26.2, 18.7, 0.3, -5.0. HRFAB-MS (3-NOBA matrix): m/z = 513.26663 (calcd. for $C_{31}H_{45}BrN_3O_6Si$, $[M]H^+$, 513.26588).

2-Bromo-2-methyl-propionic acid 1-(*tert*-butyl-dimethyl-silanyloxymethyl)-2-[2-(2-diphenylacetylamino-acetylamino)-acetylamino]-ethyl ester (2.7)

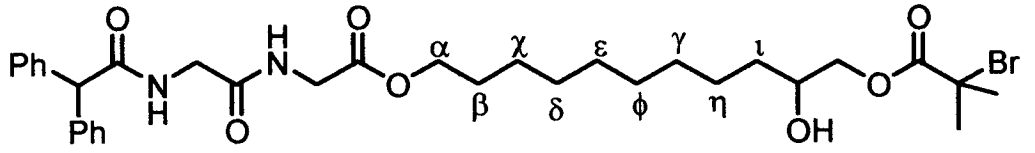
To a stirred solution of **2.6** (1 g, 1.9 mmol) and imidazole (560 mg, 8.2 mmol) in CH_2Cl_2 (50 mL) under nitrogen was added dropwise 2-bromo-2-methylpropanoyl bromide (540 mg, 289 µl, 2.3 mmol) in CH_2Cl_2 (30 mL) over 30 min. The reaction was stirred for 2 h and quenched with 2 mL water. The solution was then washed with dilute acid (3 x 50 mL), base (3 x 50 mL), and brine (3 x 50 mL), dried over Na_2SO_4, filtered and concentrated under reduced pressure to yield a pale brown foam. The crude product was purified by column chromatography (silica, methylene chloride) to give the pure product as a colourless solid (**2.7**, 720 mg, crude yield 55 %); ^{1}H NMR (400 MHz, $CDCl_3$) δ 7.33 (10H, m, Ph), 7.20 (1H, t, *J* = 6.0 Hz, NH), 6.91 (1H, t, *J* = 6.0 Hz, NH), 6.70 (1H, t, *J* = 6.0 Hz, NH), 5.01 (1H, s, $Ph_2C\underline{H}$), 4.96 (1H, m, C<u>H</u>OCO), 3.95 (2H, m, CH_2OSi), 3.82 (2H, d, *J* = 6.0 Hz, NHC<u>H</u>$_2$), 3.72 (2H, d, *J* = 6.0 Hz, NHC<u>H</u>$_2$), 3.59 (1H, ddd, *J* = 14.0 Hz, 6.0 Hz, 4.0 Hz, NHC<u>H</u>H'CHOCO), 3.44 (1H, ddd, *J* = 14.0 Hz, 6.0 Hz, 4.0 Hz, NHCH<u>H</u>'CHOCO), 1.91 (6H, app d, *J* = 4.0 Hz, (C<u>H</u>$_3$)$_2$CBr), 0.91 (9H, s, (C<u>H</u>$_3$)$_3$CSi), 0.08 (6H, s, (C<u>H</u>$_3$)$_2$Si); ^{13}C NMR (100 MHz, $CDCl_3$) δ 173.3, 169.5, 168.8, 139.4, 129.3, 127.8, 77.6, 74.9, 62.9, 60.8, 59.2, 43.9, 43.4, 40.6, 30.9, 26.1, 21.4, 14.6; HRFAB-MS (3-NOBA matrix): *m/z* = 662.22583 (calcd. for $C_{31}H_{45}BrN_3O_6Si$, $[M]H^+$, 662.22610).

[2](1,7,14,20-Tetraaza-2,6,15,19-tetraoxo-3,5,9,12,16,18,22,25-tetrabenzocyclohexacosane)-2-bromo-2-methyl-propionic acid 1-(*tert*-butyl-dimethyl-silanyloxymethyl)-2-[2-(2-diphenylacetylamino-acetylamino)-acetylamino]-ethyl ester rotaxane (2.8)

To a stirred solution of **2.7** (720 mg, 1.09 mmol) and di-(*iso*-propyl)ethylamine (4.2 g, 5.8 mL, 32.6 mmol) in anhydrous chloroform (100 mL) under a nitrogen atmosphere was added simultaneously *para*-xylylenediamine (1.78 g, 13.1 mmol) in anhydrous chloroform (50 mL) and isophthaloyl dichloride (2.65 g, 13.1 mmol) in anhydrous chloroform (50 mL) by syringe pump over the course of 3h. The reaction was allowed to stir for 14 h before being filtered, the organics washed with dilute acid (3 x 100 mL) and brine (3 x 100 mL), dried over Na_2SO_4, filtered and evaporated under reduced pressure. The crude product was purified by column chromatography (SiO_2, 4:1 $CHCl_3$ / CH_3COCH_3) to yield a slightly impure product

2.8 (50 mg, 3.8 %); ^{1}H NMR (400 MHz, $CDCl_3$) * denotes macrocycle protons δ 8.25 (2H, s, ArH*), 8.15 (4H, bdd, ArH*), 7.60 (4H, t, J = 7.5 Hz, NH*), 7.56 (2H, t, J = 6.0 Hz, ArH*), 7.25- 7.11 (10H, m, Ph_2C), 7.02 (8H, s, ArH*), 6.99 (1H, bt, NH), 6.65 (1H, t, J = 6.0 Hz, NH), 5.99 (1H, t, J = 6.0 Hz, NH), 4.88 (1H, sextet, J = 5.0 Hz, C<u>H</u>OCO), 4.44 (8H, bddd$_{ABX}$, ArC<u>H</u>$_2$*), 3.65 (2H, bd, J = 6.0 Hz), 3.61 (1H, m, NHC<u>H</u>H'CHOCO), 3.21 (1H, m, NHCH<u>H</u>'CHOCO), 3.17 (2H, d, J = 6.0 Hz), 3.08 (2H, bdd), 1.86 (6H, s, (C<u>H</u>$_3$)$_2$CBr), 0.86 (9H, s, (C<u>H</u>$_3$)$_3$CSi), 0.04 (6H, 2s, (C<u>H</u>$_3$)$_2$Si); HRFAB-MS (3-NOBA matrix): *m/z* = 1194.43722 (calcd. for $C_{63}H_{73}BrN_7O_{10}Si$, [M]H+, 1194.43716).

2-Bromo-2-methyl-propionic acid 11-[2-(2-diphenylacetylamino-acetylamino)-acetoxy]-2-hydroxy-undecyl ester (2.10)



To a stirred mixture of (2-Diphenylacetylamino-acetylamino)-acetic acid 10,11-dihydroxy-undecyl ester **2.9** (1 g, 2 mmol) and triethylamine (0.87 g, 8.6 mmol) in CH_2Cl_2 (50 mL) under a nitrogen atmosphere was added 2-bromo-2-methyl-propanoyl bromide (0.99 g, 0.53 mL, 4.3 mmol) in CH_2Cl_2 (10 mL) over 10 min. The reaction was allowed to stir for 1 h. The reaction was then washed with sodium bicarbonate solution (3 x 50 mL), dilute acid (3 x 50 mL) and brine (3 x 50 mL), dried over Na_2SO_4, filtered and evaporated to dryness under reduced pressure. The crude product was purified (SiO_2, Et_2O/EtOAc) to yield the desired product as a pale yellow oil (**2.10**, 740 mg, 57 %). ^{1}H NMR (400 MHz, $CDCl_3$) δ 7.38 -7.29 (10H, m, Ph), 6.57 (1H, t, J = 6.0 Hz, NH), 6.43 (1H, t, J = 6.0 Hz, NH), 5.02 (1H, s, Ph_2C<u>H</u>), 4.55 (1H, dd, J = 3.0Hz, 11.5 Hz, C<u>H</u>H'OCO), 4.18 (2H, t, J = 7.0 Hz, CH_2), 4.11 (1H, dd, J = 7.0 Hz, 11.5 Hz, CH<u>H</u>'OCO), 4.03 (4H, app. t, J = 6.0 Hz, 2 x NHC<u>H</u>$_2$), 3.92 (1H, m, C<u>H</u>OH), 1.98 (6H, s, (C<u>H</u>$_3$)$_2$CBr), 1.68-1.58 (4H, m, J = 7.0 Hz, 2 x CH_2), 1.53 (2H, m, CH_2),1.33 (10H, bs, 5 x CH_2); ^{13}C NMR (100 MHz, $CDCl_3$) δ

139.4, 129.4, 127.7, 77.9, 70.6, 66.6, 43.7, 41.7, 33.6, 31.1, 29.8, 29.7, 29.7, 29.4, 28.8, 26.1, 25.7.

2-Bromo-2-methyl-propionic acid 1-(*tert*-butyl-dimethyl-silanyloxymethyl)-10-[2-(2-diphenylacetylamino-acetylamino)-acetoxy]-decyl ester (2.12)

(The attempted synthesis of 2-Bromo-2-methyl-propionic acid 2-(*tert*-butyl-dimethyl-silanyloxy)-11-[2-(2-diphenylacetylamino-acetylamino)-acetoxy]-undecyl ester (**2.11**))

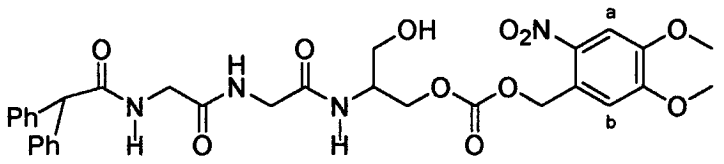
A solution of **2.10** (400 mg, 0.60 mmol), imidazole (123 mg, 1.8 mmol), *tert*-butyldimethylsiloxyl chloride (109 mg, 0.73 mmol) and a catalytic amount of 4-(dimethylamino)pyridine in CH_2Cl_2 (25 mL) was allowed to stir for 12 h. The reaction was washed with acid (3 x 25 mL), base (3 x 25 mL) and brine (3 x 25 mL), dried over Na_2SO_4, filtered and evaporated to dryness. The crude material was purified by column chromatography (SiO_2, Et_2O / EtOAc). No desired product **2.11** was observed, and the pure product **2.12** was obtained as an oil (**2.12**, 56 mg, 12 %). ^{1}H NMR (400 MHz, $CDCl_3$) δ 7.37- 7.26 (10H, m, Ph), 6.84 (1H, t, J = 6.0 Hz, NH), 6.64 (1H, t, J = 6.0 Hz, NH), 5.00 (1H, s, $Ph_2C\underline{H}$), 4.98- 4.92 (1H, m, C$\underline{H}$OCO), 4.14 (2H, t, J = 6.0 Hz, CH_2), 4.02 (2H, d, J = 6.0 Hz, NHC$\underline{H}_2$), 3.96 (2H, d, J = 6.0 Hz, NHC$\underline{H}_2$), 3.68 (2H, m, C$\underline{H}$H'OSi), 1.96 (6H, s, $(C\underline{H}_3)_2$CBr), 1.68 (4H, bs, 2 x CH_2), 1.31 (12H, bs, 6 x CH_2), 0.91 (9H, s, $(C\underline{H}_3)_3$CSi), 0.08 (6H, s, $(C\underline{H}_3)_2$Si); ^{13}C NMR (100 MHz, $CDCl_3$) δ 173.4, 170.0, 169.5, 139.44, 129.4, 127.8, 77.5, 76.8, 66.1, 64.5, 59.1, 56.7, 43.8, 41.6, 31.2, 30.7, 29.7, 28.9, 26.3, 25.3, -5.5.

***N*-({[(2-Hydroxy-1-hydroxymethyl-ethylcarbamoyl)-methyl]-carbamoyl}-methyl)-2,2-diphenyl-acetamide (2.13)**

(2-Diphenylacetylamino-acetylamino)-acetic acid ethyl ester **2.2** (740 mg, 2.08 mmol) and serinol (200 mg, 2.19 mmol) were refluxed in toluene (50 mL) overnight. The resulting off-white precipitate was filtered and recrystallised from ethanol / hexane to yield a white solid (**2.13**, 790 mg, 95 %); ^{1}H NMR (400 MHz, d_6-DMSO)

δ 8.51 (1H, t, J = 6.0 Hz, NH), 8.10 (1H, t, J = 6.0 Hz, NH), 7.55 (1H, d, J = 7.0 Hz, NH), 7.33 – 7.22 (10H, m, Ph), 5.08 (1H, s, $Ph_2C\underline{H}$), 4.61 (2H, t, OH), 3.79 (2H, d, J = 6.0 Hz, $NC\underline{H}_2$), 3.73 (2H, d, J = 6.0 Hz, $NHC\underline{H}_2$), 3.71 (1H, m, $NC\underline{H}$), 3.40 (4H, t, J = 6.0 Hz, $C\underline{H}_2O$); ^{13}C NMR (100 MHz, d_6-DMSO) δ 171.9, 169.2, 168.8, 140.7, 129.0, 128.6, 127.0, 60.4, 56.5, 53.3, 42.6, 42.3; HRFAB-MS (3-NOBA matrix): m/z = 400.18736 (calcd. for $C_{21}H_{26}N_3O_5$, $[M]H^+$, 400.18725).

Carbonic acid 4,5-dimethoxy-2-nitro-benzyl ester 2-[2-(2-diphenylacetylamino-acetylamino)-acetylamino]-3-hydroxy-propyl ester (2.14)



To a stirred solution of **2.13** (500 mg, 1.25 mmol) in pyridine (2 mL) and chloroform (10 mL) and dimethylformamide (1 mL) was added nitroveratrylchloroformate (260 mg, 0.94 mmol) in one aliquot. The reaction was monitored by TLC until no starting chloroformate remained. The reaction was washed with 1M HCl (3 x 25 mL), water (25 mL), dried over $MgSO_4$ and evaporated to dryness. The crude product was purified by column chromatography (silica, ethyl acetate) to collect the pure product as a yellow solid (**2.14**, 450 mg, 56 %). ^1H NMR (400 MHz, $CDCl_3$) δ 7.71 (1H, s, Ph_a), 7.38 – 7.22 (10 H, m, Ph), 7.04 (1H, s, Ph_b), 6.90 (1H, d, J = 7.0 Hz), 6.65 (1H, t, J = 6.0 Hz, NH), 6.49 (1H, t, J = 6.0 Hz, NH), 5.54 (2H, d_{AB}, J = 2.0 Hz, $PhC\underline{H}_2$), 4.99 (1H, s, $Ph_2C\underline{H}$), 4.23 (2H, d, J = 6.0 Hz, $C\underline{H}_2OCO$), 4.12 (1H, bm, $NC\underline{H}$), 4.06 – 3.97 (3H, s, OMe), 3.95 (3H, s, OMe), 3.91 – 3.76 (4H, m, 2 x NCH_2), 3.58 – 3.47 (1H, bm, $C\underline{H}H'OH$), 3.44 – 3.46 (1H, bm, $CH\underline{H}'OH$), 3.31 – 3.34 (1H, bm, $CHH'O\underline{H}$); ^{13}C NMR (100 MHz, $CDCl_3$) δ 173.2, 169.3, 154.8, 154.1, 148.9, 140.2, 139.3, 129.2, 127.9, 126.4, 110.9, 108.6, 67.3, 66.6, 63.9, 59.1, 57.0, 56.8, 47.8, 44.1;

2-Bromo-2-methyl-propionic acid 3-(4,5-dimethoxy-2-nitro-benzyloxycarbonyloxy)-2-[2-(2-diphenylacetylamino-acetylamino)-acetylamino]-propyl ester (2.15)

To a stirred solution of **2.14** (1.14 g, 1.78 mmol), 2-bromo-2-methylpropionic acid (0.45 mg, 2.68 mmol) and DMAP (0.33 g, 2.68 mmol) in CH_2Cl_2 (50 mL) at 0°C was added EDCI (0.51 g, 2.68 mmol). The reaction was left to stir overnight. TLC analysis showed the reaction to be complete and the reaction was washed with 1M HCl (3 x 50 mL), saturated $NaHCO_3$ (3 x 50 mL) and water (50 mL), dried over $MgSO_4$ and evaporated to dryness to yield the crude product as a yellow solid. The product was purified by column chromatography (silica, 3 % methanol / CH_2Cl_2) to yield the pure thread as a yellow solid (**2.15**, 1.21 g, 94 %). ^{1}H NMR (400 MHz, $CDCl_3$) δ 7.69 (1H, s, Ph), 7.33 – 7.20 (10H, m, Ph), 7.01 (1H, s, Ph), 6.69 (1H, d, *J* = 7.0 Hz, NH), 6.65 (1H, t, *J* = 6.0 Hz, NH), 6.44 (1H, t, *J* = 6.0 Hz, NH), 5.55 (1H, AB, *J* = 14.0 Hz, C<u>H</u>H'Ph), 5.49 (1H, AB, *J* = 14.0 Hz, C<u>H</u>H'Ph), 4.97 (1H, s, $Ph_2C\underline{H}$), 4.47 (1H, m, NCH), 4.22 – 4.10 (4H, m, 2 x CH_2O), 3.97 (3H, s, OMe), 3.93 (3H, s, OMe), 3.92 – 3.81 (4H, m, 2 x NCH_2), 1.88 (3H, s, CH_3CBr), 1.87 (3H, s, CH_3CBr).

[2](1,7,14,20-Tetraaza-2,6,15,19-tetraoxo-3,5,9,12,16,18,22,25-tetrabenzocyclohexacosane)-2-bromo-2-methyl-propionic acid 3-(4,5-dimethoxy-2-nitro-benzyloxycarbonyloxy)-2-[2-(2-diphenylacetylamino-acetylamino)-acetylamino]-propyl ester rotaxane (2.16)

To a stirred solution of thread **2.15** (540 mg, 750 μmol) and triethylamine (2.53 mL, 18.0 mmol) in chloroform (25 mL) was added separate solutions of *p*-xylenediamine (1.22 g, 9.00 mmol) in chloroform (40 mL) and isophthaloyl chloride (2.3 g, 9.00 mmol) in chloroform (40 mL) dropwise over three hours. On completion the reaction was filtered and washed with 1M HCl (3 x 100 mL), saturated $NaHCO_3$ (3 x 100 mL), and water (3 x 100 mL), dried over $MgSO_4$ and evaporated to dryness. The crude mixture was redissolved in CH_2Cl_2 (5 mL) and washed through a silica plug with 4 % methanol / CH_2Cl_2 to yield the rotaxane product as a bright yellow solid (**2.16**, 40 mg, 4 %); ^{1}H NMR (400 MHz, d_6-DMSO) δ 8.43 (2H, bt, *J* = 1.5 Hz, ***C***), 8.35 (4H, bt, ***D***), 8.25 (1H, d, *J* = 6.0 Hz, N<u>H</u>CH), 8.01 (4H, dd, *J* = 1.5, 8.0 Hz, ***B***), 7.65 (1H, s, Ph), 7.64 – 7.59 (3H, m, ***A***, NH), 7.56 (1H, t, *J* = 6.0 Hz, NH), 7.25 –

7.12 (10H, m, Ph), 7.11 (1H, s, Ph), 7.01 (8H, s, ***F***), 5.41 (1H, AB, J = 13.5 Hz, CHH'Ph), 5.38 (1H, d_{AB}, J = 13.5 Hz, CHH'Ph), 5.03 (1H, s, Ph_2CH), 4.31 (4H, ABX, J = 2.5, 14.0 Hz, ***E***), 4.22 (4H, ABX, J = 4.0, 14.0 Hz, ***E***), 4.12 – 4.03 (5H, m, NCH, $C(CH_2)_2$), 3.86 (3H, s, OMe), 3.81 (3H, s, OMe), 3.10 (1H, ABX, J_{AB} = 17.0 Hz, $J_{AX} = J_{BX}$ = 5.0 Hz, NCHH'), 3.04 (1H, ABX, J_{AB} = 17.0 Hz, $J_{AX} = J_{BX}$ = 5.0 Hz, NCHH'), 2.93 (1H, ABX, J_{AB} = 17.0 Hz, $J_{AX} = J_{BX}$ = 5.0 Hz, NCHH'), 2.83 (1H, ABX, J_{AB} = 17.0 Hz, $J_{AX} = J_{BX}$ = 5.0 Hz, NCHH'), 1.80 (3H, s, CH_3CBr), 1.79 (3H, s, CH_3CBr); ^{13}C NMR (100 MHz, d_6-DMSO) δ 171.9, 170.8, 168.5, 166.4, 148.6, 140.4, 137.3, 137.1, 134.5, 130.8, 129.0, 128.9, 128.8, 128.5, 127.0, 126.2, 125.1, 112.4, 108.6, 66.5, 66.4, 63.8, 57.2, 56.5, 55.2, 47.1, 43.9, 43.8, 41.6, 30.4; HRFAB-MS (3-NOBA matrix): m/z = 1319.39410 (calcd. for $C_{67}H_{68}BrN_8O_{16}$, $[M]H^+$, 1319.39367).

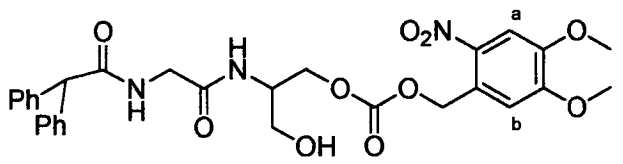
Diphenylacetylamino-acetic acid ethyl ester (2.17)

To a stirred solution of glycine ethyl ester hydrochloride (10 g, 71.6 mmol) and triethylamine (30.0 mL, 215 mmol) in CH_2Cl_2 (250mL) under a nitrogen atmosphere was added diphenylacetyl chloride (18.2 g, 78.8 mmol) in CH_2Cl_2 (50mL) dropwise over 1hr and left to stir for 24h. The reaction was then washed with saturated sodium bicarbonate solution (3 x 100mL) and water (3 x 100mL), dried over $MgSO_4$, filtered and concentrated under reduced pressure. Recrystallisation of the resulting yellow solid from toluene yielded the product as a white solid (**2.17**, 19.5 g, 92 %); ^1H NMR (400 MHz, d_6-DMSO) δ 8.72 (1H, t, J = 6.0 Hz, NH), 7.34 – 7.22 (10H, m, Ph), 5.05 (1H, s, Ph_2CH), 4.09 (2H, q, J = 7.0 Hz, OCH_2), 3.87 (2H, d, J = 6.0 Hz, NCH_2), 1.17 (3H, t, J = 7.0 Hz, CH_3); ^{13}C NMR (100 MHz, d_6-DMSO) δ 173.1, 168.8, 140.7, 128.9, 128.6, 127.0, 62.2, 56.6, 42.5, 14.5; HRFAB-MS (3-NOBA matrix): m/z = 298.14438 (calcd. for $C_{18}H_{20}NO_3$, $[M]H^+$, 298.14432).

***N*-[(2-Hydroxy-1-hydroxymethyl-ethylcarbamoyl)-methyl]-2,2-diphenyl-acetamide (2.18)**

A solution of **2.17** (12.0 g, 42 mmol) and serinol (4.06 g, 0.045 mmol) was refluxed in toluene overnight. The reaction was allowed to cool and the resulting off-white precipitate was filtered and recrystallised from ethanol / hexane to yield the product as a white solid (**2.18**, 12.5 g, 91 %). ^{1}H NMR (400 MHz, d_6-DMSO) δ 8.45 (1H, t, J = 6.0 Hz, NH), 7.60 (1H, d, J = 7.0 Hz, NH), 7.33 – 7.14 (10H, m, Ph), 5.09 (1H, s, $Ph_2C\underline{H}$), 4.67 (2H, t, J = 5.0 Hz, OH), 3.76 (2H, d, J = 6.0 Hz, NCH_2), 3.72 (1H, m, NCH), 3.40 (4H, m obscured by H_2O, CH_2O); ^{13}C NMR (100 MHz, d_6-DMSO) δ 171.7, 168.8, 140.7, 128.9, 128.6, 127.0, 60.3, 56.6, 53.2, 42.5; HRFAB-MS (3-NOBA matrix): m/z = 343.16571 (calcd. for $C_{19}H_{23}N_2O_4$, $[M]H^+$, 343.16578).

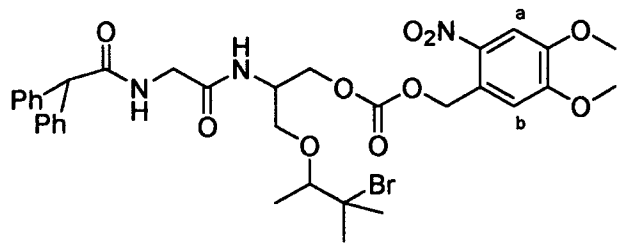
Carbonic acid 4,5-dimethoxy-2-nitro-benzyl ester 2-(2-diphenylacetylamino-acetylamino)-3-hydroxy-propyl ester (2.19)



To a solution of **2.18** (6 g, 17.6 mmol) in pyridine (20 mL) and chloroform (70 mL) and dimethylformamide (10 mL) was added nitroveratrylchloroformate (1 g, 3.6 mmol) in one aliquot. The reaction was monitored by TLC, and on consumption of starting material the reaction was diluted with diethyl ether. The precipitate of PN72 was filtered and washed with CH_2Cl_2. The remaining solution was washed with 1M HCl (3 x 100 mL) and water (100 ml), dried over $MgSO_4$ and evaporated to dryness. The crude product was purified by column chromatography (silica, 3% methanol / CH_2Cl_2) to yield a yellow solid (**2.19**, 680 mg, 32 %). ^{1}H NMR (400 MHz, $CDCl_3$) δ 7.71 (1H, s, Ph_a), 7.33 – 7.25 (10H, m, Ph), 7.04 (1H, d, J = 7.0 Hz, NH), 7.03 (1H, s, Ph_b), 6.92 (1H, bt, J = 6.0 Hz, NH), 5.54 (2H, d_{AB}, J = 2.0 Hz, $OC\underline{H}_2Ph$), 4.88 (1H, s, $Ph_2C\underline{H}$), 4.22 – 4.05 (3H, m, NCH, CH_2OCO), 3.86 (3H, s, OMe), 3.84 (4H, m, OMe, NC$\underline{H}$H'), 3.72 (1H, ABX, J = 5.0, 17.0 Hz, NCH$\underline{H}$'), 3.46 (1H, bt, $C\underline{H}_2OH$) 3.31 (2H, t, J = 6.0 Hz, $CH_2O\underline{H}$); ^{13}C NMR (100 MHz, $CDCl_3$) δ 173.2, 169.3, 154.8, 154.1, 148.9, 140.2, 139.3, 129.2, 127.9, 126.4, 110.9, 108.6, 67.3, 66.6, 63.9,

59.1, 57.0, 56.8, 47.8, 44.1; HRFAB-MS (3-NOBA matrix): *m/z* = 582.20795 (calcd. for $C_{29}H_{32}N_3O_{10}$, $[M]H^+$, 582.20877).

2-Bromo-2-methyl-propionic acid 3-(4,5-dimethoxy-2-nitro-benzyloxycarbonyloxy)-2-(2-diphenylacetylamino-acetylamino)-propyl ester (2.20)



To a stirred solution of **2.19** (680 mg, 1.17 mmol), DMAP (214 mg, 1.75 mmol) and 2-bromo-2-methylpropionic acid (293 mg, 1.75 mmol) in CH_2Cl_2 (40 mL) at 0°C was added EDCI (336 mg, 1.75 mmol). The reaction was stirred overnight. TLC analysis showed the reaction to be complete. The solution was washed with 1M HCl (3 x40 mL), saturated $NaHCO_3$ (3 x 40 mL) and water (40 mL), dried over $MgSO_4$ and evaporated to dryness to yield the crude product as a yellow solid. The product was purified by column chromatography (silica, CH_2Cl_2) to yield the pure thread as a yellow solid (**2.20**, 712 mg, 83 %). ^1H NMR (400 MHz, $CDCl_3$) δ 7.62 (1H, s, Ph_a), 7.24 – 7.14 (10H, m, Ph), 6.94 (1H, s, Ph_b), 6.88 (1H, d, *J* = 7.0 Hz, NH), 6.57 (1H, t, *J* = 6.0 Hz, NH), 5.46 (2H, s, $OC\underline{H}_2Ph$), 4.89 (1H, s, $Ph_2C\underline{H}$), 4.42 (1H, m ABX, NCH), 4.16 – 4.09 (4H, m ABX, 2 x CH_2O), 3.86 (8H, m, 2 x OMe , NCH_2), 1.80 (3H, s, $C\underline{H}_3CBr$), 1.79 (3H, s, $C'H_3CBr$); ^{13}C NMR (100 MHz, $CDCl_3$) δ 173.4, 171.7, 169.3, 154.8, 154.1, 148.9, 140.2, 139.3, 129.2, 127.9, 126.4, 110.9, 108.6, 67.3, 66.6, 63.9, 59.1, 57.0, 56.8, 56.0, 47.8, 44.1, 31.0, 30.9; HRFAB-MS (3-NOBA matrix): *m/z* = 730.16131 (calcd. for $C_{33}H_{37}BrN_3O_{11}$, $[M]H^+$, 730.16115).

[2](1,7,14,20-Tetraaza-2,6,15,19-tetraoxo-3,5,9,12,16,18,22,25-tetrabenzocyclohexacosane)-2-bromo-2-methyl-propionic acid 3-(4,5-

dimethoxy-2-nitro-benzyloxycarbonyloxy)-2-(2-diphenylacetylamino-acetylamino)-propyl ester rotaxane (2.21)

To a stirred solution of thread **2.20** (500 mg, 684 μmol) and triethylamine (1.04 mL, 10.3 mmol) in chloroform (25 mL) was added separate solutions of *p*-xylenediamine (560 mg, 4.11 mmol) in chloroform (20 mL) and isophthaloyl chloride (890 mg, 4.11 mmol) in chloroform (20 mL) dropwise over three hours. On completion the reaction was washed through a silica plug with 10 % methanol / CH_2Cl_2 to remove the solids and triethylamine, then evaporated to dryness. The crude mixture was purified by column chromatography (silica, 3% methanol / CH_2Cl_2) to recover the unconsumed thread (300 mg, 60 %) and to yield the pure rotaxane product as a bright yellow solid (**2.21**, 190 mg, 22%). ^{1}H NMR (400 MHz, $CDCl_3$) δ 8.19 (2H, s, C), 8.09 (4H, t, J = 6.0 Hz, B), 7.53 (4H, m, A, Ph_a, NH), 7.34 (4H, bdt, D), 7.28 – 7.14 (10H, m, Ph), 6.96 (8H, s, F), 6.81 (1H, s, Ph_b), 5.86 (1H, bt, NH), 5.46 (1H, d_{AB}, J = 13.0 Hz, OCHH'Ph), 5.18 (1H, d_{AB}, J = 13.0 Hz, OCHH'Ph), 4.54 – 4.45 (4H, bm, E), 4.40 (1H, s, Ph_2CH), 4.37 – 4.31 (4H, bm, E'), 4.29 – 4.27 (1H, bm, NCH), 4.18 – 4.07 (4H, bm, CH_2O, $C'H_2O$), 3.96 (3H, s, OMe), 3.86 (3H, s, OMe), 2.64 (2H, dq, J = 4.0 Hz, 18 Hz, NCH_2), 1.83 (3H, s, CH_3CBr), 1.81 (3H, s, CH_3CBr); ^{13}C NMR (100 MHz, $CDCl_3$) δ 172.5, 171.5, 169.9, 167.1, 154.8, 149.0, 140.1, 139.0, 137.7, 134.7, 134.6, 134.4, 131.7, 129.5, 129.4, 129.2, 129.8, 128.0, 125.7, 124.8, 111.5, 108.8, 67.7, 66.2, 63.4, 61.8, 58.7, 56.9, 56.0, 48.2, 44.6, 42.5, 30.8; HRFAB-MS (3-NOBA matrix): m/z = 1262.37275 (calcd. for $C_{65}H_{65}BrN_7O_{15}$, $[M]H^+$, 1262.37220).

Typical Polymerisation Procedure

Polymerisation reactions were carried out at 90 °C using *N*-(*n*-pentyl)-2-pyridyl-methanimine as bidentate ligand for copper complexation. A typical polymerisation recipe is based on 30-volume % monomer in toluene. The ratio of monomer:initiator:CuBr:ligand is 150:1:1:2 on a molar basis.

For Poly(Methyl Methacrylate) (pMMA):

Rotaxane initiator (**2.21**, 23.6 mg, 18.7 μmol), monomer (0.3 mL, 2.8 mmol), d_8-toluene (0.6 mL), and ligand (6.6 mg, 37.4 μmol) were charged into a NMR tube fitted with a Young tap, which was placed under an inert nitrogen atmosphere by one freeze-pump-thaw cycle. Copper(I) bromide (0.1 mL, 2.7 mg, 18.7 μmol) from a degassed stock solution in toluene under inert atmosphere was added to the NMR tube, and the contents shaken. The NMR tube placed in the NMR spectrometer, heated to 90 °C, and ^{1}H NMR spectra (shimmed on dummy sample of d_6-toluene) were taken every minute. After 125 minutes (64 % conversion) the sample was removed from the spectrometer. The reaction was passed through a plug of alumina with dichloromethane, and the product purified by precipitation in *n*-hexane.

Octadecanoyl chloride (Stearic acid chloride)

Stearic acid (3 g, 10.6 mmol) was dissolved in methylene chloride (20 mL) and stirred vigorously. Dimethylformamide (1 mL) was added to catalyse the reaction. Oxalyl chloride, 2M in CH_2Cl_2, (5.3 mL, 10.6 mmol) was added dropwise over one hour and the reaction was allowed to proceed until effervescence was no longer observed. The completed reaction was evaporated to dryness. The product was used without further purification. ^{1}H NMR (400 MHz, $CDCl_3$) δ 2.32 (2H, t, J = 8.0 Hz, α-CH_2), 1.63 (2H, bt, J = 8.0 Hz, β-CH_2), 1.36 – 1.26 (28H, bs, CH_2), 0.89 (3H, bt, J = 6.0 Hz); ^{13}C NMR (100 MHz, $CDCl_3$) δ 174.9, 34.5, 32.3, 30.1, 30.0, 29.8, 29.7, 29.6, 29.5, 25.3, 23.0, 14.5.

Octadecanoic acid 3-(4,5-dimethoxy-2-nitro-benzyloxycarbonyloxy)-2-(2-diphenylacetylamino-acetylamino)-propyl ester (2.22)

To a stirred solution of **2.19** (120 mg, 206 μmol) and triethylamine (24 μL, 172 μmol) in methylene chloride (25 mL) was added a solution of Octadecanoyl chloride (Stearic acid chloride) (63 mg, 208 μmol), synthesised in the previous step, in methylene chloride (10 mL) dropwise. The reaction was allowed to stir for one hour and was then washed with 1M HCl (3 x40 mL), saturated $NaHCO_3$ (3 x 40 mL) and

water (40 mL), dried over $MgSO_4$ and evaporated to dryness to yield the pure product as a yellow oil (**2.22**, 170 mg, 91%). ^{1}H NMR (400 MHz, $CDCl_3$) δ 7.72 (1H, s, Ph_a), 7.34 – 7.24 (10H, m, Ph), 7.04 (1H, s, Ph_b), 6.78 (1H, d, J = 7.0 Hz, NH), 6.57 (1H, t, J = 6.0 Hz, NH), 5.55 (2H, s, $OC\underline{H}_2Ph$), 4.98 (1H, s, $Ph_2C\underline{H}$), 4.42 (1H, m ABX, NCH), 4.27 – 4.04 (4H, m ABX, 2 x CH_2O), 3.96 (8H, m, 2 x OMe , NCH_2), 2.27 (2H, t, J = 7.0 Hz, $O_2CC\underline{H}_2$), 1.58 (2H, bm, $O_2CCH_2C\underline{H}_2$), 1.26 (28H, bs, 14 x $C\underline{H}_2$), 0.89 (3H, bt, J = 7.0 Hz, $C\underline{H}_3$); ^{13}C NMR (100 MHz, $CDCl_3$) δ 173.9, 173.3, 169.3, 154.8, 154.1, 148.8, 139.3, 139.2, 129.2, 129.2, 129.2, 129.2, 127.8, 127.8, 127.8, 126.5, 110.7, 110.7, 108.6, 77.7, 77.4, 77.1, 67.2, 66.7, 62.5, 59.0, 57.0, 56.9, 56.8, 56.8, 47.9, 47.9, 44.1, 34.3, 32.3, 30.1, 30.0, 29.8, 29.7, 29.6, 29.5, 25.1, 23.0, 14.5.

[2](1,7,14,20-Tetraaza-2,6,15,19-tetraoxo-3,5,9,12,16,18,22,25-tetrabenzocyclohexacosane)-octadecanoic acid 3-(4,5-dimethoxy-2-nitro-benzyloxycarbonyloxy)-2-(2-diphenylacetylamino-acetylamino)-propyl ester rotaxane (2.24)

To a stirred solution of thread **2.22** (170 mg, 188 μmol) and triethylamine (378 μL, 2.82 mmol) in chloroform (10 mL) was added separate solutions of *p*-xylenediamine (153 mg, 1.13 mmol) in chloroform (10 mL) and isophthaloyl chloride (225 mg, 1.13 mmol) in chloroform (10 mL) dropwise over two hours. On completion the reaction was washed through a silica plug with 10 % methanol / CH_2Cl_2 to remove the solids and triethylamine, then evaporated to dryness. The crude mixture was purified by column chromatography (silica, 2% methanol / CH_2Cl_2) to recover the unconsumed thread (**2.22**, 50 mg, 29 %) and to yield the pure rotaxane product as a bright yellow powder (**2.24**, 42 mg, 25%); ^{1}H NMR (400 MHz, $CDCl_3$) δ 8.19 (2H, s, C), 8.09 (4H, t, J = 6.0 Hz, B), 7.82 (1H, bs, NH), 7.53 (4H, m, A, Ph_a), 7.34 (4H, dt, J = 5.0 17.0 Hz, D), 7.22 (8H, m, Ph), 7.14 (2H, m, Ph), 6.98 (8H, s, F), 6.81 (1H, s, Ph_b), 5.73 (1H, bt, NH), 5.46 (1H, d_{AB}, J = 14.0 Hz, OC$\underline{H}$H'Ph), 5.18 (1H, d_{AB}, J = 14.0 Hz, OCH$\underline{H}$'Ph), 4.54 – 4.45 (4H, bm, E), 4.37 – 4.31 (5H, bm, $Ph_2C\underline{H}$, NC$\underline{H}$*, E'), 4.18 – 4.00 (4H, bm, CH_2O, C'H_2O), 3.96 (3H, s, OMe), 3.85 (3H, s, OMe), 2.72 (2H, dq, J = 4 Hz, 18 Hz, NCH_2), 2.21 (2H, t, J = 7.0 Hz, $O_2CC\underline{H}_2$), 1.49 (2H,

bquintet, $O_2CCH_2C\underline{H}_2$), 1.34- 1.12 (28H, bm, 14 x $C\underline{H}_2$), 0.88 (3H, t, J = 7.0 Hz, $C\underline{H}_3$); ^{13}C NMR (100 MHz, $CDCl_3$) δ 173.6, 172.6, 169.8, 166.8, 154.8, 153.8, 140.1, 138.9, 137.6, 137.6, 134.3, 131.7, 131.7, 129.4, 129.4, 129.2, 129.1, 128.8, 128.1, 128.1, 125.5, 124.4, 111.6, 108.9, 72.7, 70.2, 68.5, 67.8, 66.5, 62.1, 58.6, 56.8, 48.4, 44.4, 32.3, 30.1, 30.1, 30.0, 30.0, 29.8, 29.7, 29.6, 29.5, 25.0, 23.0, 14.5.

Triacontanoic acid 3-(4,5-dimethoxy-2-nitro-benzyloxycarbonyloxy)-2-(2-diphenylacetylamino-acetylamino)-propyl ester (2.23)

To a stirred solution of **2.19** (64 mg, 0.11 mmol), Triacontanoic acid (50 mg, 0.11 mmol) and DMAP (27 mg, 0.22 mmol) in methylene chloride (30 mL) at 0°C was added EDCI (42 mg, 0.22 mmol). The reaction was left overnight, then washed with 1M HCl (3 x40 mL), saturated $NaHCO_3$ (3 x 40 mL) and water (40 mL), dried over $MgSO_4$ and evaporated to dryness to yield the product as a yellow oil (**2.23**, 65 mg, 58%); ^1H NMR (400 MHz, $CDCl_3$) δ 7.72 (1H, s, Ph_a), 7.34 – 7.24 (10H, m, Ph), 7.04 (1H, s, Ph_b), 6.58 (1H, d, J = 7.0 Hz, NH), 6.37 (1H, t, J = 6.0 Hz, NH), 5.55 (2H, s, $OC\underline{H}_2Ph$), 4.98 (1H, s, $Ph_2C\underline{H}$), 4.42 (1H, m ABX, NCH), 4.27 – 4.04 (4H, m ABX, 2 x CH_2O), 3.96 (8H, m, 2 x OMe, NCH_2), 2.27 (2H, t, J = 7.0 Hz, $O_2CC\underline{H}_2$), 1.58 (2H, bm, $O_2CCH_2C\underline{H}_2$), 1.26 (52H, bs, 26 x $C\underline{H}_2$), 0.89 (3H, bt, J = 7.0 Hz, $C\underline{H}_3$); ^{13}C NMR (100 MHz, $CDCl_3$) δ 173.9, 173.3, 169.3, 154.8, 154.1, 148.8, 139.3, 139.2, 129.4, 129.4, 128.0, 128.0, 127.8, 127.8, 127.8, 126.5, 110.7, 110.7, 108.6, 77.7, 77.4, 77.1, 67.2, 66.7, 62.5, 59.0, 57.0, 56.9, 56.8, 56.8, 47.9, 47.9, 44.1, 34.3, 32.3, 30.1, 30.0, 29.8, 29.7, 29.6, 29.5, 25.1, 23.0, 14.5.

[2](1,7,14,20-Tetraaza-2,6,15,19-tetraoxo-3,5,9,12,16,18,22,25-tetrabenzocyclohexacosane)-triacontanoic acid 3-(2-nitro-4,5-dimethoxy-benzyloxycarbonyloxy)-2-(2-diphenylacetylamino-acetylamino)-propyl ester rotaxane (2.25)

To a stirred solution of thread **2.23** (65 mg, 64 μmol) and triethylamine (127 μL, 910 μmol) in chloroform (10 mL) was added separate solutions of *p*-xylenediamine (49 mg, 360 μmol) in chloroform (10 mL) and isophthaloyl chloride (73 mg, 360 μmol)

in chloroform (10 mL) dropwise over two hours. On completion the reaction was washed through a silica plug with 10 % methanol / CH_2Cl_2 to remove the solids and triethylamine, then evaporated to dryness. The crude mixture was purified by column chromatography (silica, 2% methanol / CH_2Cl_2) to yield the pure rotaxane product as a bright yellow powder (**2.25**, 19 mg, 19%); ^{1}H NMR (400 MHz, $CDCl_3$) δ 8.19 (2H, s, C), 8.09 (4H, t, J = 6.0 Hz, B), 7.72 (1H, bs, NH), 7.53 (4H, m, A, Ph_a), 7.34 (4H, dt, J = 5.0, 17.0 Hz, D), 7.22 (8H, m, Ph), 7.14 (2H, m, Ph), 6.98 (8H, s, F), 6.81 (1H, s, Ph_b), 5.73 (1H, bt, NH), 5.46 (1H, d_{AB}, J = 13.0 Hz, OCHH'Ph), 5.18 (1H, d_{AB}, J = 13.0 Hz, OCHH'Ph), 4.54 – 4.45 (4H, bm, E), 4.37 – 4.31 (5H, bm, Ph_2CH, NCH*, E'), 4.18 – 4.00 (4H, bm, CH_2O, $C'H_2O$), 3.96 (3H, s, OMe), 3.85 (3H, s, OMe), 2.72 (2H, dq, J = 4.0 Hz, 18.0 Hz, NCH_2), 2.21 (2H, t, J = 7.0 Hz, O_2CCH_2), 1.49 (2H, bquintet, $O_2CCH_2CH_2$), 1.34- 1.10 (52H, bm, 26 x CH_2), 0.89 (3H, t, J = 7.0 Hz, CH_3).

2.5 References

(1) Balzani, V.; Credi, A.; Raymo, F. M.; Stoddart, J. F., *Angew. Chem. Int. Ed.*, **2000**, *39*, 3348-3391.

(2) Leigh, D. A.; Troisi, A.; Zerbetto, F., *Angew. Chem. Int. Ed.*, **2000**, *39*, 350-353.

(3) Lane, A. S.; Leigh, D. A.; Murphy, A., *J. Am. Chem. Soc.*, **1997**, *119*, 11092-11093.

(4) Anelli, P. L.; Spencer, N.; Stoddart, J. F., *J. Am. Chem. Soc.*, **1991**, *113*, 5131-5133.

(5) Herrmann, W.; Keller, B.; Wenz, G., *Macromolecules*, **1997**, *30*, 4966-4972.

(6) Mason, P. E.; Bryant, W. S.; Gibson, H. W., *Macromolecules*, **1999**, *32*, 1559-1569.

(7) Matyjaszewski, K.; Xia, J., *Chem. Rev.*, **2001**, *101*, 2921-2990; Matyjaszewski, K., *Chem. Eur. J.*, **1999**, *5*, 3095-3102.

(8) Leigh, D. A.; Moody, K.; Smart, J. P.; Watson, K. J.; Slawin, A. M. Z., *Angew. Chem., Int. Ed. Eng.*, **1996**, *35*, 306-310.

(9) Kidd, T. J.; Leigh, D. A.; Wilson, A. J., *J. Am. Chem. Soc.*, **1999**, *121*, 1599-1600.

(10) Leigh, D. A.; Murphy, A.; Smart, J. P.; Slawin, A. M. Z., *Angew. Chem., Int. Ed. Eng.*, **1997**, *36*, 728-732.

(11) Holmes, C., *J. Org. Chem.*, **1997**, *62*, 2370-2380.

Chapter 3

A Tight Fit: Rotaxane Formation with a Highly Preorganised Template Assisted by Aromatic Stacking Interactions

Declaration: All compounds besides thread **3.1** and rotaxane **3.2** have been reported elsewhere and were synthesised by persons other than the author, Phillip Nash.

3.1 Introduction

Aromatic interactions are probably the least understood of the weak non-covalent forces. Unlike hydrogen bonds, which are well understood, strong, single point electrostatic interactions with a well-defined geometry, aromatic interactions are much less well-defined. Due to their weak strength (~1- 2 kcal mol^{-1} compared to ~5-7 kcal mol^{-1} for N-H···O and O-H···O hydrogen bonds)[1] they usually play a secondary role in intermolecular associations, which has made their study and observation difficult. In fact, they may well have gone unnoticed until recently if it were not for the strongly-coloured charge-transfer complexes[2] that they sometimes form.*

A great deal of research in the last fifteen years[2,3] has seen an extension of the classical concept of hydrophobically driven association to the realisation of many different types of aromatic association (*e.g.* C-H···π, offset π–π stacking, edge-to-face, O-H···π hydrogen bonds).[4] As they can form associations in a variety of ways,

* These coloured charge-transfer complexes were for a long time considered to be the main contribution to aromatic associations. Since then it has been shown that electrostatic interactions are the dominant factor in determining associations, with charge transfer contributing very little to the overall stability. Charge-transfer is simply an occasional consequence of certain types of electrostatic interaction.

and the strength of these interactions is dependant of a number of factors (e.g. dispersion energies based on size / shape complementarity, electrostatic interactions based on quadrupole moment positioning or π-electron distributions, and desolvation effects) the prediction of potential associations is a non-trivial exercise.

Because of their weak strength, the contributions aromatic interactions make to the stability of intermolecular complexes is usually swamped by the stronger interactions essential to the formation of stable complexes in the first instance. As a result of this the importance of aromatic interactions was for a long time overlooked.[5]

Hunter and co-workers have carried out much research into the nature of aromatic interactions.[1,6] Until recently, these types of studies had to be done in the absence of other, stronger binding interactions, but he has designed an elegant system to determine the binding contribution from aromatic interactions in the presence of stronger intermolecular interactions using chemical double-mutant cycles (see figure 3.1).[7] These systems use hydrogen-bonding interactions to form strong intermolecular complexes, and then, by using the binding energies from a cycle of structurally-similar complexes, one can cancel the hydrogen-bonding contribution to the overall binging energy in the original system to obtain the contribution from only the aromatic stacking interactions.

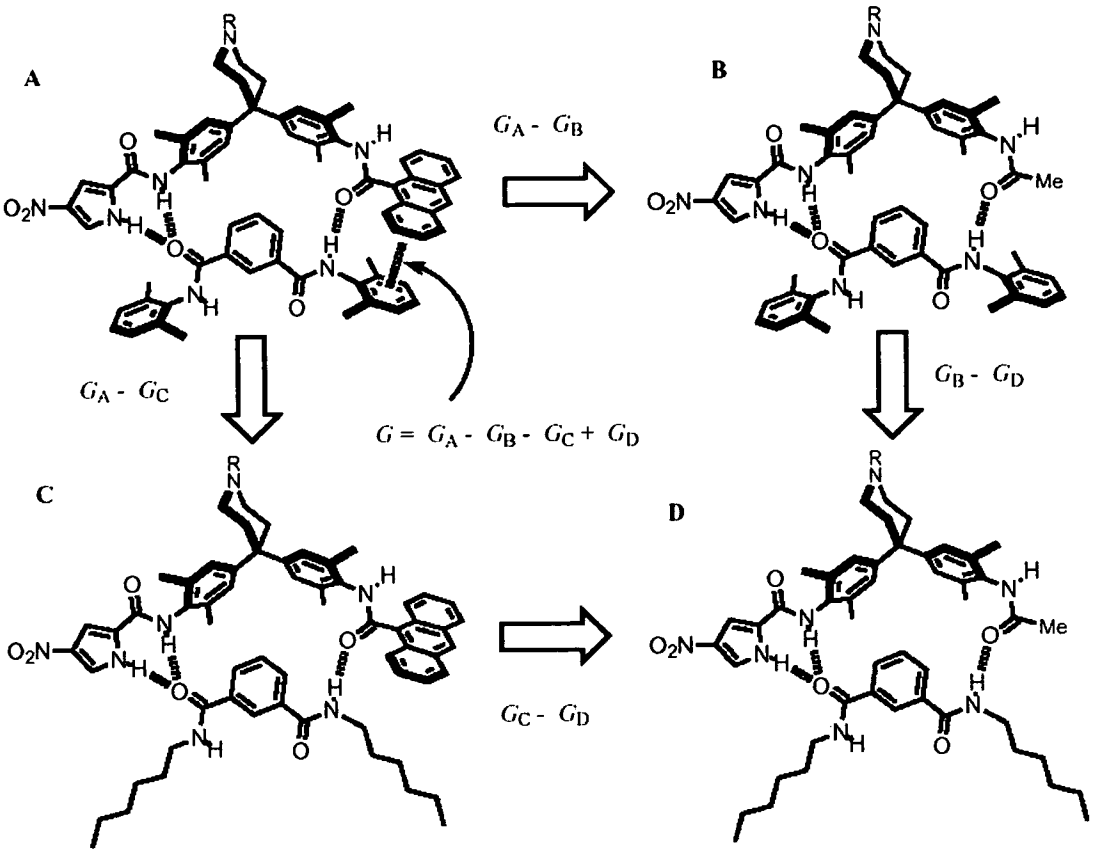


Figure 3. 1 Hunter's use of a chemical double-mutant cycle to measure aromatic stacking contributions to the overall association energy.

Stoddart has made use of aromatic stacking interactions to template rotaxane and catenane synthesis (see figure 3.2).[8,9] Despite the strongly-coloured charge-transfer complex that indicates a binding association involving aromatic stacking interactions, the main driving force for association is actually hydrogen-bonding from the α-protons of the bipyridinium unit to the oxygens of the crown ether.[8,10] In fact intermolecular associations are not formed in the absence of hydrogen bonding interactions.[11]

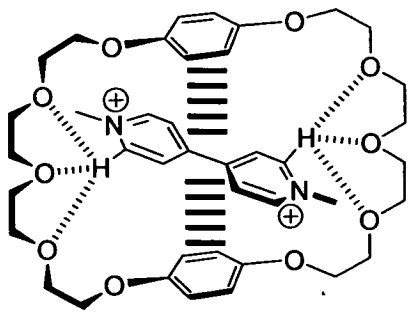


Figure 3. 2 Stoddart's aromatic stacking template, which makes use of hydrogen bonds to form complexes. The polarised nature of the α-CH bond allows it to act as a hydrogen-bond donor.

Hydrogen bonding interactions have been used by Leigh to template benzylic amide macrocycle formation around a suitable template by means of a five molecule condensation reaction to form rotaxanes (see figure 3.3).[12,13] The reaction proceeds via a linear macrocycle-precursor, which is relatively long-lived because the two reactive ends are far apart from one another in the preferred *syn-anti* conformation.[14,15] Binding to the thread forces the linear species to become the u-shaped, *syn-syn* conformation so that two bifurcated hydrogen bonds can be formed. This binding-event brings the two reactive ends of the macrocycle-precursor into close proximity, thereby favouring the ring-closing reaction, and forming the macrocycle around the thread, hence forming the rotaxane.

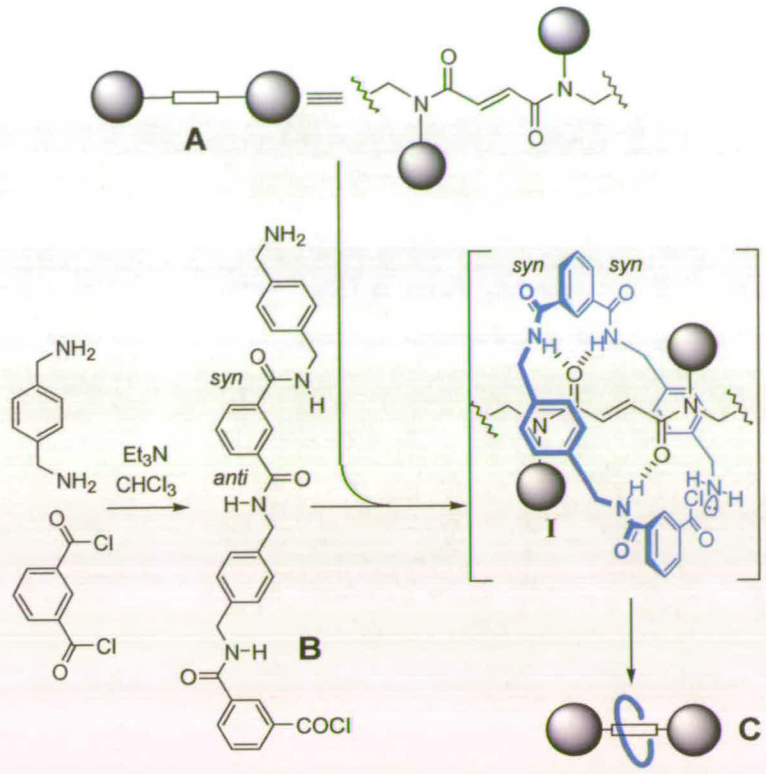


Figure 3. 3 Formation of a rotaxane (C) from a thread (A) via a linear, macrocycle-precursor (B).

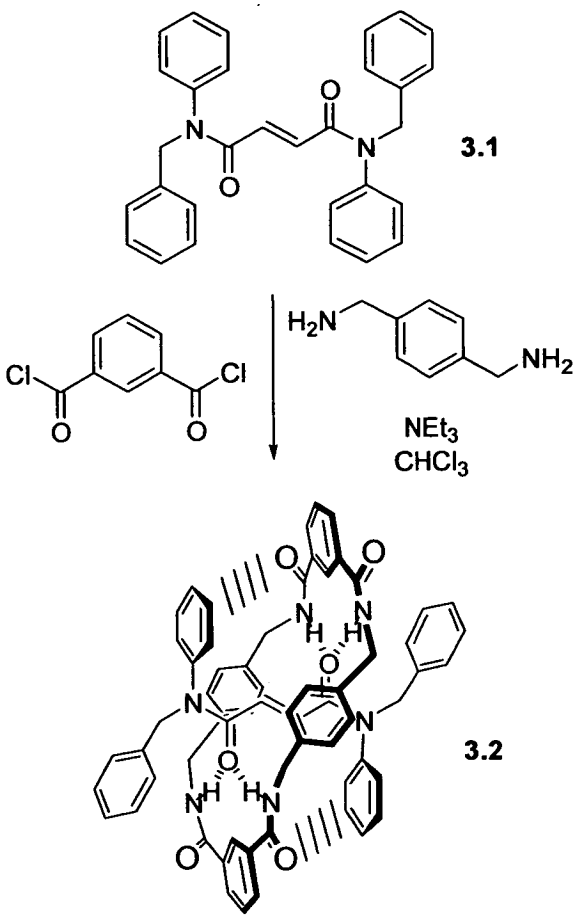
These rotaxanes have been shown to tolerate a wide range of structural diversity in the design of the thread and the components of the macrocycle.[12] A variety of amide-based threads have been shown to template rotaxane formation with a wide degree of success, with yields anywhere between 0.2- 97%. The ability of a template to form rotaxanes, in terms of its rotaxane yield, has been used to determine the features necessary in a good template and improve our understanding of such systems.

Fumaramide based threads have produced the highest yields of rotaxanes (up to 97%) because of their rigidity and the way the hydrogen bond acceptors in the template are preorganised for rotaxane formation.[16] Tertiary amide-based fumaramide threads have also been used to form rotaxanes.[16-18] These benefit from much improved solubility and hence, better processability (*e.g.* larger scale reactions and purification are easier), but the associated disadvantages of tertiary amides have resulted in their less than widespread general use. Tertiary amide-based threads

produce lower yields of rotaxane, even with the ideally-arranged fumaramide template, because of steric repulsions. Another disadvantage of tertiary amides is due to the partial double bond character of the amide bond. This results in mixtures of rotamers, the populations of which are determined by the relative stabilities, and which exchange slowly in solution ($\Delta G^{\ddagger}$ ~18- 20 kcal mol^{-1}). This problem is further complicated in systems with asymmetrical tertiary amides (*i.e.* $R^1CONR^2R^3$). These mixtures of rotamers tend to become even more complicated in rotaxane systems where the macrocycle can influence the rotamer populations, presumably for steric reasons, to give different populations of Z,Z-, Z,E- and E,E- amide rotamers. The ^1H NMR spectra of these rotaxanes tend to be complicated and are not easily interpreted.

Here we describe the synthesis of a novel tertiary amide-based [2]rotaxane in high yield. The high yielding template incorporates N-aryl amide moieties, which appear as a single rotamer in solution and in the solid-state. The N-aryl group employs aromatic stacking interactions to assist in the templating of the macrocycle-precursor during rotaxane formation, and thus overcomes the steric repulsions usually associated tertiary amide units. The thread and macrocycle show a good size/ shape complementarity that is key to strong aromatic interactions.

3.2 Results and Discussion



Scheme 3. 1 Rotaxane formation via rigid tertiary-fumaramide template.

The bis(N-benzyl-N-phenyl-)fumaramide thread, **3.1**, was synthesised in one step from the commercially available fumaryl chloride and N-benzylaniline in 96% yield. Only one set of ^{1}H NMR signals can be observed in solution, which denotes that one of the rotamer conformations is much more stable. NOESY NMR showed that the dominant rotamer was determined to have the N-aryl ring in a transoid arrangement to the carbonyl group (as drawn in scheme 3.1). Prior research into N-aryl tertiary amides has found that the aromatic ring is not conjugated with the amide group and prefers to sit orthogonal.[19] This suggests that steric repulsion between the ring protons and carbonyl (in the cisoid rotamer) and the fumaramide double-bond proton (in the preferred transoid rotamer) is a more important factor in determining the

conformations than the electronic stabilisation affording by the extended conjugation of the π-system.

Treatment of **3.1** with six equivalents of *p*-xylylene diamine and isophthaloyl dichloride ($CHCl_3$, Et_3N, 3 h, ~10 mM) resulted in complete consumption of the thread. The crude reaction mixture was purified by column chromatography to give the rotaxane **3.2** in 94% yield (see scheme 3.1). This high-yield is remarkable in that the thread contains two tertiary amides, usually considered poor templates for rotaxane formation. This fact is highlighted by comparing the contrasting rotaxane yields obtained from a variety of threads based on the rigid fumaramide template (see figure 3.4 and table 3.1).

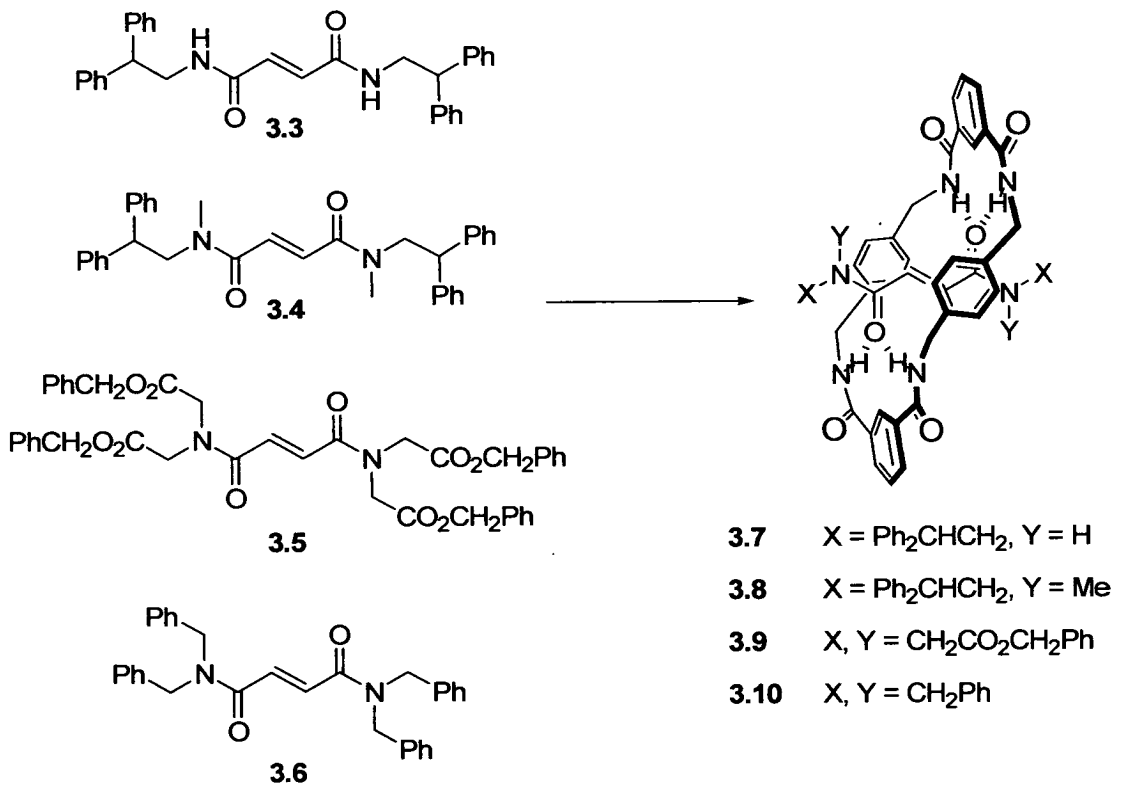


Figure 3.4 Various fumaramide-based threads, 3.3- 3.6, that have been used to template rotaxane formation, 3.7- 3.10 respectively.

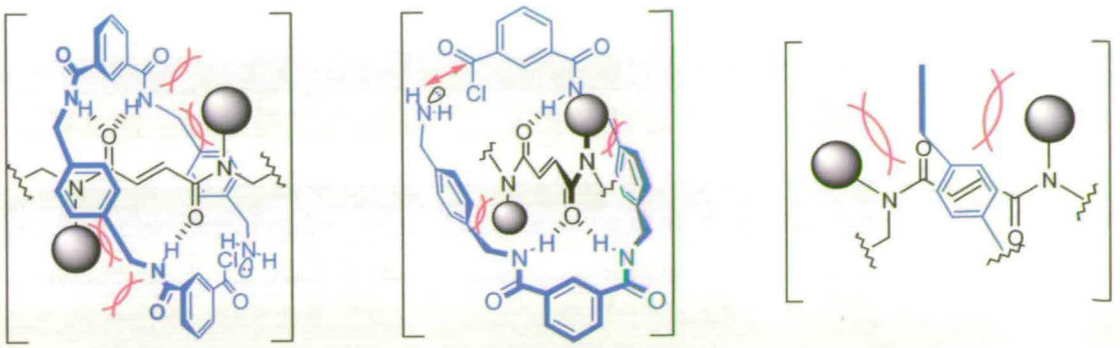
Thread	[2]Rotaxane yield %
3.1	94
3.3[16]	97
3.4[18]	33
3.5[16]	67
3.6[17]	60

Table 3.1 Table of threads with respective [2]rotaxane yields.

The success of the fumaric template has been highlighted by the secondary amide based template, **3.3** which gives [2]rotaxane in a "world record" 97%. On replacing secondary amides with tertiary amides in the thread, the rotaxane yield is seen to drop significantly. The N,N'-dimethylated thread, **3.4**, gives an especially low 33% yield of rotaxane. This is probably a consequence of steric mismatching of the {E,E}- and /or {E,Z}- tertiary amide rotamers with the macrocycle-precursor, *i.e.* the E- rotamer conformations present the very bulky stopper group towards the macrocycle binding sites and effectively templating is 'switched-off' when these rotamers are present. Better yields are obtained with the symmetrical tertiary amide templates, **3.5** and **3.6**, with yields of 67% and 60% respectively. Although each amide in these threads has two identical bulky substituents, compared to the N,N'-dimethylated thread **3.4** which has one small and one very large substituent, the benzyl and benzyl ester groups of **3.5** and **3.6** respectively must be sufficiently small so as to not block the hydrogen bonding sites, unlike the 2,2-diphenylethyl group in **3.4**.

The N,N'-diphenyl thread **3.1** is clearly an exception to the observed trend generating rotaxane in 94% yield. An explanation for the observed lower yields for tertiary amide threads can be given as they present a larger steric bulk than secondary amide threads (see figure 3.5), and have two fewer hydrogen bond donors to provide extra hydrogen bonding interactions.*

* Although amide protons are often not seen to provide hydrogen bonds in the solid –state structure of fumaramide-based rotaxanes, evidence for their role is provided by an associated downfield chemical shift compared to the thread in the ^{1}H NMR spectrum. Although their role appears to be secondary in



I II III

Figure 3. 5 I) Steric repulsions between tertiary amide substituents and macrocycle precursor that disfavour the clipping reaction in rotaxane sysnthesis (only steric interactions from one tertiary amide substiuent are shown in any diagram for clarity). II) How repulsive interactions with the xylylene units disfavours ring closing. III) How the hydrogen bonding interaction responsible for binding the macrocycle-precursor may be strained by steric repulsions.

Single crystals of **3.2** suitable for investigation by X-ray crystallography by SMART diffractometer were obtained by slow evaporation of a dichloromethane / methanol solution. The crystal structure (see figure 3.6) shows that the amides of the macrocycle form four bifurcated hydrogen bonds with the amide carbonyls of the thread and that the macrocycle sits in an energetically favourable chair conformation. The electron-rich N-phenyl of the thread also forms an offset π–π stack with the electron-deficient isophthaloyl unit of the macrocycle. The observed interaromatic separation of approximately 3.5 Å is also optimal for aromatic stacking interactions. The desire for the isophthaloyl unit to associate in a π–π stack is such that the amides of the macrocycle are no longer co-planar with the isophthaloyl unit, but twisted into a less-energetically favourable out-of-plane conformation with torsion angles of 169.0° and 157.7°.

---

the stabilisation of the rotaxane, they may be important in templating the macrocycle-precursor. They do however provide an entropic stabilisation, by providing more low energy degrees of freedom for the immobilised macrocycle and helping to facilitate the pirouetting motion of the macrocycle.

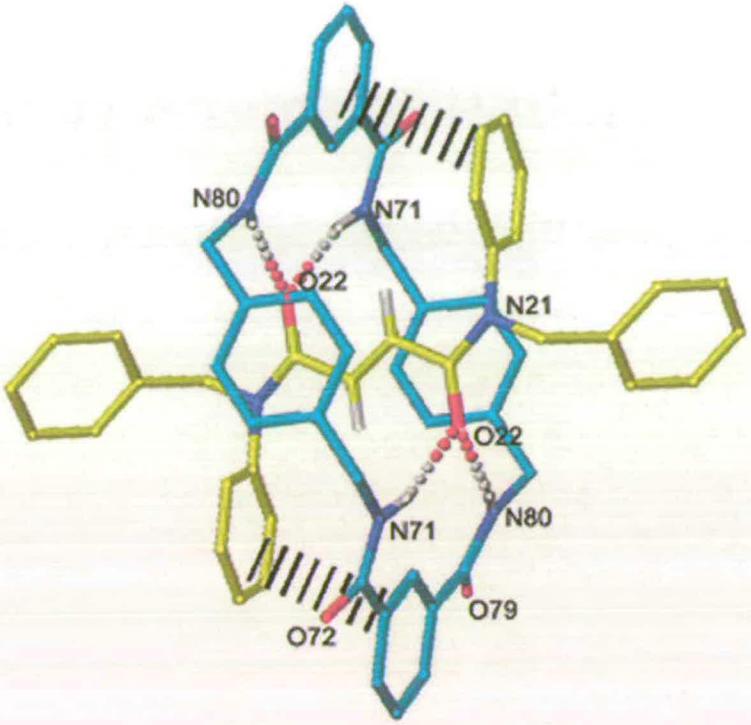


Figure 3. 6 X-ray crystal structure of the fumaramide [2]rotaxane 3.2 (for clarity one structure in the unit cell is omitted, macrocyclic carbon atoms are coloured blue, and thread carbon atoms are yellow; oxygen atoms are red, nitrogen dark blue, and selected hydrogen white. Only one of symmetrically equivalent heteroatoms has been labelled. Intramolecular hydrogen bond distances (Å) are the following: O22-HN71 2.15, O22-HN80 2.45. Interaromatic distance (as indicated) is estimated to be 3.5 Å.

The effect the aromatic stacking interaction has on the solid-state structure is highlighted by looking at the crystal structure of the secondary fumaramide rotaxane **3.7** (see figure 3.7). The macrocycle again sits in a chair conformation and forms four bifurcated hydrogen bonds with the thread. The thread hydrogen bond-donors are satisfied by intermolecular interactions with dimethylformamide, which also pack to form π-stacks between the isophthaloyl and stopper-phenyl groups. In this case, the macrocycle amides sit in-plane with the isophthaloyl unit.

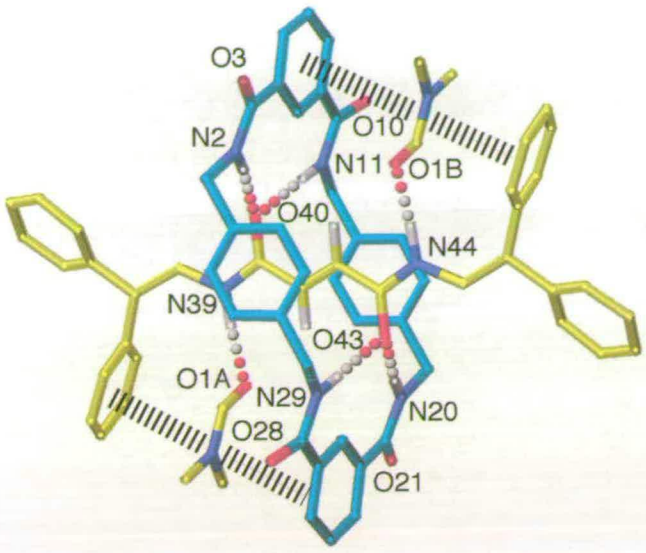


Figure 3. 7 X-ray crystal structure of the fumaramide [2]rotaxane 3.7. Intramolecular hydrogen bond distances (Å): O40–HN2/O43–HN20 1.98, O40–HN11/O43–HN29 2.06.

On comparing the two crystal structures, it becomes apparent that the aromatic stacking interaction is quite significant. In both structures the macrocycles form bifurcated hydrogen bonds. In secondary amide rotaxane **3.7**, both hydrogen bond distances are similar at 1.98 Å and 2.06 Å, but in tertiary amide rotaxane **3.2** one of the bifurcated hydrogen bonds is significantly longer with distances 2.15 Å and 2.45 Å. This is a result of the isophthaloyl unit straining the hydrogen bonds to maximise its interaction with the N-phenyl group. The energetic stabilisation offered by this interaction must be fairly significant to offset the unfavourable weakening of an amide hydrogen bond, and the unfavourable twisting out-of-plane of the amides with the isophthaloyl unit.

The *N,N,N',N'*-tetrabenzyl thread **3.6** is closer in structure to the N-aryl thread **3.1** with both being tertiary amides. The crystal structure of the corresponding rotaxane **3.10** highlights the difference in intercomponent interactions between the two tertiary amide rotaxanes (see figure 3.8). Firstly, no stacking can be observed between the isophthaloyl unit and the benzyl groups. Secondly four strong hydrogen bonds with bond lengths 1.90 and 2.01 are present, which is more similar to the secondary amide

rotaxane **3.7** structure than that of the N-aryl rotaxane **3.2**. The amides of the macrocycle are out-of-plane with the isophthaloyl unit, although this is due to the isophthaloyl unit twisting to accommodate an intermolecular offset stack with a benzyl unit, which would not be a factor in solution.

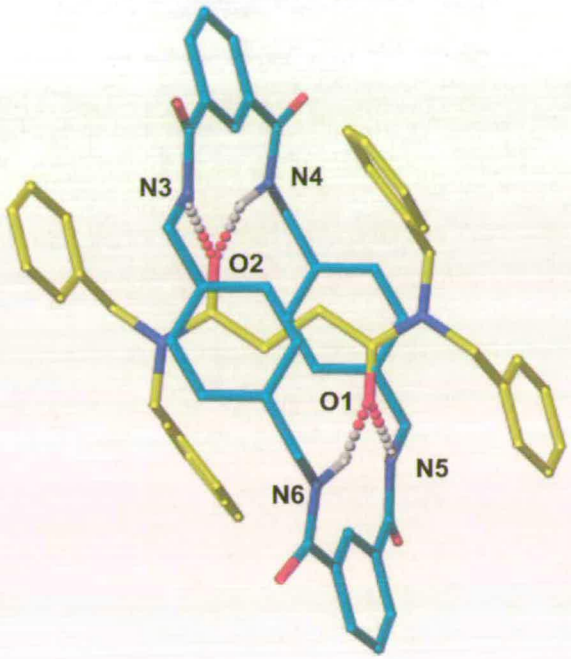


Figure 3. 8 X-ray crystal structure of [2]rotaxane 3.10. Intramolecular hydrogen bond distances (Å): O2–HN3/O1–HN5 1.90, O2–HN4/O1–HN6 2.01.

The crystal structure of the methylated rotaxane **3.8** shows that the macrocycle adopts a strange, almost linear conformation, but shows reasonably strong hydrogen bonds of 2.22 Å and 1.94 Å, and no evidence of any aromatic interactions that would assist in the templating of the macrocycle (see figure 3.9). Again, the tetrabenzyl ester rotaxane **3.9** shows no evidence of an aromatic interaction that would assist in the formation of rotaxane (see figure 3.10).

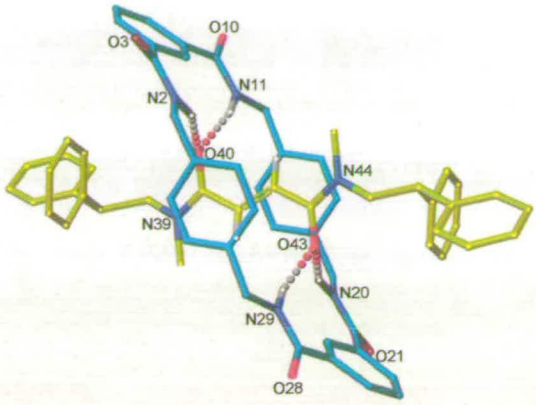


Figure 3. 9 X-Ray crystal structure of [2]rotaxane 3.8. Intramolecular hydrogen bond distances (Å): O40–HN2/O43–HN20 = 2.22, O40–HN11/O43–HN29 = 1.94.

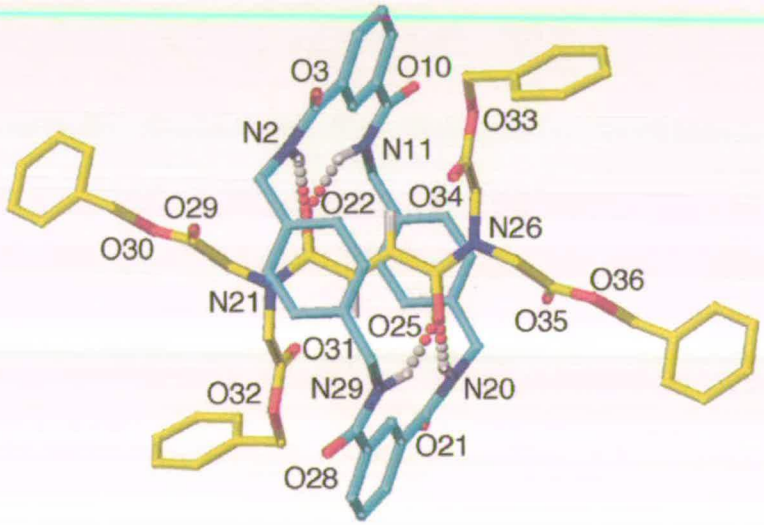


Figure 3.10 X-ray crystal structure of the tertiary amide fumaramide [2]rotaxane 3.9. Intramolecular hydrogen bond distances (Å): O22–HN2/O25–HN20 2.16, O22–HN11/O25–HN29 2.40.

The solid-state structures of these rotaxanes do not give the full picture of the nature of this aromatic interaction. Using ^{1}H NMR allows us to discern important information on the solution-state structures of these rotaxanes. By comparing the ^{1}H NMR of the thread **3.1** and rotaxane **3.2** (see figure 3.11) it is possible to see the effect the aromatic stacking has on the rotaxane spectrum. The usual features associated with rotaxane are present. The protons of the fumaric double bond are

shifted 1.3 ppm upfield as a result of the shielding by the xylylene units. Evidence of a close N-phenyl / isophthalyl contact in solution, supporting a positive aromatic interaction, is shown by the shielding experienced by the N-phenyl protons (H_a). These N-phenyl protons are shifted upfield, with H_a experiencing the most shielding (0.96 ppm) as it sits directly above the centre of the isophthalyl aromatic ring, and with H_b shielded less (0.22 ppm) and H_c experiencing only a little shielding (0.08 ppm).

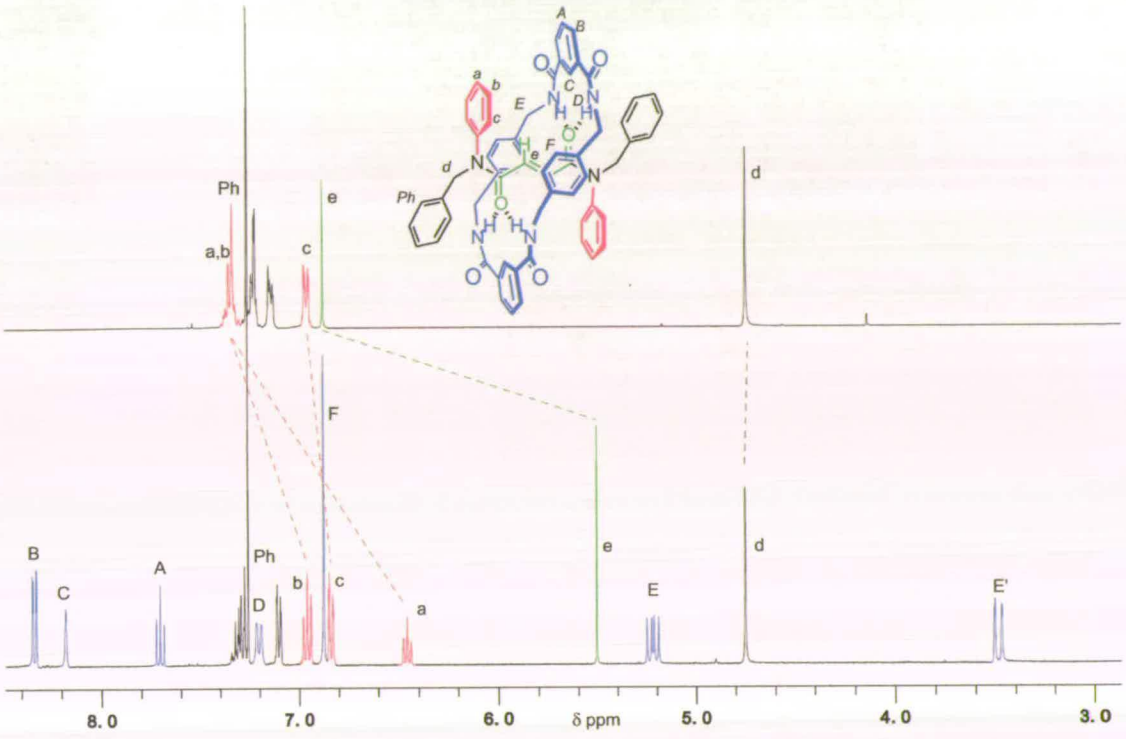


Figure 3. 11 ^{1}H NMR spectra ($CHCl_3$, 298K, 400 MHz) of thread 3.1 (top) and rotaxane 3.2 (bottom).

Comparing the rotaxane spectra for the N-phenyl rotaxane **3.2**, the secondary amide rotaxane **3.7** and the tetrabenzyl tertiary amide rotaxane **3.10** supports the argument for a favourable aromatic interaction, and highlights the differences between these rotaxanes in solution (see figure 3.12). The rotaxane spectra all show similar features indicating a similar solution state structure to each other, and to the crystal structures. The olefinic protons also experience a similar degree of shielding (compared to their respective threads) in all three rotaxanes ($\Delta\delta$ ~1.5 ppm). The relative shifts of the macrocycle amide protons H_D provides an indication as to the strength of the

hydrogen bonds in each of the rotaxanes, with their downfield position related to strength of hydrogen bonding interaction they are involved with. Hydrogen bonding strength is greatest in the secondary amide rotaxane **3.7** (δ H_D = 7.82 ppm), with weaker hydrogen bonding indicated in the tertiary amide rotaxanes (δ H_D = 7.05 and 7.20 ppm for **3.10** and **3.2** respectively). The evidence suggests that hydrogen bonds are typically weaker in tertiary amide rotaxanes due to steric repulsions, which is consistent with the solid-state structure. Typically H_C is used to provide another indication of hydrogen bonding strength. This is because it experiences a stronger downfield shielding effect when its proximity to the amide carbonyl is increased on increasing hydrogen-bond strength. Here though it provides further evidence for an aromatic interaction. In rotaxanes **3.7** and **3.10**, H_C appears at around 8.6 and 8.4 ppm respectively, indicating the relative strengths of the hydrogen bonding interactions. In **3.2** H_C appears much lower at 8.1 ppm, despite H_D indicating a comparable hydrogen bonding strength to that in **3.10**. This is a result of the upfield shielding it experiences from its proximity to the N-phenyl ring.

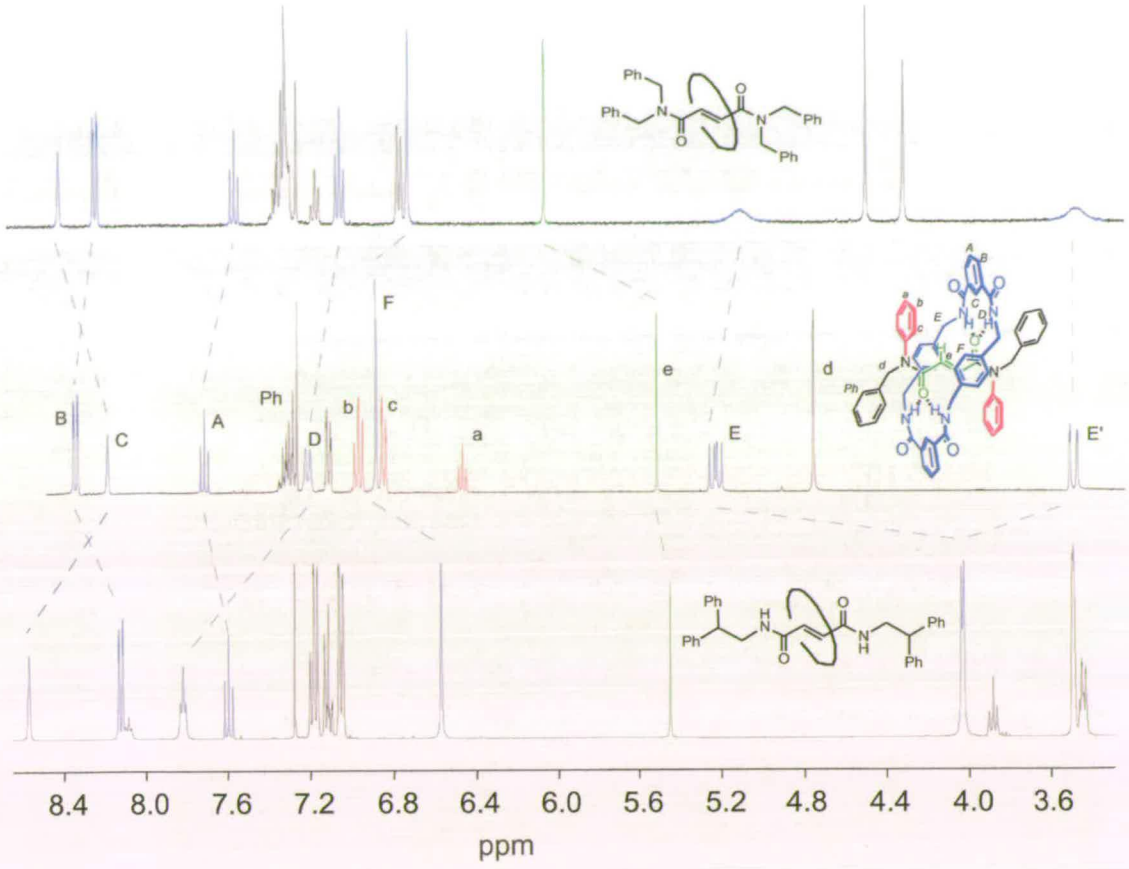


Figure 3. 12 ^{1}H NMR spectra ($CHCl_3$, 298K, 400 MHz) of rotaxanes 3.10, 3.2, and 3.7, which highlights the differences between these rotaxanes.

The dynamics of these rotaxanes also provides some interesting insights into these rotaxane templates. The macrocycle in rotaxane systems can undergo a pirouetting motion, which involves a 180° circumrevolution and a ring flipping process.[15,20] During this process the macrocyclic benzyl protons (H_{Eaxial} and $H_{Eequatorial}$) undergo chemical exchange, and this process can be observed in the proton NMR. In each of the three rotaxanes the H_E protons appear differently at 298K, appearing fully resolved into a single H_E peak in **3.7**, as two broad peaks just below the coalescence point in **3.10**, and fully resolved into two sharp signals in **3.2**. This observation shows that the rate of circumrotation at room temperature is getting slower as bulkier groups are introduced to the templates (fastest to slowest is the secondary amide, N,N-dibenzyl tertiary amide to N-benzyl-N-phenyl tertiary amide) (see figure 3.13). This rate at which this process occurs is usually used to determine the relative strength of hydrogen bonding between the macrocycle and the thread, as these

hydrogen bonds must be broken in order to complete the rotation. In this case, the circumrotation rate gives an indicatation of the steric environment of the macrocycle, as the ring flipping process becomes more unfavourable in tightly constrained environments.

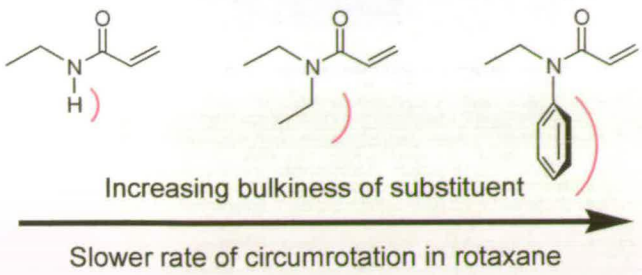


Figure 3. 13 Showing the increase in N-substituent size and the relative rates of circumrotation.

This visual observation is more than supported when the activation energy barriers for circumrotation are calculated using VT ^{1}H NMR or spin polarisation transfer by selective inversion recovery (SPT-SIR) techniques.[20,21] Energy barriers were obtained of 11.5 ±0.2 kcal mol^{-1} for **3.7** (by SPT-SIR, 298 K), 13.4 ±0.1 kcal mol^{-1} (by coalescence, 298 K)[22] for **3.10**, and 18.9 ±0.1 kcal mol^{-1} for **3.2** (SPT-SIR, 348 K)! This incredible leap in energy barrier for the circumrotation process (in fact, similar to the energy barrier of tertiary amide rotation ~18.4 kcal mol^{-1}) highlights the very tightly constrained steric environment that the macrocycle occupies in rotaxane **3.2**. The fact that rotaxane **3.2** forms in almost quantitative yield in such a sterically crowded environment is remarkable, especially when the less constrained template **3.6** gives rotaxane **3.10** in only 60% yield.

The fact that the energy barrier for circumrotation in rotaxane **3.2** is comparable to the energy barrier for the tertiary amide rotation may suggest that the N-phenyl group must first rotate from trans- to the carbonyl to cis- in order to relieve the tightly constrained environment of the macrocycle, which provides it with the space necessary for circumrotatation.

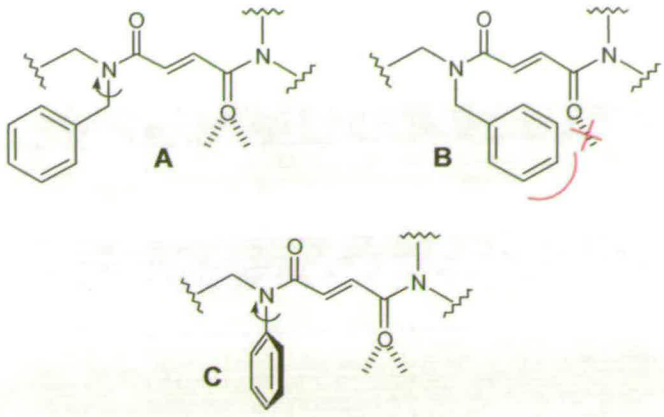


Figure 3. 14 Showing how freedom of rotation around the N-benzyl bond in 3.6 can reveal (A) and obscure (B) the hydrogen bonding sites on the thread and disfavour rotaxane formation, whereas rotation around the N-ph bond (C) does not cause the same increase in steric bulk around the hydrogen bonding site.

Although the difference in activation energy of cricumrotation reveals the steric constraints in the rotaxane environment, the real difference in template efficiency comes from the ability of the two templates to bind to the rotaxane intermediate, the linear macrocycle-precursor. The difference between the two sterically crowded tertiary amide templates **3.6** and **3.2** is in the nature of the steric substituents (see figure 3.14). The N-benzyl groups, although constrained by the slow rotation around the amide N-CO bond, have freedom of rotation around the N-CH_2 bond. This freedom of rotation means that, in the thread, the benzyl groups can obstruct the amide carbonyl responsible for forming the hydrogen bonds that template rotaxane formation, and can destabilise an already bound macrocycle-precursor. The N-benzyl-N-phenyl thread **3.1**, as a result of its preference for the N-phenyl group to be trans to the carbonyl group and orthogonal to the amide group, only has a restricted rotation around the N-Ph bond. This limited movement does not obscure the template or destabilise the binding of the rotaxane intermediate. In fact, the rotaxane intermediate binding is enhanced by the favourable aromatic stacking interaction discussed previously rather than reduced by steric repulsions. Once the macrocycle-precursor is bound, the subsequent clipping reaction to close the macrocycle is kinetically controlled. This means that although the macrocycle has no freedom to

pirouette in rotaxane **3.2** because the bulky substituents, this has no effect on the ability of the thread to template the rotaxane formation.

3.3 Conclusions

Tertiary amide-based templates have generally been overlooked as rotaxane templates due to the associated low yields and complications as a result of different rotamer populations. The novel tertiary amide unit incorporating an N-phenyl substituent overcomes these problems, with only one preferred rotamer conformation observable in solution and the solid-state and an associated large rotaxane yield, as well as giving rise to unique dynamic properties in the corresponding rotaxanes.

The success of the template stems from the preorganisation of the N-phenyl substituents, which allow the presentation of the binding sites of the thread without obstruction, and offer no steric, repulsive interactions to destabilise the hydrogen-bonded intermediate. In fact, attractive offset π–π stacking interactions serve to further stabilise the bound rotaxane intermediate. The rigidity of the template, from the preorganised binding sites to the transoid arrangement of N-phenyl groups, makes the thread a 'perfect fit' for the macrocycle. This fact is highlighted by the rotaxane dynamics. The very high energy-barrier for the pirouetting motion is as a result of the inflexible nature of the bulky stopper groups. Although they allow very efficient templating, they present large steric obstacles to the macrocycle during the circumrotation / ring flipping motion.

3.4 Experimental

But-2-enedioic acid bis-(benzyl-phenyl-amide) (3.1)

To a stirred solution of N-benzylaniline (500 mg, 2.73 mmol, 2.2 eq) and triethylamine (523 μL, 3.83 mmol, 3 eq) in methylene chloride (50 mL) was added

fumaryl chloride (134 μL, 1.24 mmol, 1 eq) in methylene chloride (10 mL) dropwise over 10 min. The reaction was left for a further 30 min before being washed with 1N HCl (3 x 50 mL), water (1 x 50 mL), dried over $MgSO_4$ and evaporated to dryness. The crude product was triturated with diethyl ether to give the pure product **3.1** as a colourless solid (532 mg, 96 %); m.p. 167-169 °C; ^{1}H NMR (400 MHz, d_6-DMSO) δ 7.48 – 7.34 (6H, m, Ph), 7.28 – 7.11 (14H, m, Ph), 6.70 (2H, bs, CH=), 4.92 (4H, bs, PhC$\underline{H}_2$); ^{13}C NMR (100 MHz, d_6-DMSO) δ 163.3, 140.9, 136.9, 131.4, 129.6, 128.6, 128.3, 127.9, 127.2, 52.3; HRFAB-MS (3-NOBA matrix): *m/z* = 447.20729 (calcd. for $C_{30}H_{27}N_2O_2$, [M]H+, 447.20725).

[2](1,7,14,20-Tetraaza-2,6,15,19-tetraoxo-3,5,9,12,16,18,22,25-tetrabenzocyclohexacosane)-but-2-enedioic acid bis-(benzyl-phenyl-amide) rotaxane (3.2)

To a stirred solution of thread **3.1** (72 mg, 161 μmol) and triethylamine (450 μL, 3.23 mmol) in chloroform (10 mL) was added separate solutions of *p*-xylenediamine (176 mg, 1.29 mmol) in chloroform (10 mL) and isophthaloyl chloride (262 mg, 1.29 mmol) in chloroform (10 mL) dropwise over two hours. On completion the reaction was filtered and washed with 1M HCl (3 x 50 mL), saturated $NaHCO_3$ (3 x 50 mL) and water (50 mL) to yield almost pure rotaxane product. The crude product was purified by column chromatography (silica, 2% methanol / methylene chloride) to yield pure rotaxane **3.2** as a white powder (149 mg, 152 μmol, 94%); decomposed > 280 °C; ^{1}H NMR (400 MHz, $CDCl_3$) δ 8.27 (4H, dd, *J* = 1.5, 8 Hz, B), 8.12 (2H, bt, *J* = 1.5 Hz, C), 7.64 (2H, t, *J* = 8 Hz, A), 7.28 – 7.18 (6H, m, *m*-PhC, *p*-PhC), 7.14 (4H, bd, *J* = 8 Hz, NH), 7.06 – 7.02 (4H, m, *o*-PhC), 6.92 – 6.87 (4H, dd, *J* = 7.5, 8.0 Hz, *m*-PhN), 6.81 (8H, s, F), 6.77 (4H, dd, *J* = 1.0, 8.0 Hz, *o*-PhN), 6.39 (2H, tt, *J* = 1.0, 7.5 Hz, *p*-PhN), 5.44 (2H, s, C$\underline{H}$=C), 5.15 (4H, dd, *J* = 9.5, 14.0 Hz, E), 4.69 (4H, s, PhC$\underline{H}_2$), 3.42 (4H, dd, *J* = 1.5, 14.0 Hz, E'); ^{13}C NMR (100 MHz, $CDCl_3$) δ 165.2, 164.8, 139.8, 137.9, 135.6, 133.5, 131.9, 129.5, 129.4, 129.3, 129.1, 129.0, 128.7, 128.5, 128.4, 127.3, 122.5, 54.7, 43.0; HRFAB-MS (3-NOBA matrix): *m/z* = 979.41816 (calcd. for $C_{62}H_{55}N_6O_6$, [M]H+, 447.20725).

X-ray Crystallographic Structure Determinations. 3.2: $C_{63}H_{58}N_6O_7$, M_r = 1011.15, crystal size 0.46 x 0.38 x 0.12 mm, triclinic P-1, a = 12.2119(14), b = 14.8497(17), c = 16.5724(19) Å, α = 111.490(2)°, β = 90.191(2)°, γ = 106.111(2)°, V = 2667.93(32) Å^3, Z = 2, ρ_{calcd} = 1.31 Mg m^{-3}; Mo X-ray radiation (SMART APEX, Edinburgh University, λ= 0.71073 Å, μ(Mo-Kα) = 0.946 mm^{-1}), T = 150(2) K. 24242 data (12569 unique, R_{int}= 0.0332, 2.3 < θ < 26.0°) were collected on a Siemens SMART CCD diffractometer using narrow frames (0.3° in ω), and were corrected semiempirically for absorption and incident beam decay (transmission 0.817 - 1.00). The structure was solved by direct methods and refined by full-matrix least-squares methods on F 2 values of all data (G. M. Sheldrick, SHELXTL Manual, Version 5, Siemens Analytical X-ray Instruments, Madison, WI, 1994) to give wR = $\{\Sigma[w(F_o^2 - F_c^2)^2]/\Sigma\{w(F_o^2)^2]\}^{1/2}$ = 0.164, conventional R = 0.063 for F values of 7376 reflections with $F_o^2 > 2\sigma(F_o^2)$, S = 1.020 for 687 parameters. Residual electron density extremes were 0.555 and –0.421 e Å^{-3}. Hydrogen atoms were added in calculated positions and constrained to a riding model. A disordered molecule of methanol could not be modelled satisfactorily and was successfully treated in the method described by van der Sluis and Spek with no significant observable effect on the main structure.

3.5 References

(1) Hunter, C. A.; Lawson, K. R.; Perkins, J.; Urch, C. J., *J. Chem. Soc., Perkin Trans. 2,* **2001**, 651-669.

(2) Hunter, C. A., *Angew. Chem.,* **1993**, *105*, 1653-1655. (See also Angew. Chem., Int. Ed., **1993**, *32*, 1584-1656).

(3) Meyer, E. A.; Castellano, R. K.; Diederich, F., *Angew. Chem. Int. Ed.,* **2003**, *42*, 1210-1250.

(4) Diederich, F.; Smithrud, D. B.; Sanford, E. M.; Wyman, T. B.; Ferguson, S. B.; Carcanague, D. R.; Chao, I.; Houk, K. N., *Act. Chem. Scand.,* **1992**, *46*,

205-215; Ferguson, S. B.; Sanford, E. M.; Seward, E. M.; Diederich, F., *J. Am. Chem. Soc.*, **1991**, *113*, 5410-5419; Smithrud, D. B.; Wyman, T. B.; Diederich, F., *J. Am. Chem. Soc.*, **1991**, *113*, 5420-5426; Ferguson, S. B.; Seward, E. M.; Diederich, F.; Sanford, E. M.; Chou, A.; Inocencio-Szweda, P.; Knobler, C. B., *J. Org. Chem.*, **1988**, *53*, 5593-5595.

(5) Burley, S. K.; Petsko, G. A., *Science*, **1985**, *229*, 23-28.

(6) Hunter, C. A.; Sanders, J. K. M., *J. Am. Chem. Soc.*, **1990**, *112*, 5525-5534; Hunter, C. A.; Singh, J.; Thornton, J. M., *Journal of Molecular Biology*, **1991**, *218*, 837-846; Hunter, C. A., *Chem. Soc. Rev.*, **1994**, *23*, 101-109; Adams, H.; Harris, K. D. M.; Hembury, G. A.; Hunter, C. A.; Livingstone, D.; McCabe, J. F., *Chem. Commun.*, **1996**, 2531-2532; Breault, G. A.; Hunter, C. A.; Mayers, P. C., *J. Am. Chem. Soc.*, **1998**, *120*, 3402-3410; Hunter, C. A.; Low, C. M. R.; Rotger, C.; Vinter, J. G.; Zonta, C., *Proc. Nat. Acad. Sci.*, **2002**, *99*, 4873-4876.

(7) Adams, H.; Carver, F. J.; Hunter, C. A.; Morales, J. C.; Seward, E. M., *Angew. Chem., Int. Ed. Eng.*, **1996**, *35*, 1542-1544; Carver, F. J.; Hunter, C. A.; Seward, E. M., *Chem. Commun.*, **1998**, 775-776; Carver, F. J.; Hunter, C. A.; Jones, P. S.; Livingstone, D. J.; McCabe, J. F.; Seward, E. M.; Tiger, P.; Spey, S. E., *Chem. Eur. J.*, **2001**, *7*, 4854-4862.

(8) Ashton, P. R.; Goodnow, T. T.; Kaifer, A. E.; Reddington, M. V.; Slawin, A. M. Z.; Spencer, N.; Stoddart, J. F.; Vicent, C.; Williams, D. J., *Angew. Chem.*, **1989**, *101*, 1404-1408.

(9) Anelli, P. L.; Spencer, N.; Stoddart, J. F., *J. Am. Chem. Soc.*, **1991**, *113*, 5131-5133; Ashton, P. R.; Grognuz, M.; Slawin, A. M. Z.; Stoddart, J. F.; Williams, D. J., *Tetrahedron Lett.*, **1991**, *32*, 6235-6238; Ashton, P. R.; Belohradsky, M.; Philp, D.; Stoddart, J. F., *J. Chem. Soc., Chem. Commun.*, **1993**, 1269-1274.

(10) Houk, K. N.; Menzer, S.; Newton, S. P.; Raymo, F. M.; Stoddart, J. F.; Williams, D. J., *J. Am. Chem. Soc.*, **1999**, *121*, 1479-1487.

(11) Hansen, J. G.; Feeder, N.; Hamilton, D. G.; Gunter, M. J.; Becher, J.; Sanders, J. K. M., *Org. Lett.*, **2000**, *2*, 449-452.

(12) Johnston, A. G.; Leigh, D. A.; Murphy, A.; Smart, J. P.; Deegan, M. D., *J. Am. Chem. Soc.*, **1996**, *118*, 10662-10663; Leigh, D. A.; Murphy, A.; Smart, J. P.; Slawin, A. M. Z., *Angew. Chem., Int. Ed. Eng.*, **1997**, *36*, 728-732; Clegg, W.; Gimenez-Saiz, C.; Leigh, D. A.; Murphy, A.; Slawin, A. M. Z.; Teat, S. J., *J. Am. Chem. Soc.*, **1999**, *121*, 4124-4129; Brouwer, A. M.; Frochot, C.; Gatti, F. G.; Leigh, D. A.; Mottier, L.; Paolucci, F.; Roffia, S.; Wurpel, G. W. H., *Science,* **2001**, *291*, 2105-2106.

(13) Lane, A. S.; Leigh, D. A.; Murphy, A., *J. Am. Chem. Soc.*, **1997**, *119*, 11092-11093; Gatti, F. G.; Leigh, D. A.; Nepogodiev, S. A.; Slawin, A. M. Z.; Teat, S. J.; Wong, J. K. Y., *J. Am. Chem. Soc.*, **2001**, *123*, 5983-5989.

(14) Carver, F. J.; Hunter, C. A.; Shannon, R. J., *J. Chem. Soc., Chem. Commun.*, **1994**, 1277-1280.

(15) Johnston, A. G.; Leigh, D. A.; Nezhat, L.; Smart, J. P.; Deegan, M. D., *Angew. Chem., Int. Ed. Eng.*, **1995**, *34*, 1212-1216.

(16) Gatti, F. G.; Leigh, D. A.; Nepogodiev, S. A.; Slawin, A. M. Z.; Teat, S. J.; Wong, J. K. Y., *J. Am. Chem. Soc.*, **2001**, *123*, 5983-5989.

(17) Altieri, A.; Gatti, F. G.; Kay, E. R.; Leigh, D. A.; Martel, D.; Paolucci, F.; Slawin, A. M. Z.; Wong, J. K. Y., *J. Am. Chem. Soc.*, **2003**, *125*, 8644-8654.

(18) Gatti, F. G.; Leon, S.; Wong, J. K. Y.; Bottari, G.; Altieri, A.; Morales, M. A. F.; Teat, S. J.; Frochot, C.; Leigh, D. A.; Brouwer, A. M.; Zerbetto, F., *Proc. Nat. Acad. Sci.*, **2003**, *100*, 10-14.

(23) Van der Sluis, P., Spek A. L., *Acta. Cryst.*, **1990**, *A46*, 194.

(19) Pederson, B. F.; Pederson, B., *Tetrahedron Lett.,* **1965**, 2995-3001; Itai, A.; Toriumi, Y.; Tomioka, N.; Kagechika, H.; Azumaya, I.; Shudo, K., *Tetrahedron Lett.,* **1989**, *30*, 6177-6180.

(20) Leigh, D. A.; Murphy, A.; Smart, J. P.; Deleuze, M. S.; Zerbetto, F., *J. Am. Chem. Soc.,* **1998**, *120*, 6458-6467.

(21) Dahlquist, F. W.; Longmur, K. J.; Du Vernet, R. B., *J. Magn. Reson.,* **1975**, *17*, 406.

(22) Sutherland, I. O., *Annu. Rep. NMR Spectrosc.,* **1971**, *4*, 71; Sandstroem, J. *Dynamic NMR Spectroscopy*; Academic Press: London, 1982.

(23) Van der Sluis, P., Spek A. L., *Acta. Cryst.*, **1990**, *A46*, 194.

Chapter 4

Macrocycle Racing 2: Using Telechelics to form [2]Polyrotaxanes

4.1 Introduction

Since the failure of the Atom Transfer Radical Polymerisation (ATRP) method of reliably growing a [2]polyrotaxane from the [2]rotaxane initiator, an alternative method was adopted. Telechelics, defined as readily-available polymers with functional groups to facilitate further functionalisation, could be utilised as the polymer moiety in the [2]polyrotaxane systems. This would eliminate the need to subject the various rotaxanes to the conditions required for ATRP polymerisation, and any subsequent purification steps.

This new approach required a change in the design of the rotaxane. The initiator, which formed part of the stopper in the thread, is no longer necessary. An alternative stopper must be included in the design. Also, a functional group must be present at the end of the thread to attach the telechelic once the rotaxane has been formed. This must be protected during the rotaxane formation step to prevent side reactions from occurring.

The preorganised fumaramide system, with reported rotaxane yields up to 97%,[1] can be employed instead of the glycyl systems previously utilised. This was not possible previously as the double bond of the fumaric system could be susceptible to attack from the radical reactants during atom transfer polymerisation (ATRP). The fumaramide system should enhance the yield of rotaxanes generated, and allow the necessary large quantities of rotaxane to be produced more efficiently.

Once the rotaxane had been formed, the plan was to attach the polymer and study the molecule according to the following scheme (see figure 4.1). Firstly, the masking group, used to protect the acid functionality, would be removed so that the polymer could be attached (step A). Then the fumaric template would be isomerised to the maleic (step B). This would switch-off the favourable hydrogen-bonding interaction between thread and macrocycle used to template the rotaxane formation, and increase the steric repulsion felt by the macrocycle. The combination of these two effects would be the driving force for the relocation of the macrocycle off the station and onto the polymer backbone. The order in which these first two steps are carried out is not important, but this order was chosen in case the increased steric strain in the maleic rotaxane caused any side reactions during the masking group-cleavage step. At this point, the polymer telechelic would be attached (step C). It is important that the polymer be attached last as it will probably be difficult to purify and therefore the need for fewer subsequent reactions is desirable. The final reaction is the cleavage of the removable stopper (step D), which would allow the macrocycle onto the polymer backbone. Then all that remains is to monitor the time over which the macrocycle appears free in solution (step E), and then repeat with different lengths of polymer chain.

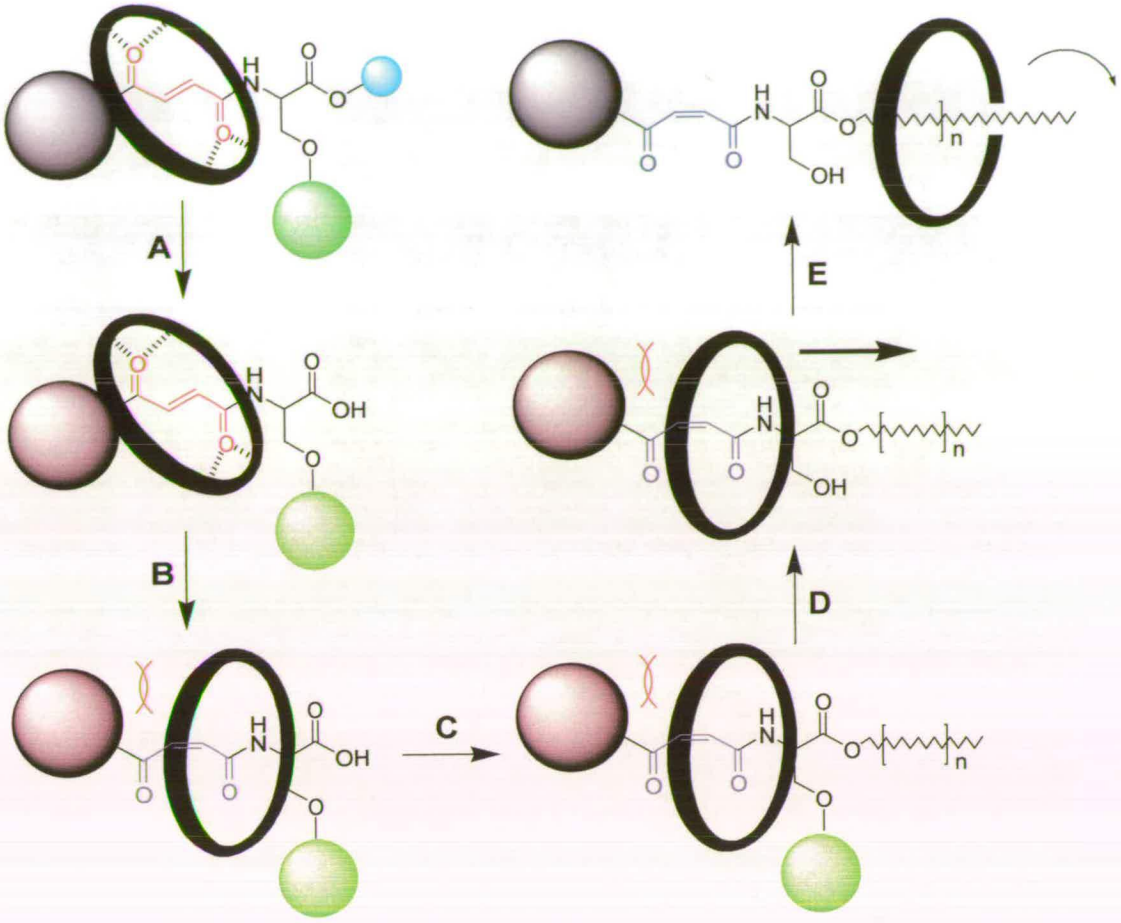


Figure 4. 1 Proposed plan for attaching polymer and studying the cleavage. A) Remove the masking group used to protect the acid functionality during rotaxane synthesis. B) Isomerise the fumaric double bond to the maleic, effectively switching-off the favourable hydrogen bonding interaction responsible for templating rotaxane. C) Attach the polymer telechelic. D) Cleave the removable stopper to allow the macrocycle onto the polymer backbone. E) Measure the rate at which free macrocycle appears in solution. The order in which steps A and B are carried out is interchangeable.

4.2 Results and Discussion

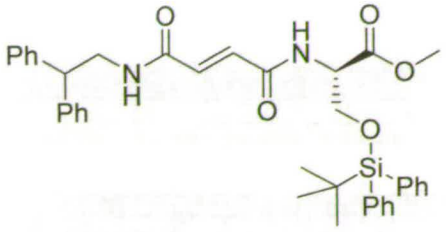
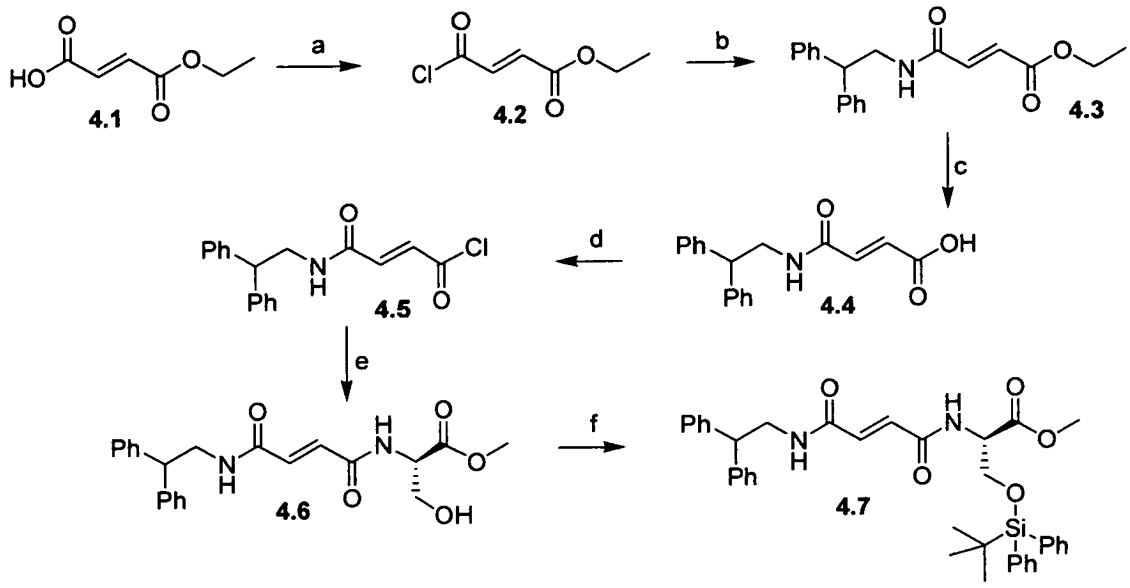


Figure 4. 2 Initial thread design.

The new template (figure 4.2) incorporates all the design features mentioned previously. The 2,2-diphenyl fumaramide portion of the molecule was incorporated into the design as this was part of the symmetrical thread (bis(2,2-diphenylethyl)-fumaramide) that yielded 97% rotaxane.[2] L-serine was chosen as a linker group because it is readily available and incorporates three different functional groups. The amine is used to complete the diamide template. The α-hydroxyl is used to attach the removable stopper, and the methyl ester is an already protected acid for attaching the telechelics. The photo-cleavable group previously used as a removable stopper (see chapter 2) was considered unsuitable for this system. Firstly, the carbonate group used to link the photocleavable group to the thread is not orthogonal with the methyl ester. This may cause complications when the methyl ester is deprotected in order to attach the telechelics. Secondly, the fumaramide system is photoactive, and readily isomerises from trans- to cis- when exposed to hν light at 254nm. Photo-isomerisation of the double bond, necessary to disrupt the strong hydrogen bonding interactions, could cause the photo-cleavage reaction to occur instead. Therefore a silyl protecting group was used instead to avoid any possible complications. A *tert*-butyldiphenylsilyl group was chosen because it is a large enough group to stopper the thread, and because it strikes a good balance between its stability as a protecting group and its cleavage kinetics under the right conditions.

The designed thread was prepared by a six-step synthesis (scheme 4.1). The synthesis was such that no column chromatography was required until after the final step to obtain the pure thread.



Scheme 4. 1 Synthetic steps to the designed thread.

Fumaric acid mono-ethyl ester **4.1** was converted to the acid chloride **4.2** using oxalyl chloride and dimethylformamide in methylene chloride (step a). Complete reaction was indicated when the initial suspension of acid starting material disappeared to leave a clear solution. This solution of acid chloride **4.2** was then added dropwise to a solution of 2,2-diphenylethylamine and triethylamine in methylene chloride (step b). A white precipitate appeared during the reaction. The product was isolated by reducing the volume of solvent, re-dissolving in hot ethanol and tipping into 1M aqueous hydrochloric acid to produce a precipitate. This was filtered, washed and dried to yield pure product **4.3** in 94% yield.

Dissolving the ester product in ethanol and treating with 1M aqueous sodium hydroxide cleaved the ethyl ester group (step c). The complete reaction was indicated by the clear solution of the acid sodium salt. The acid product was precipitated out of solution by acidifying the solution with 1M aqueous hydrochloric acid. This was filtered, washed and dried to leave the pure acid **4.4** in 93% yield.

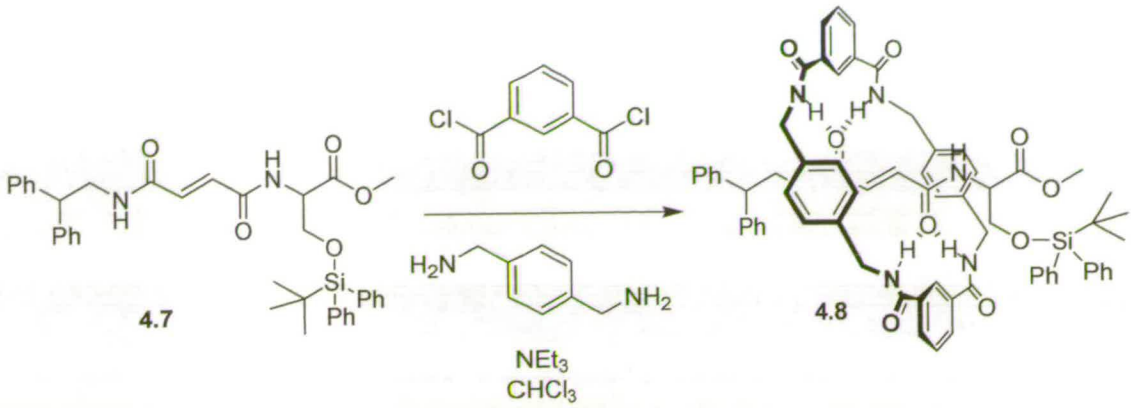
The acid **4.4** was converted to the acid chloride **4.5** using oxalyl chloride and dimethylformamide in methylene chloride (step d). Again complete reaction was

indicated when the initial suspension of acid disappeared to become a clear solution of acid chloride **4.5**. The solution of acid chloride was then added dropwise to an ice-cold solution of L-serine methyl ester hydrochloride and triethylamine in methylene chloride (step e). A precipitate appeared during the course of the reaction. The reaction was reduced in volume, re-dissolved in hot ethanol and the crude product precipitated out of solution by tipping into 1M aqueous hydrochloric acid. The white precipitate was filtered, washed and dried and then recrystallised from methanol to give the pure product **4.6** in 78% yield.

The final step in the synthesis was to attach the silyl-protecting group. This was achieved by reacting **4.6** in the presence of imidazole with an excess of *tert*-butyldiphenyl silyl chloride in methylene chloride. The reaction was washed with water, dried and reduced in volume. The crude product was purified by column chromatography to remove the silyl by-products and give the pure thread **4.7** in 95% yield.

The thread **4.7** was synthesised with an overall yield of 65%. This represents a significant step up from the yield of the initiator thread synthesised previously (see chapter 2). In addition, the elimination of column chromatography in all but the final steps of synthesis allows the thread to be made on a much larger scale, and also makes this a more facile and efficient synthesis.

The rotaxane **4.8** was formed from thread **4.7** using eight equivalents of isophthaloyl chloride and *p*-xylylene diamine with triethylamine in chloroform (scheme 4.2). The crude reaction mixture was separated by column chromatography to give the desired rotaxane **4.8** in 30% yield.



Scheme 4. 2 Rotaxane synthesis from thread **4.7**.

The low rotaxane yield proved a disappointment considering that the fumaramide template has been associated with the almost quantitative conversion of thread to rotaxane (*e.g.* in the first reported case of bis(diphenylethyl)fumaramide), and that the production of large quantities of rotaxane was desirable for use in subsequent steps.

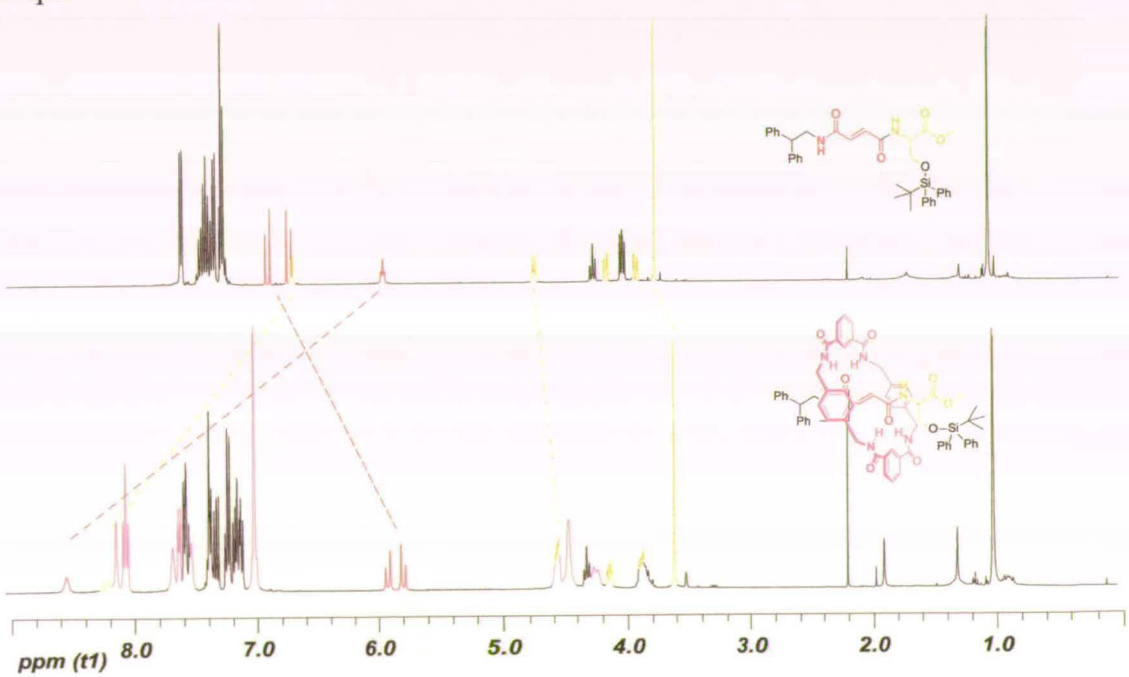


Figure 4. 3 ^{1}H NMR spectra (400 MHz, $CDCl_3$, 298K) of thread **4.7** and rotaxane **4.8**.

Analysis of the ^{1}H NMR spectra of the thread **4.7** and rotaxane **4.8** (figure 4.3) gives us interesting information on the rotaxane system. Firstly, the fumaric protons

experience shielding from the macrocycle xylylene rings. Also of note is that the protons of the methyl ester, the serine chiral centre and even the *t*-butyl group also experience some shielding. This suggests that the macrocycle sits in close promixity to these groups. Both amides of the thread appear very far downfield, indicating a strong hydrogen bonding interaction with the macrocycle. This suggests that the macrocycle does not adopt the doubly-bifurcated hydrogen bonding co-conformation with the thread carbonyls that is usually observed in fumaric systems.[2] The benzylic protons of the macrocycle appear as several signals (δ 4.2- 4.7 ppm), suggesting that they each experience different environments, and only undergo slow exchange by pirouetting. This all suggests that the macrocycle is in a sterically crowded environment, and is forced to adopt an unusual co-conformation with the thread. This would explain the low yield of rotaxane that was obtained.

The next step was the removal of the methyl ester masking group and subsequent coupling to the various poly(ethylene glycol) chains. A convenient method that could couple the PEG chains in one step without the need for initial deprotection of the methyl ester would be to use a transesterification catalyst. Bis(chlorodibutyltin oxide) was chosen, because it often catalyses transesterification cleanly under mild conditions.[3]

Using one equivalent of rotaxane, various amounts of PEG and tin catalyst, and refluxing in a variety of solvents, no reaction could be observed and unconsumed starting materials were recovered in all cases (see table 4.1).

Equivalents Tin catalyst	Equivalents PEG	Solvent	Result
0.1	2	Toluene	Limited solubility No reaction
0.1	2	1,2-Dichloroethane	No reaction
0.5	2	1,2-Dichloroethane	No reaction
1	10	1,2-Dichloroethane	No reaction
1	50	None	No reaction Decomposition after extended reaction periods

Table 4.1 Transesterification reaction conditions used in the attempted synthesis of polyrotaxanes. In each case the reactions were left for a period of one week at reflux in the reported solvent, or 150 °C in the solvent-free reaction.

Since the PEG coupling could not be achieved in one step by means of a transesterification reaction, an alternative approach was adopted. The methyl ester masking-group would have to be removed to reveal the carboxylic acid group prior to attaching the polymer telechelic.

The simplest method of methyl ester cleavage was saponification using aqueous sodium hydroxide. The *tert*-butyldiphenylsilyl (TPS) stopper group should be stable to the basic conditions, but attempts using several different reaction conditions led to decomposition, indicated by the precipitation of free macrocycle. This was attributed to the undesired and unexpected cleavage of the TPS protecting group. A search of the literature indicated that although methyl esters can be selectively cleaved under basic conditions in the presence of a TPS group, there was no literature precedent for the selective cleavage of a methyl ester in such close proximity and such a sterically constrained environment around a TPS group. The presence of non-covalently bound macrocycle may have also introduced some 'mechanical strain' or steric repulsion with the TPS group and thereby increasing its susceptibility to cleavage under basic conditions.

Due to the lack of success in cleaving the methyl ester, and a lack of material, a new thread was designed (see figure 4.4), this time incorporating two design improvements over the previously synthesised thread. A new aromatic tertiary amide stopper group has replaced the secondary amide stopper group. The aromatic tertiary amide group has the advantages of an alkyl tertiary amide in that the thread displays improved solubility,[2] and is less prone to self-aggregation, which allows large quantities of rotaxane to be synthesised and purified, whilst avoiding the disadvantages such as mixtures of rotamers and low rotaxane yields. A benzyl ester masking group is also included in the design as it can be removed selectively by hydrogenolysis and is a totally orthogonal protecting group to the silyl ether.

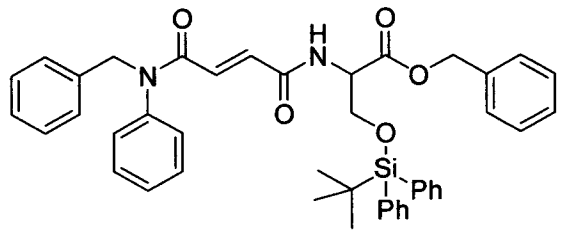
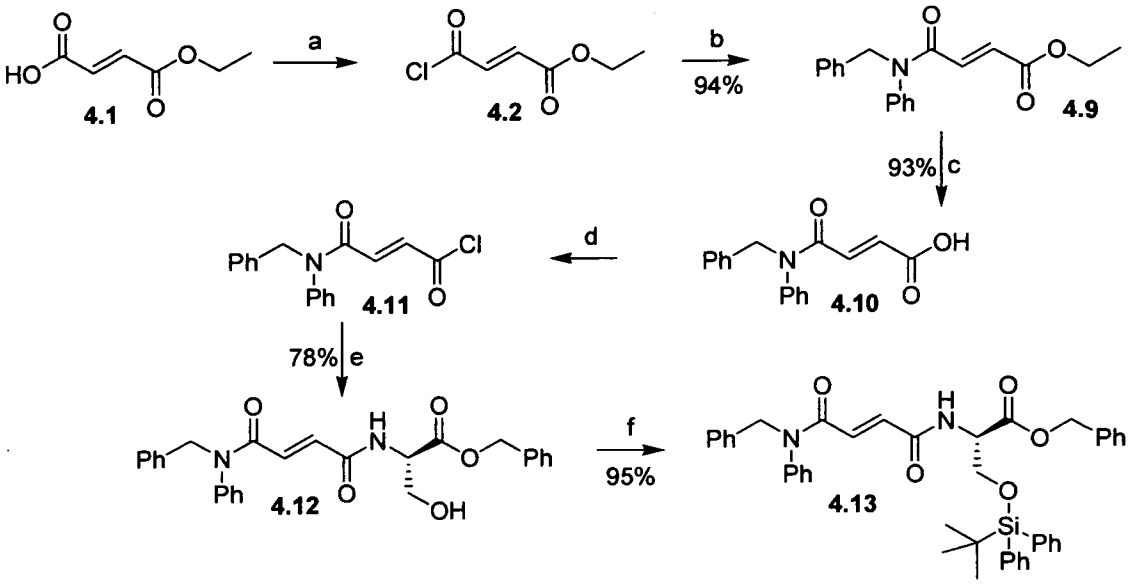


Figure 4. 4 New thread design.

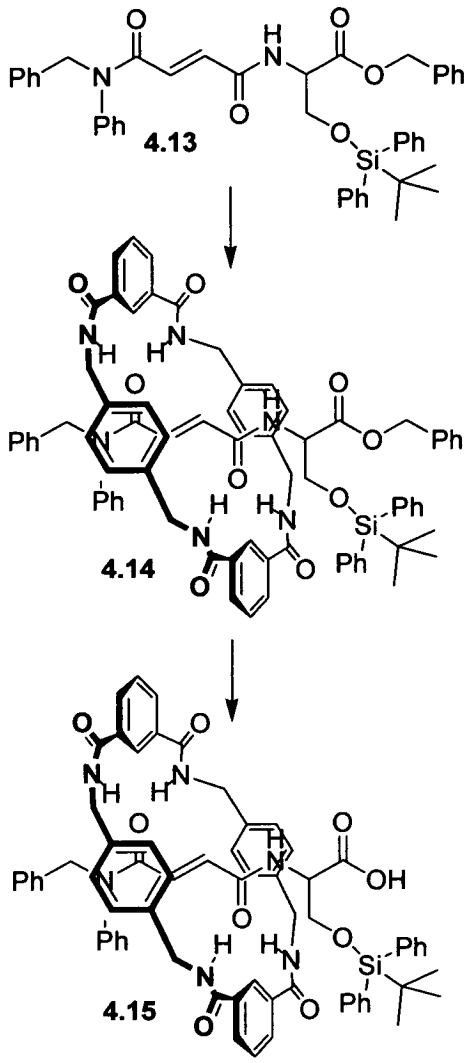
The designed thread was prepared in a six-step synthesis similar to that of the previous thread (see scheme 4.3).



Scheme 4. 3 New thread **4.13** synthetic scheme.

Conditions: (a) $(COCl)_2$ / DMF / CH_2Cl_2; (b) *N*-benzylaniline / NEt_3 / CH_2Cl_2; (c) 1N NaOH / EtOH; (d) $(COCl)_2$ / DMF / CH_2Cl_2; (e) serine-*O*-benzyl ester.HCl / NEt_3 / CH_2Cl_2; (f) *t*-butyldiphenylsilyl chloride / imidazole / CH_2Cl_2.

The improved solubility of the various thread precursors allowed a large quantity, 3g, of thread **4.13** to be synthesised, in one sequence of high-yielding steps, in an overall yield of 53%.



Scheme 4. 4 Rotaxane synthesis and subsequent deprotection of the masking group.

Due to the high thread solubility, the subsequent rotaxane formation was carried out on all three grams of thread using the rotaxane conditions: five equivalents of p-xylylenediamine, five equivalents of isophthaloyl dichloride and ten equivalents of triethylamine in 200 mL chloroform. The reaction produced, in a single step, an unprecedented three grams of rotaxane **4.14** in an overall yield of 54% (see scheme 4.4). The 54% yield obtained could perhaps have been improved if the standard eight equivalents of reagents had been used. Only five equivalents of diacid chloride and diamine were used in order to limit the production of side products (*e.g.* catenane, triethylamine hydrochloride and oligomers) that would trivialise the purification of

such a large quantity of rotaxane. Since the thread could be recovered and recycled, the trade-off of ease of purification over yield seemed reasonable.

The rotaxane **4.14** was then twice subjected to hydrogenolysis conditions with the benzyl masking group cleaved using hydrogen and palladium on carbon in methanol to give the free acid rotaxane **4.15** in overall 75% yield. Each time the hydrogenolysis reaction failed to go to completion, perhaps due to poisoning of the catalyst by an undetectable impurity (by ^{1}H NMR and UV), but unreacted starting material was recovered and recycled in each case.

Analysis of the proton NMR of the thread **4.13**, rotaxane **4.14**, and 'unmasked' rotaxane **4.15** again gives interesting information on the rotaxane system (see figure 4.5). The rotaxane **4.14** spectrum shows that the fumaric protons are shielded by the macrocycle xylylene rings, although one experiences much more shielding than the other one. The N-aryl ring experiences significant shielding from the isophthalyl ring, and the N-benzyl protons of the stopper are also shielded. The macrocycle benzyl protons appear as a broad peak, suggesting that circumrotation of the macrocycle is slow at room temperature. The two diastereotopic protons of the O-benzyl masking group now appear well separated in the spectrum, as each experiences different shielding from the macrocycle.

Removal of the benzyl ester masking group is shown by the lack of corresponding signals in the proton NMR spectrum of rotaxane **4.15**. The spectrum also shows that the N-benzyl protons are no longer symmetrical and experience different amounts of shielding. The amide proton of the thread appears much further downfield indicating a strong hydrogen bonding interaction, probably with the newly revealed acid.

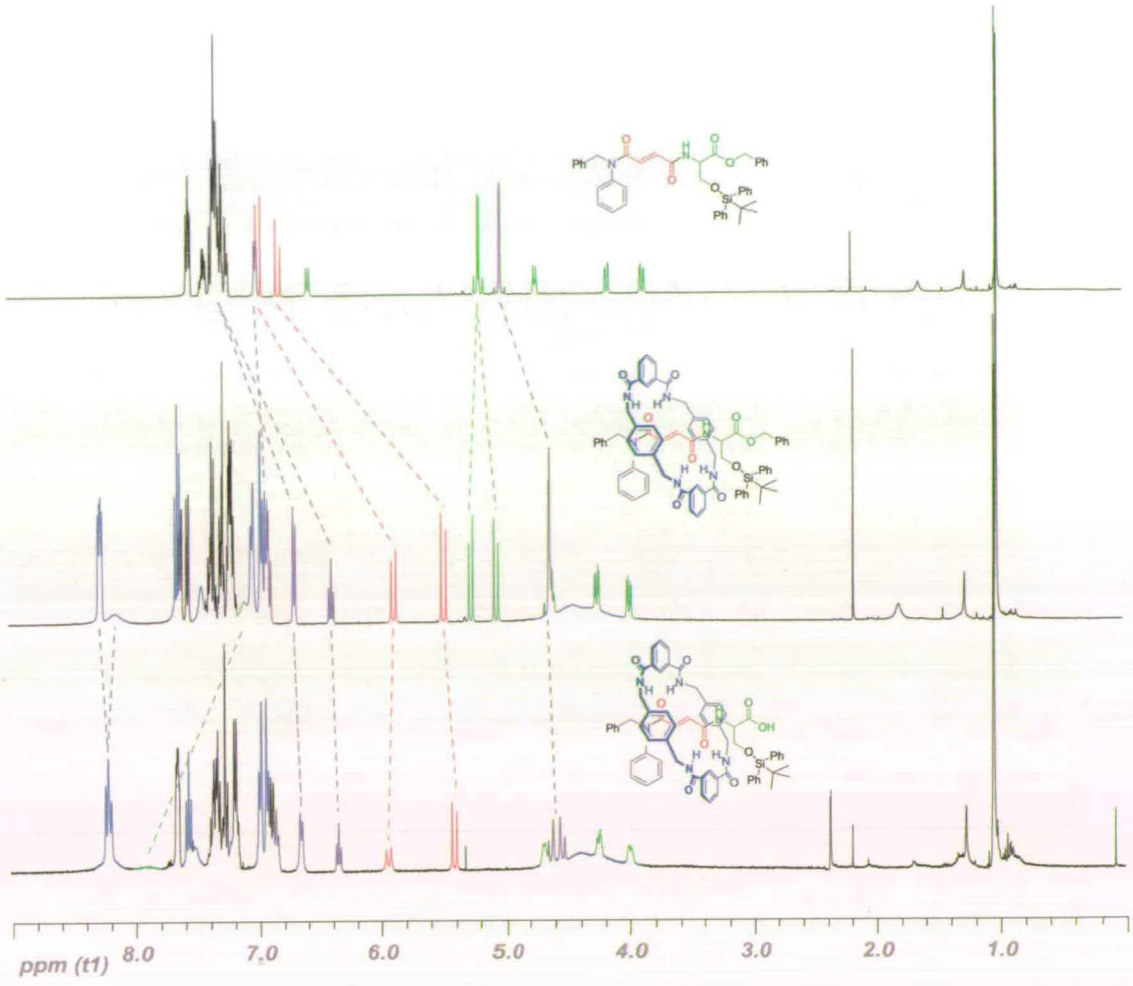


Figure 4. 5 ^{1}H NMR (400 MHz, $CDCl_3$, 298K) showing the thread **4.13**, rotaxane **4.14** and 'unmasked' rotaxane **4.15**.

The next step was to isomerise the fumaric double bond to the maleic. Normally, the photoisomerisation reaction reaches the photostationary state within 20 minutes,[4] giving approximately 60% maleic product. Unfortunately, isomerisation on rotaxane **4.15** and **4.14** produced almost no maleic rotaxane (scheme 4.5), even when exposed for several hours (<5% by ^{1}H NMR analysis of the crude. The maleic product was not isolated). The reaction was repeated under a variety of conditions (254 nm, 356 nm with additional photosensitizers (*e.g.* benzophenone, xanthone),[4,5] but no improvement could be observed.

The failure of the isomerisation could be a result of the tightly constrained environment around the fumaric bond of the thread. The stoppers are large, bulky

groups and the macrocycle further increases the steric bulk around the double bond. This may prevent the photo-excited state from forming, or may disfavour relaxation of the excited state back in the 'cis-' direction to give the maleic double bond (see figure 4.6).[6] Anderson and coworkers have observed a similar effect in one of their azobenzene-rotaxanes, where an encapsulating α-cyclodextrin prevents isomerisation of the double bond.[7]

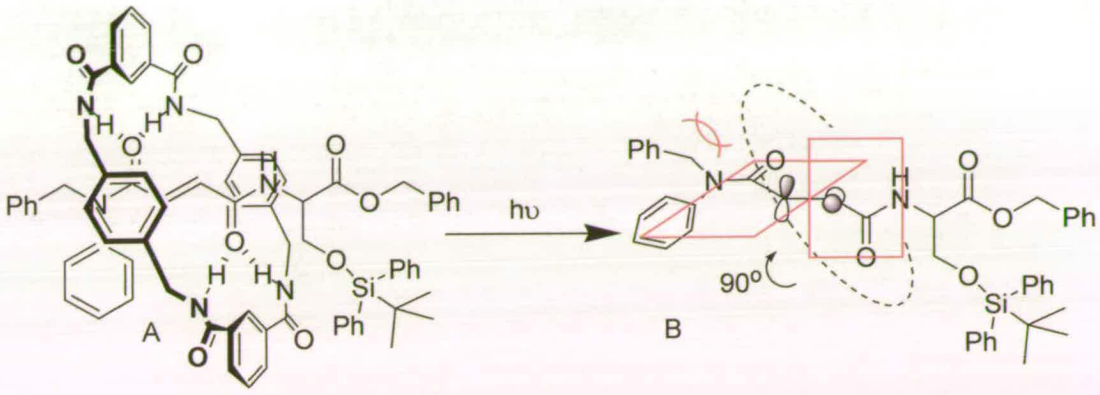
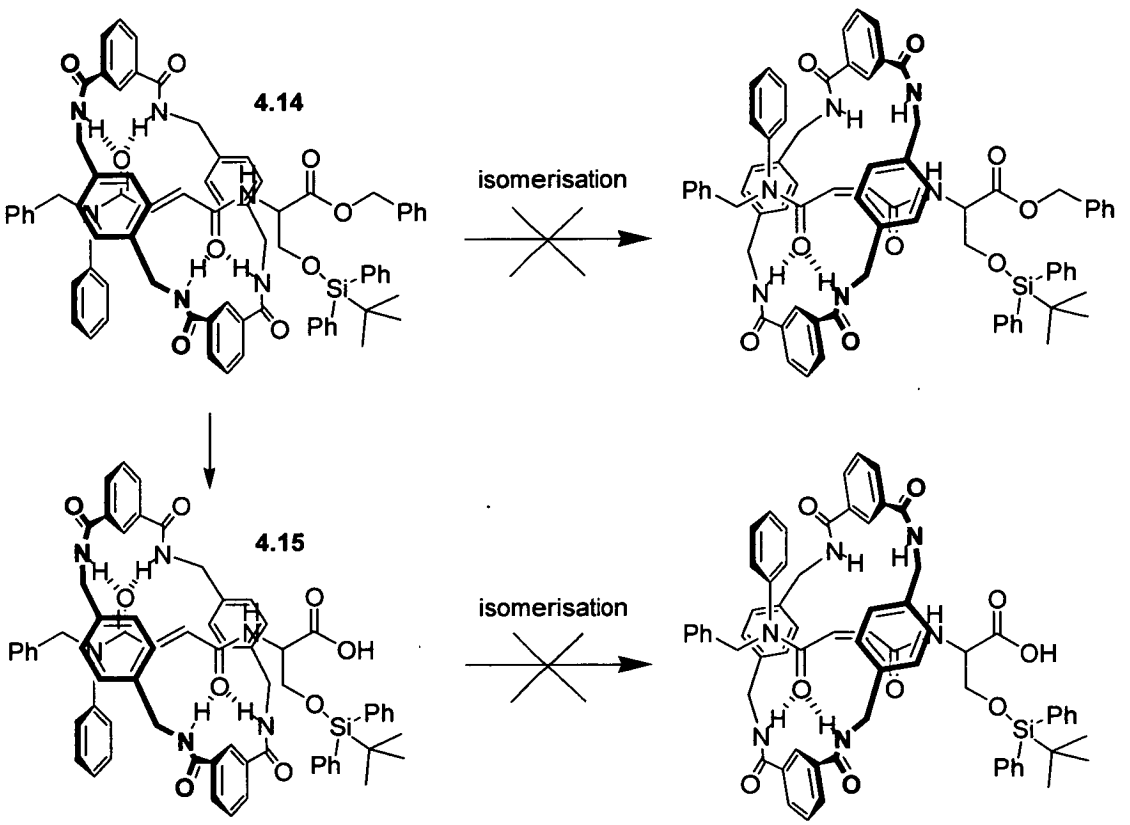


Figure 4. 6 Photo-excitation of the rotaxane **A** should produce the triplet-state **B** in which the π-bond is broken and the p-orbitals turn orthogonal to each other. Steric repulsions from the macrocycle (omitted for clarity) and the stoppers may prevent relaxation in the cis- direction to give the maleic double bond.

It was decided to continue without isomerising the double bond. This would mean that the strong hydrogen bonding interactions would still be present when the removable stopper was removed in the [2]polyrotaxane. This would affect the study, as the macrocycle would still prefer to sit over the station rather than move along the polymer backbone. It was hoped that by conducting the study in dimethylsulfoxide or methanol, the hydrogen bonding interactions between thread and macrocycle could be disrupted and the macrocycle would move off the station and onto the polymer backbone.



Scheme 4. 5 The failed attempts to isomerise rotaxanes **4.14** and **4.15**.

The remaining step was to couple the various length poly(ethylene glycol) chains to the free acid group in rotaxane **4.15**. Several attempts were made to couple PEG 350 monomethyl ether to the free acid of rotaxane **4.15**. Formation of an acid chloride, whilst avoiding the acidic side products associated with oxalyl chloride, could be

achieved using triphenylphosphine and carbon tetrachloride, but subsequent reaction with PEG and triethylamine led again to decomposition. Finally several attempts were made using pivaloyl chloride to form a mixed anhydride, and then subsequently reacting with PEG. Careful control of the conditions avoided the appearance of the precipitate associated with decomposition.

A sample of rotaxane in tetrahydrofuran and three equivalents of triethylamine were cooled to -78°C, and one equivalent of pivaloyl chloride was added. The reaction was allowed to warm to room temperature during which time the colour could be seen to change from colourless to a clear fluorescent green colour. The reaction was left for two hours before being cooled to -78°C again, and a solution of two equivalents of PEG was added. The reaction was allowed to warm to room temperature, and the vivid green colour changed to a vivid yellow colour.

Although it appeared that a reaction was occurring, disappointingly analysis using either 1H NMR or mass spectrometry could detect no evidence of polyrotaxane formation.

4.3 Conclusion

Although no poly[2]rotaxane could be synthesised, significant progress has been made towards the synthesis of the target. Many threads have been synthesised, and their suitability for use as rotaxane auxiliaries has been investigated. The design of the rotaxane auxiliary has evolved such that large quantities of rotaxane can be produced in high yield, which is highly desirable for generating quantities suitable for further functionalisation and study. Initially (see chapter 2) rotaxanes were generated on 200 mg scales with 4% yield. Through the study of these and subsequent systems, the templates have been redesigned and culminated in the production of a template that can produce large quantities of rotaxane (3 g in one rotaxane step) in high yield (54% under non-standard conditions). An orthogonal protecting group has also been incorporated, and been shown to cleave cleanly to allow the rotaxane auxiliary to be further functionalised. It remains now that the

work must be continued to develop the methodology for attaching polymer telechelics to the auxiliary, and to complete the study.

4.4 Experimental

3-Chlorocarbonyl-acrylic acid ethyl ester (4.2)

To a stirred suspension of fumaric acid monoethyl ester **4.1** (5 g, 34.7 mmol) and dimethylformamide (5 mL) in methylene chloride (100 mL) was dropwise added oxalyl chloride, 2M solution in methylene chloride, (18.2 mL, 36.4 mmol). The reaction was allowed to proceed until it became a clear solution and no further effervescence could be observed. The product **4.2** in solution was used without further purification in the next step.

3-(2,2-Diphenyl-ethylcarbamoyl)-acrylic acid ethyl ester (4.3)

To a stirred solution of 2,2-diphenylethylamine (7.5 g, 38.1 mmol) and triethylamine (5.3 mL, 38.1 mmol) in methylene chloride (100 mL) at 0°C was added the fresh solution of **4.2** (prepared in the previous step) dropwise over one hour. A precipitate appeared in the solution. The reaction was left for one hour, and then concentrated under reduced pressure to yield an off-white slurry. The crude product was then redissolved in hot ethanol and tipped in 1M HCl to produce a clear white precipitate. The product was filtered, washed with water and dried under high vacuum to yield to pure product as a white solid (**4.3**, 11.6 g, 94%); m.p. 133 °C; ^{1}H NMR (400 MHz, d_6-DMSO) δ 8.62 (1H, t, J = 6 Hz, NH), 7.35 – 7.14 (10H, m, Ph), 6.95 (1H, d, J = 15 Hz, NHCOC<u>H</u>=C), 6.53 (1H, d, J = 15 Hz, C=C<u>H</u>COO), 4.27 (1H, t, J = 8 Hz, $Ph_2C\underline{H}$), 4.16 (2H, q, J = 7 Hz, OCH_2), 3.86 (2H, dd, J = 6 Hz, 8 Hz, CH_2N), 1.23 (3H, t, J = 7 Hz, CH_3); ^{13}C NMR (100 MHz, d_6-DMSO) δ 165.0, 164.0, 141.9, 136.5, 130.4, 129.2, 128.4, 127.4, 61.6, 50.8, 44.6, 14.5; MS (FAB): m/z = 324 [$(M+H)^+$]; Anal. Calcd. for $C_{20}H_{21}NO_3$: C 74.28, H 6.55, N 4.33. Found: C 74.83, H 6.91, N 4.38.

3-(2,2-Diphenyl-ethylcarbamoyl)-acrylic acid (4.4)

To a stirred suspension of **4.3** (10 g, 30.9 mmol) in ethanol (100 mL) was added 1M NaOH (aq) (50 mL). Over the course of one hour the reaction became clear. The reaction was cooled and acidified by dropwise addition of concentrated HCl with stirring. A white precipitate appeared and was filtered, washed with water and dried under high vacuum. The white solid was found to be the desired pure product (**4.4**, 8.5 g, 93%). ^{1}H NMR (400 MHz, d_6-DMSO) δ 12.88 (1H, bs, COOH), 8.60 (1H, t, J = 6 Hz, NH), 7.36 – 7.21 (10H, m, Ph), 6.90 (1H, d, J = 15 Hz, NHCOC<u>H</u>=C), 6.51 (1H, d, J = 15 Hz, C=C<u>H</u>COO), 4.27 (1H, t, J = 8 Hz, Ph_2C<u>H</u>), 3.86 (2H, dd, J = 6, 8 Hz, CH_2N). ^{13}C NMR (100 MHz, d_6-DMSO) δ 168.0, 164.0, 142.3, 132.6, 130.4, 129.2, 128.4, 127.4, 50.8, 44.6. MS (FAB): m/z = 296 [$(M+H)^+$]; Anal. Calcd. for $C_{18}H_{17}NO_3$: C 73.20, H 5.80, N 4.70. Found: C 73.10, H 5.20, N 4.73.

3-(2,2-Diphenyl-ethylcarbamoyl)-acryloyl chloride (4.5)

To a stirred suspension of **4.4** (1 g, 3.39 mmol) and dimethylformamide (1 mL) in methylene chloride (50 mL) was dropwise added oxalyl chloride, 2M solution in methylene chloride, (1.7 mL, 36.4 mmol). The reaction was allowed to proceed until it became a clear yellow solution and no further effervescence could be observed. The product **4.5** in solution was used without further purification in the next step.

2-[3-(2,2-Diphenyl-ethylcarbamoyl)-acryloylamino]-(S)-3-hydroxy-propionic acid methyl ester (4.6)

To a stirred solution of L-serine methyl ester hydrochloride (580 mg, 3.7 mmol) and triethylamine (1.05 mL, 7.5 mmol) in methylene chloride (30 mL) at 0°C was added the fresh solution of **4.5** (prepared in the previous step) dropwise over one hour. A precipitate appeared in the solution. The reaction was left for one hour, and then concentrated under reduced pressure to yield an off-white slurry. The crude product was then redissolved in hot ethanol and tipped into 1M HCl to produce a white

precipitate. The product was filtered, washed with water and dried under high vacuum. The crude product was recrystallised from hot methanol to yield to pure product as a white solid (**4.6**, 1.05 g, 78%). ^{1}H NMR (400 MHz, d_6-DMSO) δ 8.83 (1H, d, J = 7 Hz, NH), 8.52 (1H, t, J = 6 Hz, NH), 7.34 – 7.17 (10H, m, Ph), 6.96 (1H, d, J = 15 Hz, C<u>H</u>=C), 6.78 (1H, d, J = 15 Hz, C=C<u>H</u>), 5.12 (1H, t, J = 6 Hz, OH), 4.44 (1H, m, NCH), 4.24 (1H, t, J = 8 Hz, Ph_2C<u>H</u>), 3.83 (2H, dd, J = 6, 8 Hz, CH_2N), 3.77 – 3.62 (2H, m, C<u>HH</u>'O), 3.64 (3H, s, OMe). ^{13}C NMR (100 MHz, d_6-DMSO) δ 170.7, 163.9, 163.6, 142.7, 135.0, 134.5, 128.5, 127.8, 126.4, 61.1, 55.0, 51.9, 50.0, 44.3; HRFAB-MS (3-NOBA matrix): *m/z* = 397.17685 (calcd. for $C_{22}H_{25}N_2O_5$, $[M]H^+$, 397.17635).

3-(*tert*-Butyl-diphenyl-silanyloxy)-2-[3-(2,2-diphenyl-ethylcarbamoyl)-acryloylamino]-propionic acid methyl ester (4.7)

To a stirred solution of **4.6** (350 mg, 880 μmol) and imidazole (120 mg, 1.76 mmol) in methylene chloride (50 mL) was added *t*-butyldiphenylsilyl chloride (250 μL, 970 μmol). The reaction was allowed to stir for three hours before another aliquot of the silyl chloride was added (200 μL, 776μmol). The reaction was monitored by TLC until starting material had been consumed. The reaction was washed with water (3 x 100 mL), dried over $MgSO_4$ and evaporated to dryness to produce an oil. The crude product was purified by column chromatography (silica, 1% methanol / methylene chloride) to yield a white foam (**4.7**, 530 mg, 95 %); ^{1}H NMR (400 MHz, d_6-DMSO) δ 8.94 (1H, d, J = 8 Hz, NH), 8.59 (1H, t, J = 6 Hz, NH), 7.58 (4H, m, PhSi), 7.42 (6H, m, PhSi), 7.30 (8H, m, Ph), 7.19 (2H, m, Ph), 7.04 (1H, J = 15 Hz, CH=C), 6.77 (1H, J = 15 Hz, CH=C), 4.61 (1H, m, NCH), 4.24 (1H, t, J = 8 Hz, Ph_2C<u>H</u>), 3.91 (1H, m, C<u>H</u>H'O), 3.81 (3H, m, CH_2N, CH<u>H</u>'O), 3.62 (3H, s, OMe), 0.95 (9H, s, $SiC(CH_3)_3$). ^{13}C NMR (100 MHz, d_6-DMSO) δ 170.1, 163.8, 163.6, 142.7, 135.0, 133.3, 132.4, 131.9, 129.9, 128.4, 127.9, 126.4, 63.3, 54.2, 52.0, 50.0, 43.3, 26.4, 18.7. HRFAB-MS (3-NOBA matrix): *m/z* = 635.29387 (calcd. for $C_{38}H_{43}N_2O_5Si$, $[M]H^+$, 635.29413).

[2](1,7,14,20-Tetraaza-2,6,15,19-tetraoxo-3,5,9,12,16,18,22,25-tetrabenzocyclohexacosane)-3-(*tert*-Butyl-diphenyl-silanyloxy)-2-[3-(2,2-diphenyl-ethylcarbamoyl)-acryloylamino]-propionic acid methyl ester rotaxane (4.8)

To a stirred solution of thread **4.7** (440 mg, 690 μmol) and triethylamine (1.94 mL, 13.9 mmol) in chloroform (30 mL) was added separate solutions of *p*-xylenediamine (754 mg, 5.54 mmol) in chloroform (20 mL) and isophthaloyl chloride (1.125 g, 5.54 mmol) in chloroform (20 mL) dropwise over two hours. Upon complete addition the reaction was left for a further 2 hours, before being filtered, reduced in volume and purified by column chromatography to give the recovered starting material and the pure product **4.8** as a colourless solid; 243 mg, 30 %; ^{1}H NMR (400 MHz, $CDCl_3$) δ 8.51 (1H, bs, NH), 8.18 (1H, bs, NH), 8.11 (2H, bt, H_C*), 8.02 (4H, t, J = 8.0 Hz, H_B*), 7.64 (2H, bt, H_D*), 7.61- 7.57 (2H, m, H_A*), 7.57- 7.52 (4H, m, Ph), 7.52- 7.45 (2H, m, H_D*), 7.38- 7.26 (6H, m, Ph), 7.23- 7.16 (4H, m, Ph), 7.16- 7.05 (6H, m, Ph), 6.98 (8H, s, H_F*), 5.88 (1H, d, J = 15.0 Hz, C=C<u>H</u>), 5.75 (1H, d, J = 15 Hz, C=C<u>H</u>), 4.58- 4.48 (3H, m, NC<u>H</u>CHH', 2 x H_E*), 4.42 (4H, bs, 4 x H_E*), 4.31- 4.24 (1H, t, J = 8.0 Hz, Ph_2C<u>H</u>), 4.24- 4.14 (2H, bd, 2 x H_E*), 4.10 (1H, dd, J = 4.0, 10.0 Hz, CHC<u>H</u>H'), 3.90- 3.74 (3H, m, CHC<u>H</u>H', C<u>H_2</u>N), 3.57 (3H, s, CO_2C<u>H_3</u>), 0.98 (9H, s, C(C<u>H_3</u>)$_3$); ^{13}C NMR (100 MHz, $CDCl_3$) δ 169.8, 166.6, 166.6, 165.8, 165.7, 141.6, 141.5, 136.8, 136.7, 135.5, 135.4, 133.4, 133.4, 132.3, 132.2, 131.3, 131.2, 130.5, 130.2, 130.1, 129.3, 129.2, 128.9, 128.8, 128.6, 128.0, 127.8, 127.1, 127.1, 124.4, 64.0, 54.8, 53.4, 52.3, 50.3, 45.2, 44.4, 26.6, 19.1; HRFAB-MS (3-NOBA matrix): *m/z* = 1167.50502 (calcd. for $C_{70}H_{71}N_6O_9Si$, $[M]H^+$, 1167.50518).

3-(Benzyl-phenyl-carbamoyl)-acrylic acid ethyl ester (4.9)

To a cooled solution of N-benzylaniline (12.8 g, 70.0 mmol) and triethylamine (7 g, 5 mL, 70.0 mmol) in dichloromethane at 0 °C was added with vigorous stirring the solution of previously formed acid chloride **4.2** (70.0 mmol) dropwise over one hour. The reaction was left to stir overnight before being washed with 1M HCl (3 x 200 mL), saturated $NaHCO_3$ solution (3 x 50 mL) and brine (3 x 50 mL), dried over

$MgSO_4$, filtered and evaporated under reduced pressure to yield the product **4.9** as a pale yellow oil (19.7 g, 63.8 mmol, 91 %); ^{1}H NMR (400 MHz, $CDCl_3$, 298K) δ 7.30- 7.24 (3H, m Ph), 7.20- 7.16 (3H, m, Ph), 7.15- 7.12 (2H, m, Ph), 6.95- 6.88 (2H, m, Ph), 6.83 (1H, d_{AB}, J = 15 Hz, C=C<u>H</u>), 6.74 (1H, d_{AB}, J = 15 Hz, C=C<u>H</u>), 4.92 (2H, s, C<u>H</u>$_2$Ph), 4.08 (2H, q, J = 7.0 Hz, OC<u>H</u>$_2$), 1.16 (3H, t, J = $CH_2C\underline{H}_3$); ^{13}C (100 MHz, $CDCl_3$, 298K) δ 165.6, 163.8, 140.4, 136.8, 134.3, 131.5, 129.7, 128.7, 128.5, 128.3, 128.1, 127.6, 61.0, 53.5, 14.1; HRFAB-MS (3-NOBA matrix): *m/z* = 310.14548 (calcd. for $C_{19}H_{20}NO_3$, $[M]H^+$, 310.14432).

3-(Benzyl-phenyl-carbamoyl)-acrylic acid (4.10)

To a stirred solution of **4.9** (10 g, 32.4 mmol) in ethanol (100 mL) was added 1N NaOH (35.0 mL, 35.0 mmol). The resulting opaque mixture was stirred for three hours, before being filtered to remove the solid di(N,N-phenylbenzyl)fumaramide impurity. The resulting clear solution was acidified with 2N HCl to produce a white precipitate that was then extracted with ethyl acetate (3 x 200 mL). The combined organic washes were washed with water (3 x 100 mL), dried over $MgSO_4$ and evaporated to dryness under reduced pressure to yield the product **4.10** as a colourless solid (7.91g, 28.1 mmol, 87 %); ^{1}H NMR (400 MHz, $CDCl_3$, 298K) δ 7.31- 6.95 (10H, m, Ph), 6.53 (1H, d_{AB}, J = 15 Hz, C=CH), 6.46 (1H, d_{AB}, J = 15 Hz, C=CH), 4.84 (2H, s, CH_2Ph); ^{13}C NMR (100 MHz, $CDCl_3$, 298K) δ 169.9, 163.9, 140.7, 136.5, 135.9, 130.9, 129.8, 128.8, 128.6, 128.5, 128.0, 127.7, 53.6; HRFAB-MS (3-NOBA matrix): *m/z* = 282.11334 (calcd. for $C_{17}H_{16}NO_3$, $[M]H^+$, 282.11302).

3-(Benzyl-phenyl-carbamoyl)-acryloyl chloride (4.11)

To a stirred solution of **4.10** (2.8 g, 9.96 mmol) and catalytic dimethylformamide (1 mL) in dichloromethane (100 mL) at 0 °C was added oxalyl chloride (2M solution in dichloromethane, 4.98 mL, 9.96 mmol) over one hour. The reaction was stirred for a further hour until effervescence could no longer be observed. The resulting acid chloride **4.11** solution was used immediately without further purification.

2-[3-(Benzyl-phenyl-carbamoyl)-acryloylamino]-3-hydroxy-propionic acid benzyl ester (4.12)

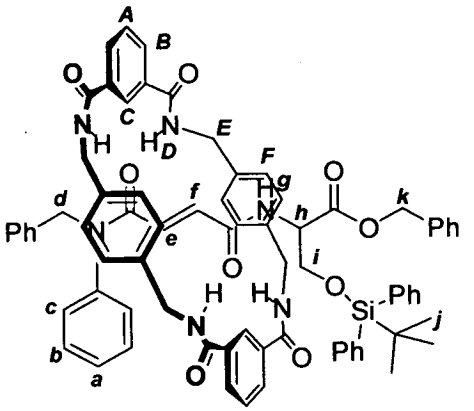
To a cooled, stirred solution of L-serine benzyl ester hydrochloride (2.54 g, 10.96 mmol) and triethylamine (2.5 g, 3.5 mL, 24.9 mmol) in dichloromethane (100 mL) at 0 °C was added the previously prepared solution of acid chloride **4.11** over one hour. The reaction was stirred for a further hour before being washed with 1M HCl (3 x 200 mL), saturated $NaHCO_3$ solution (3 x 50 mL) and water (3 x 50 mL), dried over $MgSO_4$, filtered and evaporated under reduced pressure to yield a yellow oil. The crude product was purified by column chromatography (SiO_2, dichloromethane / methanol) to yield the pure product **4.12** as a colourless oil (3.88 g, 8.47 mmol, 85 %); ^{1}H NMR (400 MHz, $CDCl_3$, 298K) δ 7.68 (1H, d, J = 7.5 Hz, NH), 7.27- 7.21 (8H, m, Ph), 7.19- 7.14 (3H, m, Ph), 7.13- 7.07 (3H, m, Ph, C=C<u>H</u>), 6.94- 6.89 (2H, m, Ph), 6.76 (1H, d, J = 15.0 Hz, C=CH), 5.10 (2H, s, NC<u>H</u>$_2$Ph), 4.92 (1H, d_{AB}, J = 14.0 Hz, OC<u>H</u>H'Ph), 4.88 (1H, d_{AB}, J = 14.0 Hz, OCH<u>H</u>'Ph), 4.58 (1H, dt, J = 3.0, 7.5 Hz, NHC<u>H</u>*), 3.94 (1H, dd, J = 3.0, 7.5 Hz, CH*C<u>H</u>H'), 3.82 (1H, dd, J = 3.0, 7.5 Hz, CH*CH<u>H</u>'), 3.67 (1H, bs, OH); ^{13}C NMR (100 MHz, $CDCl_3$, 298K) δ 170.1, 164.6, 164.3, 141.0, 136.8, 135.4, 133.9, 131.5, 129.7, 128.6, 128.5, 128.4, 128.3, 128.1, 128.0, 127.5, 67.3, 62.8, 55.4, 53.5; HRFAB-MS (3-NOBA matrix): *m/z* = 459.19100 (calcd. for $C_{27}H_{27}N_2O_5$, $[M]H^+$, 459.19200).

2-[3-(Benzyl-phenyl-carbamoyl)-acryloylamino]-3-(*t*-butyl-diphenyl-silanyloxy)-propionic acid benzyl ester (4.13)

To a stirred solution of **4.12** (3.88g, 8.47 mmol, 1 eq.) and imidazole (1.73 g, 25.4 mmol, 3 eq.) in dichloromethane (100 mL) was added *tert*-butyldiphenylsilyl chloride (4.64 g, 4.39 mL, 16.9 mmol, 2 eq.). The reaction was allowed to stir for 48 hours during which the evolution of a white precipitate of imidazole hydrochloride was be observed. The completed reaction was filtered and reduced in volume under reduced pressure to around 10 mL. The crude product was purified by column chromatography (SiO_2, 0.6 % methanol / dichloromethane) to give the pure product

4.13 as a colourless oil (6.23 g, 6.67 mmol, 79 %); ^{1}H NMR (400 MHz, $CDCl_3$, 298K) δ 7.57 -7.51 (4H, m, Ph), 7.45- 7.39 (2H, m, Ph), 7.38- 7.20 (18H, m, Ph), 7.02- 6.98 (2H, m, Ph), 6.96 (1H, d, J = 15.0 Hz, C=C<u>H</u>), 6.81 (1H, d, J = 15.0 Hz, C=C<u>H</u>), 6.56 (1H, d, J = 8.0 Hz, NH), 5.19 (1H, d_{AB}, J = 12.0 Hz, OC<u>H</u>H'Ph), 5.16 (1H, d_{AB}, J = 12.0 Hz, OCH<u>H</u>'Ph), 5.03 (1H, d_{AB}, J = 14.0 Hz, NC<u>H</u>H'Ph), 5.00 (1H, d_{AB}, J = 14.0 Hz, NCH<u>H</u>'Ph), 4.71 (1H, dt, J = 2.5, 8.0 Hz, NHC<u>H</u>*), 4.15 (1H, dd, J = 2.5, 10.0 Hz, CH*C<u>H</u>H'), 3.86 (1H, dd, J = 2.5, 10.0 Hz, CH*CH<u>H</u>'), 1.01 (9H, s, C(C<u>H</u>$_3$)$_3$); ^{13}C NMR (100 MHz, $CDCl_3$, 298K) δ 169.8, 164.3, 163.6, 158.1, 141.0, 136.9, 135.5, 135.4, 135.0, 129.9, 129.7, 128.7, 128.6, 128.5, 128.4, 128.3, 128.1, 127.9, 127.8, 127.6, 67.5, 64.1, 54.5, 53.6, 26.8, 19.3; HRFAB-MS (3-NOBA matrix): m/z = 697.31015 (calcd. for $C_{43}H_{45}N_2O_5Si$, $[M]H^+$, 697.30978).

[2](1,7,14,20-Tetraaza-2,6,15,19-tetraoxo-3,5,9,12,16,18,22,25-tetrabenzocyclohexacosane)-2-[3-(Benzyl-phenyl-carbamoyl)-acryloylamino]-3-(*t*-butyl-diphenyl-silanyloxy)-propionic acid benzyl ester rotaxane (4.14)



To a stirred solution of **4.13** (3.00 g, 3.21 mmol, 1eq.) in chloroform (50 mL) was added simultaneously solutions of *p*-xylylene diamine (2.62 g, 19.3 mmol, 6 eq.) and triethylamine (4.86 g, 6.75 mL, 48.2 mmol, 15 eq.) in chloroform (50 mL), and isophthaloyl chloride (3.91 g, 19.3 mmol, 6 eq.) in chloroform (50 mL) via syringe pump over three hours. After addition the reaction was stirred for a further hour before being filtered and reduced in volume under reduced pressure. The crude reaction mixture was then purified by column chromatography (SiO_2) to recover unconsumed starting material (**4.13**, 0.96 g, 32 %) with 0.8 % methanol / dichloromethane, and the desired rotaxane product as a white solid with 1.2 %

methanol dichlormethane (**4.14**, 2.54 g, 1.73 mmol, 54 %); ^{1}H NMR (400 MHz, $CDCl_3$, 298K) δ 8.25 (4H, bm, ***B***), 8.16 (2H, bs, ***C***), 7.64- 7.51 (6H, m, ***A***, Ph, ***g***), 7.39-7.23 (10H, m, Ph), 7.23- 7.13 (8H, m, Ph, ***D***), 7.07- 6.97 (6H, m, Ph, ***F***), 6.96-6.84 (8H, m, Ph, ***F'***), 6.78 (2H, abd, J = 7.5 Hz, ***b***), 6.49 (1H, dt, J = 7.5, 1.0 Hz, ***a***), 5.77 (1H, ad, J = 15.0 Hz, C=C<u>H</u>), 5.49 (1H, ad, J = 15.0 Hz, C=C<u>H</u>), 5.23 (1H, d, J = 12.0 Hz, ***k***), 5.04 (1H, d, J = 12.0 Hz, ***k'***), 4.62 (1H, bd_{AB}, J = 14.0 Hz, ***d***), 4.62 (1H, bd_{AB}, J = 14.0 Hz, ***d'***), 4.54 (1H, dt, J = 3.5, 7.0 Hz, ***h***), 4.50- 4.37 (4H, bm, ***E***), 4.32- 4.16 (5H, bm, ***E'***, ***i***), 3.95 (1H, ddd, J = 1.0, 10.5, 4.5 Hz, ***i'***), 0.99 (9H, bs, ***j***); ^{13}C NMR (100 MHz, $CDCl_3$, 298K) δ 191.9, 169.2, 165.8, 165.6, 164.4, 158.1, 139.7, 137.3, 155.5, 135.4, 134.8, 133.6, 133.5, 132.1, 131.8, 131.7, 130.9, 130.4, 130.2, 129.5, 129.3, 129.2, 128.7, 128.6, 128.5, 128.4, 128.3, 128.1, 127.9, 127.1, 123.3, 116.3, 67.7, 63.6, 63.6, 55.4, 54.7, 26.7, 19.2; HRFAB-MS (3-NOBA matrix): m/z = 1229.52340 (calcd. for $C_{75}H_{73}N_6O_9Si$, $[M]H^+$, 1229.52083).

[2](1,7,14,20-Tetraaza-2,6,15,19-tetraoxo-3,5,9,12,16,18,22,25-tetrabenzocyclohexacosane)-2-[3-(Benzyl-phenyl-carbamoyl)-acryloylamino]-3-(*t*-butyl-diphenyl-silanyloxy)-propionic acid rotaxane (4.15)

To a stirred solution of **4.14** (100 mg, 68 μmol) in ethyl acetate (20 mL) was added a catalytic amount of palladium on activated carbon (5 mg). The closed vessel was evacuated and purged with hydrogen three times before being left under a positive pressure of hydrogen for 24 hours. The reaction vessel was evacuated and purged three times with hydrogen again before being left under a positive pressure of hydrogen for a further 24 hours. The reaction was filtered through celite and evaporated to dryness under reduced pressure. The product was recovered pure as a colourless powder (**4.15**, 89 mg, 64 μmol, 95 %); ^{1}H NMR (400 MHz, $CDCl_3$, 298K) δ 8.23- 8.15 (6H, m, ***B***,***C***), 7.90 (1H, bs, ***g***), 7.61 (4H, d, J = 7.0 Hz, Ph), 7.54 (2H, t, J = 7.5 Hz, **A**), 7.40 (2H, bt, Ph), 7.37- 7.27 (7H, m, Ph), 7.27- 7.07 (10H, m, Ph), 6.97 (4H, d_{AB}, J = 7.5Hz, ***F***), 6.90 (6H, m, Ph, ***F'***), 6.85 (2H, abt, J = 7.0 Hz, ***b***), 6.65 (2H, d, J = 8.0 Hz, ***c***), 6.36 (1H, t, J = 7.0 Hz, ***a***), 5.81 (1H, d, J = 15 Hz, C=C<u>H</u>), 5.45 (1H, d, J = 15 Hz, C=C<u>H</u>), 4.60 (3H, m, ***d***, ***g***), 4.46- 4.35 (4H, bm, ***E***), 4.30-4.14 (5H, bm, ***E'***, ***i***), 3.95 (1H, dd, J = 10.0, 4.0 Hz, ***i'***), 1.02 (9H, s, ***j***); ^{13}C NMR

(100 MHz, $CDCl_3$, 298K) δ 187.0, 168.1, 166.0, 165.5, 164.4, 139.7, 137.2, 137.1, 135.5, 135.4, 135.3, 133.2, 133.2, 132.3, 132.2, 131.9, 131.8, 131.7, 130.3, 130.1, 129.4, 129.3, 129.2, 129.1, 129.1, 129.0, 128.5, 128.3, 128.3, 128.2, 128.0, 127.8, 127.1, 125.2, 123.3, 63.7, 55.2, 54.7, 43.7, 26.7, 19.2; HRFAB-MS (3-NOBA matrix): *m/z* = 1139.47327 (calcd. for $C_{68}H_{67}N_6O_9Si$, $[M]H^+$, 1139.47388).

4.5 References

(1) Altieri, A.; Bottari, G.; Dehez, F.; Leigh, D. A.; Wong, J. K. Y.; Zerbetto, F., *Angew. Chem. Int. Ed.*, **2003**, *42*, 2296-2300.

(2) Gatti, F. G.; Leigh, D. A.; Nepogodiev, S. A.; Slawin, A. M. Z.; Teat, S. J.; Wong, J. K. Y., *J. Am. Chem. Soc.*, **2001**, *123*, 5983-5989.

(3) Otera, J., *Chem. Rev.*, **1993**, *93*, 1449-1470.

(4) Gatti, F. G.; Leon, S.; Wong, J. K. Y.; Bottari, G.; Altieri, A.; Morales, M. A. F.; Teat, S. J.; Frochot, C.; Leigh, D. A.; Brouwer, A. M.; Zerbetto, F., *Proc. Nat. Acad. Sci.*, **2003**, *100*, 10-14.

(5) Brouwer, A. M.; Fazio, S. M.; Frochot, C.; Gatti, F. G.; Leigh, D. A.; Wong, J. K. Y.; Wurpel, G. W. H., *Pure Appl. Chem.*, **2003**, *75*, 1055-1060.

(6) Saltiel, J.; Sears, J., D. F.; Ko, D.-H.; Park, K.-M. In *CRC Handbook of Organic Photochemistry and Photobiology*; Horspool, W. M., Song, P.-S., Eds.; CRC Press: Boca Raton, New York, London, Tokyo, 1995, pp 3-15.

(7) Stanier, C. A.; Alderman, S. J.; Claridge, T. D. W.; Anderson, H. L., *Angew. Chem. Int. Ed.*, **2002**, *41*, 1769-1772.

Chapter 5

Using Symmetrical Molecular Shuttles to Study the Mechanism of Intercomponent Motion in Rotaxanes

Declaration: NMR experiments were carried out by Emilio Perez.

5.1 Introduction

Molecular shuttles, two station [2]rotaxanes, have received much attention in the pursuit of developing molecular machines since the first symmetrical shuttle was reported in 1991 (see figure 5.1).[1] In this interlocked system, the macrocycle was observed to 'shuttle' between the two identical binding sites, or stations, effectively half-occupying each one. The authors concluded their study by proposing the use of different stations to desymmetrise the system, in order to control the relative positions of the two components, as a possible route towards making switching devices. Since this time, almost all research into molecular shuttles has focused on developing them into functional molecular machines.[2]

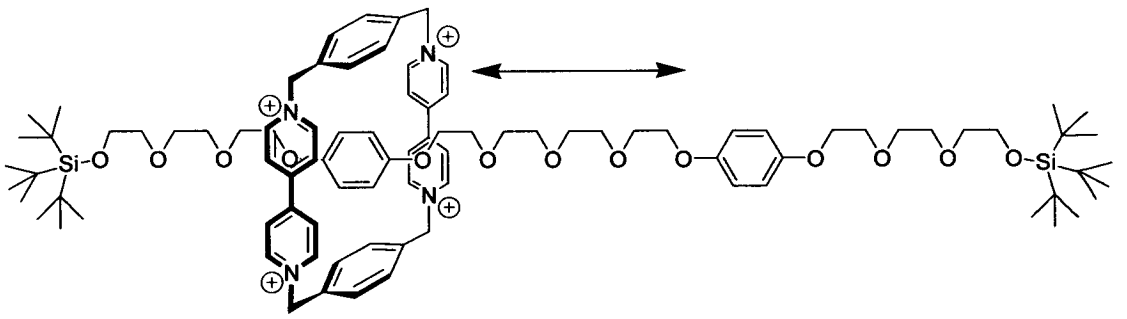


Figure 5. 1 Symmetrical molecular shuttle synthesised by Stoddart.[1]

The route by which shuttles are being developed involves incorporating two different stations, one of which can be selectively addressed using some external stimulus, *e.g.* light, heat, chemical- or electrochemical- energy, to change the relative binding

affinities of one station compared to another. This line of research has produced some remarkable prototype devices such as a light-driven[3] and electrochemically-driven piston,[4] an acid / base- and electrochemically-driven switching device,[5] and also a three station, unidirectional [3]catenane rotor.[6]

With such focus on designing molecular devices, the original, symmetrical design of molecular shuttle has been almost overlooked as a subject for study. In 1997, Leigh and co-workers designed a series of three shuttles using a hydrogen-bonded [2]rotaxane system incorporating two peptide stations separated by different spacers (see figure 5.2).[7] The synthesis of several shuttles allowed them to study the systems in more depth and several interesting observations were made. Firstly, on altering the distance separating the stations, the rate of shuttling was affected. The presence of a longer chain separating the two stations decreased the rate of shuttling, therefore also increasing the activation energy barrier for the shuttling process. Also, oxidising a sulfur atom within the alkyl chain to a sulfoxide and then a sulfone had no effect on the rate of shuttling, despite the obvious change in size and hydrogen bonding-ability of the sulfur group between the two stations. Shuttling was only disrupted when the sulfur group was functionalised with an N-tosyl group, large enough to block the macrocycle from passing over. The authors offered no explanation for these observations.

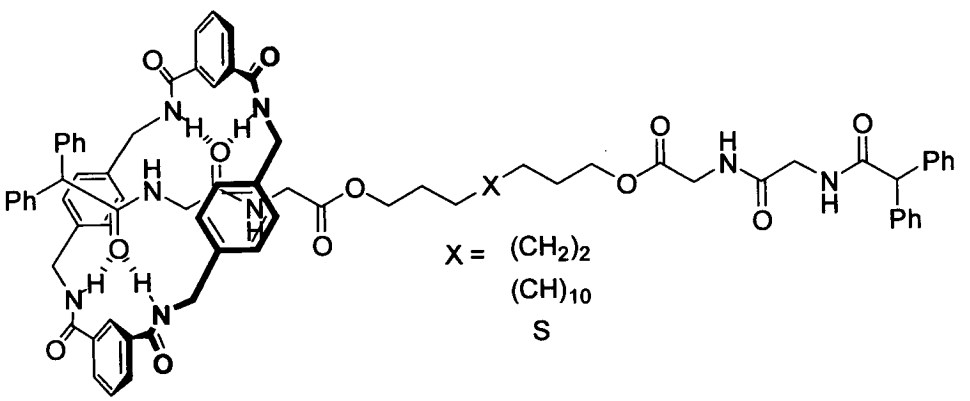


Figure 5. 2 Peptide-based molecular shuttle of Leigh.

The fact that the rate of shuttling is dependent on the length of the separating alkyl chain, at first, seems reasonable given that the macrocycle has a longer distance to travel between stations, but this observation is taken from the classical viewpoint of a macroscopic system. On looking at the system in terms of energetics, the length dependence of the rate is harder to explain. The difference in rates of exchange means that there must be a difference in the energy barriers for the shuttling process in the different systems (see figure 5.3). Since the most energetically significant process one can envision is the breaking of the four strong hydrogen bonds at the station, this should be the rate-determining step of the shuttling process. There is no obvious explanation as to where the length dependence of the shuttling process comes from, as this should not affect the rate at which the hydrogen bonds at the identical stations in each system are broken. Equally, if the alkyl chain had an effect on the shuttling rate, why is the rate unaffected by the different sized groups in the chain?

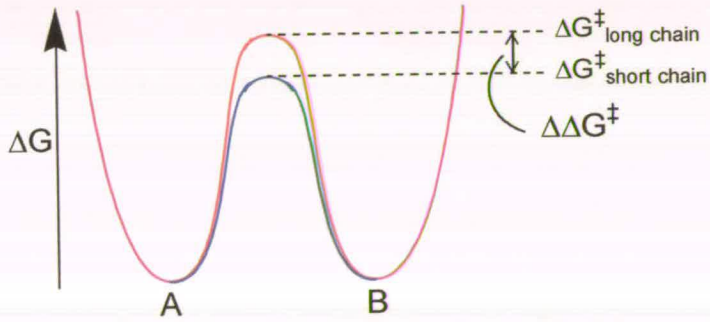


Figure 5. 3 The energy profile for the shuttling process between stations A and B. The height of the barrier (the activation energy) must be higher in the longer chain systems to explain the difference in shuttling rate. This difference in activation energy ($\Delta\Delta G^{\ddagger}$) must be a result of the different length alkyl chains as the stations are the same in both systems.

The answer to this riddle lies in the mechanism of the macrocyclic motion, *i.e.* how the macrocycle gets from station A to station B. Once the macrocycle has left the station, motion along the alkyl chain is probably as a result of a diffusional process, *e.g.* Brownian motion. This mode of motion could explain the observed length dependence of the shuttling rate. The macrocycle will spend relatively a large amount of time sat on a station, before it gains sufficient energy to break all four

restraining hydrogen bonds in order to move away from the station. The macrocycle motion along the alkyl chain will occur on a much faster time-scale than this off-station process, and therefore the speed of motion has no bearing on the rate of shuttling. This is opposite to the clasical view of the system, where the macrocycle has further to travel and will therefore take longer to get there. Instead it is the diffusional nature of the motion that dictates the length dependence of shuttling. As the macrocycle moves via diffusional instead of inertial motion, travel in the backwards direction is equally likely as in the forward direction. This introduces the possibility of the macrocycle returning to the station it has just left, and not undergoing exchange. Thus, the shuttling process is dependent on two factors: 1) the motion of the macrocycle off the station, involving the energetically costly process of breaking four hydrogen bonds, and 2) the statistical probability of the macrocycle reaching the other station, therefore undergoing exchange, instead of returning undetected to its starting point. Therefore, although there is only one energetically costly step in the shuttling process, *i.e.* the macrocycle moving off the station, the breaking of the binding interaction may have to be repeated many times before actual exchange takes place, and exchange becomes less likely as the chain gets longer.

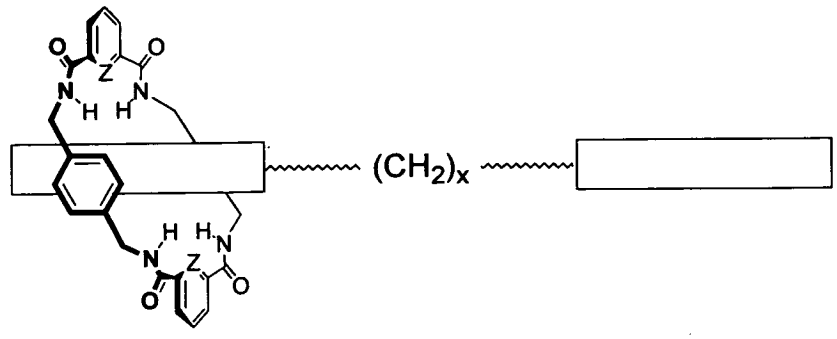
Another alternative mechanism of macrocyclic motion between stations could be due to the two stations associating in solution. If the unoccupied station associates with the macrocycle at the occupied station, it may provide a means for the intercomponent hydrogen bonds to be broken, and therefore catalyse the macrocycle leaving the station. Since the association of the two chain ends is entropically unfavourable due to the necessary ordering of the alkyl chain, this mechanism would also explain the length dependence of the shuttling motion, as increasing the alkyl chain length makes the end group association less likely to occur.

In order to prove which of these theories is correct, another series of molecular shuttles has been designed and synthesised. A greater range of data will be collected to show the how the length dependence changes with respect to length of alkyl spacer, station binding strength and the type of macrocycle. This should help

improve our understanding of molecular shuttle systems in general and allow us to better predict the behaviour of more complicated systems.

5.2 Results and Discussion

A series of molecular shuttles was synthesised, with each [2]rotaxane system incorporating two identical stations, either succinic amide ester- or a fumaric- based, an alkyl chain and a macrocycle (see figure 5.4). The two different types of station were used in the shuttle series to compare the difference in binding ability[8] and shuttling rate between the two. Different length alkyl spacers, C2 to C12, were used in order to observe how the shuttling rate changes on increasing the length of the spacers. Different macrocycles, isophthaloyl- or *endo*-pyridyl-, were also used in the series in order to observe whether a change in binding strength affects the shuttling behaviour. The nomenclature used to refer to the individual shuttles incorporates the type of station used, **A** for succinic amide ester- and **B** for fumaric-based, the macrocycle used, **I** for isophthaloyl, **P** for *endo*-pyridyl, and the length of the alkyl spacer, indicated by the number of carbons in the chain.



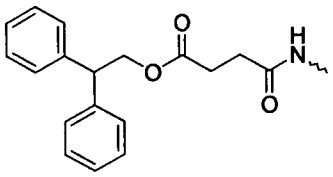
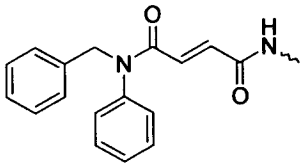
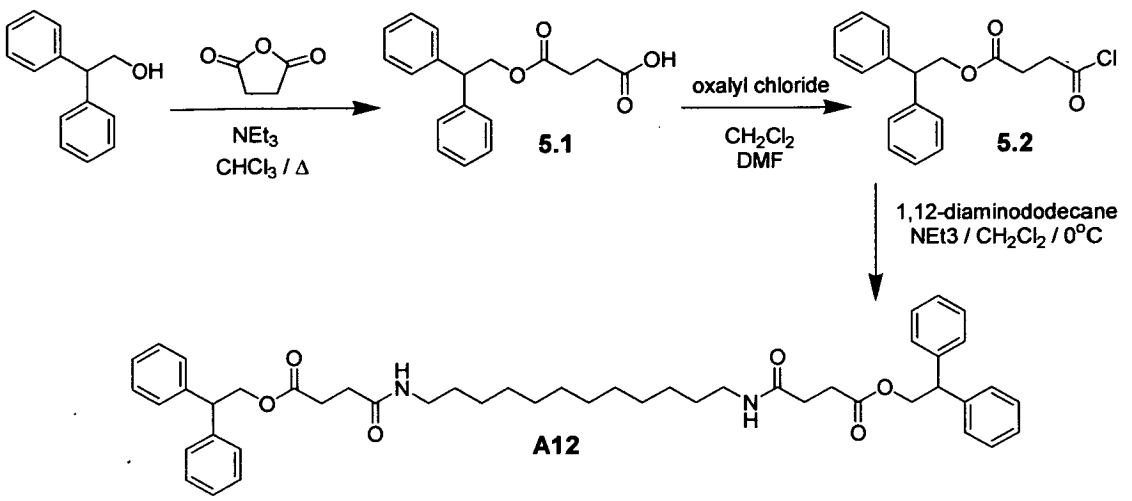
	x	Z	Name
	12	CH	**AI 12**
	12	N	**AP 12**
	12	CH	**BI 12**
	10	CH	**BI 10**
	8	CH	**BI 8**
	6	CH	**BI 6**
	4	CH	**BI 4**
	2	CH	**BI 2**
	12	N	**BP 12**
	6	N	**BP 6**

Figure 5. 4 The series of molecular shuttles synthesised indicating the different stations, length of alkyl spacer and macrocycle that were used, and the nomenclature used to refer to them.

5.2.1 Synthesis

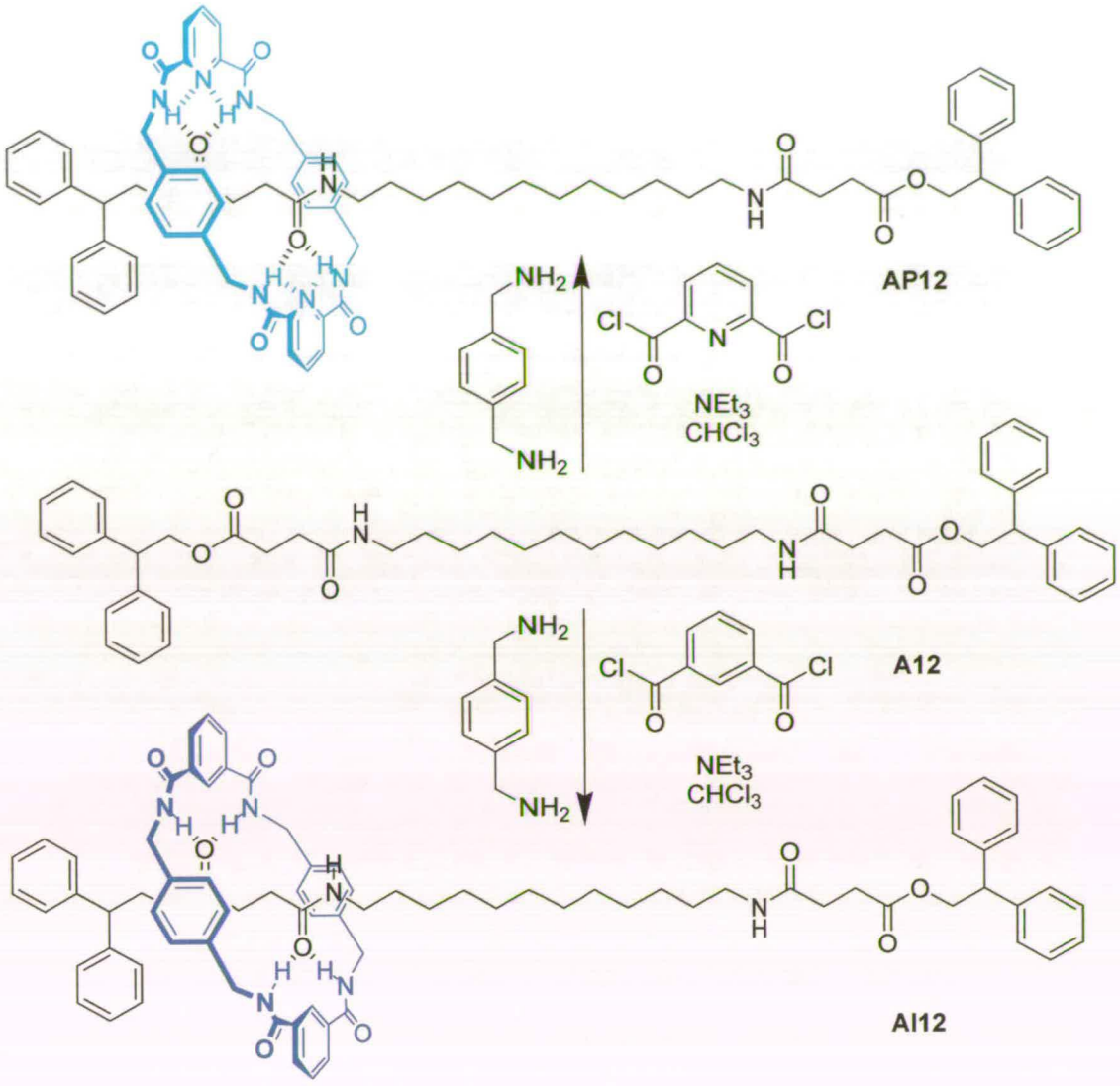
The succinic amide ester based thread was synthesised in three steps (see scheme 5.1). Firstly refluxing succinic anhydride and 2,2-diphenylethanol ($CDCl_3$, 60°C,

24h) produced the stoppered succinic acid **5.1** in 80% yield. The acid chloride **5.2** was then formed using oxalyl chloride with catalytic dimethylformamide (methylene chloride, 2.5 h). This was used, without further purification, to form the thread **A12** in 72% yield by dropwise addition to a solution of the 1,12-diaminododecane ($CHCl_3$, triethylamine, 2.5 h).



Scheme 5. 1 Synthesis of the succinic amide ester-based thread **A12** in three steps.

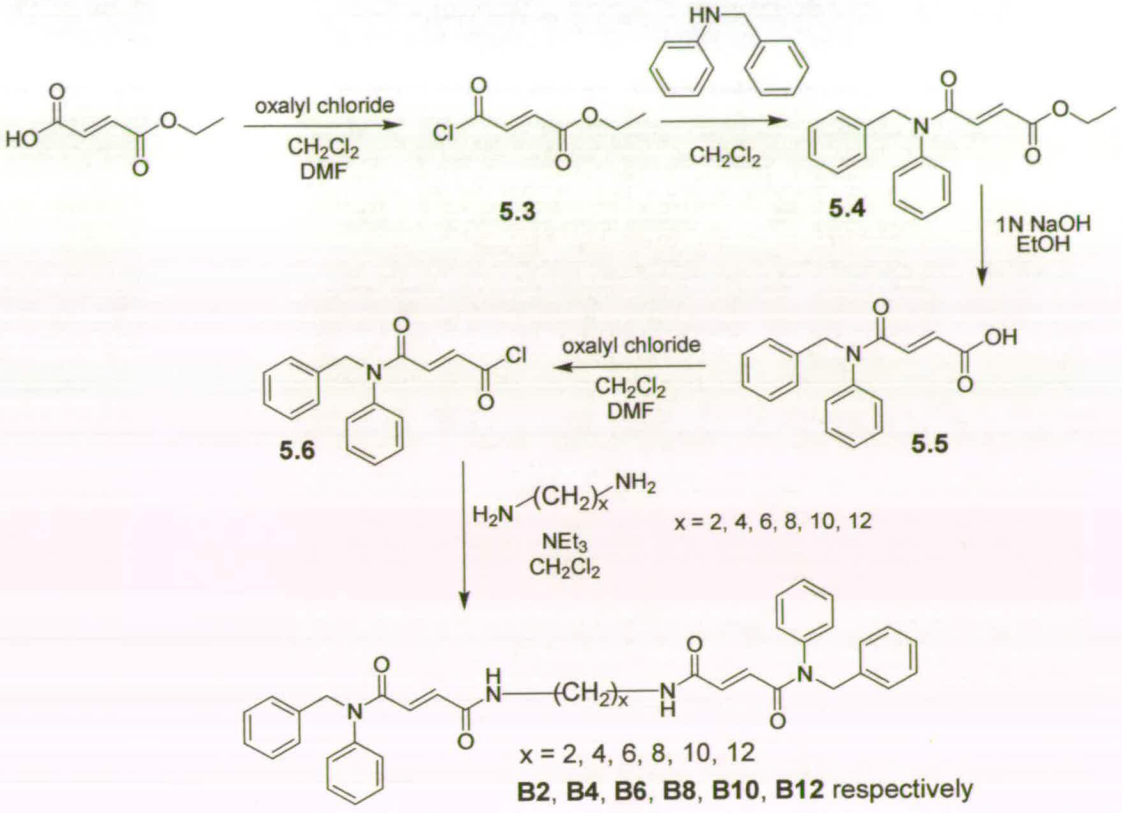
The corresponding isophthaloyl and *endo*-pyridyl rotaxanes, **AI12** and **AP12** respectively, were synthesised by simultaneous addition of solutions of the respective di-acid chlorides and *p*-xylelenediamine / triethylamine to solutions of the thread (chloroform, 4 hours) (see scheme 5.2). The rotaxanes **AI12** and **AP12** were isolated from the unconsumed thread in 16 % and 6.2 % yield.



Scheme 5. 2 Synthesis of the rotaxanes **AI12** and **AP12** from thread **A12**.

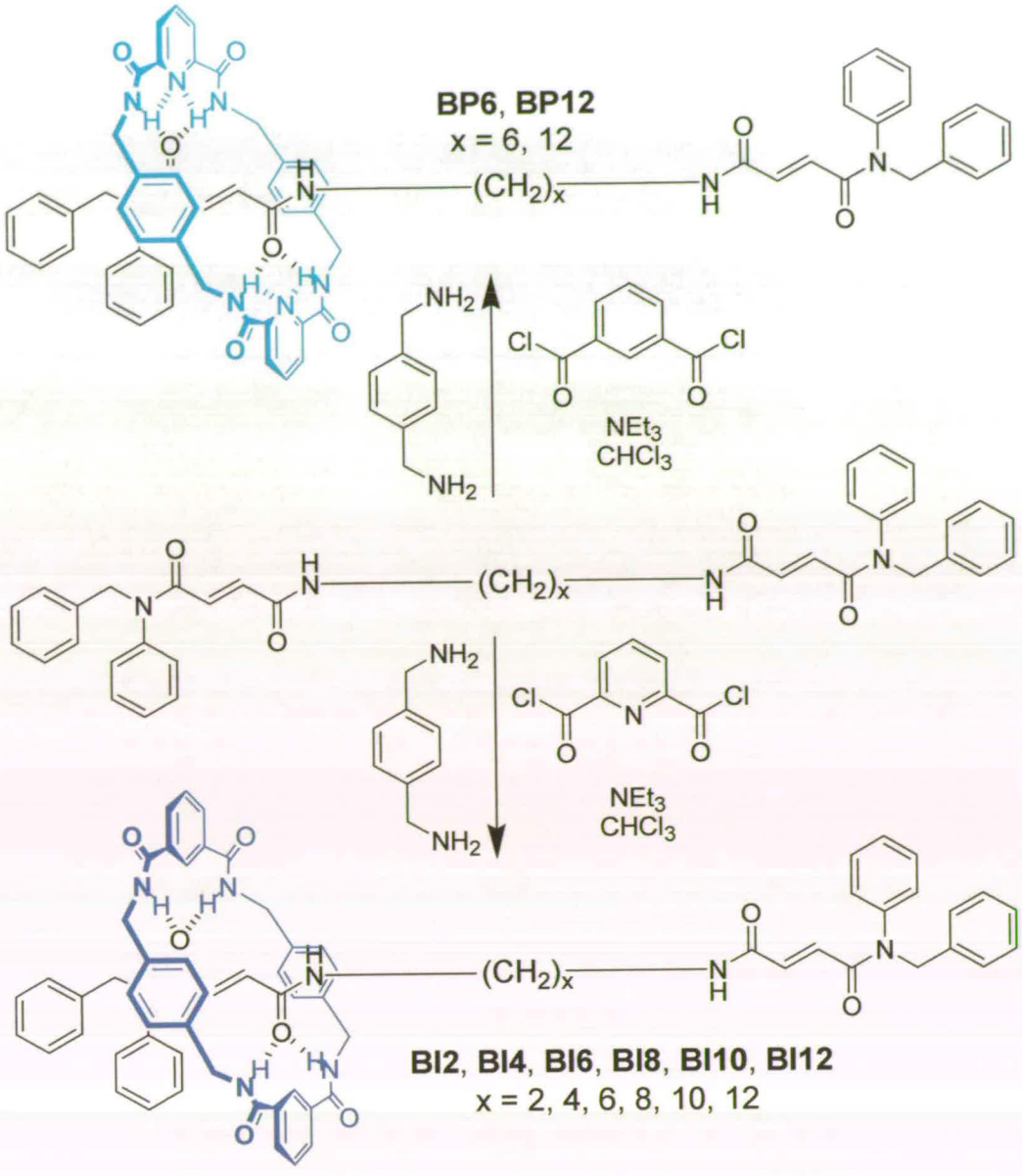
The fumaric-based threads were synthesised in five steps (see scheme 5.3). Firstly, the acid chloride **5.3** of fumaric acid mono ethyl ester was formed using oxalyl chloride and catalytic dimethylformamide (methylene chloride, 2 h) and used, without further purification, to form the stoppered fumaric ester **5.4** in 91 % yield by dropwise addition to a cooled solution of N-benzylaniline and triethylamine (methylene chloride, 0 °C, 24 h). The ethyl ester of **5.4** was then saponified with 1N sodium hydroxide (ethanol, 3 h) and the acid **5.5** was recovered in 87 % yield by extracting the acidified solution. The acid chloride **5.6** was then formed using oxalyl chloride and catalytic dimethylformamide (methylene chloride, 2 h), which was

again used without further purification. Adding a solution of the acid chloride **5.6** to a cooled solution of the respective diamines formed the series of different length threads, **B2**, **B4**, **B6**, **B8**, **B10** and **B12** respectively (methylene chloride, NEt_3, 0 °C, 2 h), which precipitated out from the reaction mixture and were isolated pure by filtration.



Scheme 5. 3 Synthesis of the fumaric-based threads **B2, B4, B6, B8, B10** and **B12** in five steps.

The corresponding isophthaloyl rotaxanes **BI2**, **BI4**, **BI6**, **BI8**, **BI10** and **BI12**, and *endo*-pyridyl rotaxanes **BP6** and **BP12** were then formed by simultaneous addition of solutions of the respective di-acid chloride (3 equivalents) and *p*-xylylenediamine (3 equivalents)/ triethylamine to solutions of the respective threads (see scheme 5.4). Only three equivalents of di-acid chloride, di-amine were used, because the fumaric template is so efficient at rotaxane formation,[9] it is necessary in order to limit the production of [3]rotaxane. The [2]rotaxanes (shuttles) were isolated in yields of 9 to 28% from the unconsumed thread and [3]rotaxanes after column chromatography.



Scheme 5. 4 Synthesis of the rotaxanes isophthaloyl rotaxanes **BI2**, **BI4**, **BI6**, **BI8**, **BI10** and **BI12**, and *endo*-pyridyl rotaxanes **BP6** and **BP12**.

5.2.2 Shuttle Dynamics

A look at the room temperature ^{1}H NMR spectra of the shuttles shows some interesting features. The usual features associated with rotaxane formation are present, e.g. appearance of macrocycle peaks in the spectrum, and shielding of some of the thread protons due to the presence of the macrocycle, compared to the uninterlocked threads, **AP12** and **BP12**. Some peaks within the spectrum appear

broad indicating an exchange process caused by shuttling of the macrocycle between the stations.[7] The ^{1}H NMR spectra of the succinic amide ester rotaxanes show similar features to each other (see figure 5.5). The succinic protons in **AP12** and **AI12** each appear as a single broad resonance and the rotaxane appears symmetrical, as the shuttling process is occurring quickly. They are also shielded differently compared to the thread **A12**. In **AP12** the succinic protons appear 1 ppm* further upfield than the thread whereas in rotaxane **AI12** they appear 0.6 ppm further upfield. The increased shielding experienced with the *endo*-pyridyl macrocycle may be due a tighter binding interaction at the station.[10]

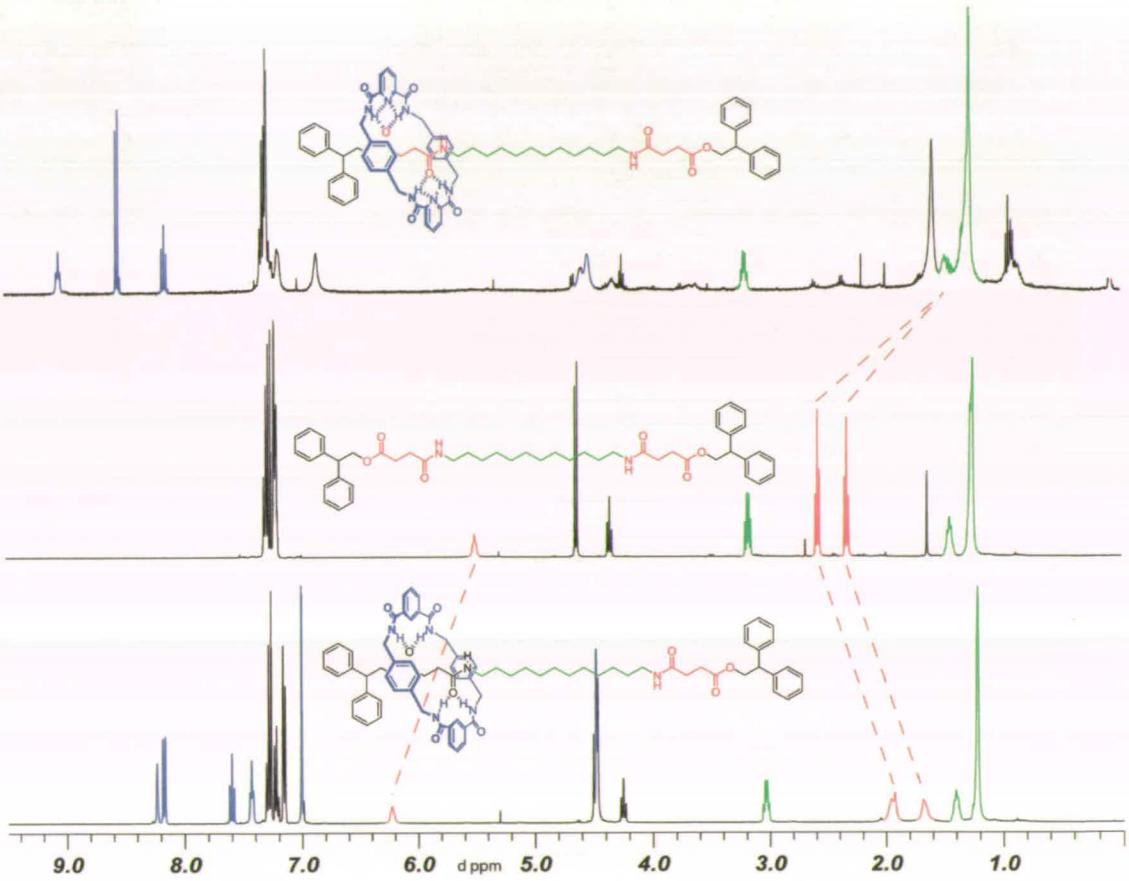


Figure 5. 5 The ^{1}H NMR spectra (400 MHz, $CDCl_3$, 298 K) of the succinic amide ester based *endo*-pyridyl rotaxane **AP12** (top), thread **A12** (middle) and isophthaloyl rotaxane **AI12** (bottom). The colours indicate the features shown in the diagrams.

* The exact position of the shielded succinic protons under the alkyl chain was determined by the ^{1}H, ^{1}H TOCSY and ^{1}H, ^{13}C HMQC.

In contrast, the room temperature ^{1}H NMR spectra of the two fumaric-based shuttles, **BP12** and **BI12**, appear very different from the spectra of the succinic amide ester-based shuttles, and from each other (see figure 5.6). The endo-pyridyl shuttle **BP12** shows doubling-up of many of the peaks, indicating that the two stations of the thread have been desymmetrised, *e.g.* the fumaric protons and the stopper benzylic protons. This is caused by the slow exchange of the macrocycle between the stations, so that only one is occupied, and therefore appears shielded with respect to the other, unoccupied station. The benzylic protons of the macrocycle are also split indicating slow piroutetting of the macrocycle around the station.[11] The ^{1}H NMR of the isophthaloyl shuttle **BI12** is broad at room temperature. It is just possible to make out the desymmetrised peaks, but the exchanging protons are quite close to the coalescence point.

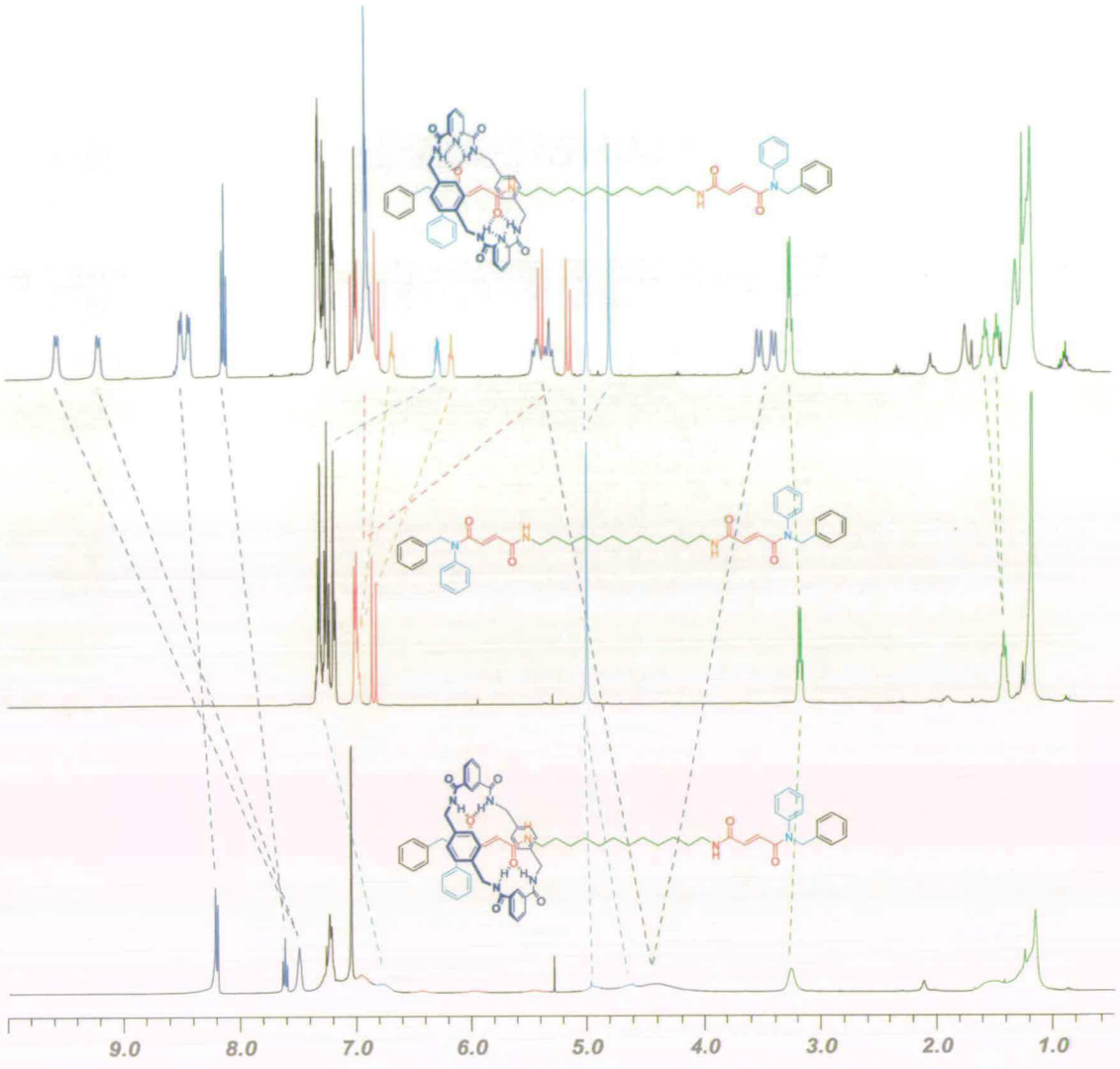


Figure 5. 6 The ^{1}H NMR spectra (400 MHz, $CDCl_3$, 298 K) of the fumaric based *endo*-pyridyl rotaxane **BP12** (top), thread **B12** (middle) and isophthaloyl rotaxane **BI12** (bottom). The colours indicate the features shown in the diagrams.

Observations from the room temperature dynamics in the ^{1}H NMR spectra of the shuttles allow us to draw some general conclusions. The endo-pyridyl macrocycle appears to bind to the stations much more tightly than the isophthaloyl macrocycle, as it undergoes slower exchange. Also, the fumaric-based rotaxanes undergo slower shuttling that the succinic amide ester rotaxanes. These two observations suggest that the choice of stations and macrocycle, *i.e.* the strength of binding interaction at the stations, has a large effect of the rate of shuttling, and the size of the activation energy barrier.

The dynamics can be better observed using Variable Temperature (VT) ^{1}H NMR. Reducing the temperature slows down the dynamic processes, and this can be observed in the VT ^{1}H NMR spectra first by broadening, then desymmetrisation of the exchanging signals. The VT spectra for **AP12** shows how the spectrum changes on reducing the temperature (see figure 5.7).

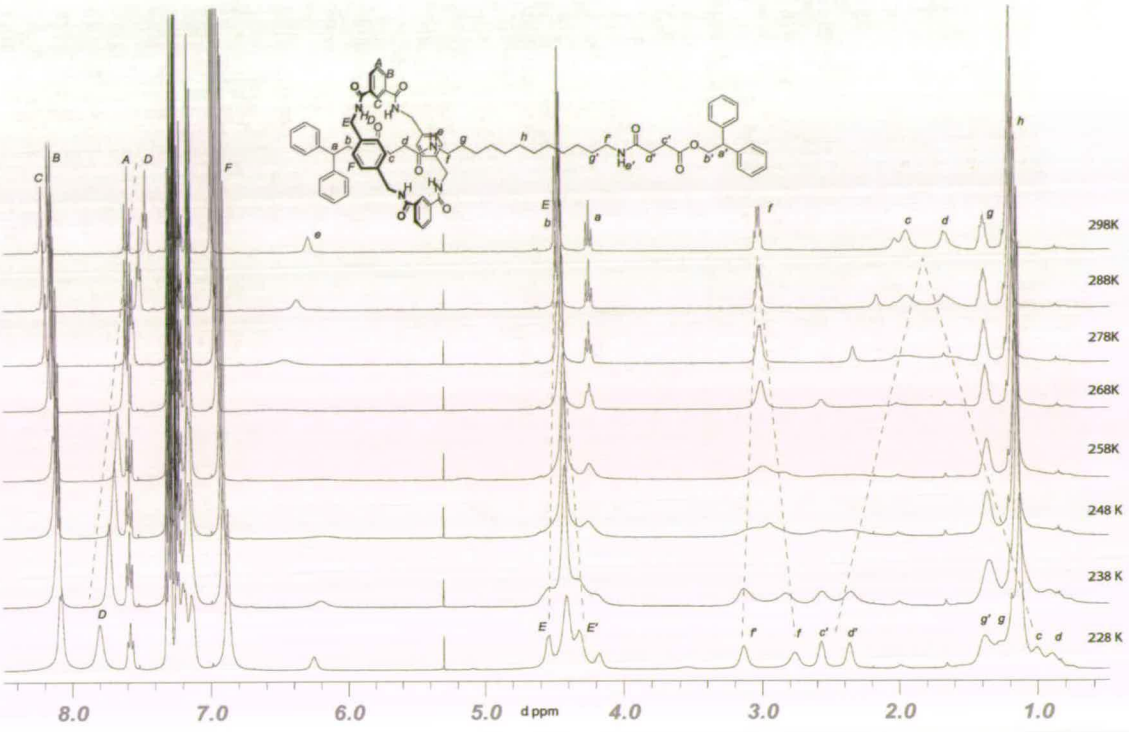


Figure 5. 7 The VT ^{1}H NMR (400 MHz, $CDCl_3$) stack plot showing how the shuttle dynamics cause broadening then desymmetrisation of the exchanging signals with reducing temperature in rotaxane **AI12**.

The VT spectra of **AI12** show that as the temperature is reduced, each of the symmetrical succinic proton signals H_c and H_d first broaden and then resolve into two separate signals as the shuttling slows down and the two stations become inequivalent, *i.e.* one occupied and the other unoccupied. Therefore, at high temperature the fast exchanging protons appear as averaged signals, with each station half-occupied and experiencing the same degree of shielding. As the temperature is reduced, the signals are desymmetrised as one station is fully occupied, feeling the

full shielding effect and the other fully unoccupied, experiencing no shielding at all. In fact, at low temperature the unshielded protons appear at the same chemical shift as they do in the thread. Besides the succinic protons, the alkyl chain α-protons H_f also undergo exchange, as they become desymmetrised at low temperature, indicating that they experience some shielding from the macrocycle also. The amide protons, H_D, shift further downfield as the temperature is reduced because the hydrogen bonding interaction gets stronger, *i.e.* the macrocycle sits more tightly on the station. It is also possible to observe another exchange process that is taking place. At very low temperatures the benzylic protons of the macrocycle, H_E, start to broaden as they become desymmetrised. The exchange process that is responsible for this phenomenon is not shuttling of the macrocycle between stations, but circumrotation or pirouetting of the macrocycle around the thread. This process has been used in the past to quantify the strength of the hydrogen bonding interactions between the thread and the macrocycle,[12] as the macrocycle must break all of the hydrogen bonding interactions and flip conformations (which brings about the chemical exchange) in order for circumrotation to occur. As the benzylic protons, H_E, are only just starting to broaden at 298 K, it appears that the rate of pirouetting is much faster than the rate of shuttling as one would expect (see figure 5.8).

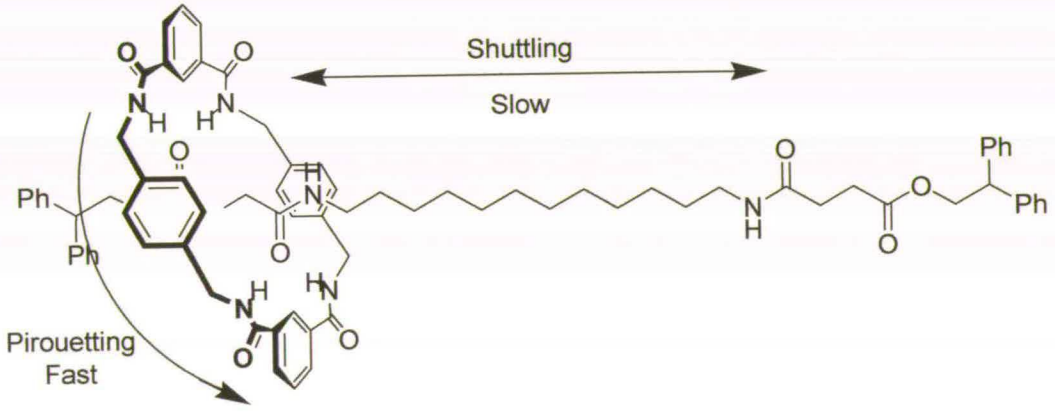


Figure 5. 8 The two exchange processes in the shuttle systems: pirouetting and shuttling.

The two different exchanges processes can be seen more clearly in the VT ^{1}H NMR spectra of the fumaric-based shuttles. The fumaric template offers a stronger hydrogen bonding interaction to the macrocycle,[12] and therefore both the dynamic process are slower than in the succinic amide ester shuttles. In the VT ^{1}H NMR

spectra of shuttle **BI12** (see figure 5.9) it is possible to observe that on reducing the temperature, the thread station peaks becomes broader until they resolve at ~263 K into two sets of peaks for the two desymmetrised ends of the thread. Cooling below this temperature sees broadening and splitting of the macrocycle peaks as the pirouetting of the macrocycle slows down, and the two isophthaloyl ends occupy different environments, *i.e.* one shielded by the N-phenyl of the thread, and the other unshielded.

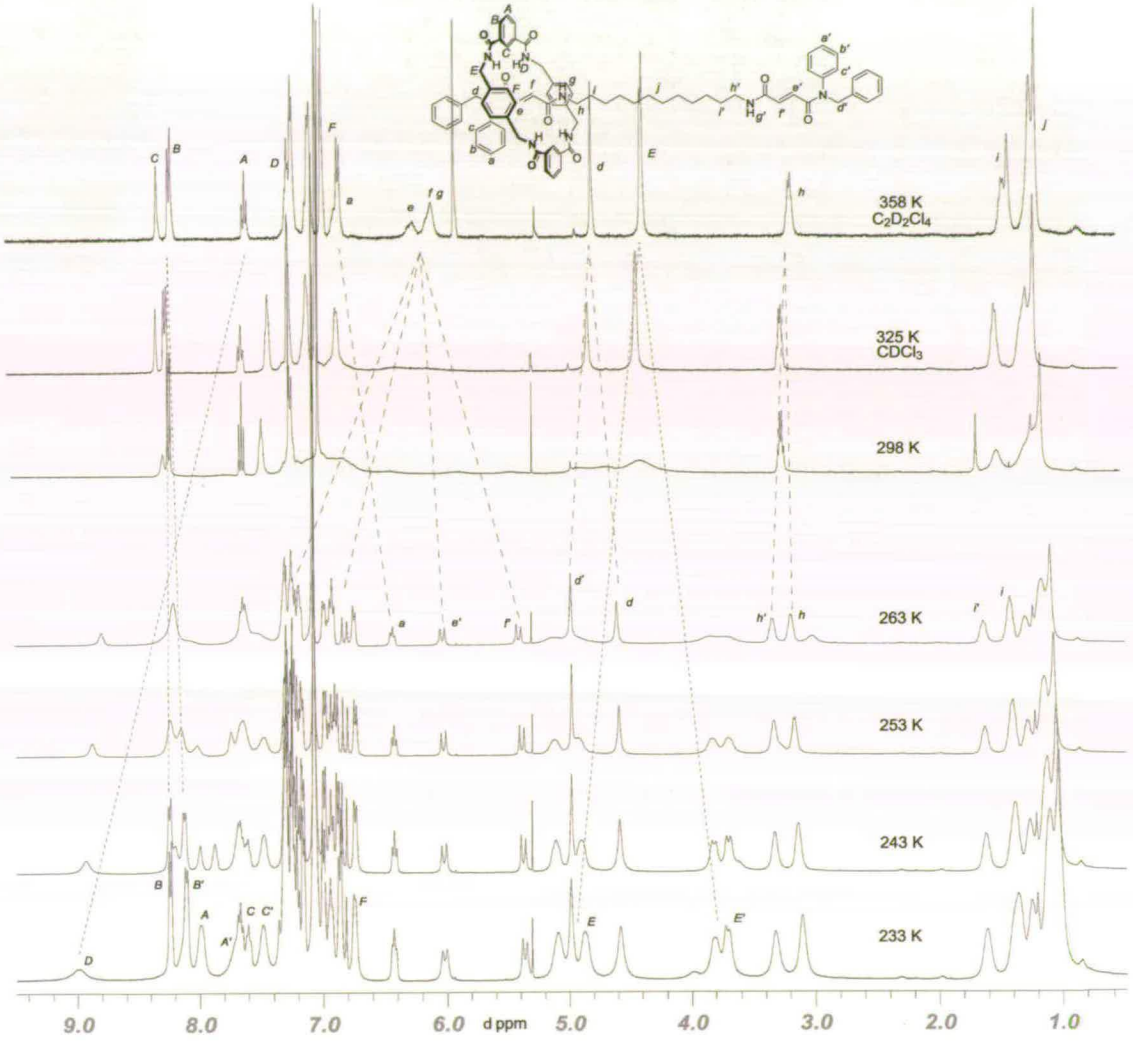


Figure 5. 9 The VT ^{1}H NMR (400 MHz, $CDCl_3$ (except top spectrum in $C_2D_2Cl_4$)) stack plot of rotaxane **BI12** showing the two different exchange processes that occur in the shuttle systems. On reducing the temperature, firstly the stations of the thread become desymmetrised, followed by the benzyl protons of the macrocycle.

From the VT NMR, it is clear that the energy barrier for shuttling is higher than that of the pirouetting, and therefore pirouetting occurs much faster than shuttling does. The fact that both exchange processes require the breaking of the intercomponent hydrogen bonds in order to exchange supports they theory that shuttling involves simply more than breaking of the hydrogen bonding interaction at the station. It may be that the shuttling and pirouetting rates are related, but seeing as the pirouetting rate is at least an order of magnitude larger than shuttling rate it is not considered in this study.

5.2.3 Kinetic Studies

The dynamic processes within the whole series of shuttles were investigated using the Spin Polarisation Transfer – Selective Inversion Recovery (SPT-SIR) ^{1}H NMR technique in order to determine the kinetics of the processes occurring in each of the shuttles.[13] This technique allows the accurate determination of the rate of exchange, k, at a range of temperatures, as long as the signals for the two exchanging sites at the chosen temperature are resolved, *i.e.* slow exchange, and that the exchange lifetimes, τ (= $1/k$), is of the same order of magnitude as the longitudinal relaxation, T_1. The experiment involves inversion of the signal due to irradiation of one of the exchanging sites using a soft 180° pulse, followed by a delay before acquisition. This leads to a decrease in signal intensity at the non-irradiated site that is dependent on the delay. Correlating this signal intensity with the delay times allows the calculation of τ, and therefore the rate of site exchange, k, can be determined.

The recorded intensities, I, for the signal at the non-irradiated site varied according to the exchange lifetime, τ, and T_1 by the biexponential function (for $\tau << T_1$):

$$I(t) = I_\infty - Y \exp(-t/\tau) + Z \exp(-t/T_1) \qquad (1)$$

Where $I(t)$ is the signal intensity for delay t in seconds, I_∞ is the signal intensity after infinite delay, and Y and Z are constants. τ for each of the system was determined by fitting the observed intensities to the five parameter exponential eq. 1.(e.g. see figure

5.10). Having established k, the activation energy for exchange was determined by extrapolation (eq. 2) of the Eyring equation:

$$\Delta G^{\ddagger} = aT(10.319 + \log(T/k)) \qquad (2)$$

where $a = 4.575 \times 10^{-3}$ (for $\Delta G^{\ddagger}$ in kcal mol^{-1}).

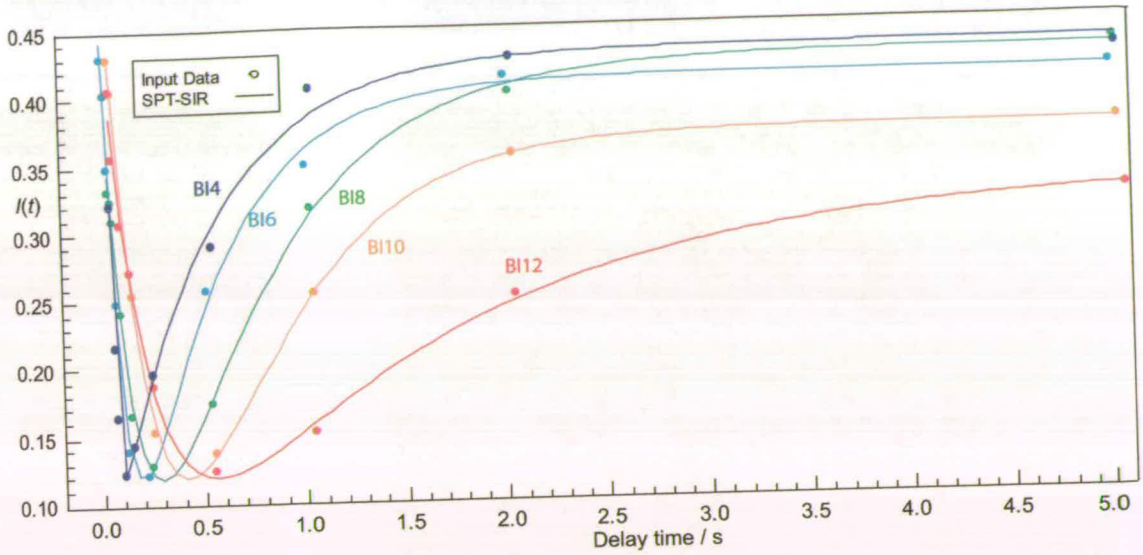


Figure 5. 10 Overlay of the plots of non-irradiated site signal intensity against the delay times for the series of different spacer-length shuttles **BI4**, **BI6**, **BI8**, **BI10**, **BI12** (CDCl3, 217.9 K). The traces show the biexponential fits used to determine the exchange lifetime, τ, and longitudinal relaxation time T1. Intensities, *I(t)*, for the various plots were normalised such that the plots reflect the loss of intensity for each signal rather than the true value of *I(t)* recorded.

All the kinetic studies were carried out in $CDCl_3$, except where otherwise stated, and the recorded temperatures are accurate to ± 0.4 K as determined by prior temperature calibration using VT ^{1}H NMR of methanol. Errors are stated for all the results, and included on all of the graphs (typically ± 0.1 kcal mol^{-1}).

Firstly, a look at the results obtained for shuttles with the different macrocycles and stations, but the same length alkyl chain, C12, shows that the activation energy of the shuttling process varies depending both on the choice of station and of macrocycle (see table 5.1). As the variations in the rates are only small*, the activation energies

* $\Delta G^{\ddagger}$ changes linearly with temperature and logarithmically with respect to changes in rate.

of the different systems are representative of the strength of interaction between each station and macrocycle.

	T / K	τ / s		k / s^{-1}		$\Delta G^{\ddagger}$ / kcal mol^{-1}		% error
AP12	238.7	0.176	± 0.045	5.7	± 1.9	13.04	± 0.15	1.1
BP12	314.6	0.177	± 0.030	5.7	± 1.1	17.37	± 0.13	0.7
AI12	197.2	0.053	± 0.015	18.9	± 7.4	10.23	± 0.14	1.3
BI12	231.7	0.222	± 0.031	4.5	± 0.7	12.76	± 0.09	0.9

Table 5. 1 Table comparing the activation energies, $\Delta G^{\ddagger}$, for the different C12 shuttles.

The table shows that shuttling is a higher energy process in the fumaric systems than in the succinic amide ester systems, and also higher for the *endo*-pyridyl- than the isophthaloyl macrocycles. This large difference can be attributed to the difference in the strength of binding interaction between the stations and the macrocycles. It tells us that, unsurprisingly, the binding strength for the fumaric stations are stronger than the succinic amide esters, as the fumaric template contains two amides and is preorganised, whereas the succinic amide ester station contains only one amide and an ester, a weaker hydrogen bond donor. Also, the endo-pyridyl macrocycle binds more strongly than the isophthaloyl macrocycle. It appears to bind more strongly to the weaker succinic amide ester station than the isophthaloyl macrocycle binds to the 'ideal' fumaric station! This is a result of the way in which these macrocycles bind to the stations (see figure 5.11).

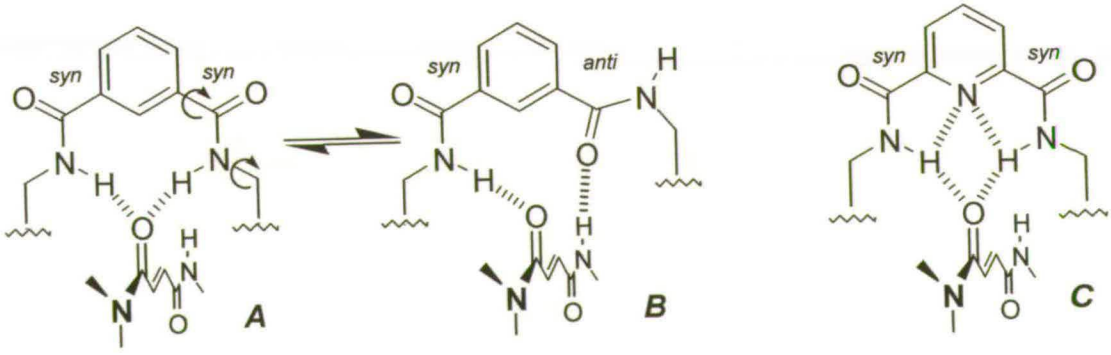


Figure 5. 11 The different binding modes of the macrocycles. The isophthaloyl macrocycle can bind to a template via a *syn-syn* (A) or a *syn-anti* (B) conformation, and these two modes

are constantly interconverting. The *endo*-pyridyl macrocycle can only bind via the *syn-syn* (C) conformation to form bifurcated hydrogen bonds.[14]

The isophthaloyl unit can bind in two different conformations to a template. In the *syn-syn* conformation two bifurcated hydrogen bonds are formed, but rotation of one amide, giving the syn-anti conformation binds via the amide proton and the carbonyl group. The *endo*-pyridyl macrocycle only binds via the *syn-syn* conformation, as this is stabilised by a positive interaction between the pyridyl nitrogen and amide protons, and the *syn-anti* conformation is destabilised by the electrostatic interaction between the pyridyl nitrogen lone pair of electrons and the carbonyl groups.[14] As a result of these different modes of binding, it is easier for the isophthaloyl macrocycle to leave the station as one of the two hydrogen bonds from each isophthaloyl group is constantly being broken and reformed as it alternates between conformations. The *endo*-pyridyl macrocycle does not have this facility, and therefore in order to leave the station it must break all four hydrogen bonds simultaneously, *i.e.* two from each pyridyl unit. This chelating effect is probably the main factor in determining the difference in the strength of binding interaction between the macrocycles.

Given more time it would have been possible to synthesise a wider variety of shuttles, with which the relative size and importance of the contributions from macrocycles and stations could be determined separately. Unfortunately, with the data from shuttles with only two different macrocycles and stations, it is not possible to draw any conclusions about the relative effect each has on the binding strength, or energy barrier of shuttling.

The kinetics of the series of shuttles with different length spacers, but the same station and macrocycle, **BI2**, **BI4**, **BI6**, **BI8**, **BI10**, **BI12**, were studied to determine how the shuttling rates and activation energies change as the length of the alkyl chain that separates the two stations is changed (see table 5.2 and figure 5.12). In the shortest shuttle, **BI2**, with the C2 alkyl chain separating the stations, shuttling could not be observed on reducing the temperature. Instead, the broad ^{1}H NMR spectrum of **BI2** at 298 K ($CDCl_3$) became more complicated on cooling than

desymmetrisation alone would account for. It is thought that the macrocycle, rather than undergo shuttling between stations at low temperature, simply preferred to bridge the two-carbon chain and bind to the internal secondary amides of each station.[15] Reducing the temperature makes this binding mode more favourable, due to its relatively high entropic cost, and therefore the populations of the different binding modes also changes with temperature. In the absence of a shuttling motion at low temperature, the C2 'shuttle', **BI2**, was excluded from the study.

	T / K	τ / s		k / s^{-1}		$\Delta G^{\ddagger}$ / kcal mol^{-1}		% error
BI12 B	217.9	0.212	± 0.0524	4.7	± 1.5	11.95	± 0.18	1.3
BI12 A	217.9	0.273	± 0.1072	3.7	± 2.3	12.06	± 0.25	1.9
BI10	217.9	0.249	± 0.0305	4.0	± 0.5	12.02	± 0.12	0.9
BI8	217.9	0.149	± 0.0015	6.7	± 0.1	11.80	± 0.06	0.5
BI6	217.9	0.098	± 0.0235	10.2	± 3.2	11.61	± 0.17	1.3
BI6	217.9	0.081	± 0.0128	12.4	± 2.3	11.53	± 0.13	1.0
BI4	217.9	0.016	± 0.0023	64.0	± 11.1	10.82	± 0.12	1.0

Table 5. 2 Table comparing the activation energies, $\Delta G^{\ddagger}$, and rates of shuttling, k, for the different length **BI** series of shuttles. Two different values of τ were obtained for each of the **BI6** and **BI12** SPT-SIR experiments, and both are included in this study.

From the table, the rate increases, and therefore the energy barrier for shuttling decreases with decreasing chain length, as would be expected knowing that there is a length dependence, but the graph of length against both rates and energy barriers shows that the trends are not linear with respect to the number of carbons (see figure 5.12).

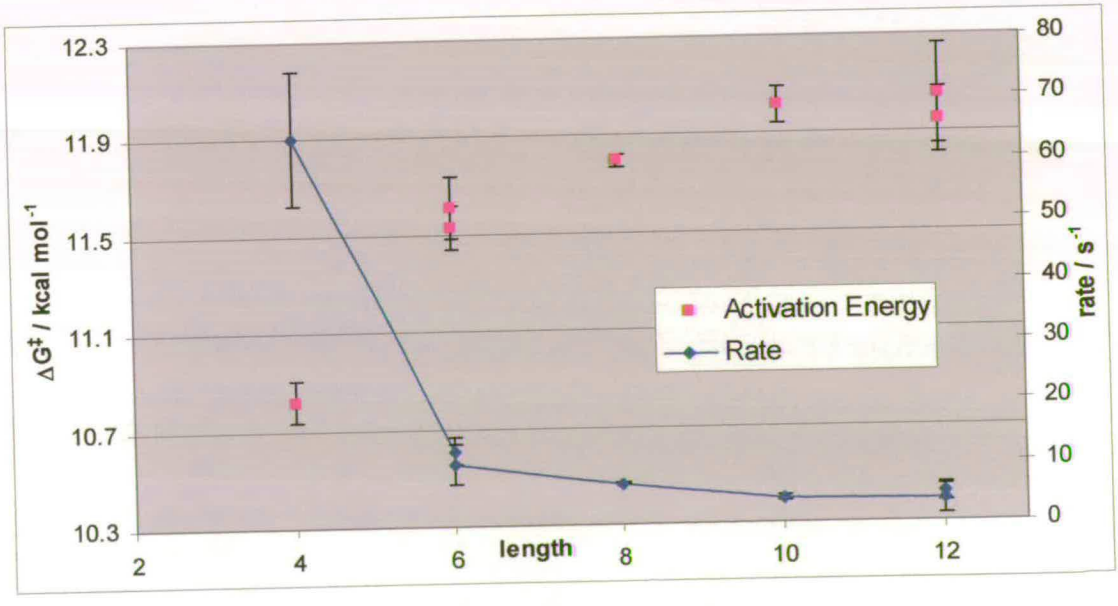


Figure 5. 12 The plot showing how the rates and activation energies for shuttling vary with increasing chain length.

One would expect that as the chain gets longer the activation energy of shuttling would increase. The graph shows that the activation energy does not increase linearly, as each successive increment in chain length becomes less significant, *i.e.* the difference between C2 and C4 is much more significant than that between C10 and C12.

The graph also suggests an explanation as to why the C2 rotaxane, **BI2**, gave a complicated low temperature ^{1}H NMR spectrum and did not undergo shuttling. If the trend indicated in the graph (figure 5.12) were extrapolated down to a two-carbon length spacer, the energy barrier for shuttling would be approximately 10.0 kcal mol^{-1}, lower than the expected energy barrier for pirouetting at around 10.5 kcal mol^{-1}.

If one now looks at how the energy barrier of shuttling in one particular shuttle, **AI12**, changes with temperature, it appears that the activation energy increases linearly with increasing temperature. Only three different temperatures were used to plot the trend due to the small range of temperatures the experiment can be conducted at. This range is defined by a temperature low enough for the exchanging signals to be resolved, and yet exchange must be fast enough to be observed. The results are supported, though, by the similar shuttle, **BP12**, which shows the same trend (see table 5.3 and figure 5.13).

	T / K	τ / s		k / s^{-1}		ΔG‡ / kcal mol^{-1}		% error
BI12	252.5	0.075	± 0.01	13.38	± 1.05	13.39	± 0.09	0.7
BI12	231.7	0.222	± 0.03	4.50	± 0.70	12.76	± 0.12	0.9
BI12	217.9	0.212	± 0.05	4.72	± 1.53	11.95	± 0.17	1.4
BP12*	289.8	0.370	± 0.84	2.70	± 95.9	16.37	± 0.74	4.5
BP12	314.6	0.177	± 0.03	5.66	± 1.14	17.37	± 0.16	0.9

* The large reported error result from two erroneous intensities, $I(t)$ observed in the SPT-SIR experiment, which resulted in a poor fitted curve ($R^2 = 0.983$). Exclusion of these points give similar values of τ recorded here, but with error of only ± 0.08s. This gives ΔG‡ value 16.4 ± 0.2 kcal mol^{-1}. Although, this is only indicative, it is probable that the value reported is more accurate than the large error value would suggest.

Table 5. 3 Table comparing the rates and activation energies for two different shuttles at several temperatures.

Both shuttles **BI12** and **BP12** show an increase in the activation energy of shuttling with temperature. This means that there is a large entropic contribution to the shuttling process. In fact, the energy barriers for both C12 fumaric shuttles display the same temperature relationship, which suggests that this entropic factor is independent of the strength of binding at the stations, as this would be different in both cases, and therefore must be due to the alkyl chain in both shuttles.

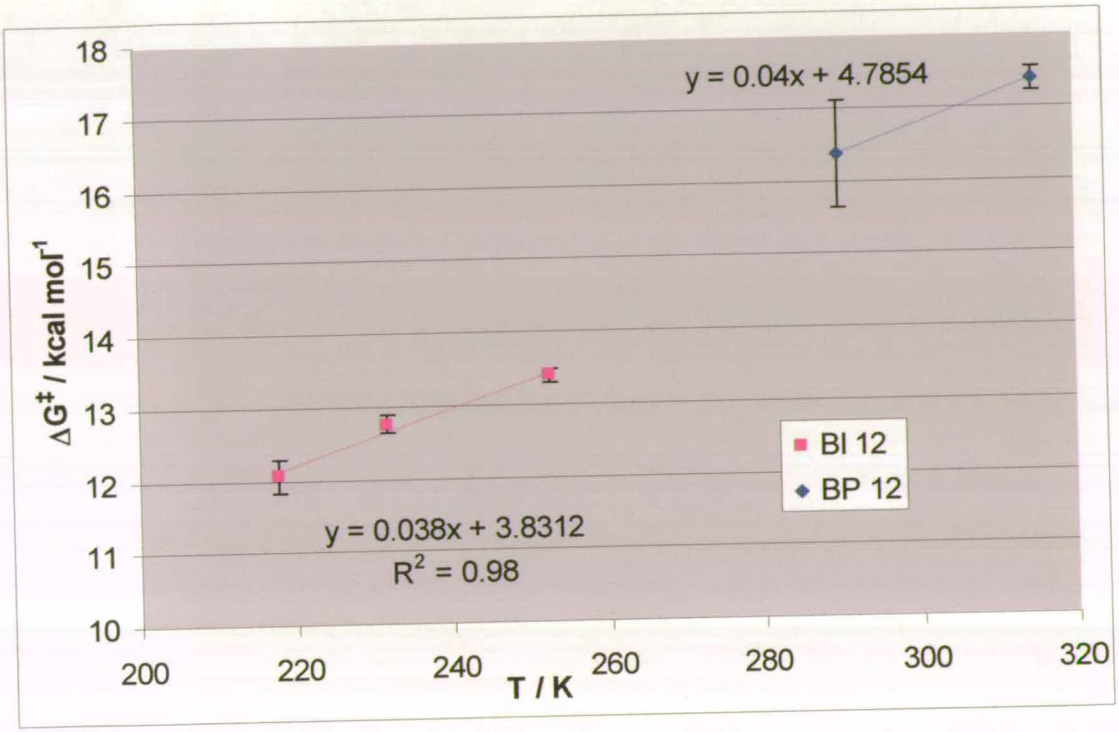


Figure 5. 13 The plot showing how the activation energy changes with temperature in two different C12 shuttles, **BI12** and **BP12**.

This theory is supported when data for the shorter chain shuttles is included in the temperature study (see figure 5.14 and table 5.4). The energy barriers for shorter chain shuttles also show a temperature dependence, increasing with increasing temperature. The slopes for the shorter chain shuttles, which indicates the entropy barrier for the shuttling process, decreases with decreasing chain length. This observation confirms the theory that the entropic contribution is due to the length of

the alkyl spacer. The decreasing entropy barrier in shorter shuttles can be rationalised as there are less translational degrees of freedom available for the unbound macrocycle in the shorter chains systems.

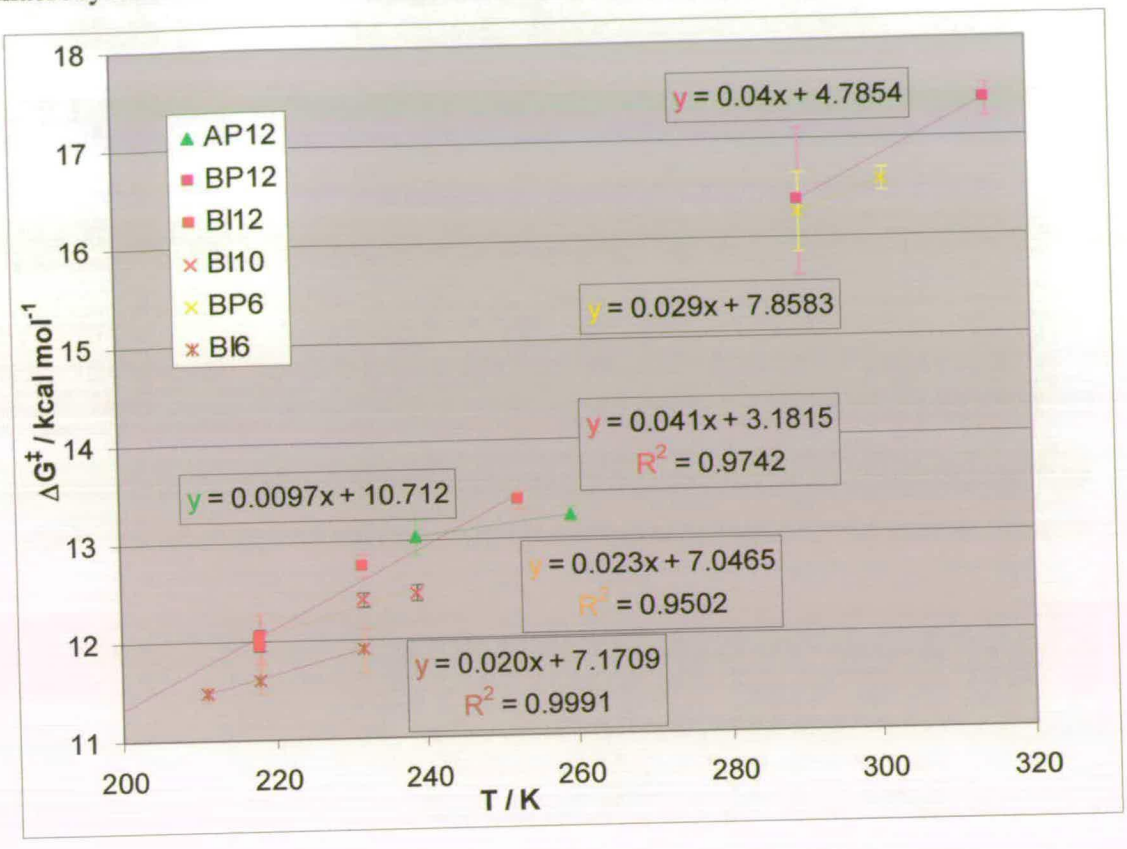


Figure 5. 14 The plot of temperature against activation energy for the different shuttles for which kinetic data was obtained at different temperatures. The best fit lines with equations are included, linking different temperature points for the same shuttles, and where this is derived from three different points, the quality of fit is indicated by R^2.

As the temperature is reduced, it appears that for the each different length series of fumaric shuttles, *i.e.* the **BI** and **BP** series, the activation energies tend towards the same value as observed for the C12 shuttles. The collected data is insufficient to determine what will occur if the temperature is further reduced. If the observed trends continued though, the rate of shuttling at low temperature would be faster in the C12 shuttles than in the C10 shuttles!

	length	T / K	τ / s		k / s^{-1}		$\Delta G^{\ddagger}$ / kcal mol^{-1}	
AP12	12	259.4	0.027	± 0.002	37.6	± 2.2	13.24	± 0.08
AP12	12	238.7	0.176	± 0.045	5.7	± 1.9	13.04	± 0.18
BP12	12	289.8	0.370	± 0.841	2.7	± 5.2	16.37	± 0.74
BP12	12	314.6	0.177	± 0.030	5.7	± 1.1	17.37	± 0.16
BP6	6	300.8	0.177	± 0.016	5.7	± 0.6	16.58	± 0.11
BP6	6	289.8	0.303	± 0.164	3.3	± 3.8	16.26	± 0.41
BI12	12	252.5	0.075	± 0.005	13.4	± 1.0	13.39	± 0.09
BI12	12	231.7	0.222	± 0.031	4.5	± 0.7	12.76	± 0.12
BI12	12	217.9	0.212	± 0.052	4.7	± 1.5	11.95	± 0.17
BI12	12	217.9	0.273	± 0.107	3.7	± 2.3	12.06	± 0.24
BI10	10	238.7	0.053	± 0.003	18.8	± 1.1	12.47	± 0.08
BI10	10	231.7	0.107	± 0.003	9.4	± 0.3	12.42	± 0.07
BI10	10	217.9	0.249	± 0.031	4.0	± 0.5	12.02	± 0.11
BI6	6	231.7	0.035	± 0.015	28.5	± 20.3	11.91	± 0.23
BI6	6	217.9	0.098	± 0.024	10.2	± 3.2	11.61	± 0.13
BI6	6	211.0	0.179	± 0.022	5.6	± 0.8	11.48	± 0.07

Table 5. 4 Table comparing the rates and activation energies for different lengths shuttles at different temperatures.

The C12 succinic amide ester shuttle, **AP12**, appears to be less dependent on temperature than the C12 fumaric shuttles. It is unclear as to why this is, as one would expect the entropy in the system, and therefore the entropy of activation to be greater, as there is an entropic contribution from the station, which loses its rotational freedom on binding the macrocycle.

5.2.4 Interpretation of Kinetic Results

From the plot of activation energy against temperature it is possible to obtain values for the enthalpy and entropy of activation for the shuttling process (see table 5.5). Although taken from only two or three points and the associated errors will probably quite significant, the values of $\Delta S^{\ddagger}$ and $\Delta H^{\ddagger}$ should give an indication of the forces driving the shuttling process.

	$\Delta H^{\ddagger}$ / kcal mol^{-1}	$\Delta S^{\ddagger}$ / cal mol^{-1} K^{-1}
AP12	10.7	-9.7
BP12	4.8	-40
BP6	7.9	-29
BI12	3.2	-41
BI10	7.0	-23
BI6	7.2	-20

Table 5. 5 Table of activation enthalpy and entropy for shuttling in several shuttles.*

The way the activation energy of shuttling breaks down into enthalpy and entropy values is quite surprising. Both C12 fumaric shuttles, **BP12** and **BI12**, appear to have relatively low enthalpies of activation, $\Delta H^{\ddagger}$ = 4.8 and 3.2 kcal mol^{-1} respectively, and larger entropic values $\Delta S^{\ddagger}$ ~ -40 cal compared to shorter chain shuttles with the same components, where the enthalpy is significantly higher, $\Delta H^{\ddagger}$ ~ 7.2, 7.0 and 7.9 kcal mol^{-1}, and the entropy, $\Delta S^{\ddagger}$, much lower at ~ -20, -23 and -29 cal for **BI6**, **BI10** and **BP6** respectively. The succinic amide ester shuttle has the highest enthalpy cost of all the shuttle systems, $\Delta H^{\ddagger}$ = 10.7 kcal mol^{-1}, and the lowest entropic cost, $\Delta S^{\ddagger}$ = 9.7 cal. This is surprising, as the succinic amide ester provides a weaker hydrogen bonding interaction to the macrocycle than the fumaric station, yet it has the highest enthalpic cost to shuttling, possibly equivalent to breaking all four hydrogen bonds between the station and macrocycle at once.

These results must reflect differences in the mechanism of the shuttling process. In the long, C12 systems, **BP12** and **BI12**, the low enthalpies of activation represent the barrier to breaking one hydrogen bond, with $\Delta H^{\ddagger}_{\text{Hydrogen bond}}$ ~ 2 - 4 kcal mol^{-1}. The higher value observed in the *endo*-pyridyl shuttle is not surprising as this macrocycle binds more tightly and therefore the breaking of a stronger hydrogen bond is more costly. The entropies of activation for both these two shuttles are approximately the same, therefore this contribution must come from the alkyl chain. The higher cost,

* Due to the low number of data points used to calculate the activation entropy and activation enthalpy for the various shuttles the approximate error is ± 100%. Although this error is large, the fact that the data in the table seem reasonable and support each other suggests that the values may be more representative than the large error would suggest.

compared to the shorter shuttles, must be due to a reduction in the degrees of freedom of the alkyl chain. This could be explained by an association of the two stations, *i.e.* the two stations interacting with the macrocycle at the same time, with the vacant station assisting in the breakage of the hydrogen bonding interactions at the other station.

The shorter chain systems do not seem to employ this mechanism of shuttling. All three shorter shuttles investigated, **BP6**, **BI6** and **BI10** show similar activation enthalpies and entropies to each other, but which are quite markedly different from the C12 shuttles, even though the C10 shuttle is only two carbons different. The enthalpy of the process is much higher, equivalent to the cost of breaking two hydrogen bonds, and the entropy cost of the process is much lower. The lower entropy cost suggests that less organisation of the alkyl chain is required.

The succinic amide ester shuttle, **AP12**, must display the high enthalpic and low entropic costs to shuttling due to a drastic difference in the shuttling mechanism, which reflects the differences in the station-macrocycle binding interactions in the succinic amide ester and the fumaric systems. The succinic amide ester template only offers a weak hydrogen bonding interaction to the macrocycle. Ironically, it is probably because of this weak interaction that the activation enthalpy is high and the entropy is low, as the enthalpy gain from association of the two weak-binding succinic amide ester stations is insufficient to offset the entropic cost of folding, and therefore all the hydrogen bonds at the occupied station, even though an overall weak interaction, must all be broken simultaneously, resulting in the large enthalpy barrier observed.

Different modes of shuttling could be the result of there being lower energy pathways available to the different shuttles, reflecting differences in their composition (see figure 5.15). Each of the different modes of shuttling would be more favourable at different temperatures, with one route being enthalpically costly (pathway **A**), therefore favourable at higher temperatures, and the other one being entropically so, and therefore favourable at lower temperatures (pathway **B1** and **B2**).

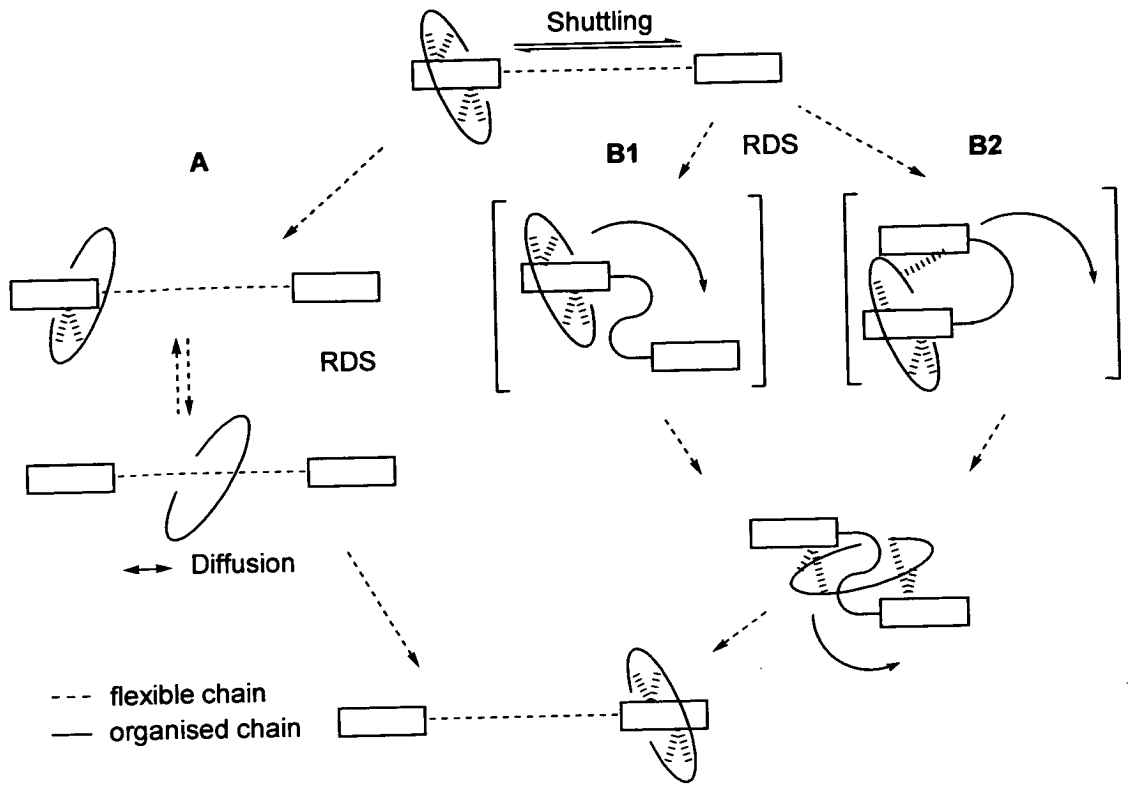


Figure 5. 15 The proposed two different mechanisms of shuttling: the enthalpically costly (A) and entropically costly (B1 and B2) paths. The rate determining steps has been indicated in each case (RDS).

At higher temperatures, the macrocycle will be rapidly dissociating / re-associating with the station, and the rate of shuttling is dependent on the diffusion of the macrocycle across the alkyl chain (mechanism **A**). This mechanism describes the high enthalpy and low entropy cost in the succinic amide ester shuttle system.

In systems with stronger binding interactions, the high enthalpic cost of breaking the hydrogen bonds, *i.e.* complete dissociation of the macrocycle from the station, makes shuttling by mechanism **A** unfavourable. Instead, it is more favourable for the vacant station to organise itself into a position where it can provide alternative hydrogen bonding interactions for the macrocycle (mechanism **B1**), thereby providing a means for the macrocycle to move off the station by breaking only two hydrogen bonds, and forming an intermediate bridging structure which reforms the four strong hydrogen bonding interactions. From this bridged intermediate, the macrocycle could simply

flip onto the previously vacant stations and thereby complete the exchange process. This would describe the shuttling process in the shorter fumaric shuttles at the low temperatures used to observe slow exchange. This may not be the case at higher temperatures when the large entropic contributions make shuttling by this mechanism unfavourable.

In the C12 systems, the mechanism appears slightly different from the shorter chain shuttles as the entropy cost is higher, and the enthalpy cost is lower, *i.e.* the equivalent of breaking only one, instead of two hydrogen bonds. This could be due to the vacant station associating with the macrocycle, thereby providing a mechanism for a single hydrogen bond to be broken, and thus forming a new hydrogen bond. This interaction would make it easier for the macrocycle to dissociate, as breaking the one remaining hydrogen bond would allow the vacant station to drag the macrocycle into the bridged intermediate structure (mechanism **B2**). It may be that only the C12 chain is of sufficient length to associate with the macrocycle in this way, or that the chain length is just too long, and therefore too entropically unfavourable to 'pre-arrange' itself as in mechanism **B1**.

The succinic amide ester system represents the case that would be observed in longer shuttles, *e.g.* a very long fumaric shuttle, where the vacant station can offer no assistance to breaking the binding interaction with the macrocycle, due to the prohibitive entropic cost. Shuttling rates and activation energies in these systems would simply be based on dissociation and diffusion of the macrocycle between stations.

Although these different shuttling mechanisms are only speculative, and require more experimental evidence to confirm the proposals, they do appear to fit the observed results, and provide a possible explanation for the observed differences in entropy and enthalpy costs to shuttling in different systems. The proposed-bridged intermediate in the shuttling mechanism **B1** and **B2** is supported by the results in

chapter six, in which a bridged structure becomes the more favourable conformation in an unsymmetrical shuttle system.

5.3 Future Work

Since the mode of shuttling appears to be much more complicated than was initially expected, further investigations should be carried out to confirm, or disprove the theories presented here. Given the time constraints, and the huge amount of work that has already gone into this investigation, it would have been difficult to investigate this problem as thoroughly as would have desired or expected, therefore it is prudent to include some suggestions to complete and extend the research presented here.

Besides the obvious extension of the study to include a wider variety of different stations and macrocycles, there are a number of experiments that can be undertaken on the shuttles already synthesised that would add weight to the findings presented here.

Firstly, the kinetics at which the pirouetting event takes place in the different shuttles should be investigated. The pirouetting motion involves the breaking of the hydrogen bonds at one station, which one would expect the energy barrier to be solely dependent on the strength of binding interaction at the station and therefore independent of alkyl chain. Yet if there is an association between stations in the shuttles, then the pirouetting energy barrier should show similar trends and relative enthalpic and entropic contributions as the shuttling energy barriers.

Secondly, if possible, the shuttling exchange kinetics should investigated at lower temperatures to determine whether the mechanism by which shuttling occurs in the systems changes to follow a lower energy pathway. The C10 shuttles are the most likely candidates to display this behaviour at temperatures just lower than the experiments were performed at.

The range of data over which the investigation was conducted could be extended by synthesising shuttles with alkyl chains longer than C12, to determine whether the observed trends continue in systems with much longer alkyl chains, and to verify

whether a very long chain fumaric system displays the same behaviour as the C12 succinic amide ester shuttle, **AP12**.

An elegant way to conclude any further investigation would be to change the composition of the spacer group. By extending the study to include rigid spacers and, for example, polyether chains, the folding mechanism proposed can be investigated and verified. Finally, by incorporating bulkier alkyl chains as spacers between stations, effects on the rate of shuttling, *i.e.* intercomponent frictional forces, can be investigated.

5.4 Conclusions

With all the focus on molecular shuttles being developed as molecular machines, it is surprising that no one has wondered by what means they operate. This investigation has looked back at the long-since overlooked symmetrical molecular shuttle systems in order to explore and attempt to explain their interesting properties.

This investigation has shown that the modes by which molecular shuttles operate is not as straightforward as one would expect from observations of the asymmetrical molecular shuttles, 'switches', or from conclusions drawn by classical interpretations of shuttle systems. In fact, the conclusions drawn from the observations in this study suggests that several shuttling mechanisms may exist, each of which come into play in different situations depending of a number of factors. These include the binding ability of stations, and the macrocycle, and the length of the spacer separating the stations, and quite possibly of the solvent in which the systems are studied.

The theories drawn from this investigation, and from future work into these symmetrical shuttle systems, should improve the understanding of intercomponent motion in mechanically interlocked architectures, and assist in the development of future molecular devices from these types of architecture.

5.5 Experimental

In rotaxane ^{1}H NMR assignments, an asterix indicates a macrocycle proton, and the capital letter suffix denotes the proton assignment as indicated in the diagrams earlier in this chapter.

Succinic acid mono-(2,2-diphenyl-ethyl) ester (5.1)

A stirred solution of succinic anhydride (505 mg, 5 mmol), 2,2-diphenylethanol (1 g, 5 mmol) and a catalytic amount of N,N-dimethylaminopyridine (50 mg, 0.5 mmol) in pyridine (5 mL) and chloroform (mL) was heated at reflux overnight. After being allowed to cool, ethyl acetate (100 mL) was added and the solution was washed with 1M HCl (3 x 50 mL). The product was then extracted with saturated $NaHCO_3$ solution (3 x 100 mL), and the combined aqueous was washed with ether (3 x 50 mL). The aqueous phase was then acidified with 2M HCl producing a white precipitate that was extracted with ethyl acetate (3 x 50 mL). The combined organics were washed with brine (1 x 50 mL), dried over Mg_2SO_4, filtered and evaporated to dryness to give the pure product as a colourless solid (**5.1**, 1.12 g, 4.0 mmol, 80 %); ^{1}H NMR (400 MHz, $CDCl_3$, 298 K) δ 11.02 (1H, bs, COO<u>H</u>), 7.25- 7.10 (10H, m, Ph), 4.58 (2H, d, J = 7.5 Hz, C<u>H</u>$_2$O), 4.29 (1H, t, J = 7.5 Hz, C<u>H</u>CH$_2$O), 2.49 (2H, d_{ABCD}, J = 18.5, 6.5, 5.5 Hz, COC<u>H</u>$_2$), 2.45 (2H, d_{ABCD}, J = 18.5, 6.5, 5.5 Hz, COC<u>H</u>$_2$); ^{13}C NMR (100 MHz, $CDCl_3$, 298 K) δ 178.3, 172.0, 141.0, 128.6, 128.2, 126.9, 67.0, 49.8, 28.8; HRFAB-MS (3-NOBA matrix): *m/z* = 299.12902 (calcd. for $C_{18}H_{19}O_4$, $[M]H^+$, 299.12833).

3-Chlorocarbonyl-propionic acid 2,2-diphenyl-ethyl ester (5.2)

To a cooled, stirred solution of **5.1** (350 mg, 1.25 mmol) and catalytic dimethylformamide (0.5 mL) in dichloromethane (30 mL) at 0 °C was added oxalyl chloride (2M solution in dichloromethane, 622 μL, 1.22mmol) over 30 min. The

reaction was left to stir for a further two hours at which point effervescence could no longer be observed. The acid chloride product **5.2** was used in the next step without isolating or further purification.

_N_-{12-[3-(2,2-Diphenyl-ethoxycarbonyl)-propionylamino]-dodecyl}-succinamic acid 2,2-diphenyl-ethyl ester rotaxane (A12)

To a stirred solution of 1,12-diaminododecane (125 mg, 0.625 mmol) and triethylamine (126mg, 175 μL, 1.25 mmol) in dichloromethane (50 mL) was added the acid chloride solution prepared in the previous step over 30 min. The reaction was left to stir for a further two hours. The completed reaction was then washed with 1M HCl (3 x 50 mL), saturated $NaHCO_3$ solution (3 x 50 mL), and water (1 x 50 mL), dried over $MgSO_4$, filtered and evaporated to dryness under reduced pressure. The crude product was purified by column chromatography (SiO_2, 1% methanol / dichloromethane) to give the desired product as a white solid (**A12**, 328 mg, 0.453 mmol, 72 %); ^{1}H NMR (400 MHz, $CDCl_3$, 298 K) δ 7.33- 7.18 (20H, m, Ph), 5.50 (2H, t, J = 6.0 Hz, NH), 4.64 (4H, d, J = 7.5 Hz, CHC$\underline{H}_2$O), 4.35 (2H, t, J = 7.5 Hz, C$\underline{H}$CH$_2$O), 3.18 (4H, dd, J = 6.0, 7.0 Hz, NHC$\underline{H}_2$), 2.58 (4H, t, J = 7.0 Hz, COC$\underline{H}_2$), 2.33 (4H, t, J = 7.0 Hz, COC$\underline{H}_2$), 1.45 (4H, quintet, J = 7.5 Hz, NHCH$_2$C$\underline{H}_2$), 1.31-1.23 (16H, m, 8 x CH_2); ^{13}C NMR (100 MHz, $CDCl_3$, 298 K) δ 172.9, 171.2, 141.0, 128.6, 128.3, 126.8, 66.9, 49.8, 39.6, 31.0, 29.7, 29.6, 29.5, 29.3, 26.9; HRFAB-MS (3-NOBA matrix): m/z = 761.45332 (calcd. for $C_{48}H_{61}N_2O_6$, $[M]H^+$, 761.45296).

[2](1,7,14,20-Tetraaza-2,6,15,19-tetraoxo-3,5,9,12,16,18,22,25-tetrabenzocyclohexacosane)-_N_-{12-[3-(2,2-diphenyl-ethoxycarbonyl)-propionylamino]-dodecyl}-succinamic acid 2,2-diphenyl-ethyl ester rotaxane (AI12)

To a stirred solution of **A12** (338 mg, 445 μmol, 1eq.) in chloroform (30 mL) was added simultaneously solutions of *p*-xylylene diamine (363 mg, 2.67 mmol, 6 eq.) and triethylamine (674 g, 936 μL, 6.67 mmol, 15 eq.) in chloroform (20 mL), and isophthaloyl chloride (542 mg, 2.67 mmol, 6 eq.) in chloroform (20 mL) via syringe

pump over three hours. After addition the reaction was stirred for a further hour before being filtered and reduced in volume under reduced pressure. The crude reaction mixture was then purified by column chromatography (SiO_2) to recover unconsumed starting material (1.4 % methanol / dichloromethane, pn 465, 200 mg, 263 μmol, 55 %), and the desired rotaxane product as a white solid (2% methanol / dichloromethane, **AI12**, 96 mg, 74 μmol, 16%); ^{1}H NMR (400 MHz, $CDCl_3$, 298 K) δ 8.24 (2H, bt, J = 1.5 Hz, H_C*), 8.18 (4H, dd, J = 1.5, 7.5 Hz, H_B*), 7.62 (2H, t, J = 7.5 Hz, H_A*), 7.45 (4H, bt, J = 5.0 Hz, H_D*), 7.33- 7.21 (14H, m, Ph), 7.19- 7.15 (8H, m, Ph), 7.02 (8H, s, H_F*), 6.23 (2H, bt, NH), 4.53- 4.44 (12H, m, $CHC\underline{H_2}O$, H_E*), 4.25 (2H, t, J = 7.5 Hz, $C\underline{H}CH_2O$), 3.04 (4H, q, J = 6.5 Hz, $C\underline{H_2}NH$), 1.96 (4H, bt, $COC\underline{H_2}$), 1.68 (4H, bt, $COC\underline{H_2}$), 1.41 (4H, bt, J = 6.5 Hz, $C\underline{H_2}CH_2NH$), 1.22 (16H, s, 8 x CH_2); ^{13}C NMR (100 MHz, $CDCl_3$, 298 K) δ 173.6, 171.7, 166.6, 140.8, 137.6, 134.1, 131.3, 129.3, 129.0, 128.7, 128.1, 127.0, 124.2, 67.3, 49.6, 44.1, 39.8, 30.0, 29.4, 29.4, 29.1, 29.1, 26.8; HRFAB-MS (3-NOBA matrix): m/z = 1293.66450 (calcd. for $C_{80}H_{89}N_6O_{10}$, $[M]H^+$, 1293.66402).

[2](1,4,7,14,17,20-Hexaaza-2,6,15,19-tetraoxo-3,5,9,12,16,18,22,25-tetrabenzocyclohexacosane)-*N*-{12-[3-(2,2-diphenyl-ethoxycarbonyl)-propionylamino]-dodecyl}-succinamic acid 2,2-diphenyl-ethyl ester rotaxane (AP12)

To a stirred solution of **AI12** (200 mg, 263 μmol, 1eq.) in chloroform (30 mL) was added simultaneously solutions of *p*-xylylene diamine (286 mg, 2.11 mmol, 8 eq.) and triethylamine (532 mg, 738 μL, 5.26 mmol, 20 eq.) in chloroform (20 mL), and 2,6-pyridine-2,6-dicarbonyl chloride (410 mg, 2.11 mmol, 8 eq.) in chloroform (20 mL) via syringe pump over three hours. After addition the reaction was stirred for a further hour before being filtered and reduced in volume under reduced pressure. The crude reaction mixture was then purified by column chromatography (SiO_2) to recover unconsumed starting material (1.4% methanol / dichloromethane, **AP12**, 132 mg, 173 μmol, 63%), and the desired rotaxane product as a white solid (21 mg, 16 μmol, 6.2%); ^{1}H NMR (400 MHz, $CDCl_3$, 325 K)δ 8.96 (4H, t, J = 6.5 Hz, H_D*), 8.53 (4H, d, J = 8.0 Hz, H_B*), 8.11 (2H, t, J = 8.0 Hz, H_A*), 7.35- 7.11 (20H, m, Ph),

6.88 (8H, s, H_F*), 5.60- 5.00 (4H, bm, C=C<u>H</u>), 4.80- 4.20 (16H, bm, 2 x C<u>H</u>C<u>H</u>$_2$O, H_E*), 3.19 (4H, q, J = 6.5 Hz, NHC<u>H</u>$_2$), 1.80- 1.40 (8H, bm, 2 x COC<u>H</u>$_2$, NHCH$_2$C<u>H</u>$_2$), 1.40- 1.20 (16H, m, 8 x CH$_2$), 1.20- 0.98 (4H, bm, 2 x COC<u>H</u>$_2$); ^{13}C NMR (100 MHz, $CDCl_3$, 298K)(macrocycle peaks broad at RT) δ 163.7, 158.0, 149.2, 140.9, 138.8, 138.5, 130.9, 128.8, 128.7, 128.6, 128.1, 127.0, 125.4, 68.2, 42.6, 39.7, 29.6, 29.5, 29.4, 29.4, 29.2, 26.9, 23.7; HRFAB-MS (3-NOBA matrix): m/z = 1295.65491 (calcd. for $C_{78}H_{87}N_8O_{10}$, $[M]H^+$, 1295.65452).

3-Chlorocarbonyl-acrylic acid ethyl ester (5.3)

To a stirred suspension of fumaric acid monoethyl ester (5 g, 34.7 mmol) and dimethylformamide (5 mL) in methylene chloride (100 mL) was dropwise added oxalyl chloride, a 2M solution in methylene chloride, (18.2 mL, 36.4 mmol). The reaction was allowed to proceed until it became a clear solution and no further effervescence could be observed. The product **5.3** in solution was used without further purification in the next step.

3-(Benzyl-phenyl-carbamoyl)-acrylic acid ethyl ester (5.4)

To a cooled solution of N-benzylaniline (12.8 g, 70.0 mmol) and triethylamine (7 g, 5 mL, 70.0 mmol) in dichloromethane at 0 °C was added with vigorous stirring the solution of previously formed acid chloride **5.3** dropwise over one hour. The reaction was left to stir overnight before being washed with 1M HCl (3 x 200 mL), saturated $NaHCO_3$ solution (3 x 50 mL) and brine (3 x 50 mL), dried over $MgSO_4$, filtered and evaporated under reduced pressure to yield the product **5.4** as a pale yellow oil (19.7 g, 63.8 mmol, 91 %); ^{1}H NMR (400 MHz, $CDCl_3$, 298K) δ 7.30- 7.24 (3H, m Ph), 7.20- 7.16 (3H, m, Ph), 7.15- 7.12 (2H, m, Ph), 6.95- 6.88 (2H, m, Ph), 6.83 (1H, d_{AB}, J = 15 Hz, C=C<u>H</u>), 6.74 (1H, d_{AB}, J = 15 Hz, C=C<u>H</u>), 4.92 (2H, s, C<u>H</u>$_2$Ph), 4.08 (2H, q, J = 7.0 Hz, OC<u>H</u>$_2$), 1.16 (3H, t, J = CH$_2$C<u>H</u>$_3$); ^{13}C (100 MHz, $CDCl_3$, 298K) δ 165.6, 163.8, 140.4, 136.8, 134.3, 131.5, 129.7, 128.7, 128.5, 128.3, 128.1, 127.6, 61.0, 53.5, 14.1; HRFAB-MS (3-NOBA matrix): m/z = 310.14548 (calcd. for $C_{19}H_{20}NO_3$, $[M]H^+$, 310.14432).

3-(Benzyl-phenyl-carbamoyl)-acrylic acid (5.5)

To a stirred solution of **5.5** (10 g, 32.4 mmol) in ethanol (100 mL) was added 1N NaOH (35.0 mL, 35.0 mmol). The resulting opaque mixture was stirred for three hours, before being filtered to remove the solid di(N,N-phenylbenzyl)fumaramide impurity. The resulting clear solution was acidified with 2N HCl to produce a white precipitate that was then extracted with ethyl acetate (3 x 200 mL). The combined organic washes were washed with water (3 x 100 mL), dried over $MgSO_4$ and evaporated to dryness under reduced pressure to yield the product as a colourless solid (**5.5**, 7.91g, 28.1 mmol, 87 %); ^{1}H NMR (400 MHz, $CDCl_3$, 298K) δ 7.31- 6.95 (10H, m, Ph), 6.53 (1H, d_{AB}, J = 15 Hz, C=CH), 6.46 (1H, d_{AB}, J = 15 Hz, C=CH), 4.84 (2H, s, CH_2Ph); ^{13}C NMR (100 MHz, $CDCl_3$, 298K) δ 169.9, 163.9, 140.7, 136.5, 135.9, 130.9, 129.8, 128.8, 128.6, 128.5, 128.0, 127.7, 53.6; HRFAB-MS (3-NOBA matrix): m/z = 282.11334 (calcd. for $C_{17}H_{16}NO_3$, $[M]H^+$, 282.11302).

3-(Benzyl-phenyl-carbamoyl)-acryloyl chloride (5.6)

To a stirred solution of **5.5** (2.8 g, 9.96 mmol) and catalytic dimethylformamide (1 mL) in dichloromethane (100 mL) at 0 °C was added oxalyl chloride (2M solution in dichloromethane, 4.98 mL, 9.96 mmol) over one hour. The reaction was stirred for a further hour until effervescence could no longer be observed. The resulting acid chloride **5.6** solution was used immediately without further purification.

General procedure for the synthesis of fumaric-based threads

To a stirred solution of the diamine (1 mmol) and triethylamine (4 mmol) in dichloromethane (40 mL) at 0 °C was added over 30 min a freshly prepared solution of acid chloride **5.6** (2 mmol) in dichloromethane (40 mL). The reaction was left for a further hour. The resulting colourless precipitate was collected by filtration, washed with cold dichloromethane (10 mL) and then diethyl ether (10 mL) and dried under vacuum to give the pure product as a colourless solid.

Selected data for **But-2-enedioic acid benzyl-phenyl-amide {12-[3-(benzyl-phenyl-carbamoyl)-acryloylamino]-dodecyl}-amide**: **B12**, 683 mg, 69 %; ^{1}H NMR (400 MHz, $CDCl_3$, 298 K) δ 7.36- 7.13 (16H, m, Ph), 7.06 (2H, d, J = 15.0 Hz, C=C<u>H</u>), 6.99 (4H, m, Ph), 6.82 (2H, d, J = 15.0 Hz, C=C<u>H</u>), 6.34 (2H, t, J = 5.5 Hz, NH), 4.99 (4H, s, $PhCH_2$), 3.22 (4H, aq, J = 6.0 Hz, NHC<u>H</u>$_2$), 1.45 (4H, bquintet, J = 7.0 Hz, $NHCH_2C\underline{H}_2$), 1.30- 1.17 (16H, m, 8 x CH_2); ^{13}C NMR (100 MHz, $CDCl_3$, 298K) δ 164.7, 164.0, 158.0, 141.0, 136.8, 134.8, 130.5, 129.7, 129.0, 128.5, 128.3, 128.2, 127.5, 125.3, 53.5, 39.8, 29.7, 29.5, 29.4, 29.1, 26.9; HRFAB-MS (3-NOBA matrix): m/z = 727.42122 (calcd. for $C_{46}H_{55}N_4O_4$, $[M]H^+$, 727.42223).

Selected data for **But-2-enedioic acid benzyl-phenyl-amide {10-[3-(benzyl-phenyl-carbamoyl)-acryloylamino]-decyl}-amide**, **B10**: 243 mg, 54 %; ^{1}H NMR (400 MHz, $CDCl_3$, 298 K) δ 7.36- 7.13 (16H, m, Ph), 7.02 (4H, m, Ph), 6.94 (2H, d, J = 15.0 Hz, C=C<u>H</u>), 6.81 (2H, d, J = 15.0 Hz, C=C<u>H</u>), 5.95 (2H, t, J = 5.5 Hz, NH), 4.99 (4H, s, $PhCH_2$), 3.26 (4H, aq, J = 6.0 Hz, NHC<u>H</u>$_2$), 1.48 (4H, bquintet, J = 7.0 Hz, $NHCH_2C\underline{H}_2$), 1.30- 1.17 (12H, m, 6 x CH_2); ^{13}C NMR (100 MHz, $CDCl_3$, 298K) δ 164.7, 164.0, 141.0, 136.8, 134.8, 130.5, 129.7, 129.0, 128.5, 128.3, 128.2, 127.5, 53.5, 39.8, 29.4, 29.1, 26.8; HRFAB-MS (3-NOBA matrix): m/z = 699.39009 (calcd. for $C_{44}H_{51}N_4O_4$, $[M]H^+$,699.39103).

Selected data for **But-2-enedioic acid benzyl-phenyl-amide {8-[3-(benzyl-phenyl-carbamoyl)-acryloylamino]-octyl}-amide**, **B8**: 102 mg, 32 %; ^{1}H NMR (400 MHz, $CDCl_3$, 298 K) δ 7.36- 7.13 (16H, m, Ph), 7.04 (2H, d, J = 15.0 Hz, C=C<u>H</u>), 6.99 (4H, m, Ph), 6.82 (2H, d, J = 15.0 Hz, C=C<u>H</u>), 6.31 (2H, t, J = 5.5 Hz, NH), 4.99 (4H, s, $PhCH_2$), 3.22 (4H, aq, J = 6.0 Hz, NHC<u>H</u>$_2$), 1.44 (4H, bquintet, J = 7.0 Hz, $NHCH_2C\underline{H}_2$), 1.30- 1.17 (8H, m, 4 x CH_2); ^{13}C NMR (100 MHz, $CDCl_3$, 298K) δ 164.7, 164.1, 141.0, 136.8, 134.7, 130.6, 129.7, 128.5, 128.5, 128.3, 128.2, 127.5, 53.5, 39.7, 29.3, 28.9, 26.7; HRFAB-MS (3-NOBA matrix): m/z = 671.35894 (calcd. for $C_{42}H_{47}N_4O_4$, $[M]H^+$, 671.35973).

Selected data for **But-2-enedioic acid benzyl-phenyl-amide {6-[3-(benzyl-phenyl-carbamoyl)-acryloylamino]-hexyl}-amide**: **B6**: 350 mg, 21 %; ^{1}H NMR (400 MHz, $CDCl_3$, 298 K) δ 7.36- 7.13 (16H, m, Ph), 6.98 (4H, m, Ph), 6.90 (2H, d, J = 15.0 Hz, C=C<u>H</u>), 6.79 (2H, d, J = 15.0 Hz, C=C<u>H</u>), 5.85 (2H, bt, NH), 4.99 (4H, s, $PhCH_2$), 3.24 (4H, aq, J = 6.0 Hz, NHC<u>H</u>$_2$), 1.46 (4H, bquintet, $NHCH_2C\underline{H}_2$), 1.27 (4H, bquintet, CH_2); ^{13}C NMR (100 MHz, $CDCl_3$, 298K) δ 164.7, 164.1, 141.0, 136.8, 134.7, 130.6, 129.7, 128.5, 128.5, 128.3, 128.2, 127.5, 53.5, 39.7, 29.3, 26.7; HRFAB-MS (3-NOBA matrix): *m/z* = 643.32829 (calcd. for $C_{40}H_{43}N_4O_4$, $[M]H^+$, 643.32843).

Selected data for **But-2-enedioic acid benzyl-phenyl-amide {4-[3-(benzyl-phenyl-carbamoyl)-acryloylamino]-butyl}-amide**: **B4** 158 mg, 35 %; ^{1}H NMR (400 MHz, $CDCl_3$, 298 K) δ 7.36- 7.13 (16H, m, Ph), 7.04- 6.97 (6H, m, Ph, C=C<u>H</u>), 6.81 (2H, d, J = 15.0 Hz, C=C<u>H</u>), 6.46 (2H, t, J = 5.5 Hz, NH), 4.99 (4H, s, $PhCH_2$), 3.22 (4H, bq, J = 6.0 Hz, NHC<u>H</u>$_2$), 1.46 (4H, bquintet, $NHCH_2C\underline{H}_2$); ^{13}C NMR (100 MHz, $CDCl_3$, 298K) δ 164.6, 164.3, 158.0, 141.0, 136.8, 134.4, 130.8, 129.8, 128.5, 128.5, 128.0, 127.6, 53.6, 39.3, 26.7; HRFAB-MS (3-NOBA matrix): *m/z* = 615.29654 (calcd. for $C_{38}H_{39}N_4O_4$, $[M]H^+$, 615.29713).

Selected data for **But-2-enedioic acid benzyl-phenyl-amide {2-[3-(benzyl-phenyl-carbamoyl)-acryloylamino]-ethyl}-amide**: **B2** 105 mg, 28 %; ^{1}H NMR (400 MHz, d_6-DMSO, 298 K) δ 8.53 (2H, bt, NH), 7.44- 7.12 (20H, m, Ph), 6.92 (2H, d, J = 15.0 Hz, C=C<u>H</u>), 6.55 (2H, d, J = 15.0 Hz, C=C<u>H</u>), 4.98 (4H, s, $PhCH_2$), 3.12 (4H, bm, NHC<u>H</u>$_2$); ^{13}C NMR (100 MHz, $CDCl_3$, 298K) δ 163.7, 163.4, 141.0, 137.0, 134.8, 129.6, 129.2, 128.4, 127.9, 127.9, 127.2, 52.2, 38.2; HRFAB-MS (3-NOBA matrix): *m/z* = 587.26625 (calcd. for $C_{36}H_{55}N_4O_4$, $[M]H^+$, 587.26583).

General procedure for the synthesis of fumaric-based isophthaloyl rotaxanes

To a stirred solution of thread (500 μmol, 1eq.) in chloroform (25 mL) was added simultaneously solutions of *p*-xylylene diamine (204 mg, 1.50 mmol, 3 eq.) and

triethylamine (526 μL, 3.75 mmol, 7.5 eq.) in chloroform (10 mL), and isophthaloyl chloride (304 mg, 1.5 mmol, 3 eq.) in chloroform (10 mL) via syringe pump over three hours. After addition, the reaction was stirred for a further hour before being filtered and reduced in volume under reduced pressure. The crude reaction mixture was then purified by column chromatography (SiO_2) to recover unconsumed starting material (1.75% methanol / dichloromethane), the desired rotaxane product as a white solid (2.25% methanol / dichloromethane) and often some [3]rotaxane. (Macrocycle and alkyl protons are often broad in ^{13}C NMR and are not reported in some cases).

Selected data for **[2](1,7,14,20-Tetraaza-2,6,15,19-tetraoxo-3,5,9,12,16,18,22,25-tetrabenzocyclohexacosane)-but-2-enedioic acid benzyl-phenyl-amide {12-[3-(benzyl-phenyl-carbamoyl)-acryloylamino]-dodecyl}-amide rotaxane, BI12**: 87 mg, 27 %; ^1H NMR (400 MHz, $CDCl_3$, 328 K) δ 8.34 (2H, bs, H_C*), 8.25 (4H, bd, J = 8.0 Hz, H_B*), 7.64 (2H, t, J = 8.0 Hz, H_A*), 7.42 (4H, bt, H_D*), 7.27- 7.21 (8H, bm, Ph), 7.17- 7.05 (8H, bm, Ph), 7.03 (8H, s, H_F*), 6.80- 6.60 (6H, bs, Ph, 2 x NH), 6.40- 5.60 (4H, bs, 2 x HC=CH), 4.87- 4.78 (4H, bs, CH_2Ph), 4.47- 4.38 (8H, bs, H_E*), 3.26 (4H, quartet, J = 6.0 Hz, $NHCH_2$), 1.54 (4H, bs, $NHCH_2CH_2$), 1.37- 1.15 (16H, bm, 8 x CH_2); ^{13}C NMR (100 MHz, $CDCl_3$, 298K) δ 166.0, 164.8, 137.3, 133.4, 131.6, 129.7, 129.6, 129.2, 128.5, 128.3, 128.0, 127.6, 123.6, 43.8, 39.8, 29.4, 29.3, 27.0; HRFAB-MS (3-NOBA matrix): *m/z* = 1259.63411 (calcd. for $C_{78}H_{83}N_8O_8$, $[M]H^+$, 1259.63339).

Selected data for **[2](1,7,14,20-Tetraaza-2,6,15,19-tetraoxo-3,5,9,12,16,18,22,25-tetrabenzocyclohexacosane)-but-2-enedioic acid benzyl-phenyl-amide {10-[3-(benzyl-phenyl-carbamoyl)-acryloylamino]-decyl}-amide rotaxane, BI10**: 33 mg, 24 %; ^1H NMR (400 MHz, $CDCl_3$, 298 K) δ 8.28 (2H, bs, H_C*), 8.23 (4H, dd, J = 1.5, 8.0 Hz, H_B*), 7.63 (2H, t, J = 8.0 Hz, H_A*), 7.50 (4H, bt, H_D*), 7.33- 7.21 (8H, bm, Ph), 7.21- 6.93 (8H, bm, Ph), 7.03 (8H, s, H_F*), 6.93- 6.77 (4H, bs, HC=CH), 5.00- 4.00 (8H, bs, H_E*), 4.96- 4.68 (4H, bs, CH_2Ph), 3.24 (4H, quartet, J = 6.0 Hz, $NHCH_2$), 1.50 (4H, bs, $NHCH_2CH_2$), 1.37- 1.15 (12H, bm, 6 x CH_2); ^{13}C NMR (100 MHz, $CDCl_3$, 298K) δ 165.9, 164.7, 137.4, 133.5, 131.6, 129.7, 129.6, 129.2, 128.5,

128.3, 127.9, 127.6, 123.6, 43.8, 39.8, 29.5, 29.3, 27.0; HRFAB-MS (3-NOBA matrix): *m/z* = 1231.60263 (calcd. for $C_{76}H_{79}N_8O_8$, $[M]H^+$, 1231.60209).

Selected data for **[2](1,7,14,20-Tetraaza-2,6,15,19-tetraoxo-3,5,9,12,16,18,22,25-tetrabenzocyclohexacosane)-but-2-enedioic acid benzyl-phenyl-amide {8-[3-(benzyl-phenyl-carbamoyl)-acryloylamino]-octyl}-amide rotaxane, BI8**: 46 mg, 28 %; ^{1}H NMR (400 MHz, $CDCl_3$, 325 K) δ 8.31 (2H, bs, H_C*), 8.23 (4H, bd, *J* = 8.0 Hz, H_B*), 7.62 (2H, t, *J* = 8.0 Hz, H_A*), 7.45 (4H, bt, H_D*), 7.33- 7.21 (8H, bm, Ph), 7.17- 6.93 (8H, bm, Ph), 7.04 (8H, bs, H_F*), 6.92- 6.78 (6H, bm, Ph, 2 x NH), 6.60- 5.90 (4H, bs, HC=CH), 4.82 (4H, bs, CH_2Ph), 4.43 (8H, bs, H_E*), 3.22 (4H, quartet, *J* = 6.0 Hz, $NHCH_2$), 1.51 (4H, bs, $NHCH_2CH_2$), 1.38- 1.22 (8H, bm, 4 x CH_2); ^{13}C NMR (100 MHz, $CDCl_3$, 298K) δ 166.0, 164.8, 137.3, 133.5, 131.6, 129.7, 129.6, 129.2, 128.5, 128.3, 127.9, 127.6, 123.6, 54.0, 43.7, 39.9, 29.7, 29.2, 29.0, 26.8; HRFAB-MS (3-NOBA matrix): *m/z* = 1203.57081 (calcd. for $C_{74}H_{75}N_8O_8$, $[M]H^+$, 1203.57079).

Selected data for **[2](1,7,14,20-Tetraaza-2,6,15,19-tetraoxo-3,5,9,12,16,18,22,25-tetrabenzocyclohexacosane)-but-2-enedioic acid benzyl-phenyl-amide {6-[3-(benzyl-phenyl-carbamoyl)-acryloylamino]-hexyl}-amide rotaxane, BI6**: 24 mg, 20 %; ^{1}H NMR (400 MHz, $CDCl_3$, 298 K) δ 8.30 (2H, bs, H_C*), 8.18 (4H, d, *J* = 8.0 Hz, H_B*), 7.58 (2H, t, *J* = 8.0 Hz, H_A*), 7.42 (4H, bt, H_D*), 7.30- 6.85 (16H, bm, Ph), 6.95 (8H, bs, H_F*), 6.83 (4H, m, Ph), 6.40 (2H, bm, C=CH), 6.10 (2H, bm, C=CH), 4.82 (4H, bs, CH_2Ph), 4.40 (8H, bs, H_E*) 3.18 (4H, bm, $NHCH_2$), 1.58 (4H, m, $NHCH_2CH_2$), 1.46 (4H, bs, 8 x CH_2); ^{13}C NMR (100 MHz, $CDCl_3$, 298K) δ 165.9, 164.9, 164.8, 140.6, 137.5, 136.3, 133.7, 133.5, 131.6, 129.6, 129.0, 128.8, 128.5, 128.3, 128.0, 127.9, 127.6, 127.5, 123.5, 54.0, 43.7, 39.3, 28.9, 25.9; HRFAB-MS (3-NOBA matrix): *m/z* = 1175.53994 (calcd. for $C_{72}H_{71}N_8O_8$, $[M]H^+$, 1175.53949).

Selected data for **[2](1,7,14,20-Tetraaza-2,6,15,19-tetraoxo-3,5,9,12,16,18,22,25-tetrabenzocyclohexacosane)-but-2-enedioic acid benzyl-phenyl-amide {4-[3-(benzyl-phenyl-carbamoyl)-acryloylamino]-butyl}-amide rotaxane, BI4**: 49 mg,

22 %; ^{1}H NMR (400 MHz, $CDCl_3$, 298 K) δ 8.29 (2H, bs, H_C*), 8.21 (4H, dd, J = 1.5, 8.0 Hz, H_B*), 7.60 (2H, t, J = 8.0 Hz, H_A*), 7.51 (4H, bt, H_D*), 7.33- 7.21 (8H, bm, Ph), 7.12- 7.03 (8H, bm, Ph), 6.96 (8H, bs, H_F*), 6.83 (4H, bs, Ph), 6.37 (2H, bs, C=CH), 6.03 (2H, bs, C=CH), 4.81 (4H, bs, CH_2Ph), 4.37 (8H, bs, H_E*) 3.20 (4H, bquartet, $NHCH_2$), 1.54 (4H, bs, $NHCH_2CH_2$); ^{13}C NMR (100 MHz, $CDCl_3$, 298K) δ 166.0, 165.1, 164.8, 140.4, 137.4, 136.1, 133.6, 133.2, 131.6, 129.7, 129.5, 129.2, 129.0, 128.7, 128.6, 128.4, 128.0, 127.5, 123.6, 54.0, 43.6, 39.6, 29.7; HRFAB-MS (3-NOBA matrix): m/z = 1147.50882 (calcd. for $C_{70}H_{67}N_8O_8$, $[M]H^+$, 1147.50819).

Selected data for **[2](1,7,14,20-Tetraaza-2,6,15,19-tetraoxo-3,5,9,12,16,18,22,25-tetrabenzocyclohexacosane)-but-2-enedioic acid benzyl-phenyl-amide {2-[3-(benzyl-phenyl-carbamoyl)-acryloylamino]-ethyl}-amide rotaxane, BI2**: 12 mg, 9 %; ^{1}H NMR (400 MHz, $CDCl_3$, 298K) δ ^{1}H NMR (400 MHz, $CDCl_3$, 298 K) δ 8.27 (2H, bs, H_C*), 8.19 (4H, dd, J = 1.5, 8.0 Hz, H_B*), 7.55 (2H, t, J = 8.0 Hz, H_A*), 7.40 (4H, bt, H_D*), 7.33- 7.21 (8H, bm, Ph), 7.12- 7.03 (8H, bm, Ph), 6.96 (8H, bs, H_F*), 6.84 (2H, bt, NH), 6.77 (4H, bs, Ph), 6.39 (2H, bs, C=CH), 6.05 (2H, bs, C=CH), 4.81 (4H, bs, CH_2Ph), 4.40 (8H, bs, H_E*) 3.34 (4H, bs, $NHCH_2$); ^{13}C NMR (100 MHz, $CDCl_3$, 298K) δ 166.1, 165.1, 164.7, 140.6, 137.4, 136.1, 133.6, 133.2, 131.6, 129.7, 129.5, 129.2, 129.0, 128.7, 128.6, 128.4, 128.0, 127.5, 123.6, 54.0, 43.6, 39.9; . HRFAB-MS (3-NOBA matrix): m/z = 1119.47743 (calcd. for $C_{68}H_{63}N_8O_8$, $[M]H^+$, 1119.47689).

General procedure for synthesis of fumaric-based *endo*-pyridyl rotaxanes

Same as for isophthaloyl rotaxanes, but with 2,6-dipyridinedicarbonyl chloride (306 mg, 1.5 mmol, 3eq.) instead of isophthaloyl chloride. Column chromatography gave unconsumed starting material (2.0% methanol / dichloromethane), and the desired rotaxane product as a white solid (2.75% methanol / dichloromethane).

Selected data for **[2](1,4,7,14,17,20-Hexaaza-2,6,15,19-tetraoxo-3,5,9,12,16,18,22,25-tetrabenzocyclohexacosane)-but-2-enedioic acid benzyl-phenyl-amide {12-[3-(benzyl-phenyl-carbamoyl)-acryloylamino]-dodecyl}-**

amide rotaxane, BP12: 73 mg, 14 %; ^{1}H NMR (400 MHz, $CDCl_3$, 298K) δ 9.55 (2H, d, *J* = 9.5 Hz, H_D*), 9.18 (2H, d, *J* = 9.5 Hz, $H_{D'}$*), 8.48 (2H, t, *J* = 7.5 Hz, H_B*), 8.41 (2H, d, *J* = 7.5 Hz, $H_{B'}$*), 8.11 (2H, t, *J* = 7.5 Hz, H_A), 7.35- 7.22 (10H, m, Ph), 7.21- 7.15 (4H, m, Ph), 7.03- 6.95 (3H, m, Ph, C=C<u>H</u>), 6.94- 6.83 (10H, m, Ph, H_F*), 6.82- 6.75 (1H, d, *J* = 15.0 Hz, C=C<u>H</u>), 6.65 (1H, t, *J* = 5.5 Hz, NH), 6.27 (1H, m, Ph), 6.14 (1H, t, *J* = 5.5 Hz, NH), 5.47- 5.23 (5H, m, C=C<u>H</u>, H_E*), 5.13 (1H, d, *J* = 15 Hz, C=C<u>H</u>), 4.97 (2H, s, d), 4.77 (2H, s, d), 3.52 (2H, d, *J* = 14Hz, $H_{E'}$*), 3.39 (2H, d, *J* = 14Hz, $H_{E'}$*), 3.24 (4H, q, *J* = 6.5 Hz, C<u>H</u>$_2$NH), 1.56 (2H, quintet, *J* = 7.0 Hz, C<u>H</u>$_2$CH$_2$NH), 1.46 (2H, quintet, *J* = 7.0 Hz, C<u>H</u>$_2$CH$_2$NH), 1.37 (4H, m, C<u>H</u>$_2$CH$_2$CH$_2$NH), 1.27- 1.14 (12H, m, 6 x C<u>H</u>$_2$); ^{13}C NMR (100 MHz, $CDCl_3$, 298K) δ 165.1, 164.7, 164.3, 164.1, 164.0, 163.1, 149.3, 149.0, 141.1, 140.1, 138.8, 138.6, 138.2, 138.0, 136.9, 136.0, 134.8, 130.4, 130.2, 129.7, 129.6, 129.0, 128.6, 128.5, 128.4, 128.3, 127.9, 127.8, 127.7, 127.5, 125.3, 124.9, 54.6, 53.5, 42.7, 42.4, 40.2, 39.7, 29.7, 29.3, 29.2, 29.1, 29.0, 27.0, 26.8; HRFAB-MS (3-NOBA matrix): *m/z* = 1261.62182 (calcd. for $C_{76}H_{81}N_{10}O_8$, $[M]H^+$, 1261.62389).

Selected data for **[2](1,4,7,14,17,20-Hexaaza-2,6,15,19-tetraoxo-3,5,9,12,16,18,22,25-tetrabenzocyclohexacosane)-but-2-enedioic acid benzyl-phenyl-amide {6-[3-(benzyl-phenyl-carbamoyl)-acryloylamino]-hexyl}-amide rotaxane, BP6**: 33 mg, 15 %; ^{1}H NMR (400 MHz, $CDCl_3$, 298K) δ 9.55 (2H, d, *J* = 9.5 Hz, H_D*), 9.16 (2H, d, *J* = 9.5 Hz, H_D'*), 8.41 (4H, bd, H_B*), 8.11 (2H, bt, *J* = 7.5 Hz, H_A*), 7.35- 7.15 (16H, m, Ph), 7.15- 7.00 (2H, m, Ph), 6.99- 6.64 (3H, m, Ph, 2 x C=C<u>H</u>, NH), 6.86 (8H, m, H_F*), 6.55- 6.40 (1H, bt, NH), 6.24 (1H, bm, Ph), 5.47- 5.23 (5H, m, C=C<u>H</u>, H_E*), 5.05 (1H, d, *J* = 15 Hz, C=C<u>H</u>), 4.99 (2H, s, C<u>H</u>$_2$Ph), 4.79 (2H, s, C<u>H</u>$_2$Ph), 3.51 (2H, d, *J* = 14Hz, E'), 3.36 (2H, d, *J* = 14Hz, E'), 3.14 (4H, bd, C<u>H</u>$_2$NH), 1.50 (2H, bm, C<u>H</u>$_2$CH$_2$NH), 1.42 (2H, bm, C<u>H</u>$_2$CH$_2$NH), 1.32 (4H, m, C<u>H</u>$_2$CH$_2$CH$_2$NH); ^{13}C NMR (100 MHz, $CDCl_3$, 298K) δ 165.0, 164.6, 164.4, 164.1, 163.9, 163.1, 149.0, 140.9, 140.2, 138.7, 138.5, 138.0, 136.7, 136.1, 134.3, 130.7, 130.6, 129.7, 129.6, 129.0, 128.6, 128.5, 128.4, 128.3, 127.9, 127.8, 127.7, 127.5, 125.3, 124.9, 54.5, 53.7, 42.5, 38.9, 38.5, 29.7, 29.6, 28.4, 25.6, 25.0; HRFAB-MS (3-NOBA matrix): *m/z* = 1177.53001 (calcd. for $C_{70}H_{69}N_{10}O_8$, $[M]H^+$, 1177.52998).

5.6 References

(1) Anelli, P. L.; Spencer, N.; Stoddart, J. F., *J. Am. Chem. Soc.*, **1991**, *113*, 5131-5133.

(2) Sauvage, J.-P., *Acc. Chem. Res.*, **1998**, *31*, 611-619; Feringa, B. L., *Acc. Chem. Res.*, **2001**, *34*, 504-513; Balzani, V.; Credi, A.; Raymo, F. M.; Stoddart, J. F., *Angew. Chem. Int. Ed.*, **2000**, *39*, 3348-3391; Blanco, M.-J.; Consuelo Jimenez, M.; Chambron, J.-C.; Heitz, V.; Linke, M.; Sauvage, J.-P., *Chem. Soc. Rev.*, **1999**, *28*, 293-305; Balzani, V.; Gomez-Lopez, M.; Stoddart, J. F., *Acc. Chem. Res.*, **1998**, *31*, 405-414; Ashton, P. R.; Ballardini, R.; Balzani, V.; Boyd, S. E.; Credi, A.; Gandolfi, M. T.; Gomez-Lopez, M.; Iqbal, S.; Philp, D.; Preece, J. A.; Prodi, L.; Ricketts, H. G.; Stoddart, J. F.; Tolley, M. S.; Venturi, M.; White, A. J. P.; Williams, D. J., *Chem. Eur. J.*, **1997**, *3*, 152-170.

(3) Brouwer, A. M.; Frochot, C.; Gatti, F. G.; Leigh, D. A.; Mottier, L.; Paolucci, F.; Roffia, S.; Wurpel, G. W. H., *Science*, **2001**, *291*, 2124-2128.

(4) Altieri, A.; Gatti, F. G.; Kay, E. R.; Leigh, D. A.; Martel, D.; Paolucci, F.; Slawin, A. M. Z.; Wong, J. K. Y., *J. Am. Chem. Soc.*, **2003**, *125*, 8644-8654.

(5) Bissell, R. A.; Cordova, E.; Kaifer, A. E.; Stoddart, J. F., *Nature*, **1994**, *369*, 133-137.

(6) Leigh, D. A.; Wong, J. K. Y.; Dehez, F.; Zerbetto, F., *Nature*, **2003**, *424*, 174-179.

(7) Lane, A. S.; Leigh, D. A.; Murphy, A., *J. Am. Chem. Soc.*, **1997**, *119*, 11092-11093.

(8) Brancato, G.; Coutrot, F.; Leigh, D. A.; Murphy, A.; Wong, J. K. Y.; Zerbetto, F., *Proc. Nat. Acad. Sci.*, **2002**, *99*, 4967-4971.

(9) Gatti, F. G.; Leigh, D. A.; Nepogodiev, S. A.; Slawin, A. M. Z.; Teat, S. J.; Wong, J. K. Y., *J. Am. Chem. Soc.*, **2001**, *123*, 5983-5989.

(10) Johnston, A. G.; Leigh, D. A.; Nezhat, L.; Smart, J. P.; Deegan, M. D., *Angew. Chem., Int. Ed.*, **1995**, *34*, 1212-1216.

(11) Gatti, F. G.; Leon, S.; Wong, J. K. Y.; Bottari, G.; Altieri, A.; Morales, M. A. F.; Teat, S. J.; Frochot, C.; Leigh, D. A.; Brouwer, A. M.; Zerbetto, F., *Proc. Nat. Acad. Sci.*, **2003**, *100*, 10-14.

(12) Gatti, F. G.; Leigh, D. A.; Nepogodiev, S. A.; Slawin, A. M. Z.; Teat, S. J.; Wong, J. K. Y., *J. Am. Chem. Soc.*, **2001**, *123*, 5983-5989.

(13) Leigh, D. A.; Murphy, A.; Smart, J. P.; Deleuze, M. S.; Zerbetto, F., *J. Am. Chem. Soc.*, **1998**, *120*, 6458-6467; Dahlquist, F. W.; Longmur, K. J.; Du Vernet, R. B., *J. Magn. Reson.*, **1975**, *17*, 406.

(14) Geib, S. J.; Hirst, S. C.; Vincent, A. D.; Hamilton, A. D., *J. Chem. Soc., Chem. Commun.*, **1991**, 1293; Hunter, C. A.; Purvis, D. H., *Angew. Chem. Int. Ed.*, **1992**, *31*, 792-795.

(15) Bottari, G.; Dehez, F.; Leigh, D. A.; Nash, P. J.; Pérez, E. M.; Wong, J. K. Y.; Zerbetto, F., *Angew. Chem. Int. Ed.*, in press.

Chapter 6

Entropy-Driven Translational Isomerism: a Tristable Molecular Shuttle

Declaration: This chapter is presented as a complete paper accepted by Angew. Chem., Int. Ed. and which is currently in press. The contribution by the co-author, Phillip Nash, is the synthesis of rotaxane **4**, and development of the synthetic method of rotaxane ***Z,Z*-5**. The rotaxane was later synthesised by Emilio Pérez. The following co-authors contributed to this work: Giovanni Bottari, Francois Dehez, David A Leigh,* Phillip J Nash, Emilio M Pérez, Jenny K Y Wong and Francesco Zerbetto*.

4.1 Introduction

Stimuli-responsive molecular shuttles translocate a macrocycle between different sites ('stations') on a rotaxane thread under the influence of an external trigger.[1] In bistable shuttles the relative macrocycle binding affinities of the stations are reversed by the stimulus, generally through it bringing about a chemical change in the molecule that targets the enthalpy of binding of the macrocycle to one or both stations.[2] Immediately following the chemical transformation the molecule is no longer in the most energetically favoured co-conformation and the macrocycle moves along the thread to its newly preferred position through biased Brownian motion as the system relaxes to the global minimum.[3] Although many external stimuli can be used to induce shuttling in this way (e.g. pH,[4] light,[5] electrochemistry[4a,6] etc.), a simple temperature change is not generally one of them.[7] The Boltzmann distribution of the macrocycle between the different binding sites within a shuttle ensures that heating or cooling changes the degree of discrimination the macrocycle expresses for the various stations, but not the actual station preference of the macrocycle. However, in principle a change of relative station binding affinity with temperature is possible since $\Delta G_{binding} = \Delta H_{binding} - T\Delta S_{binding}$. If the entropy terms are sufficiently different then the relative binding affinity of the macrocycle for the two stations can be reversed by increasing or lowering the temperature. Here we describe an example of this phenomenon.[8] The

[2]rotaxane where it occurs is, in fact, a tristable molecular shuttle, **1**; the first rotaxane in which a ring can be switched between three different positions on a thread (Figure 1).[9]

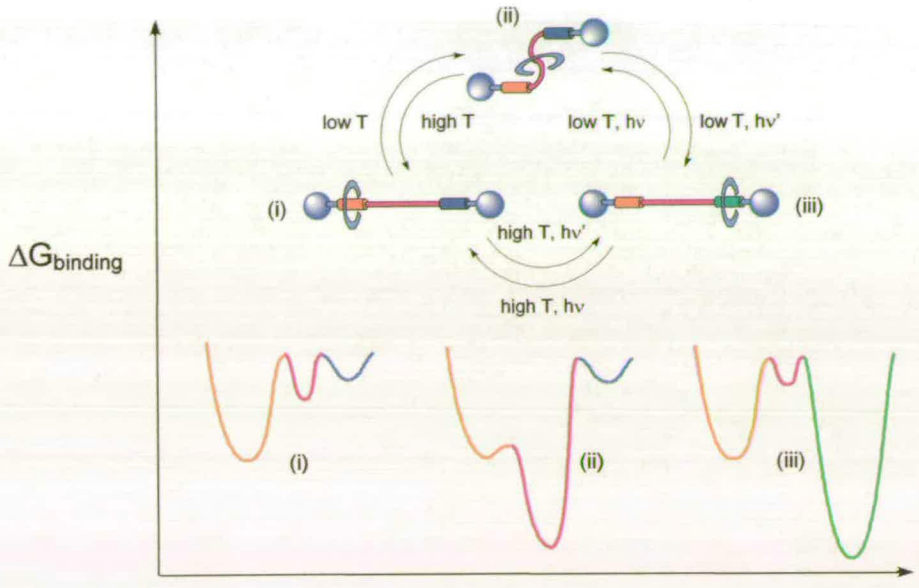
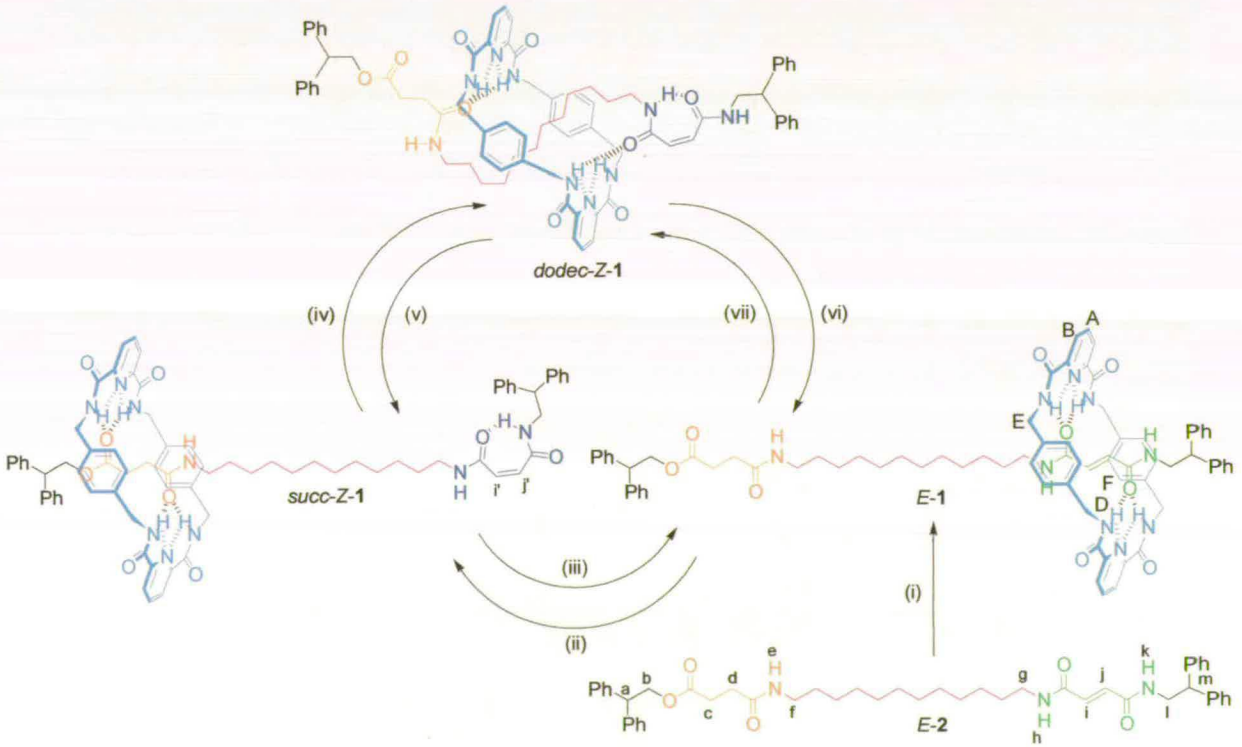


Figure 1 Macrocycle translation in a tristable molecular shuttle. Macrocycle movement between (i) and (ii) is an entropy-driven process involving no change to the covalent structure of the molecule.

4.2 Results and Discussion

Rotaxane *E*-**1** was prepared in 32% yield from thread *E*-**2** (Scheme 1). *E*-**2** has previously[5g] been utilized as the thread for a light- and heat-switchable bistable molecular shuttle, **3**, and contains two sites designed to hydrogen bond to a benzylic amide macrocycle, namely a fumaramide group (shown in green) and a succinic amide-ester (orange) unit, separated by a dodecane chain (purple). Shuttle **1** differs from **3** only in that the macrocycle contains *endo*-pyridine units instead of isophthalamide groups. Photoisomerisation of *E*-**1** at 254 nm afforded the *cis*-rotaxane *Z*-**1** in 54% yield. Since the xylylene units of the macrocycle shield the encapsulated regions of the thread, the position of the ring in *E*- and *Z*-**1** could be determined by comparing the chemical shift of the protons in the [2]rotaxanes with those of the corresponding threads (Figure 2).



Scheme 1 A tristable molecular shuttle, **1**. (i) pyridine 2,6-dicarbonyl chloride, *p*-xylylenediamine, Et_3N, $CHCl_3$, 32%; (ii) hν 254 nm, 20 mins, CH_2Cl_2, 298 K, 54% or hν 350 nm, catalytic benzophenone, 5 min, 65%; (iii) hν 312 nm, 35 mins, CH_2Cl_2, 298 K, >95% or hν 400-670 nm, catalytic Br_2, 2 mins, CH_2Cl_2, 298 K, ~100%; (iv) $CDCl_3$, 258 K, 85%; (v) $CDCl_3$, 308 K, 90%; (vi) hν 312 nm, 35 mins, CH_2Cl_2, >95% or hν 400-670 nm, catalytic Br_2, 2 mins, CH_2Cl_2, ~100%; (vii) hν 254 nm, 20 mins, $CDCl_3$, 258 K, 54%.

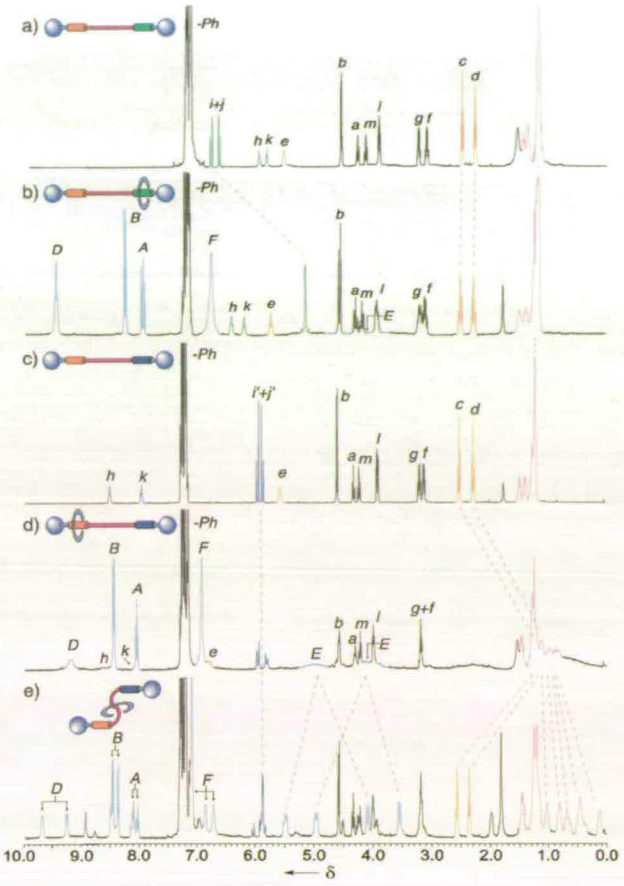


Figure 2 400 MHz ^{1}H NMR spectra in $CDCl_3$ of (a) thread *E*-**2** at 298K, (b) rotaxane *E*-**1** at 298K, (c) thread *Z*-**2** at 308K, (d) rotaxane *Z*-**1** at 308K and (e) rotaxane *Z*-**1** at 258K. The assignments correspond to the lettering shown in Scheme 1.

The ^{1}H NMR spectra (400 MHz, 298K, Figure 2a and b) confirm the position of the macrocycle over the fumaramide station of *E*-**1** in $CDCl_3$. The olefin protons H_i and H_j are shielded by more than 1.5 ppm in the rotaxane relative to the thread, while the chemical shifts of the succinic amide-ester protons H_c and H_d are unchanged. Lowering the temperature had no effect on the chemical shift values, the only significant change in the spectra being that the macrocycle H_E protons sharpen as the ring pirouetting about the thread becomes slow on the NMR timescale.

In *Z*-**1**, the strong binding fumaramide station is replaced with a group of much poorer macrocycle binding affinity (maleamide) and we expected the macrocycle to be displaced to the succinic amide ester site on the thread (i.e. co-conformer *succ*-*Z*-**1**), as occurs with *Z*-**3**.[5g] Whilst the chemical shifts differences (>1.2 ppm, COSY) of the H_c and H_d protons confirm that this is largely the case[10] at room temperature and higher (e.g. 308 K, Figure 2d), to our surprise the ^{1}H NMR spectrum of *Z*-**1** proved highly temperature dependent. Indeed, at 258 K

(Figure 2e) the major signals for H_c and H_d of *Z*-**1** appear at the same chemical shifts as they do in the thread (*Z*-**2**). Not only that, but the olefin protons $H_{i'}$ and $H_{j'}$ are also unchanged indicating that the macrocycle is not primarily located over either of the designed stations! In fact, it is the alkyl protons of the C_{12} chain that experience significant upfield shifts (up to 1 ppm at 258 K), showing that the pyridine macrocycle is actually positioned over the C_{12} unit. In order to satisfy the macrocycles hydrogen bonding requirements, the amide groups of the thread must still act as hydrogen bond acceptors and so the alkyl chain presumably adopts some form of folded "S-shape" conformation so that the amides at both ends of the chain can reach the macrocycle binding sites, accounting for the shielding seen for the alkyl protons (Scheme 1, co-conformer *dodec-Z*-**1**). Interestingly, two sets of signals are observed for the macrocycle indicating that the two halves of the ring experience magnetically different environments (i.e. pirouetting of the macrocycle about the S-shaped thread is slow on the NMR timescale at 258 K).

What is the reason for *Z*-**1**'s unexpected behavior? The reversal of the binding affinity of the macrocycle for the succinic amide-ester and the alkyl chain stations at different temperatures suggests that the $T\Delta S$ term is reversing the relative $\Delta G_{binding}$ of the two stations (Figure 1). In co-conformer *succ-Z*-**1** two hydrogen bonds from the macrocycle occur to an ester carbonyl group, a significantly weaker[11] interaction than an amide-amide hydrogen bond, whereas in the *dodec-Z*-**1** co-conformer four intercomponent amide-amide hydrogen bonds can be formed, providing ~2 kcal mol^{-1}[11] greater enthalpic stabilization. It seems that at low temperatures the energy gain from forming the two extra amide-amide hydrogen bonds overcomes the entropic cost required for the thread to bridge the macrocycle binding sites; a C_{12} chain has >500,000 (3^{12}) possible C-C rotamers and a significant number of these degrees of freedom must be lost upon forming the *dodec-Z*-**1** structure. Raising the temperature increases the contribution of the $T\Delta S$ term to the $\Delta G_{binding}$ of the *dodec-Z*-**1** co-conformer much more than for *succ-Z*-**1** until, at higher temperatures, the relative stabilities of the two positional isomers are actually reversed and the *Z*-rotaxane predominantly adopts the enthalpically weaker but entropically more favorable *succ-Z*-**1** co-conformation. Indeed, evidence that the stability of *dodec-Z*-**1** is much more temperature-dependent than *succ-Z*-**1** is provided by molecular dynamics simulations (see experimental section).

The structural requirements for temperature to markedly affect the position of the macrocycle on the thread are quite specific (Figure 3). Similar rotaxanes missing either station (**4**, *Z*,*Z*-**5**)

or without the *endo*-pyridyl macrocycle (*Z*-**3**) do not show the same temperature-dependent ^{1}H chemical shifts as *Z*-**1**. However, the "S" shape of the *dodec*-*Z*-**1** co-conformer binding site is, remarkably, observed in the solid state structure of an isophthalamide macrocycle-containing [2]rotaxane of a thread consisting of two amide groups separated by a C_{12} chain (**6**, Figure 4). In fact, this type of structure may be a reasonably low energy co-conformation for many two amide-station [2]rotaxanes with flexible spacers, which with particular molecular components (poor alternative binding stations) and the right environmental conditions (low temperature), can sometimes become the global minimum arrangement seen for *Z*-**1** at 258 K.

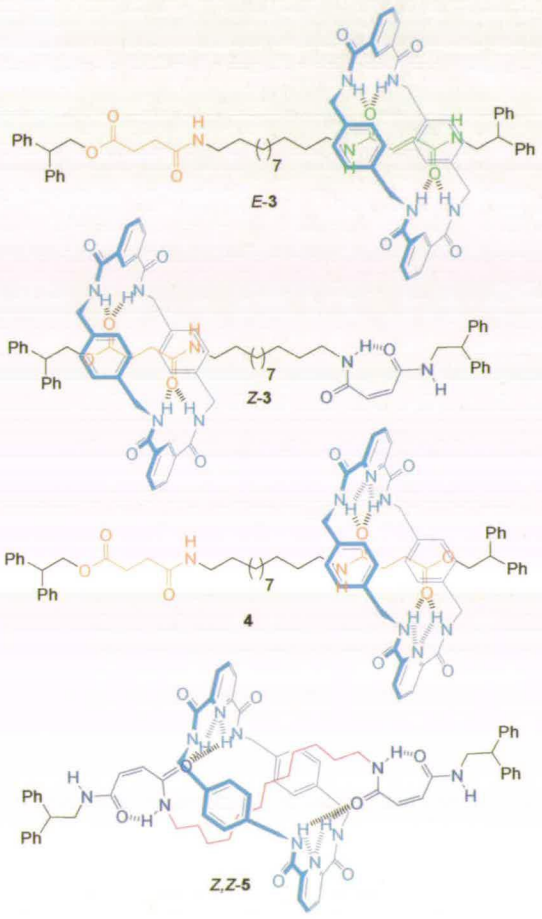


Figure 3 Rotaxane structures related to *Z*-**1** which do not show temperature-dependent translational isomerism.

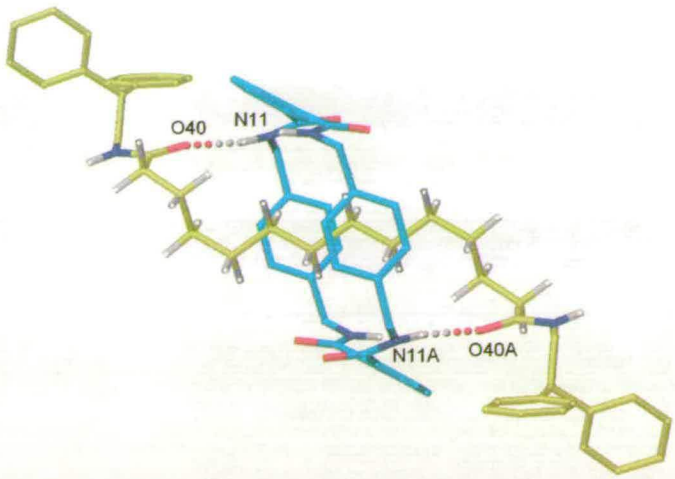


Figure 4 *X*-Ray crystal structure of a benzylic isophthalamide macrocycle-based [2]rotaxane **6** where two amide groups are separated by a C_{12} alkyl chain. The carbon atoms of the macrocycles are shown in blue, carbon atoms of the threads in yellow, oxygen atoms in red and nitrogen atoms in dark blue. The amide and C_{12} methylene hydrogen atoms are shown in white while all others are removed for clarity. Intramolecular hydrogen bond distances and angles: O40-HN11/O40A-HN11A 1.92 Å, 156.4°.

4.3 Conclusions

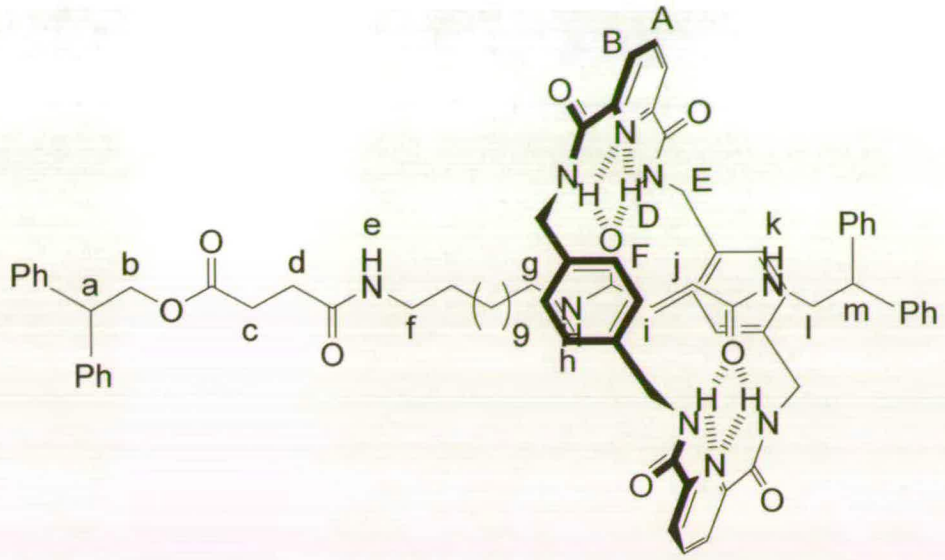
Changing the position of a macrocycle on a thread by varying the temperature is potentially a useful means of controlling translational isomerism in a rotaxane, not least because no chemical reaction is involved and no change to the covalent structure of the molecule occurs. The photostationary state of **1** at 312 nm consists of >95% of the *trans*-isomer (again, dissimilar behavior to shuttle **3** where the steady state at 312 nm is ~55:45 *E*:*Z*). This provides the tristable shuttle with the intriguing property that, starting with the ring on the central station (i.e. *dodec*-*Z*-**1**), the macrocycle can be moved selectively in one direction along the thread by irradiation with light at 312 nm, or selectively in the other direction by simply raising the temperature.

Keywords: entropy-driven motion, molecular shuttles, rotaxanes, molecular machines.

4.4 Experimental Section

The synthesis and the spectroscopic data of the precursors to rotaxanes *E*-**1** and *Z*-**1** have been reported elsewhere.

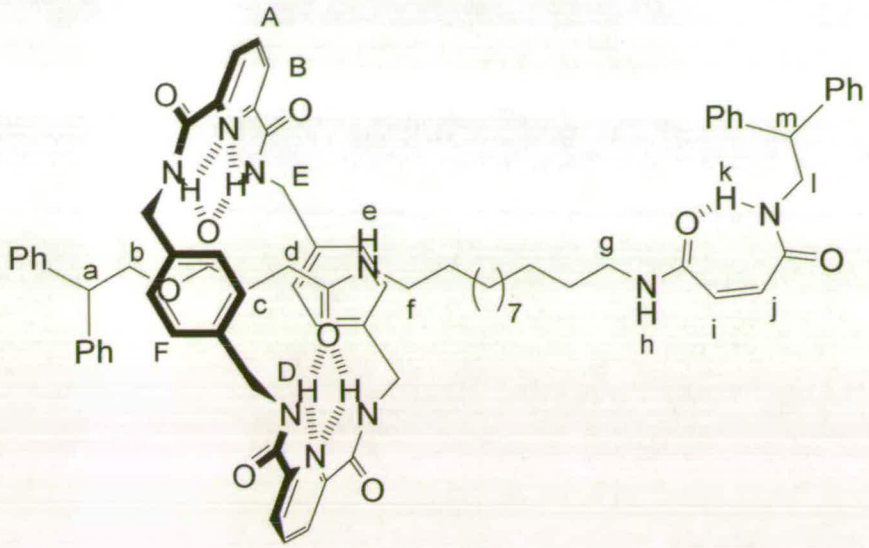
[2]-(1,4,7,14,17,20-Hexaaza-2,6,15,19-tetraoxo-3,5,9,12,16,18,22,25 – tetrabenzocyclohexacosane)-((*E*)-*N*-{12-[3-(2,2-diphenylethylcarbamoyl)-acryloylamino]-dodecyl}-succinamic acid 2,2-diphenylethyl ester)-rotaxane, *E*-1.



Rotaxane *E*-**1** was prepared from the thread *E*-**1** (0.19 g, 0.25 mmol) using a general procedure previously described[5g] for the synthesis of benzylic amide macrocycle-containing [2]rotaxanes. The crude product was subjected to column chromatography on silica gel using a gradient of CH_2Cl_2 to CH_2Cl_2/EtOAc (80/20) as eluent to obtain the desired compound as a colorless solid (*E*-**1**, 0.10 g, 32%). ^{1}H NMR (400 MHz, $CDCl_3$, 298K): δ = 9.47 (m, 4H, N*H*$_D$), 8.36 (d, *J* = 7.6 Hz, 4H, C*H*$_B$), 8.04 (t, *J* = 7.7 Hz, 2H, C*H*$_A$), 7.33-7.17 (m, 20H, ArC*H*), 6.82 (br s, 8H, ArC*H*$_F$), 6.12 (br s, 1H, N*H*$_k$), 6.05 (br s, 1H, N*H*$_h$), 5.73 (t, *J* = 5.3 Hz, 1H, N*H*$_e$), 5.22 (d, *J* = 14.5 Hz, 1H, C*H*$_{i\ or\ j}$), 5.16 (d, *J* = 14.5 Hz, 1H, C*H*$_{i\ or\ j}$), 4.80-3.70 (br m, 8H, C*H*$_E$), 4.63 (d, *J* = 7.6 Hz, 2H, C*H*$_b$), 4.34 (t, *J* = 7.6 Hz, 2H, C*H*$_a$), 4.22 (t, *J* = 8.0 Hz, 1H, C*H*$_m$), 3.97 (m, 2H, C*H*$_l$), 3.25 (dt, 2H, C*H*$_g$), 3.16 (dt, 2H, C*H*$_f$), 2.56 (t, *J* = 6.8 Hz, 2H, C*H*$_c$), 2.32 (t, *J* = 6.8 Hz, 2H, C*H*$_d$), 1.55 (m, 2H, -C*H*$_2$-CH$_f$), 1.44 (m, 2H, -C*H*$_2$-CH$_g$), 1.35-1.17 (m, 16H, -C*H*$_2$-); ^{13}C NMR (100 MHz, $CDCl_3$,): δ = 172.8 (CO succinic), 171.1 (CO succinic), 165.2 (CO fumaric), 164.9 (CO fumaric), 163.6 (CO macrocycle), 149.1, 141.4, 141.0, 138.7 (*C*H$_A$), 137.9, 129.0, 128.6 (*C*H$_F$), 128.2, 127.8, 127.3, 126.8, 124.9 (*C*H$_B$), 66.9 (*C*H$_b$), 50.3 (*C*H$_m$), 49.8 (*C*H$_a$), 44.7 (*C*H$_l$), 40.2 (*C*H$_g$), 39.6 (*C*H$_f$), 31.0 (*C*H$_d$), 29.7 (*C*H$_c$), 29.5, 29.4, 29.3, 29.2, 29.1, 27.0, 26.8; HRMS (FAB) Calcd. for $C_{78}H_{86}N_9O_9$ $[M+H]^+$ 1292.65485. Found 1292.65598.

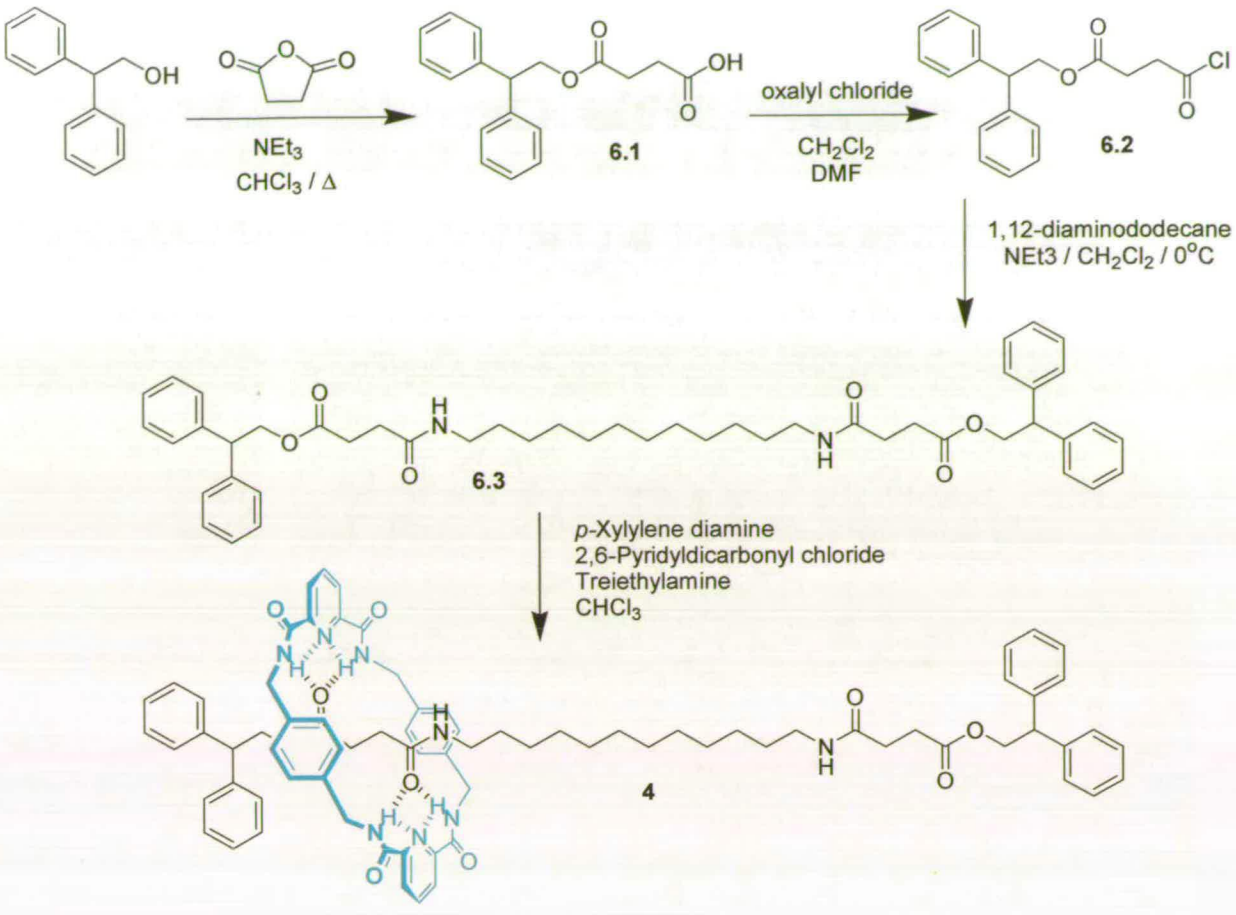
[2]-(1,4,7,14,17,20-Hexaaza-2,6,15,19-tetraoxo-3,5,9,12,16,18,22,25 –

tetrabenzocyclohexacosane)-((*Z*)-*N*-{12-[3-(2,2-diphenylethylcarbamoyl)-acryloylamino]-dodecyl}-succinamic acid 2,2-diphenylethyl ester)-rotaxane, *Z*-1.



Rotaxane *Z*-**1** was obtained by photochemical isomerisation of *E*-**1** (0.05 g, 0.04 mmol) at 254 nm in CH_2Cl_2 for 15 mins. The solution was concentrated under reduced pressure and subjected to chromatography on silica gel using a gradient of $CHCl_3$/EtOAc 3/1 as eluent to obtain the desired compound as a colorless solid (*Z*-**1**, 0.027 g, 54%). ^{1}H NMR (400 MHz, $CDCl_3$, 308K): δ = 9.21 (s, 4H, NH_D), 8.64 (br s, 1H, NH_h), 8.47 (d, J = 7.8 Hz, 4H, CH_B), 8.09 (br s, 1H, NH_k), 8.07 (t, J = 7.7 Hz, 2H, CH_A), 7.35-7.12 (m, 20H, ArC*H*), 6.94 (br s, **8**H, ArCH_F), 6.88 (br s, 1H, NH_e), 5.97 (d, J = 13.4 Hz, 1H, C$H_{i' \text{ or } j'}$), 5.83 (d, J = 13.4 Hz, 1H, C$H_{i' \text{ or } j'}$), 5.25-4.79 (br m, 4H, CH_E), 4.59 (d, J= 7.1 Hz, 2H, CH_b), 4.39- 3.88 (br m, 4H, CH_E), 4.31 (t, J= 7.1 Hz, 1H, CH_a), 4.24 (t, J= 8.0 Hz, 1H, CH_m), 4.01 (br dd, 2H, CH_l), 3.21 (br m, CH_g + CH_f), 1.52-0.45 (br m, -CH_2- + CH_c + CH_d); ^{13}C NMR (100 MHz, $CDCl_3$): δ = 174.2 (*C*O), 171.9 (*C*O), 163.5 (*C*O), 158.1 (*C*O), 149.1 (*C*O), 141.0, 138.7, 129.0, 128.8, 128.6, 128.1, 127.7, 127.3, 126.9, 125.4, 60.4, 50.9, 49.7, 42.9, 39.7, 29.7, 29.5, 29.4, 29.2, 29.2, 26.8; HRMS (FAB) Calcd. for $C_{78}H_{86}N_9O_9$ $[M+H]^+$ 1292.65485. Found 1292.65564.

Synthesis of rotaxane 4



Scheme S 1 Synthesis of the disuccinic amide ester rotaxane **4**.

Succinic acid mono-(2,2-diphenyl-ethyl) ester (6.1)

A stirred solution of succinic anhydride (505 mg, 5 mmol), 2,2-diphenylethanol (1 g, 5 mmol) and a catalytic amount of N,N-dimethylaminopyridine (50 mg, 0.5 mmol) in pyridine (5 mL) and chloroform (mL) was heated at reflux overnight. After being allowed to cool, ethyl acetate (100 mL) was added and the solution was washed with 1M HCl (3 x 50 mL). The product was then extracted with saturated $NaHCO_3$ solution (3 x 100 mL), and the combined aqueous was washed with ether (3 x 50 mL). The aqueous phase was then acidified with 2M HCl producing a white precipitate that was extracted with ethyl acetate (3 x 50 mL). The combined organics were washed with brine (1 x 50 mL), dried over Mg_2SO_4, filtered and evaporated to dryness to give the pure product as a colourless solid (**6.1**, 1.12 g, 4.0 mmol, 80 %); ^{1}H NMR (400 MHz, $CDCl_3$, 298 K) δ 11.02 (1H, bs, COO<u>H</u>), 7.25- 7.10 (10H, m, Ph), 4.58 (2H, d, J = 7.5 Hz, C<u>H</u>$_2$O), 4.29 (1H, t, J = 7.5 Hz, C<u>H</u>CH$_2$O), 2.49 (2H, d$_{ABCD}$, J = 18.5, 6.5, 5.5 Hz, COC<u>H</u>$_2$), 2.45 (2H, d$_{ABCD}$, J = 18.5, 6.5, 5.5 Hz, COC<u>H</u>$_2$); ^{13}C NMR (100 MHz,

$CDCl_3$, 298 K) δ 178.3, 172.0, 141.0, 128.6, 128.2, 126.9, 67.0, 49.8, 28.8; HRFAB-MS (3-NOBA matrix): *m/z* = 299.12902 (calcd. for $C_{18}H_{19}O_4$, $[M]H^+$, 299.12833).

3-Chlorocarbonyl-propionic acid 2,2-diphenyl-ethyl ester (6.2)

To a cooled, stirred solution of **6.1** (350 mg, 1.25 mmol) and catalytic dimethylformamide (0.5 mL) in dichloromethane (30 mL) at 0 °C was added oxalyl chloride (2M solution in dichloromethane, 622 μL, 1.22mmol) over 30 min. The reaction was left to stir for a further two hours at which point effervescence could no longer be observed. The acid chloride product **6.2** was used in the next step without isolating or further purification.

***N*-{12-[3-(2,2-Diphenyl-ethoxycarbonyl)-propionylamino]-dodecyl}-succinamic acid 2,2-diphenyl-ethyl ester rotaxane (6.3)**

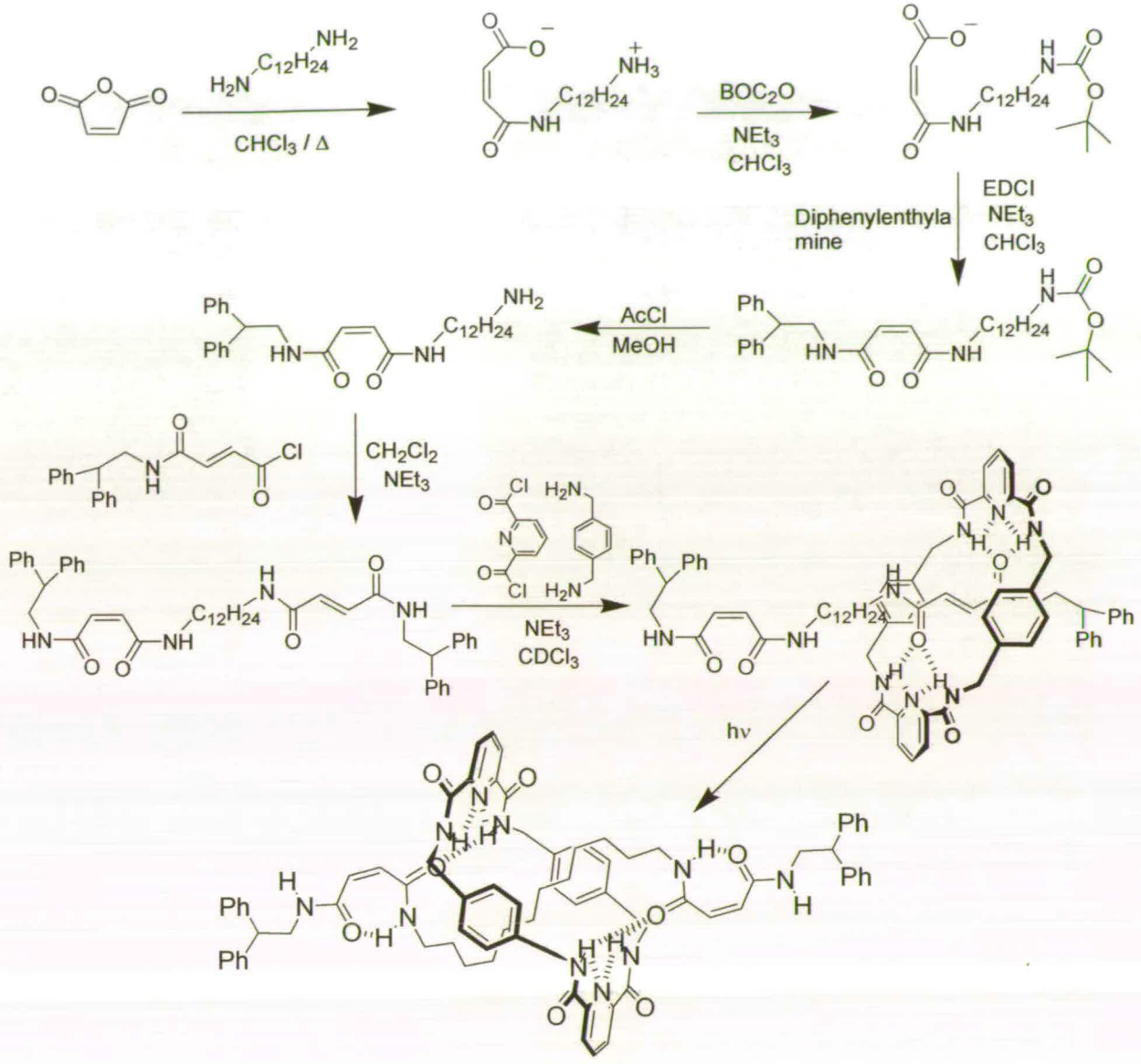
To a stirred solution of 1,12-diaminododecane (125 mg, 0.625 mmol) and triethylamine (126mg, 175 μL, 1.25 mmol) in dichloromethane (50 mL) was added the acid chloride solution **6.2** prepared in the previous step over 30 min. The reaction was left to stir for a further two hours. The completed reaction was then washed with 1M HCl (3 x 50 mL), saturated $NaHCO_3$ solution (3 x 50 mL), and water (1 x 50 mL), dried over $MgSO_4$, filtered and evaporated to dryness under reduced pressure. The crude product was purified by column chromatography (SiO_2, 1% methanol / dichloromethane) to give the desired product as a white solid (**6.3**, 328 mg, 0.453 mmol, 72 %); ^1H NMR (400 MHz, $CDCl_3$, 298 K) δ 7.33-7.18 (20H, m, Ph), 5.50 (2H, t, *J* = 6.0 Hz, NH), 4.64 (4H, d, *J* = 7.5 Hz, $CHC\underline{H}_2O$), 4.35 (2H, t, *J* = 7.5 Hz, $C\underline{H}CH_2O$), 3.18 (4H, dd, *J* = 6.0, 7.0 Hz, $NHC\underline{H}_2$), 2.58 (4H, t, *J* = 7.0 Hz, $COC\underline{H}_2$), 2.33 (4H, t, *J* = 7.0 Hz, $COC\underline{H}_2$), 1.45 (4H, quintet, *J* = 7.5 Hz, $NHCH_2C\underline{H}_2$), 1.31-1.23 (16H, m, 8 x CH_2); ^{13}C NMR (100 MHz, $CDCl_3$, 298 K) δ 172.9, 171.2, 141.0, 128.6, 128.3, 126.8, 66.9, 49.8, 39.6, 31.0, 29.7, 29.6, 29.5, 29.3, 26.9; HRFAB-MS (3-NOBA matrix): *m/z* = 761.45332 (calcd. for $C_{48}H_{61}N_2O_6$, $[M]H^+$, 761.45296).

[2](1,4,7,14,17,20-Hexaaza-2,6,15,19-tetraoxo-3,5,9,12,16,18,22,25-tetrabenzocyclohexacosane)-*N*-{12-[3-(2,2-diphenyl-ethoxycarbonyl)-propionylamino]-dodecyl}-succinamic acid 2,2-diphenyl-ethyl ester rotaxane (4)

To a stirred solution of **6.3** (200 mg, 263 μmol, 1eq.) in chloroform (30 mL) was added simultaneously solutions of *p*-xylylene diamine (286 mg, 2.11 mmol, 8 eq.) and triethylamine (532 mg, 738 μL, 5.26 mmol, 20 eq.) in chloroform (20 mL), and 2,6-pyridine-2,6-dicarbonyl chloride (410 mg, 2.11 mmol, 8 eq.) in chloroform (20 mL) via syringe pump over three hours. After addition the reaction was stirred for a further hour before being filtered and reduced in volume under reduced pressure. The crude reaction mixture was then purified by column chromatography (SiO_2) to recover unconsumed starting material (1.4% methanol / dichloromethane, **4**, 132 mg, 173 μmol, 63%), and the desired rotaxane product as a white solid (21 mg, 16 μmol, 6.2%); ^{1}H NMR (400 MHz, $CDCl_3$, 325 K)δ 8.96 (4H, t, J = 6.5 Hz, H_D*), 8.53 (4H, d, J = 8.0 Hz, H_B*), 8.11 (2H, t, J = 8.0 Hz, H_A*), 7.35- 7.11 (20H, m, Ph), 6.88 (8H, s, H_F*), 5.60- 5.00 (4H, bm, C=C$\underline{H}$), 4.80- 4.20 (16H, bm, 2 x C$\underline{H}$C$\underline{H_2}$O, H_E*), 3.19 (4H, q, J = 6.5 Hz, NHC$\underline{H_2}$), 1.80- 1.40 (8H, bm, 2 x COC$\underline{H_2}$, NHCH$_2$C$\underline{H_2}$), 1.40- 1.20 (16H, m, 8 x CH_2), 1.20- 0.98 (4H, bm, 2 x COC$\underline{H_2}$); ^{13}C NMR (100 MHz, $CDCl_3$, 298K)(macrocycle peaks broad at RT) δ 163.7, 158.0, 149.2, 140.9, 138.8, 138.5, 130.9, 128.8, 128.7, 128.6, 128.1, 127.0, 125.4, 68.2, 42.6, 39.7, 29.6, 29.5, 29.4, 29.4, 29.2, 26.9, 23.7; HRFAB-MS (3-NOBA matrix): *m/z* = 1295.65491 (calcd. for $C_{78}H_{87}N_8O_{10}$, $[M]H^+$, 1295.65452).

Developed Synthetic Route to Rotaxane *Z,Z*-5

Due to the insolubility of the Z,Z-thread in non-polar solvents necessary for rotaxane formation, the corresponding *endo*-pyridyl rotaxane ***Z,Z*-5** had to be synthesised by an indirect route. Several synthetic routes were explored, but only one proved successful. The molecule eventually synthesised according to scheme shown below (see scheme S 2).



Scheme S 2 The successful synthetic pathway developed to make rotaxane ***Z,Z*-5**.

Details of X-Ray Crystal Structure Determination

Crystallographic data for **6** (excluding structure factors) have been deposited with the Cambridge Crystallographic Data Centre as supplementary publication numbers CCDC-213301. Copies of the data can be obtained free of charge on application to The Director, CCDC, 12 Union Road, Cambridge CB2 1EZ, UK (fax: +44-1223-336-033; e-mail: teched@chemcrys.cam.ac.uk).

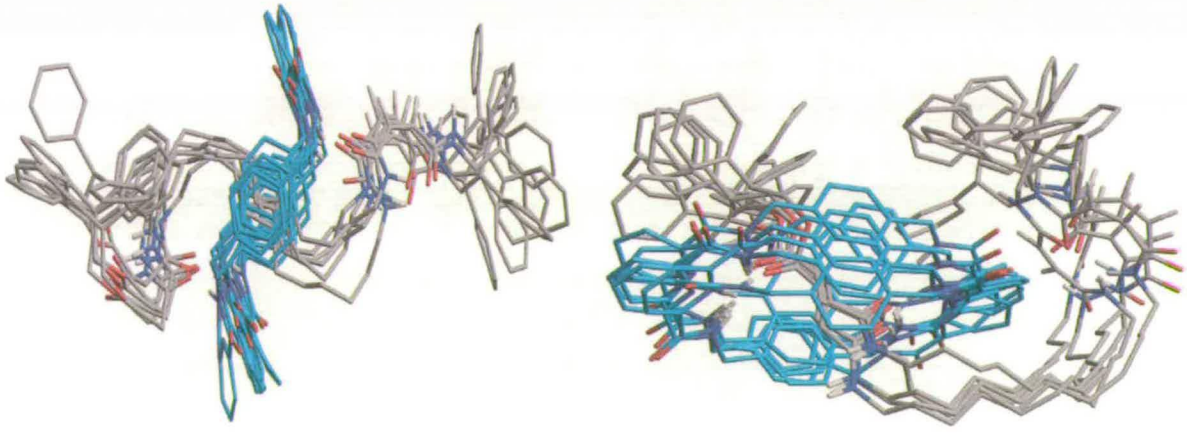
X-ray crystallographic data for compound 6 ($CHCl_3$/ether).

$C_{74}H_{80}N_6O_6$, M = 1149.44, crystal size 0.10 × 0.05 × 0.05 mm, monoclinic, $P2_1/c$, a = 11.4490(18), b = 8.8620(14), c = 31.166(5) Å, β = 94.141(4)°, V = 3153.9(9) Å^3, Z = 2, ρ_{calcd}

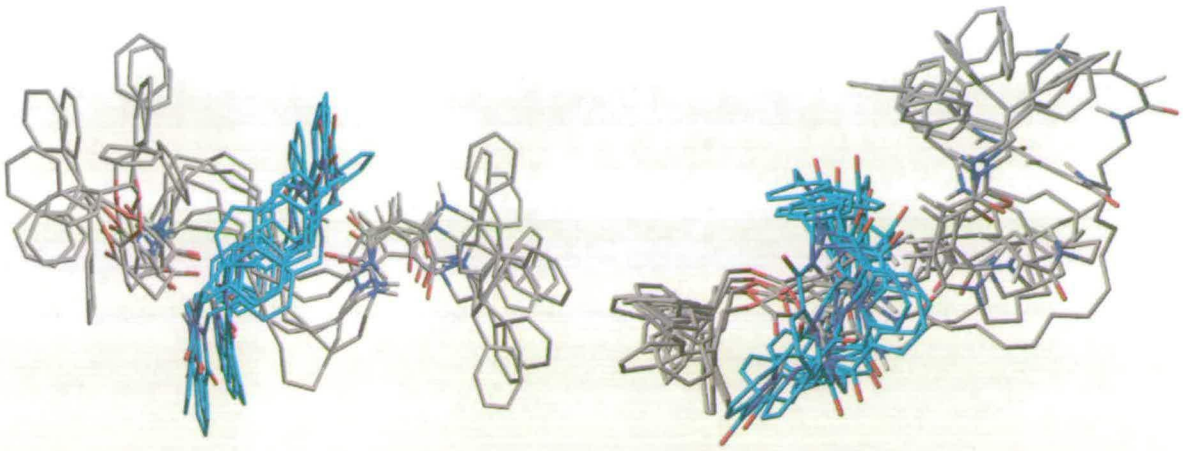
= 1.210 Mg m^{-3}; synchrotron radiation (CCLRC Daresbury Laboratory Station 9.8, silicon monochromator, λ = 0.68950 Å), μ = 0.077 mm^{-1}, T = 150(2) K. 10273 data (3210 unique, R_{int} = 0.0846, 2.07 < θ < 20.00°), were collected on a Siemens SMART CCD diffractometer using narrow frames (0.3° in ω), and were corrected semi-empirically for absorption and incident beam decay. The structure was solved by direct methods and refined by full-matrix least-squares on F^2 values of all data (G. M. Sheldrick, SHELXTL manual, Siemens Analytical *X*-ray Instruments, Madison WI, USA, 1994, version 5) to give $wR = \{\Sigma[w(F_o^2-F_c^2)^2]/\Sigma[w(F_o^2)^2]\}^{1/2}$ = 0.2654, conventional R = 0.1046 for F values of 3210 reflections with $F_o^2 > 2\sigma(F_o^2)$, S = 1.142 for 393 parameters. Residual electron density extremes were 0.563 and –0.765 $Å^{-3}$. Amide hydrogen atoms were refined isotropically with the remainder constrained; anisotropic displacement parameters were used for all non-hydrogen atoms.

Computation Simulations

Simulations of Z-**1** were carried out at 258 and 298 K. Both the proposed *dodec-* and the *succ-* co-conformers were studied using molecular dynamics. While obtaining quantitative values of entropy from molecular modelling in solution is extremely difficult and requires very long computation times, the dynamics can still show the origin of the entropic effect. Figures S1a and S1b overlap six conformations, taken every 100 ps at 258 K, of the two main co-conformers. It appears that the alkane chain of the S-shaped system is nearly static. Some mobility is observed for the stoppers of the maleamide station (see also below).



a) b)



c) d)

Figure S1 Superimposition of the motions of Z-**1** (a) *dodec*- co-conformer at 258 K, (b) *succ*- co-conformer at 258 K, (c) *dodec*- co-conformer at 298 K, (d) *succ*- co-conformer at 298 K.

Similarly, figures S1c and S1d overlap six conformations obtained at 298 K. Substantially larger movements of chain and stoppers are observed. For the *dodec*- co-conformer, however, the centre of the dodecanyl moiety is locked in place by the macrocycle and therefore the amplitude of its displacement is reduced. The pictures confirm that the alkane chain of the S-shaped system has a higher rigidity, *i.e.,* lower entropy, than in the succinic bonded rotaxane.

A more quantitative approach considers the variation in time of the average interaction energy between macrocycle and thread. This is not an instantaneous value, rather it is the mean value obtained from the energies calculated up to a given moment in time. If the simulation is sufficiently long, the value eventually converges. Figure S2 (top) shows that in 200-300 ps, the interaction energy of the *dodec*-conformer readily converges. Satisfactorily, the interaction energy is larger at the lower temperature, where the system has a better chance to be static and little or no slippage occurs.

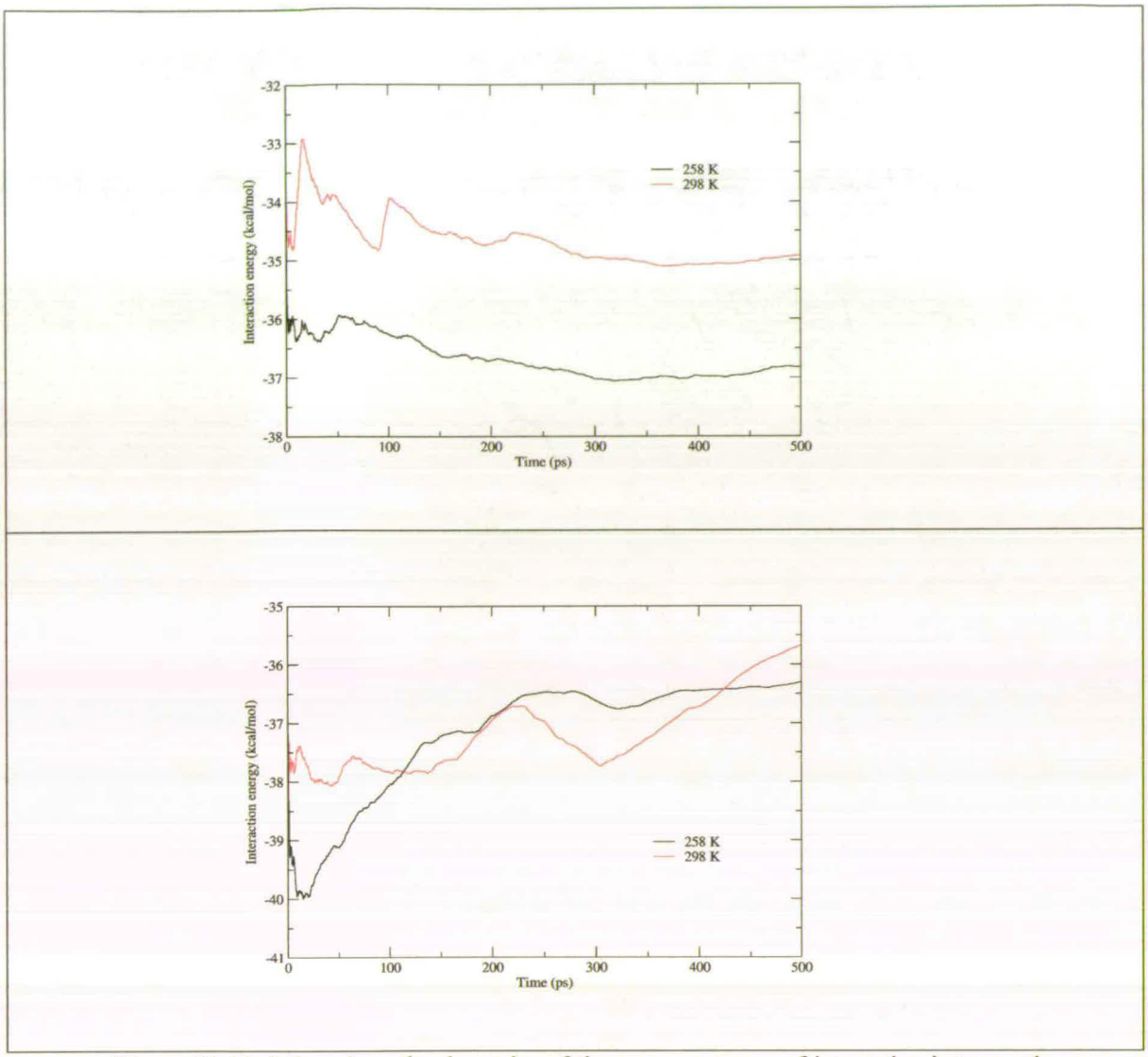


Figure S2 Variation along the dynamics of the average energy of interaction between the macrocycle and the thread. Top: *dodec-* co-conformer; bottom: *succ-* co-conformer.

Figure S2 (bottom) shows that in the *succ-* co-conformer, at 258 K, the average macrocycle-thread interaction still converges, although with some difficulty, in a similar time. At 298 K, instead, the energy is still varying after 500 ps of dynamics. From the comparison of figures S1b and S1d, the origin of the varying interaction can be assigned to the "banging" of the phenyl stoppers of the maleamide unit on the macrocycle. At 258 K, the stopper and ring form a stable π-stack; at 298 K the π-stack is broken and formed periodically. The macrocycle-thread interaction is different when the π-complex is present. To reach a constant average value the process of breaking and forming the π-stack, which is still faster than the nmr timescale, must be sampled several times. This relatively slow motion becomes only activated

with temperature and provides the crucial entropic contribution to the stability of the *succ*-co-conformer.

Computational details

Molecular dynamics calculations of Z-**1** were performed in $CHCl_3$ with the TINKER program[12] using the MM3 model[13] that has been successful in previous investigations on related systems.[14] Initially, both conformers were optimized in the vacuum. Equilibration was then performed for 50 ps (the S-shaped system had the constraint of cross hydrogen bonding of the macrocycle with the two stations). Several cycles of simulated annealing with temperatures up to 1000 K selected the most stable geometries in the vacuum. The rotaxane was then inserted in a cubic box of 45 Å side with 669 solvent molecules. NVT simulations were performed with a time step of 1 fs and a cutoff radius of 15 Å. At either 258 or 298 K, the schedule consisted of (i) 50 ps with the geometry of the rotoxane frozen, (ii) 500 ps of equilibration, (iii) 500 ps of acquisition.

4.5 References

1. *Molecular Catenanes, Rotaxanes and Knots*, J.-P. Sauvage, C. Dietrich-Buchecker, Eds.; Wiley-VCH: Weinheim, **1999**. b) V. Balzani, A. Credi, F. M. Raymo, J. F. Stoddart *Angew. Chem.* **2000**, *112*, 3483-3530; *Angew. Chem. Int. Ed.* **2000**, *39*, 3348-3391. c) Special issue on *Molecular Machines*: *Acc. Chem. Res.* **2001**, *34*, 409-522. d) M. Venturi, A. Credi, V. Balzani, *Molecular Devices and Machines - A Journey into the Nanoworld*, Wiley-VCH: Weinheim, **2003**.

2. Exceptions are environment-sensitive shuttles where the preferred position of the macrocycle is determined by the differing solvation of the binding sites in various solvent systems. a) A. S. Lane, D. A. Leigh, A. Murphy, *J. Am. Chem. Soc.* **1997**, *119*, 11092-11093. b) C. Gong, H. W. Gibson, *Angew. Chem.* **1997**, *109*, 2426-2428, *Angew. Chem., Int. Ed. Engl.* **1997**, *36*, 2331-2333. c) T. Da Ross, D. M. Guldi, A. Farran Morales, D. A. Leigh, M. Prato, R. Turco, *Org. Lett.* **2003**, *5*, 689-691. Indeed, as an alternative to cooling to 258 K in $CDCl_3$ the macrocycle in *Z*-**1** (but not *E*-**1**) can be positioned over the dodecane chain at room temperature by dissolving it in d_6-DMSO.

3. The energy potentially available to do useful mechanical work through such a process corresponds to the $\Delta\Delta G_{binding}$ of the macrocycle for the two stations in the chemically transformed shuttle.

4. R. A. Bissell, E. Córdova, A. E. Kaifer, J. F. Stoddart, *Nature* **1994**, *369*, 133-137. b) P. R. Ashton, R. Ballardini, V. Balzani, I. Baxter, A. Credi, M. C. T. Fyfe, M. T. Gandolfi, M. Gómez-López, M.-V. Martínez-Díaz, A. Piersanti, N. Spencer, J. F. Stoddart, M. Venturi, A. J. P. White, D. J. Williams, *J. Am. Chem. Soc.* **1998**, *120*, 11932-11942. c) J. W. Lee, K. Kim, K. Kim, *Chem. Commun.* **2001**, 1042-1043. d) A. M. Elizarov, S.-H. Chiu, J. F. Stoddart *J. Org. Chem.* **2002**, *67*, 9175-9181.

5. H. Murakami, A. Kawabuchi, K. Kotoo, M. Kunitake, N. Nakashima, *J. Am. Chem. Soc.* **1997**, *119*, 7605-7606. b) N. Armaroli, V. Balzani, J. P. Collin, P. Gaviña, J. P. Sauvage, B. Ventura, *J. Am. Chem. Soc.* **1999**, *121*, 4397-4408. c) P. R. Ashton, R. Ballardini, V. Balzani, A. Credi, K. R. Dress, E. Ishow, C. J. Kleverlaan, O. Kocian, J. A. Preece, N. Spencer, J. F. Stoddart, M. Venturi, S. Wenger, *Chem. Eur. J.* **2000**, *6*, 3558-3574. d) A. M. Brouwer, C. Frochot, F. G. Gatti, D. A. Leigh, L. Mottier, F. Paolucci, S. Roffia, G. W. H. Wurpel, *Science* **2001**, *291*, 2124-2128. e) G. W. H. Wurpel, A. M. Brouwer, I. H. M. van Stokkum, A. Farran, D. A. Leigh, *J. Am. Chem. Soc.* **2001**, *123*, 11327-11328. f) C. A. Stanier, S. J. Alderman, T. D. W. Claridge, H. L. Anderson, *Angew. Chem.* **2002**, *114,* 1847-1850; *Angew. Chem. Int. Ed.* **2002**, *41*, 1769-1772. g) A. Altieri, G. Bottari, F. Dehez, D. A. Leigh, J. K. Y. Wong, F. Zerbetto, *Angew. Chem.* **2003**, *115,* 2398-2402; *Angew. Chem. Int. Ed.* **2003**, *42*, 2296-2300.

6. a) P.-L. Anelli, M. Asakawa, P. R. Ashton, R. A. Bissell, G. Clavier, R. Górski, A. E. Kaifer, S. J. Langford, G. Mattersteig, S. Menzer, D. Philp, A. M. Z. Slawin, N. Spencer, J. F. Stoddart, M. S. Tolley, D. J. Williams, *Chem. Eur. J.* **1997**, *3*, 1113-1135. b) J.-P. Collin, P. Gaviña, J.-P. Sauvage, *New J. Chem.* **1997**, 525-528. c) N. Armaroli, V. Balzani, J.-P. Collin, P. Gaviña, J.-P. Sauvage, B. Ventura, *J. Am. Chem. Soc.* **1999**, *121*, 4397-4408. d) R. Ballardini, V. Balzani, W. Dehaen, A. E. Dell'Erba, F. M. Raymo, J. F. Stoddart, M. Venturi, *Eur. J. Org. Chem.* **2000**, 591-602. e) C. P. Collier, J. O. Jeppesen, Y. Luo, J. Perkins, E. W. Wong, J. R. Heath, J. F. Stoddart, *J. Am. Chem. Soc.* **2001**, *123*, 12632-12641.

7. A temperature change has been used to induce shuttling by bringing about a *cis-trans* isomerization reaction in one of the stations [ref 5g]. For a [2]rotaxane where a temperature increase is used to overcome a significant kinetic barrier to shuttling following a chemical change see ref 4c. A bistable [2]rotaxane that appears to undergo translational isomerism as a result of differences in the entropy of solvation of two stations has recently been reported [J. O. Jeppesen, K. A. Nielsen, J. Perkins, S. A. Vignon, A. Di. Fabio, R. Ballardini, M. T. Gandolfi, M. Venturi, V. Balzani, J. Becher, J. F. Stoddart, *Chem. Eur. J.* **2003**, *9*, 2982-3007]

8. A series of interesting theoretical designs for entropy-driven mechanical motion in mechanically interlocked molecules have recently been suggested [A. Hanke, R. Metzler, *Chem. Phys. Lett.* **2002**, *359*, 22-26].

9. For other types of tristable switch see a) (supramolecular) P. R. Ashton, V. Balzani, J. Becher, A. Credi, M. C. T. Fyfe, G. Mattersteig, S. Menzer, M. B. Nielsen, F. M. Raymo, J. F. Stoddart, M. Venturi, D. J. Williams, *J. Am. Chem. Soc.* **1999**, *121*, 3951-3957. b) (molecular) F. M. Raymo, S. Giordani, A. J. P. White, D. J. Williams, *J. Org. Chem.* **2003**, *68*, 4158-4169. c) ([2]- and [3]catenanes) D. A. Leigh, J. K. Y. Wong, F. Dehez, F. Zerbetto, *Nature* **2003**, *424*, 174-179.

10. At 308 K the ratio of *succ-Z*-**1**:*dodec-Z*-**1** is ~90:10; at 258 K it is ~15:85.

11. F. G. Gatti, D. A. Leigh, S. A. Nepogodiev, A. M. Z. Slawin, S. J. Teat, J. K. Y. Wong, *J. Am. Chem. Soc.* **2001**, *123*, 5983-5989.

12. J. W. Ponder, F. Richards, *J. Comput. Chem.* **1987**, *8*, 1016-1024.

13. N. L.Allinger,; Y. H. Yuh, J. H. Lii, *J. Am. Chem. Soc.* **1989**, *111*, 8551-8582.

14. F. Biscarini, M. Cavallini, D. A. Leigh, S. Leon, S. J. Teat, J. K. Y. Wong, F. Zerbetto, *J. Am. Chem. Soc.* **2002**, *124*, 225-233; V. Bermudez, N. Capron, T. Gase, F. G. Gatti, F. Kajzar, D. A. Leigh, F. Zerbetto, S. W. Zhang, *Nature* **2000**, *406*, 608-611.